UNIVERSIDADE ESTADUAL DE CAMPINAS
FACULDADE DE ENGENHARIA MECÂNICA
E INSTITUTO DE GEOCIÊNCIAS

VICTOR DE SOUZA RIOS

NEW METHODOLOGIES FOR UPSCALING OF HIGHLY HETEROGENEOUS RESERVOIRS AND MISCIBLE GAS FLOODING PROCESSES IN NUMERICAL RESERVOIR SIMULATION

NOVAS METODOLOGIAS PARA A TRANSFERÊNCIA DE ESCALA DE RESERVATÓRIOS ALTAMENTE HETEROGÊNEOS E PROCESSOS DE INJEÇÃO DE GÁS MISCÍVEL NA SIMULAÇÃO NUMÉRICA DE RESERVATÓRIOS

CAMPINAS
2021

VICTOR DE SOUZA RIOS

NEW METHODOLOGIES FOR UPSCALING OF HIGHLY HETEROGENEOUS RESERVOIRS AND MISCIBLE GAS FLOODING PROCESSES IN NUMERICAL RESERVOIR SIMULATION

NOVAS METODOLOGIAS PARA A TRANSFERÊNCIA DE ESCALA DE RESERVATÓRIOS ALTAMENTE HETEROGÊNEOS E PROCESSOS DE INJEÇÃO DE GÁS MISCÍVEL NA SIMULAÇÃO NUMÉRICA DE RESERVATÓRIOS

Thesis presented to the School of Mechanical Engineering and the Institute of Geosciences of the University of Campinas in partial fulfillment of the requirements for the degree of Doctor in Petroleum Sciences and Engineering in the area of Reservoirs and Management.

Tese apresentada à Faculdade de Engenharia Mecânica e Instituto de Geociências da Universidade Estadual de Campinas como parte dos requisitos exigidos para a obtenção do título de Doutor em Ciências e Engenharia de Petróleo na área de Reservatórios e Gestão.

Supervisor: Prof. Dr. Denis José Schiozer

Co-supervisor: Dr. Luiz Otávio Schmall dos Santos

Este exemplar corresponde à versão final da Tese defendida pelo aluno Victor de Souza Rios e orientada pelo Prof. Dr. Denis José Schiozer e coorientada pelo Dr. Luiz Otávio Schmall dos Santos.

_____

Assinatura do Orientador

CAMPINAS

2021

Ficha catalográfica
Universidade Estadual de Campinas
Biblioteca da Área de Engenharia e Arquitetura
Rose Meire da Silva - CRB 8/5974

R479n

Rios, Victor de Souza, 1987-
New methodologies for upscaling of highly heterogeneous reservoirs and miscible gas flooding processes in numerical reservoir simulation / Victor de Souza Rios. – Campinas, SP : [s.n.], 2021.

Orientador: Denis José Schiozer.
Coorientador: Luiz Otávio Schmall dos Santos.
Tese (doutorado) – Universidade Estadual de Campinas, Faculdade de Engenharia Mecânica.

1. Reservatórios de petróleo. I. Schiozer, Denis José, 1963-. II. Santos, Luiz Otávio Schmall dos. III. Universidade Estadual de Campinas. Faculdade de Engenharia Mecânica. IV. Título.

Informações para Biblioteca Digital

Título em outro idioma: Novas metodologias para a transferência de escala de reservatórios altamente heterogêneos e processos de injeção de gás miscível na simulação numérica de reservatórios
Palavras-chave em inglês:
Petroleum reservoir
Área de concentração: Reservatórios e Gestão
Titulação: Doutor em Ciências e Engenharia de Petróleo
Banca examinadora:
Denis José Schiozer [Orientador]
Philippe Remy Bernard Devloo
Célio Maschio
Daniel Nunes de Miranda Filho
Valcir Tadeu Beraldo
Data de defesa: 26-02-2021
Programa de Pós-Graduação: Ciências e Engenharia de Petróleo

Identificação e informações acadêmicas do(a) aluno(a)
- ORCID do autor: https://orcid.org/0000-0003-0291-9486
- Currículo Lattes do autor: http://lattes.cnpq.br/1749877620969357

UNIVERSIDADE ESTADUAL DE CAMPINAS

FACULDADE DE ENGENHARIA MECÂNICA

E INSTITUTO DE GEOCIÊNCIAS

TESE DE DOUTORADO

NEW METHODOLOGIES FOR UPSCALING OF HIGHLY HETEROGENEOUS RESERVOIRS AND MISCIBLE GAS FLOODING PROCESSES IN NUMERICAL RESERVOIR SIMULATION

Autor: Victor de Souza Rios
Orientador: Prof. Dr. Denis José Schiozer
Coorientador: Dr. Luiz Otávio Schmall dos Santos

A Banca Examinadora composta pelos membros abaixo aprovou esta Tese:

Prof. Denis José Schiozer, Presidente
UNICAMP

Prof. Philippe Remy Bernard Devloo
UNICAMP

Dr. Célio Maschio
UNICAMP

Dr. Daniel Nunes de Miranda Filho
PETROBRAS

Dr. Valcir Tadeu Beraldo
CONSULTOR

A Ata da defesa com as respectivas assinaturas dos membros encontra-se no processo de vida acadêmica do aluno.

Campinas, 26 de fevereiro de 2021.

DEDICATION

*I dedicate this thesis to the memory of my beloved daughter, **Catarina**, who taught me how to become a better version of myself, even under the hardest circumstances. I deeply wish you were here! I miss you every single day of my life! I love you, my baby daughter.*

*I also dedicate this work to my beloved wife, **Carina**, the prettiest smile I have ever seen. Your strength and support make me feel everything is possible. Thank you so much!*

*Finally, this scientific contribution is dedicated to my precious daughter, **Lavínia**, who has been the reason of my happiness, helping me to stay focused, when nearly losing my mind. My intent is to make you proud, dear daughter.*

ACKNOWLEDGMENTS

Firstly, I thank God for always illuminating my path and blessing my choices.

I would like to express my gratitude to my supervisor, Prof. Denis José Schiozer, for his guidance and support during my research.

Also, I would like to extend my gratitude to my co-supervisor, Dr. Luiz Otávio Schmall dos Santos, for his tireless support and attention. I am grateful for everything I learned from him since 2013. It is an honor to have him as my tutor and friend.

My sincere thanks go to Prof. Arne Skauge for providing my wife and me with an amazing experience in Bergen. In addition to the high-level technical discussions and his extraordinary ability to share knowledge, his attention and goodwill were a true blessing during our nine-month stay in Norway. Thank you, Professor!

Additionally, I would like to thank Petrobras for the opportunity of accomplishing this goal. My sincere thanks to Daniel Nunes de Miranda Filho, Luiz Otávio Schmall dos Santos, Roberta Alves Mendes, Antônio Carlos Capeleiro Pinto and Priscila Moczydlower for their intense support to get this journey started. As I get back to the office, I intend to keep helping Petrobras with the best of my knowledge.

Furthermore, I thank my colleagues at Unicamp and UNISIM group, especially Dr. Guilherme Daniel Avansi, for his friendship and partnership in some publications; M.Sc. Gilson Moura da Silva Neto, for the long technical discussions both in Brazil and in Norway; and M.Sc. Vinicius de Souza Rios, my brother, for his immense help all along the years. My work would not have been the same without his insights and suggestions.

Finally, with humble heart, I would like to express my extreme gratitude to my family: to my parents, João and Vera, my heroes, who are responsible for this achievement; to my brothers, João and Vinicius, who have been lifetime companions and permanent sources of inspiration; to my wife, Carina, for her love and unconditional support during all these years of study; and to my daughters, Catarina and Lavínia, for proving that I can be much stronger than I thought. This achievement would not have been possible without you all. Thank you so much!

“If one does not know to which port one is sailing, no wind is favorable.”

Lucius Annaeus Seneca

RESUMO

A simulação numérica de reservatórios é uma ferramenta valiosa para auxiliar o processo de tomada de decisão nas atividades da indústria de petróleo e gás. No entanto, a modelagem numérica em escala de campo de reservatórios complexos e heterogêneos ainda é desafiadora. Em tais reservatórios, modelos geológicos detalhados são necessários para garantir uma representação adequada das principais heterogeneidades e caminhos preferenciais. No entanto, altos custos computacionais e longos tempos de execução de simulação tornam esses modelos detalhados inviáveis para uso em avaliações dinâmicas. Portanto, a transferência de escala de um modelo geológico é uma etapa crucial nos estudos de engenharia de reservatório para permitir execuções de simulação em escala de campo com tempo e custo compatíveis com as necessidades da indústria. No entanto, as simplificações resultantes de modelos em escala grosseira podem afetar os resultados devido à perda de resolução de fenômenos de pequena escala, a representação média da heterogeneidade sub-malha e a dispersão numérica, especialmente em campos de petróleo sujeitos à injeção de gás miscível. Neste trabalho, exploramos o problema de transferência de escala como um todo e propomos soluções para cobrir algumas lacunas importantes ainda presentes na literatura atual, especialmente em sistemas altamente heterogêneos e com injeção de gás miscível. Desenvolvemos um procedimento de transferência de escala de dupla porosidade e dupla permeabilidade para permitir a representação de heterogeneidades de sub-malha no modelo de escala grosseira. Essa técnica é baseada na divisão do meio poroso em dois níveis guiados pela análise de capacidade de fluxo e de armazenamento e pelo Coeficiente de Lorenz, ambos calculados com propriedades estáticas (permeabilidade e porosidade) a partir de um modelo de referência em escala fina. Esta metodologia permite a adaptação de um modelo geológico fino altamente heterogêneo a um modelo de simulação em escala grosseira que representa as principais heterogeneidades do reservatório e possíveis caminhos preferenciais. Além disso, para o processo de injeção de gás miscível, desenvolvemos uma técnica baseada no emprego de um modelo de fluido alternativo, também conhecido como pseudo-fluido, com uma pseudo pressão mínima de miscibilidade (PMMP) acima dos valores experimentais para fornecer um deslocamento mais próximo do imiscível. Esta solução não viola o comportamento de fases e garante a formação de duas fases de hidrocarbonetos no reservatório. Então, a permeabilidade relativa ao gás desempenha um papel nos resultados da simulação e pode ser usada para melhorar as curvas de produção do modelo grosso. A técnica é aplicada em duas etapas: primeiro, o modelo de pseudo-fluido é

gerado e, em seguida, pseudo-curvas de permeabilidade relativa são usadas para melhor ajustar as curvas de produção. Como contribuições adicionais, propomos um fluxo de trabalho geral para orientar o processo de transferência de escala, dividindo a abordagem de acordo com as limitações mais críticas do problema, que podem ser genericamente divididas em dois grupos: (Grupo 1) limitações de modelagem estática e (Grupo 2) especificidades de dinâmica de fluxo. Além disso, motivado pela falta de procedimentos práticos para melhorar os resultados em escala grosseira com múltiplas realizações, também propomos um procedimento de transferência de escala probabilístico para sistemas composicionais com injeção de gás miscível. Resumindo, as principais contribuições deste trabalho são: (1) uma técnica de transferência de escala robusta para sistemas altamente heterogêneos; (2) um procedimento consistente de transferência de escala composicional para processos de injeção de gás miscível. Além disso, as contribuições adicionais são (1) um fluxo de trabalho geral para guiar o procedimento de transferência de escala de acordo com as limitações mais importantes de cada problema; e (2) um procedimento de transferência de escala probabilístico para simulação de composição de problemas de injeção de gás miscível.

Palavras-Chave: simulação numérica de reservatório; transferência de escala; transferência de escala com dupla porosidade/dupla permeabilidade; injeção de gás miscível; fluxo de trabalho geral para transferência de escala; transferência de escala em múltiplas realizações.

ABSTRACT

Numerical reservoir simulation is a valuable tool to assist the decision-making processes in the oil and gas industry. Nevertheless, field-scale numerical modeling of complex heterogeneous reservoirs remains a challenge. In such reservoirs, detailed geological models are required to ensure a proper representation of the key heterogeneities and main preferential pathways. However, high computational costs and long simulation run-times make such detailed models unfeasible for dynamic assessments. Therefore, the upscaling of a geological model is a crucial step in reservoir engineering studies to enable field-scale simulation runs with time and cost compatible with the industrial needs. Although, the simplifications resulting from coarse-scale models may degenerate results due to resolution loss of small-scale phenomena, average representation of sub-grid heterogeneity and numerical dispersion, especially in oil fields subject to miscible gas flooding. In this work, we explore the upscaling problem as a whole and propose solutions to cover some important gaps still present in the current literature, especially in the upscaling of highly heterogeneous systems and modeling of miscible gas flooding displacements. We developed a dual-porosity/dual-permeability upscaling process to enable the representation of sub-grid heterogeneities in a coarse-scale model. This technique is based on splitting the porous media into two levels, guided by a flow and storage capacity analysis and the Lorenz Coefficient, both calculated from permeability and porosity data from a fine-scale reference model. This methodology allows the transformation of a fine highly heterogeneous geological model into a coarse-scale simulation model that represents the main reservoir heterogeneities and possible preferential paths. Additionally, for miscible gas flooding processes, we developed a technique employing an alternative fluid model, also known as pseudo-fluid, with a pseudo minimum miscibility pressure (PMMP) higher than the experimental values, to provide an immiscible-like displacement. This solution honors the thermodynamic phase behavior and ensures the formation of two hydrocarbon phases in the reservoir. Furthermore, the gas relative permeability affects simulation results and can be used to improve the coarse model production curves. The technique is applied in two steps: first, the pseudo-fluid model is generated, then pseudo relative permeability curves are used to better match the production curves. As additional contributions, we propose a general upscaling workflow to guide the coarsening process by splitting the approach according to the most critical limitations of the problem, generically divided into two groups: (Group 1) static modeling limitations; and (Group 2) flow-dynamics specifics. Besides, motivated by the lack

of practical procedures to improve coarse-scale results at the ensemble-level, we also propose a probabilistic upscaling procedure for compositional systems with miscible gas injection. Summarizing, the main contributions of this work are: (1) a robust upscaling technique for highly heterogeneous systems; and (2) a consistent compositional upscaling procedure for miscible gas flooding processes. Moreover, the additional contributions are (1) a general upscaling workflow to guide the coarsening procedure according to the most important limitations of each problem; and (2) an ensemble-level upscaling procedure for compositional simulation of miscible gas injection problems.

Key Word: numerical reservoir simulation; upscaling techniques; dual porosity/dual permeability upscaling; miscible gas flooding; general upscaling workflow; ensemble-level upscaling.

CONTENTS

1 INTRODUCTION

Field-scale representation of heterogeneous reservoirs remains a challenge in numerical reservoir simulation. In such reservoirs, detailed geological models are important to properly represent the main heterogeneities. However, the resulting models are nearly impossible to be considered for dynamic evaluations due to high computational costs and long simulation run-times. Therefore, upscaling of geological models is a key step in reservoir engineering studies, but it needs to be carefully performed since it can introduce sensible errors to the simulation, such as: loss of resolution of small-scale phenomena, unsuited representation of sub-grid heterogeneity and preferential pathways and increased numerical dispersion, especially in oil fields with miscible gas flooding as an enhanced oil recovery method, continuously or alternatively with water (WAG). For this reason, various upscaling techniques have been proposed throughout the years with an increasing complexity level, depending on the static and dynamic challenges represented by each reservoir and production strategy. Detailed and comprehensive reviews on several techniques are provided by Wen and Gomez-Hernández (1996), Renard and de Marsily (1997), Farmer (2002) and Durlofsky (2003).

In practical simulation studies, single-phase upscaling techniques are valuable tools and the most applied methodologies. They can provide satisfactory results for some two- and three-phase flow problems when the reservoir system is not highly heterogeneous or has a low mobility-ratio. The most frequently used method to upscale porosity from a fine-scale model is the volumetric-weighted arithmetic average, because of the preserved pore volume (Durlofsky, 2003). For permeability upscaling, there are three important methods: (i) averaging, which considers horizontal arithmetic average and vertical harmonic average; (ii) Cardwell-Parsons directional averaging (Cardwell and Parsons, 1945); and (iii) flow-based upscaling with closed boundary conditions (Christie, 1996; Kumar et al., 1997). In general, flow-based upscaling methods are more widely considered as reference approaches because of their generality and flexibility (Chen and Durlofsky, 2006).

In traditional upscaling procedures, a group of fine-scale cells is averaged to obtain only one cell with uniform properties, corresponding to a coarse-scale cell. Thus, sub-grid heterogeneities and dynamic features (such as viscous instabilities) tend to be homogenized and each upscaled grid block smooths the behavior of several fine-scale grid cells. Dynamic evaluations with coarse-scale models in these situations tend to overestimate the sweep

efficiency of the injected fluids. That happens mainly because the preferential paths due to high permeability contrasts and viscous fingers are homogenized in each coarse-scale cell.

Accordingly, for multiphase flow applications, additional effort is usually required to obtain a useful upscaled model. Generally, for water or immiscible gas flooding simulation processes, a two-phase upscaling procedure is recommended. In this case, the use of pseudo-relative permeability curves is one of the most used methods to improve the results of coarse-scale simulation models, when fine-scale simulation results are available. On the other hand, for miscible gas flooding processes, this strategy cannot be applied directly and a compositional upscaling approach is recommended.

Miscible gas flooding is an effective oil recovery method that recently gained special attention in Brazil, especially after the pre-salt giant oil fields were discovered. The oil present in some of the main reservoirs in the Brazilian pre-salt area has significant amounts of dissolved CO_2, in mole percentages that may exceed 30%. Besides, even when the main destination for the decontaminated produced gas is to be exported by pipeline to an onshore processing facility, the CO_2-rich gas stream needs to be reinjected after offshore separation, so that the export gas can meet the CO_2 pipeline and emission specifications. Moreover, in some situations, the total produced gas reinjection into the reservoir may occur either as part of an enhanced oil recovery strategy or due to the unavailability of an export system (Moczydlower et al., 2019, Pizarro et al., 2017). Additionally, experimental data suggest that, at reservoir pressure and temperature conditions of some pre-salt areas, CO_2-rich gas presents favorable miscible behavior, which promotes its injection as an attractive enhanced oil production alternative.

Various approaches have been proposed for upscaling compositional flow simulations, roughly divided into four categories. Each category is described next.

The first upscaling category is represented by the method of transport coefficients (also known as α-factors), proposed by Backer and Fayers (1994). The α-factors consist of modifiers introduced in the flow terms to relate compositions of the fluids flowing out of large grid blocks to the average compositions of those fluids within the grid block. Together with pseudo-relative permeability curves, the coefficients are then considered to improve coarse-scale compositional simulations.

A second upscaling category is based on the Sorm method (Hiraiwa and Suzuki, 2007), which models a bypassed oil fraction in the porous media by excluding this immobile saturation from the flash calculations. In this method, there is no mass transfer between the

bypassed oil saturation and the flowing fluids. This assumption is the main disadvantage of this method, which makes the bypassed oil totally unrecoverable.

A third upscaling category introduces a dual-porosity/dual-permeability (DP/DP) representation of the reservoir in which the porous space is divided into two systems, one with the main flow areas and another with the regions more likely to be bypassed. The mass transfer between the flowing and bypassed systems can represent the non-equilibrium behavior at the sub-grid scale. This type of approach was recently considered by Evazi and Jessen (2014), Zhang and Okuno (2015). However, only the methodology proposed by Zhang and Okuno (2015) focused on representing the bypassed oil fraction in a compositional simulation of gas flooding.

The fourth upscaling category involves the modification of the thermodynamic properties of the components to match fine-scale fluxes in a coarse-scale. This approach is valid to overcome one important and fundamental limitation of compositional simulation: the local equilibrium assumption, which allows the fluids to become perfectly mixed and in equilibrium within each grid block. This condition may be valid at fine-scale systems, but it is not reasonable for typical simulation grid block sizes. Iranshahr et al. (2014) developed a compositional upscaling formulation, considering a non-equilibrium thermodynamic condition in the coarse-scale models. They introduced the use of upscaled functions to reproduce this effect. This approach was extended by Salehi (2013, 2016), introducing a physical non-equilibrium term for the local thermodynamic constraints, which was also converted to a transport coefficient like the α-factors. These approaches allowed the coarse-scale simulation results to better represent the small-scale curves and component rates, but with an impact on the simulation time. Moreover, these techniques tend to be highly dependent on the fine-scale well scheme and dynamic configurations used to modify the coarse-scale models, but the authors did not explore this limitation.

Nevertheless, despite the wide discussions on upscaling techniques in the literature, critical gaps remain. Among them, we highlight the coarse-scale representation of highly heterogeneous reservoirs and the upscaling of miscible gas flooding cases, either continuous or WAG. For these problems, the available upscaling techniques still lack performance (computational time to generate the coarse models), flexibility (possibility to be applied to different problems with satisfactory results) and robustness (capability to provide improved results when different flow conditions, well configuration and recovery methods are considered).

Furthermore, most of the existing upscaling techniques aim at reproducing fine-scale results of a single geological realization, i.e., deterministically. However, probabilistic approaches and uncertainty quantification studies are a reality in reservoir engineering activities. The simulation of multiple geological realizations is required for these tasks. There is little research reported up to now on this subject. Chen and Durlofsky (2008) proposed an ensemble-level upscaling approach in which upscaled two-phase functions are numerically generated for a portion of the coarse-scale blocks and statistically estimated for the others. Li and Durlofsky (2016) also developed an ensemble level upscaling (EnLU) procedure for compositional systems, enabling efficient generation of multiple coarse models for use in uncertainty quantification. Although a close match between fine and coarse P10, P50 and P90 production rate curves was achieved, it required that 10% of the fine-scale models were simulated to calibrate the data, which can be prohibitive, when these reference/fine models take several hours or days for a single run.

Therefore, no universal method can provide reliable coarse-scale simulation models, since the upscaling problem averages a complex combination of static and dynamic features of a fine-scale reference model. Hence, prior knowledge and understanding of the problem is required for selection of the most appropriate upscaling technique or group of approaches.

This thesis focuses on filling some important gaps still present in the upscaling literature. The backbone of this work comprises some main objectives: (i) the proposal of solutions for an improved coarse-scale representation of highly heterogeneous reservoirs and (ii) an effective procedure for the compositional upscaling of miscible gas flooding displacements. Two additional contributions involve (i) the proposition of a global upscaling procedure to properly guide the coarsening process and (ii) the development of an ensemble-level upscaling procedure, mainly for miscible gas flooding problems.

Our first main goal is the proposal of a new dual-porosity/dual-permeability (DP/DP) upscaling technique for highly heterogeneous reservoirs inspired by Evazi and Jessen (2014). Their work proposed a methodology to arrange the pore space into two levels of porosity based on fine-scale streamline information, adapting the coarse model with a DP/DP formulation. They obtained improved coarse-scale models with accurate results; however, their approach presented two important drawbacks: (i) the overall workflow to obtain the coarse models can be costly due to the requirement of streamline simulations for the fine-scale model, and (ii) the use of fine-scale results to divide the porous media can make the strategy highly dependent on the well locations and flow rates. In our work, we use flow and storage capacity

analyses and the Lorenz Coefficient (Lorenz, 1905; Jensen et al., 2000) applied to the static information of a fine-scale model to split the porous media into two levels: one representing the primary flow regions, while the other stands for the secondary flow regions. With the splitting of fine-scale cells, directional upscaling for permeability is performed for each group. The proposed methodology presents two significant improvements over other upscaling techniques: (i) the attainment of coarse-scale models is less time-consuming, since no dynamic responses of fine-scale models are used; and (ii) the coarse models are independent from the drainage plan or well flow rates in the fine-scale models.

Our second main goal involves the development of a methodology for a robust upscaling of compositional displacements. The technique is applied in two steps: first, an alternative fluid model is generated to deal with the compositional local equilibrium limitation on the coarse scale. Then, pseudo-relative permeability curves are used to better fit the simulated fine-scale model production curves. This technique improves the representation of the coarse-scale results – production curves, sweep efficiency and gas saturation map profile – and it can be used in any compositional simulator, providing a flexible and computationally efficient approach. Thus, this procedure provides a better representation of the small-scale phenomena, when miscible gas flooding is performed.

Additionally, we propose a general upscaling workflow that leads to a practical stepwise procedure. The upscaling problem is generically divided considering the nature of the effects into groups that require different approaches: (Group 1) static modeling limitations; and (Group 2) flow-dynamics specifics. The proposed workflow guides the upscaling process by enabling the most adequate approach selection, either Group 1 or Group 2, according with the limitations of the problem. The workflow also promotes a better understanding of the upscaling problem as a whole, leading to improved and robust coarse-scale simulation models. The noteworthy upscaling techniques that we developed for highly heterogeneous reservoir and miscible displacements are solutions for Group 1 and Group 2 approaches, respectively.

Finally, motivated by the lack of practical procedures to improve coarse-scale results at the ensemble-level, we show that both new upscaling techniques we propose can be satisfactorily applied to probabilistic studies with cost-effective workflows.

1.1 The Problem and Motivation

The upscaling of detailed geocellular models in reservoir simulation has been investigated for decades, with improved solutions proposed all along. However, there are still some important gaps in the current literature. In this context, what motivates this work is the

lack of robust and practical solutions for the upscaling of highly heterogeneous reservoirs and modeling of miscible gas flooding displacements. The challenges for obtaining useful coarse-scale models under these conditions arise from different sources, requiring a broader understanding of the problem. For instance, to represent the key reservoir heterogeneities in a coarse model, the upscaling procedure must capture the sub-grid features and the non-uniform flow behavior within a coarse grid block. On the other hand, for miscible displacements, the coarse-scale limitations are related to dynamic specifics, mainly the representation of small-scale viscous instabilities and the overestimation of compositional effects due to the grid block size.

To clearly state our motivation and qualitatively illustrate the groups of phenomena that make the generation of upscaled models a challenging task, two case-studies are presented. Some critical aspects in which traditional upscaling techniques fail are highlighted in the 2D studies.

The synthetic case-studies are inspired by the SPE-10th benchmark model. Both fine-scale models present 60 x 220 grid block cells, each with area of 6.096 x 3.048 m^2. One model is a homogeneous reservoir with constant porosity and permeability, while the other is a channelized system with high permeability in the channels and low permeability in the remaining areas. These models are upscaled using traditional flow-based technique to coarser systems with grid block cells of 24.348 x 12.192 m^2, which represents an upscaling ratio (UR) of 16. Figure 1 shows the permeability maps for all the models, except the coarse-scale homogeneous model, since it is equal to its fine-scale, except for the discretization.

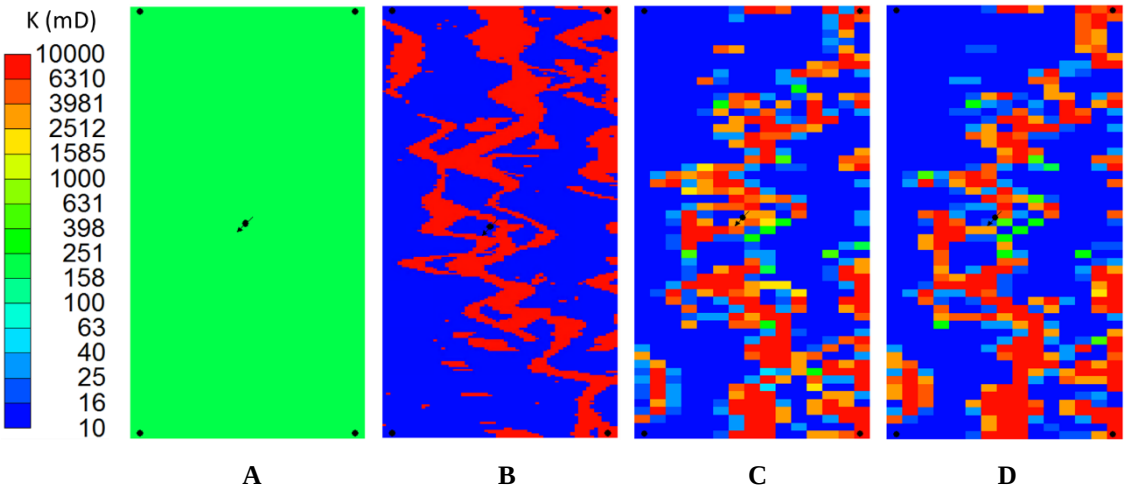

Figure 1. Permeability maps: A - Homogeneous Reservoir; B – Fine-scale channelized Reservoir; C – Coarse-scale channelized, I direction; D – Coarse-scale channelized, J direction.

The reservoir fluid is a light oil characterized by seven pseudo-components, as presented by Rios et al. (2017, 2019). The initial GOR is 215 m^3/m^3 and the saturation pressure is 400 bar, while the initial reservoir temperature and pressure are 93,9 °C and 610 bar, respectively. There is no free gas and the initial water saturation is 0.2. Additional information on the numerical models is summarized in Tables 1 and 2.

Each model considers four qualitative dynamic evaluations. First, we perform water flooding with matched viscosity for injected water and reservoir oil. Then, CO_2-rich miscible gas flooding is conducted with three different viscosity ratios (VR): matched viscosity (VR = 1) and two unfavorable displacement conditions with VR of 7.5 and 75.

Table 1 - Summary of static properties.

	Porosity	K **(mD)**
Homogeneous	0.2	Constant = 200
Channelized	0.2	10 – 10 000

Table 2 – Additional information about the numerical models (BHP is bottom hole pressure and EoS is equation of state)

Number of cells	Fine-Scale = 13 200 Coarse-Scale = 825
Simulator type	Compositional
Fluid Model	EoS with 7 components
Producer BHP	500 bar
Injection Rate	1/2000 PV/day
Relative Permeability curves	Corey type: $n_o = n_w = n_l = n_g = 2$; $K_{rw\ max} = 0.45$; $K_{ro\ max} = 0.8$; $K_{rg\ max} = 0.9$; $S_{orw} = 0.2$

The comparison between fine- and coarse-scale results for the homogeneous reservoir is presented in Figure 2, while for the channelized system is shown in Figure 3. For the water flooding process, we compare the water saturation maps (images A and E), and for the miscible gas flooding evaluations, the global CO_2-molar fraction is compared (images B, C, D, F, G, and H). The maps for the respective fine and coarse models are chosen at the same simulation-time to allow a direct comparison.

First, for the homogeneous reservoir, we evaluate the simplest system in terms of static properties, with a trivial upscaling. For matched viscosity water flooding, a stable displacement is obtained and we verify a consistent agreement between fine- and coarse-scale water saturation behavior, as shown in maps A and E of Figure 2. In fact, a matched viscosity immiscible displacement in a homogeneous system forms the most controlled environment,

where numerical dispersion could affect the coarse-scale results. However, since the UR is not high, this effect has limited impact.

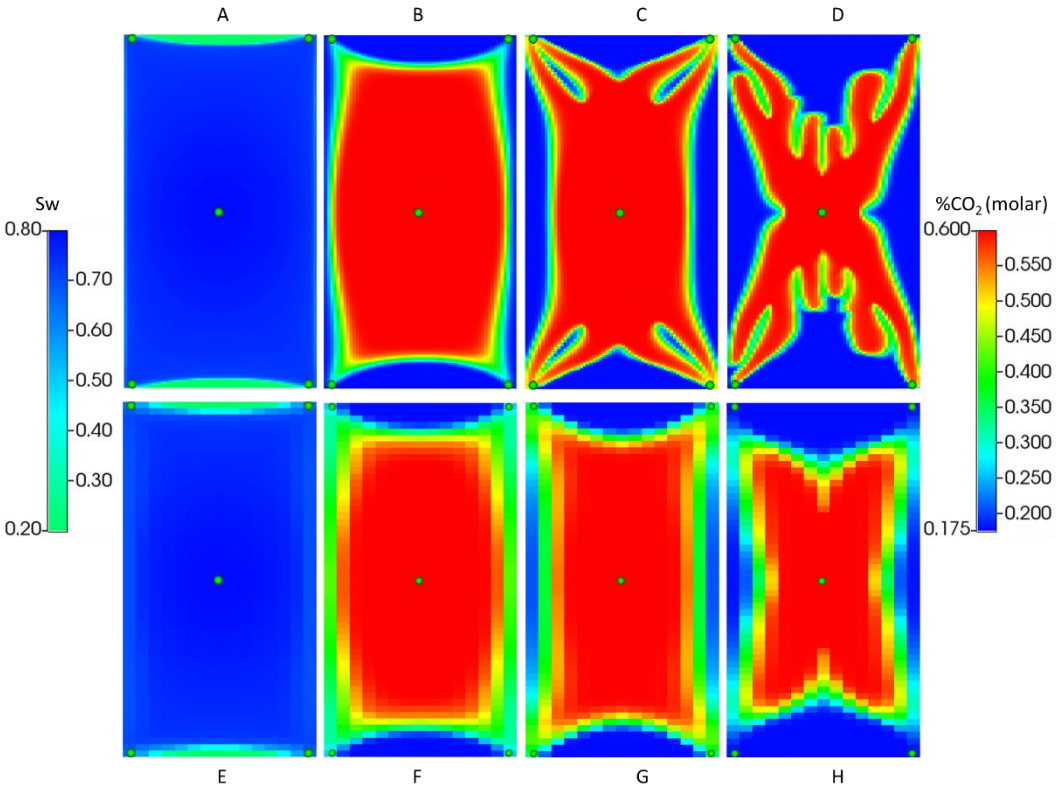

Figure 2. Homogeneous reservoir: A, B, C and D refer to fine-scale; E, F, G and H refer to coarse-scale. A and E are water saturation; B and F are CO_2-molar fraction for VR 1; C and G are CO_2-molar fraction for VR 7.5; D and H are CO_2-molar fraction for VR 75.

For the CO2-rich miscible gas flooding cases, the complexity level increases due to the compositional effects and the formation of viscous fingers triggered by the unfavorable viscosity ratio. Even for the matched viscosity scenario, the upscaled model does not present the same accuracy observed for the water flooding case. The difference happens because the coarse grid block size artificially increases the mass transfer between the injected gas and the oil in the forward front neighborhood. As a result, the compositional effects are overestimated and the coarse model tends to artificially increase the sweep efficiency. We can observe this fact by comparing Figures 2.B and 2.F.

In addition, we emphasize that the small-scale instabilities intensify for higher VR. This phenomenon is not captured by the coarse model with traditional upscaling approaches, as noted when comparing maps Figures 3.C and 3.G and Figures 3.D and 3.H. Besides not representing the viscous instabilities, the compositional effects are also not properly captured. Therefore, even when a homogenous reservoir is considered, the dynamic specifics of the

miscible gas flooding process make the upscaling problem challenging, thus requiring practical solutions for overcoming this issue.

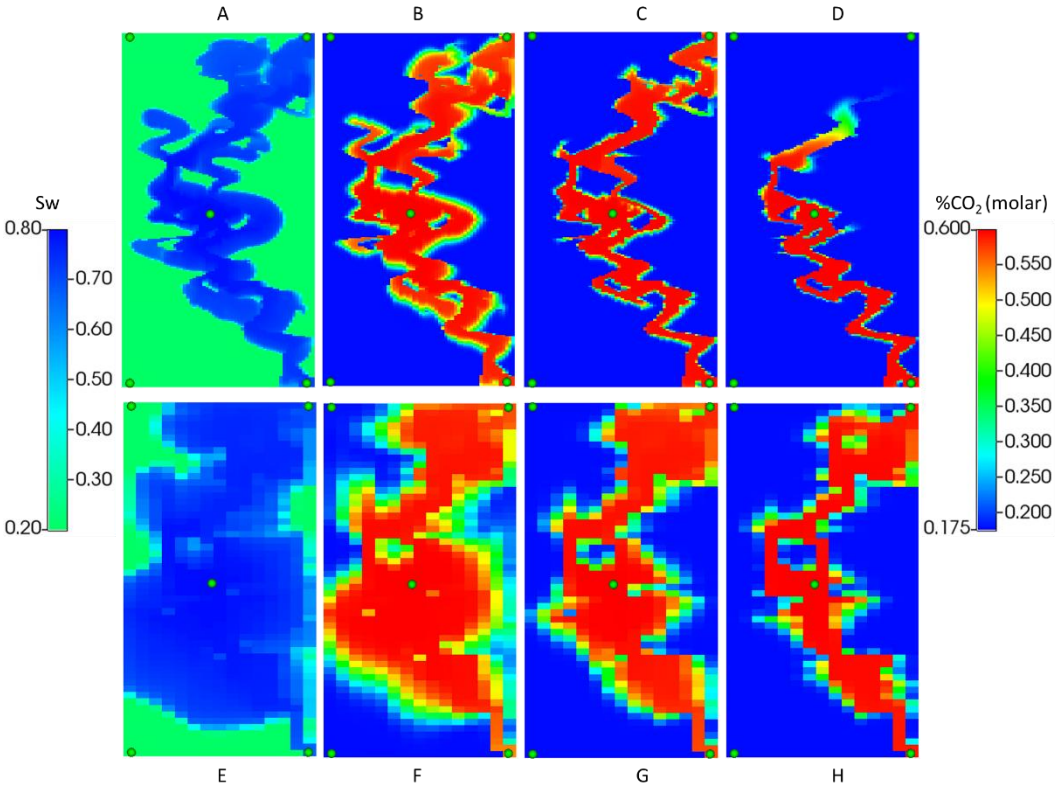

Figure 3. Channelized reservoir: A, B, C and D refer to fine-scale; E, F, G and H refer to coarse-scale. A and E are water saturation; B and F are CO_2-molar fraction for VR 1; C and G are CO_2-molar fraction for VR 7.5; D and H are CO_2-molar fraction for VR 75.

Performing the same comparisons for the channelized reservoir, a new set of observations is found. Comparing the fine- and coarse-scale maps presented in Figure 3, we can generally observe that the coarse models overestimate the sweep efficiency. This statement is valid even for the matched viscosity water flooding evaluation. It becomes even more intense for the miscible gas flooding cases. Nevertheless, the injected fluid flows through the high permeability preferential pathways regardless of the fluid nature and VR. Although the considerations regarding the compositional effects are also valid, in such a channelized system, the heterogeneity representation is the most critical issue, despite the dynamic evaluation to be performed.

In summary, from the dynamic evaluations and the discussions on the motivational case-studies, we can highlight the following aspects:

1) Even when the permeability upscaling is trivial, the capability of a coarse-scale model to represent the fine-scale behavior is highly dependent on the dynamic evaluation to be performed. Both the nature of the injected fluid and the

viscosity ratio can impact the coarse-scale representation of small-scale phenomena.

2) For highly heterogeneous systems, such as the channelized case, some areas in the reservoir tend to concentrate the flow. These regions are usually smoothed in the upscaling process, which makes the coarse-scale model overestimate the sweep efficiency of the injected fluid.
3) Miscible gas flooding processes are particularly challenging. First, the gas viscosity is usually much lower than the oil viscosity, which leads the development of viscous fingering. Also, the injected gas and the reservoir oil, under miscible conditions, always form a single-phase fluid. Thus, the use of pseudo-relative permeability is useless for the improvement of the coarse-scale responses.
4) The evaluation of immiscible displacement with a stable condition is a simple and effective procedure to investigate the permeability upscaling impact on the coarse-scale results. This statement was verified with the two motivational cases. For the homogeneous reservoir, this exercise confirmed the expectation that permeability upscaling was not an issue. However, the upscaled results for the channelized case were optimistic even for the stable flow evaluation, which means that the permeability representation is critical on the coarse model.

It is important to note that although several upscaling solutions have been proposed in the last decades, dealing with the upscaling of highly heterogeneous reservoirs and miscible displacements remains a challenge. Therefore, overcoming these limitations becomes the main concern of this thesis.

Additionally, in the Brazilian oil and gas production scenario, the oil fields located in the pre-salt area of Santos Basin are already the main hydrocarbon producers and represent the future of Brazilian production. The first pre-salt discovery occurred in 2006, with oil production starting in 2010. Despite its short development period, production already exceeded 1.5 million barrels of oil per day in 2018, with more than 20 platforms in operation. This mark surpassed production in the United Kingdom or in Oman, each with an average production of 1.0 million barrels of oil per day in 2017 (Petrobras-Blog Fatos e Dados, 2018).

Therefore, considering the increased importance of pre-salt oil fields in the upcoming years, production forecast for the pre-salt fields must be accurately obtained from rigorous simulation models with critical implications in the field development plans. Therefore, the building of effective simulation models becomes mandatory, which is only possible with

consistent upscaling techniques. Notwithstanding, it is highlighted that some of the biggest pre-salt oil fields consist of highly heterogeneous carbonate reservoirs requiring the reinjection of CO_2-rich gas. These factors strengthen the motivation for our work towards developing robust upscaling techniques, which are the main subjects of the upcoming chapters.

1.2 Objectives

This research is geared towards the development of new techniques involving fluid and rock characterization for the upscaling from fine to coarse-scale models. We propose methodologies that cover some critical gaps still present in the upscaling literature.

To fulfill such important task, we establish the following specific objectives:

- develop a consistent and cost-effective upscaling procedure for highly heterogeneous reservoirs, enabling the coarse-scale simulation models to properly represent the main reservoir heterogeneities and possible channels;
- generate a robust approach to overcome the challenging limitations of the representation of compositional miscible CO_2-rich gas injection in coarse-scale simulation models.

We also have two additional objectives:

- propose a practical and global procedure to guide the upscaling problem according to the most significant limitations in each case;
- provide an ensemble-level procedure for upscaling miscible gas flooding processes.

1.3 Structure and Description of the Thesis

This work is structured on eight scientific articles organized into two groups; six of them form the backbone of the thesis and are presented from Chapters 2 to 7, while two others are included in Appendices A and B to complement the research.

Articles 1 and 2 address the methodologies to deal with the upscaling challenges of miscible gas displacement and highly heterogeneous reservoirs, constituting the foundation of this work. In Article 3, we extend the compositional upscaling technique proposed in Article 1 for probabilistic applications. With Article 4, the DP/DP upscaling technique from Article 2 is expanded for field-scale 3D systems. For these problems, a near-well treatment is proposed to improve the profiles of production/injection wells. Then, Article 5 provides a general upscaling workflow to guide the selection of proper techniques according to limitations of each problem.

Finally, Article 6 applies the global upscaling workflow to miscible gas flooding and lays out a compilation of the previous works.

This section summarizes the six main articles in the thesis, detailing their contributions and links towards achieving the research objectives. The two complementary articles are also described in connection with the core of the research.

1.3.1 Article 1: New Upscaling Technique for Compositional Reservoir Simulations of Miscible Gas Injection

V.S. Rios, L.O.S. Santos, F.B. Quadros, D.J. Schiozer

Journal of Petroleum Science and Engineering, 2019, v. 175, p. 389–406

This article proposes a new compositional upscaling technique to overcome critical limitations related to the representation of miscible gas injection processes with coarse-scale simulation models. The main problems are associated with the difficulty in representing unstable flow and channeling on a coarse scale. The involved phenomena tend to disappear with the smoothing of the forward fronts and loss of resolution of the small-scale instabilities, which tends to create an optimistic bias on the production forecast.

The proposed methodology is applied in two steps: (1) an alternative fluid model is generated to deal with the compositional local equilibrium limitation; and (2) pseudo-relative permeability curves are used to better fit the simulated fine-scale model production curves. The new technique improves the coarse-scale results – production curves, sweep efficiency, and gas saturation map profile – in different scenarios of heterogeneity, well configuration, and flow velocities.

The use of a pseudo-fluid model to better represent the small-scale inefficiencies in a coarse-scale model is a key novelty of this study. This procedure enables a proper representation of the small-scale inefficiencies within a coarse grid block cell by reducing the local displacement efficiency due to the thermodynamic equilibrium under miscible conditions. We provide some additional comments regarding the generation of alternative equations of state for a group of experimental data in Appendix C.

The main contribution of this article to the thesis is to provide a robust and effective upscaling technique for miscible processes, which is useful to overcome Group 2 limitations on the global upscaling procedure that we propose in Article 5 and expand in Article 6. It is a continuation and evolution of Article 7, which is presented in Appendix A. In this article, we expand the discussions with the inclusion of new case-studies and additional evaluations.

1.3.2 Article 2: Upscaling Technique for Highly Heterogeneous Reservoirs Based on Flow and Storage Capacity, and Lorenz Coefficient

V.S. Rios, L.O.S. Santos, D.J. Schiozer

SPE Journal, 2020

This article presents a new dual-porosity dual-permeability (DP/DP) upscaling technique for highly heterogeneous reservoirs, inspired by Evazi and Jessen (2014). We apply classic reservoir engineering concepts (flow and storage capacity analysis and the Lorenz Coefficient) to the static properties of a fine-scale reference model to split the porous media into two levels: one representing the main flow regions – called primary system - and the other, the secondary flow regions – called secondary system. With the splitting of fine-scale cells, directional upscaling for permeability is performed for each group. This technique allows the adaptation of a fine highly heterogeneous geological model to a coarse-scale simulation model in a DP/DP approach and represents the main reservoir heterogeneities and possible preferential paths.

This work provides two significant improvements over other upscaling techniques, that result in: (1) less time-consumption to obtain coarse-scale models since no dynamic responses of fine-scale models are used; and (2) independence of the drainage plan or well flow rates of the fine-scale models.

The main contribution of this work to the thesis is the development of a consistent upscaling procedure to improve the coarse-scale representation of highly heterogeneous systems. This technique is the groundwork to overcome Group 1 limitations on the global upscaling procedure that we propose in Article 5.

1.3.3 Article 3: A Practical Probabilistic Upscaling Workflow for Compositional Reservoir Simulations of Miscible Gas Injection

Victor S. Rios, Vinicius S. Rios, L.O.S. Santos, D.J. Schiozer

Presented at the SPE Virtual Europec Conference, 1-3 Dec 2020

This article extends the compositional upscaling technique presented in Article 1 to be applied to multiple permeability realizations. The proposed workflow considers the Koval Factor, calculated for the fine-scale models, as a guide for selecting representative fine-scale models to train the pseudo-functions and improve the coarse-scale results. The approach also

uses the concept of splitting the porous media into primary and secondary systems, proposed in Article 2, to provide more flexibility to the distribution and creation of the pseudo-functions.

This work is motivated by the lack of practical ensemble-level upscaling procedures, in which the main goal is not a realization-by-realization agreement but an improved uncertainty quantification and representation of a group of models. Therefore, this article's main contribution to the thesis is to provide an effective ensemble-level upscaling and allow the two-step methodology proposed in Article 1 to be also useful for probabilistic studies.

1.3.4 Article 4: Improving Coarse-Scale Simulation Models with a Dual-Porosity Dual-Permeability Upscaling Technique and a Near-Well Approach

Victor de Souza Rios, Denis José Schiozer, Luiz O. S. dos Santos, Arne Skauge

Journal of Petroleum Science and Engineering, 2021, v. 198, March 2021, 108132

This article presents a continuation of Article 2. It focuses on improving the representation of small-scale heterogeneities in coarse models and expands the DP/DP upscaling technique to be applied to 3D highly heterogeneous porous media. As a new implementation to generalize the previously published approach, specific near-well treatment is considered to improve the overall flow distribution in the wells; with this procedure, the coarse model better represents the production and injection profiles throughout the wells. Therefore, the final coarse-scale model can represent the main reservoir heterogeneities and possible preferential pathways, while improving the definition of well productivity and injectivity indices.

Therefore, this work represents an evolution of the evolved upscaling procedure for highly heterogeneous reservoirs presented in Article 2 and is a key contribution to the thesis, since it enables the application of the DP/DP upscaling to complex field-scale reservoirs.

1.3.5 Article 5: A General Upscaling Workflow Applied to Highly Detailed Heterogeneous Reservoirs Under Near-Miscible WAG flood

Victor de Souza Rios, Arne Skauge, Ken Sorbie, Gang Wang, Denis José Schiozer, Luiz O. S. dos Santos

To be submitted to a peer-reviewed journal

This work represents a new contribution to the upscaling literature, since it provides a practical global procedure to guide the upscaling process to be conducted according to the most critical limitations of each problem. This article proposes a stepwise workflow to deal

with the upscaling problems consistently, guiding the improvement of the coarse-scale models according to the problem limitations, which can be generically divided into two groups: (Group 1) static modeling limitations; and (Group 2) flow-dynamics specifics.

Accordingly, the upscaling techniques proposed in the previous articles are important allies to overcome Group 1 (Articles 2 and 4) and Group 2 (Article 1) limitations. Nevertheless, by following the general upscaling workflow steps, the required effort to improve the coarse-scale results can be geared towards the actual key issues of each problem.

1.3.6 Article 6: Differences in the Upscaling Procedure for Compositional Reservoir Simulations of Immiscible and Miscible Gas Flooding

Victor de Souza Rios, Arne Skauge, Ken Sorbie, Gang Wang, Denis José Schiozer, Luiz O. S. dos Santos

To be presented at SPE Reservoir Simulation Conference held in Galveston, Texas, USA, 4-6 Oct 2021

This article presents an application of the general upscaling workflow proposed in Article 5 to immiscible and miscible gas flooding displacements. Additionally, it explores the differences between immiscible and miscible processes from the upscaling point of view.

For immiscible displacement situations, accurate results can be obtained with the coarse models, after a proper permeability upscaling procedure and use of pseudo-relative permeability curves to improve the dynamic responses. Miscible displacements, however, require a specific treatment of the fluid modeling process to overcome the limitations arising from the thermodynamic equilibrium assumption. For all situations, the workflow proposed in Article 5 can lead to a robust choice of techniques to satisfactorily improve the coarse-scale simulation results.

In this work, the results of Articles 1, 2, 4 and 5 are directly applied and tested in challenging highly refined case-studies. For this reason, one important result of this study to the thesis is that it summarizes some of the main contributions of the previous work and highlights the links between them.

1.3.7 Article 7: Methodology to Improve Miscible Gas Injection Forecast Based on a Field Scale Simulation Model

V.S. Rios, L.O.S. Santos, F.B. Quadros, R. Lykawka, D.J. Schiozer

Presented at the Offshore Technology Conference Brasil held in Rio de Janeiro, Brazil, 24–26 October 2017

This article is the foundation for the research performed in Article 1. It presents the two-step methodology for the compositional upscaling of miscible gas flooding processes for the first time. This work is placed in Appendix A, since Article 1 expands the studies and provides a deeper discussion on the problem with additional case studies and applications. Nevertheless, this work provides significant value to the thesis, thus becoming a complementary article.

1.3.8 Article 8: Practical Workflow to Improve Numerical Performance in Time-Consuming Reservoir Simulation Models Using Submodels and Shorter Period of Time

V.S. Rios, Avansi, G. D., D.J. Schiozer

Journal of Petroleum Science and Engineering, v. 195, December 2020, 107547

This article proposes a practical workflow to improve the numerical performance of reservoir simulation models. It indirectly relates to the overall objectives of the upscaling problems since it may significantly contribute to the performance enhancements of complex models. The proposed procedure is simple and can provide remarkable results in enhancing the numerical performance of such models.

This work is added as an appendix to the thesis, because the search for numerical performance is one of the main reasons we need to work with coarse-scale models. Consequently, a workflow that helps with this task is an important contribution for reservoir engineering daily activities.

2 ARTICLE 1: NEW UPSCALING TECHNIQUE FOR COMPOSITIONAL RESERVOIR SIMULATIONS OF MISCIBLE GAS INJECTION

V.S. Rios, L.O.S. Santos, F.B. Quadros, D.J. Schiozer

Journal of Petroleum Science and Engineering, 2019, v. 175, p. 389–406

Abstract

The use of compositional reservoir simulation is necessary to better represent the physical phenomena associated with enhanced oil recovery methods, particularly with miscible or near-miscible gas injection processes. However, upscaling of the geological fine model is required because computational costs can make it unpractical to perform compositional simulations in fine-scale models. Therefore, upscaling of fine-scale geological models is important and the use of coarse-scale models in reservoir simulation is necessary to reduce computational time. However, it can degenerate results due to loss of resolution of the small-scale phenomena, averaging of sub-grid heterogeneity and numerical dispersion, especially in oil fields where miscible gas is injected, continuously or alternatively with water (WAG).

In black oil simulations, errors of the upscaling process are usually mitigated with the use of pseudo relative permeability curves when two-phase immiscible displacement is considered. In compositional reservoir simulation of miscible gas injection, the interaction between thermodynamic phase behavior and the sub-grid heterogeneities significantly increase the challenge of the upscaling procedures.

This work presents a new technique for a robust upscaling of compositional displacements allowing a better representation of the small-scale results when miscible gas injection is considered, as in cases in which the produced gas is partially or totally reinjected in the reservoir. It can be applied in any compositional simulator with no need to adapt any transport coefficient or to use dual porosity dual permeability models, thus providing a flexible and computationally efficient approach.

The proposed technique is based on employing an alternative fluid model with a pseudo minimum miscibility pressure (PMMP) above experimental values, in order to ensure an immiscible displacement. This solution does not violate the phase behavior and ensures formation of two hydrocarbon phases in the reservoir. Therefore, the gas relative permeability plays a role on the simulation results and can be used for an improved fit of the fine model production curves. The technique is applied in two steps, first an alternative fluid model is generated and then pseudo relative permeability curves are used to better fit the production curves.

In this study, problems that occur when upscaling is applied in fields with miscible gas injection were investigated. We show that the proposed technique can significantly improve the coarse-scale results – production curves, sweep efficiency and gas saturation map profile - in different scenarios of heterogeneity. Three case studies were evaluated and compared with the standard

static upscaling processes. Additionally, we show improvements in the production curve results and physical representation of gas injection behavior.

Introduction

Miscible gas injection is an effective enhanced oil recovery method and has gained special attention recently, especially after the pre-salt oil fields discoveries. This method can improve oil production due to the formation of a miscible front, but field scale representation is challenging since several small-scale phenomena are smoothed in the simulation grid.

In this context, the highlight is the formation of an unstable front, known as viscous fingers, and the channeling effect, which happens due to permeability contrasts in heterogeneous environments. Several authors have studied the mechanisms and solutions for the representation of these phenomena.

Wagoner et al. (1991) evaluated, for different degrees of heterogeneity measured by the Dykstra-Parson index, whether a given flow condition would be dominated by viscous fingers, dispersion, or channeling. Araktingi & Orr (1993) studied the dominance conditions between viscous fingers and channeling. Additionally, these authors proposed a heterogeneity index capable of evaluating the dominant process.

Haajizadeh et al. (2000) showed that an optimal configuration may exist for the grid block size of simulation model that allows for partially canceling errors associated with the loss of smaller scale heterogeneities. The authors also emphasize that the simulations in coarse meshes present a large numerical dispersion, which softens the forward front, masking the viscous fingers. On the other hand, refining the grid without refining the geological discretization potentiates grid orientation effects.

Many authors studied problems related to grid discretization in cases of unstable flow. Sajjadi & Azaiez (2006) evaluated the unstable flow in thermal processes in which the miscible front propagates faster than the thermal front due to the formation of viscous fingers. Doorwar and Mohanty (2015) proposed a methodology for grouping the fingers observed in small scale into a single finger that would represent the total set and thus would correct the final recovery estimates. Lou et al. (2016) studied the representation of viscous fingers in cases of water injection in viscous oil. In this work, the authors proposed a correlation to estimate parameters to be incorporated in the simulation with the objective of better representing the recovery obtained for different speeds of exploitation.

Other authors proposed methodologies for better representing small-scale results in coarse-scale simulation models. Backer and Fayers (1994) developed the method of transport

coefficients (also known as α-factors), which consists in modifiers introduced in the flow terms to relate compositions of the fluids flowing out of a large grid block to the average compositions of those fluids within the grid block. Together with the use of pseudo relative permeability curves, they tested the method for various fluid systems with improved accuracy in the results, especially in terms of component production rates for the cases considered. Christie and Clifford (1998) also used the α-factor approach, but they used streamline techniques to generate a fine-scale solution. However, no pseudo-relative curves were used, because they only considered single-phase flow problems.

Coats el al. (2004) used another type of study, which considers modeling residual oil saturation in miscible and immiscible gas flooding. In these techniques, an amount of oil is bypassed and excluded from the flash calculations but responds to pressure changes. This method has an important disadvantage since no mass flux is allowed between the bypassed residual oil and the flowing fractions.

Evazi and Jessen (2014) developed a technique, for highly heterogeneous reservoirs, in which the pore space is arranged into two levels of porosity based on fine-scale streamline information, and a dual-porosity dual-permeability (DP/DP) flow model is adapted to simulate the coarse-scale model. They demonstrated that DP/DP coarse-models predict the breakthrough time accurately and are less sensitive to the level of upscaling, compared to conventional single-porosity upscaling. However, the DP/DP model may be too time-consuming to be considered in field scale applications.

Li (2014, 2016) have extended the method of transport coefficient to include treatment of near-well upscaling. These techniques, however, increase the simulation time due to the calculation of the coefficients. Iranshahr et al. (2014) developed a new compositional upscaling formulation, considering the system to be out of thermodynamic equilibrium on the coarse-scale models. They introduced the use of upscaled functions to reproduce this effect. This approach was extended by Salehi (2013, 2016), introducing a physical non-equilibrium term for the local thermodynamic constraints, which was also converted to a transport coefficient similar to the α-factors. These approaches allowed the coarse-simulation results to better represent the small-scale curves and component rates, but with an impact on the simulation time.

An initial validation of the methodology was presented by Rios et al. (2017). In this work we focused on describing the methodology in more details and capturing new reservoir geological features to prove the versatility and robustness of the technique. We first present the problem and the details regarding upscaling of compositional simulation of miscible gas

injection. After that, the case studies are described. The technique is applied in three cases: two 2D models and one 3D, based on the SPE10 problem (Christie and Blunt, 2001). The first 2D case study was also presented by Rios et al. (2017) and the other two are new applications to show the robustness of the technique in different complexity level for simulation models. Then, the simulation results and some important numerical aspects of the simulations are discussed. Finally, the main results and contributions of this work are summarized in the conclusion.

The Problem and Methodology

In the management of an oil field, it is common to create a refined model to properly represent the main reservoir heterogeneities. However, to evaluate the dynamic behavior, it is usual to perform upscaling for a geocellular model with a reduced number of cells, thus enabling the reservoir flow simulation to run in a time compatible with the needs of the industry. In order to show the effect of this upscaling in the simulation flow and to discuss the problem we aim at solving in this work, we first created a refined model constructed with cells of 5 x 5 m² and average thickness of approximately 0.5 m. The first upscaling was performed only vertically, resulting in average thicknesses of approximately 1.7 m and preserving the remaining dimensions in 5 x 5 m². After that, we performed an upscale in the horizontal direction to achieve the 100 x 100 m^2 industry standard.

Our first concern was to evaluate the impact of permeability upscaling method. For this purpose, three methods were considered: averaging, which considers arithmetic average horizontally and harmonic average vertically, Cardwell-Parsons directional averaging method (Cardwell and Parsons, 1945) and flow-based upscaling with closed boundary conditions (Kumar et al., 1997).

In this analysis, we compared the refined model, shown in the first image of Figure 1 to the upscaled model with 100 x 100 m² considering each one of the above-mentioned methods. To investigate the dynamic response, a pair of wells was diagonally placed in the reservoir and two different recovery methods were conducted keeping the reservoir pressure at the original level: water injection and first contact miscible gas injection. For the latter, we used a seven-pseudo-component fluid model – the same fluid model presented by Rios et al. (2017) - injecting CO_2-rich miscible gas. Table 1 highlights the parameters used in the Peng-Robinson (PR) equation of state (EoS), while Table 2 shows the binary interaction coefficients.

When water is continuously injected, all the upscaling methods presented similar results. Besides that, the upscaled models presented closer results when compared to the fine scale reference model. These comparisons can be visualized in Figure 2. On the other hand, for

miscible gas injection, even though the upscaling methods presented almost the same results for the coarse scale models, the oil recovery in the fine scale model was considerably smaller, as shown in Figure 3.

Since the upscaling methods provided similar results, we used the flow-based upscaling technique with closed boundary conditions for all the subsequent analysis. Further comparisons on permeability upscale methods were performed by Shehata et al, 2012.

Figures 2 and 3 also suggest that, in case of miscible gas injection, another issue arises. These Figures indicate that for the same static models, water injection presented similar results when comparing coarse and fine scale modes. On the other hand, for miscible gas injection, the coarse scale models overestimated the recovery.

In order to better highlight the problem, further upscaling of the fine model, using flow-based upscaling technique with closed boundary conditions, were made to grids sizes of 10 x 10 m², 50 x 50 m², and the already mentioned 100 x 100 m² (final simulation grid block size) cells, maintaining the mean vertical thickness of 1.7 m.

In order to study the phenomenon associated with miscible gas injection, a single layer representative of a stratigraphic subzone with different levels of refinement was considered. Therefore, we first analyzed the 2D effects. Figure 1 shows the permeability maps for the four different levels of refinement used, highlighting the smoothening of the heterogeneity with the upscaling process (Rios, et al. (2017)).

In each of the four models, a pair of wells was considered, and first contact miscible gas injection was performed. For this purpose, the seven-pseudo-component fluid model highlighted in Tables 1 and 2 was also considered.

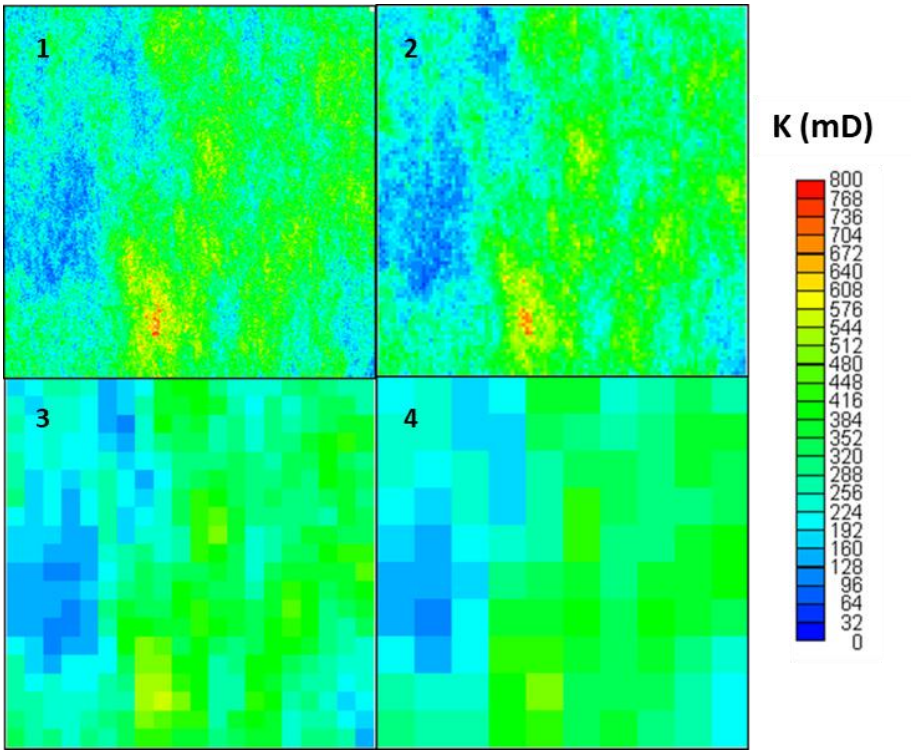

Figure 1. Absolute permeability map with emphasis on the different scales of the reservoir model and the associated loss of heterogeneity. In the figure, we have cell sizes of (1) 5 x 5 m², (2) 10 x 10 m², (3) 50 x 50 m² and (4) 100 x 100 m². Rios et al. (2017)

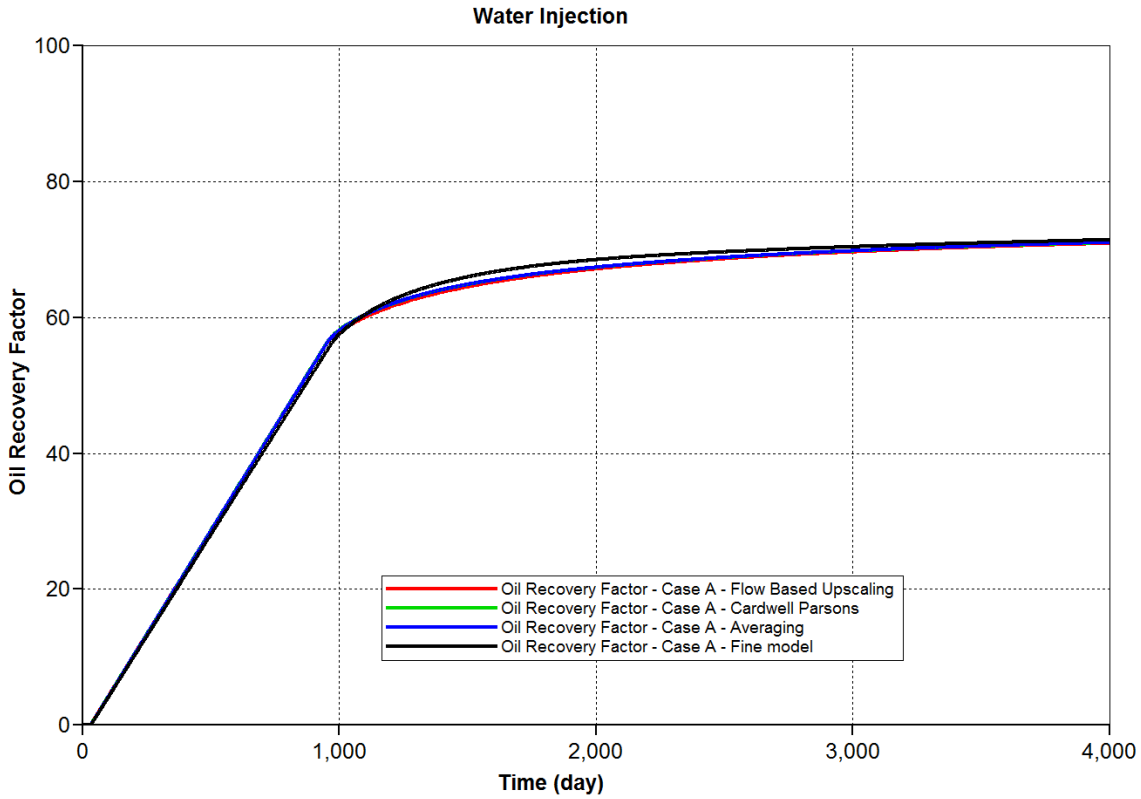

Figure 2. Oil recovery factor behavior with water injection considering the fine scale model and the upscaled coarse models with three different upscaling methods

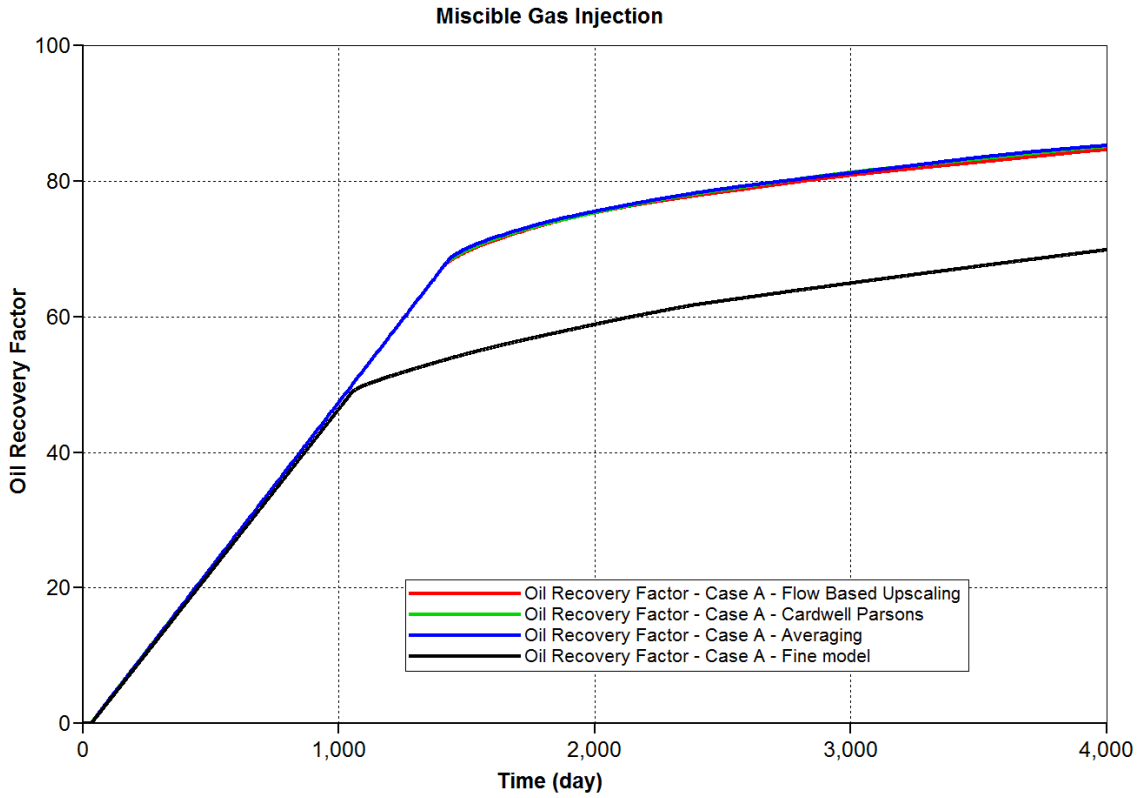

Figure 3. Oil recovery factor behavior with miscible gas injection considering the fine scale model and the upscaled coarse models with three different upscaling methods

Table 1. Parameters of the equation of state for a miscible fit - Peng-Robinson

	P_c(MPa)	T_c(K)	ω	MW	Vshift
PC1	7.38	304.2	0.23	44.0	-0.0718
PC2	4.59	190.2	0.01	16.1	0.0468
PC3	3.42	369.0	0.20	36.8	0.0282
PC4	2.40	614.9	0.51	168.2	0.0075
PC5	1.82	778.5	0.72	241.1	-0.0053
PC6	1.09	796.7	1.18	363.5	0.1956
PC7	0.71	1078.1	1.33	785.3	0.1741

Table 2. Binary interaction coefficients for a miscible fit

PC1	0						
PC2	0.15	0					
PC3	0.16	0.03	0				
PC4	0.15	0.07	0	0			
PC5	0.13	0.09	0	0	0		
PC6	0.09	0.12	0	0	0	0	
PC7	0.02	0.16	0	0	0	0	0

Evaluating the injection of CO_2-rich gas, the injection well is positioned in the lower left corner and producer in the upper right corner. It is possible to visualize the importance of a robust upscaling technique for compositional reservoir simulation of miscible process.

Figure 4 shows the four simulated cases of miscible gas injection for the different levels of refinement. It is observed that there is significant difference in the results. Furthermore, the coarser meshes, with smoothened small-scale phenomena and sub-grid heterogeneity, tend to increase the sweep efficiency and overestimate the final recovery (more optimistic results). Figure 3 shows saturation maps for the four simulated cases. This figure indicates viscous finger effects acting strongly on the fine-scale miscible injection.

Figures 4 and 5 show the importance of small-scale phenomena and the upscaling process on the smoothening of the miscible gas injection front. In this case, the instability represented by the viscous fingering is lost as the model gets coarser and, consequently, the oil recovery is overestimated in the coarser models.

Computational time can make fine-scale simulation models impossible to be used for production forecast and all the analyses performed during an oil field development plan and production life. Although the coarse-scale models have several limitations, they are also needed for compositional reservoir simulation, particularly when miscible gas injection is applied to large oil fields.

One important step for an effective technique to improve these upscaling results is a proper understanding of the small-scale results and their physical behavior before considering the coarse-scale in which compositional simulations runs are performed. In order to make meaningful comparisons, the fine-grid gas saturation is averaged over the corresponding coarse grid, as shown in Figure 6.

As it can be observed in Figure 6, gas saturation map in fine-scale model presents only values 0 or 1, due to the first contact miscible displacement. However, when this map is averaged to the coarse-scale, gas saturation values vary between 0 and 1. Thus, the resulting gas saturation map is more likely to represent an immiscible displacement than a first contact miscible process in the coarse-scale. Therefore, for an effective upscaling process, coarse-scale simulation runs need to reproduce this gas saturation variation. Furthermore, standard static upscaling alone cannot be considered when compositional simulations need to be performed. It is necessary to work on dynamic compositional upscaling techniques to better represent the coarse-scale model results.

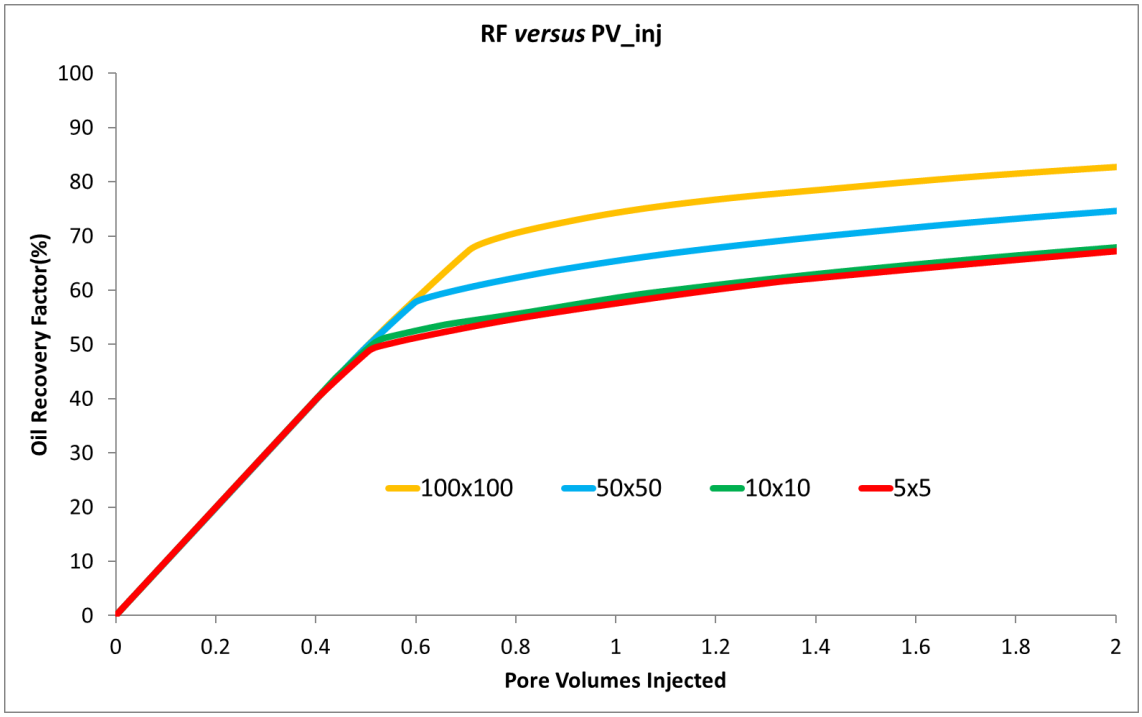

Figure 4. Recovery factor versus pore volumes injected for the case of CO_2-rich gas injection. Rios et al. (2017)

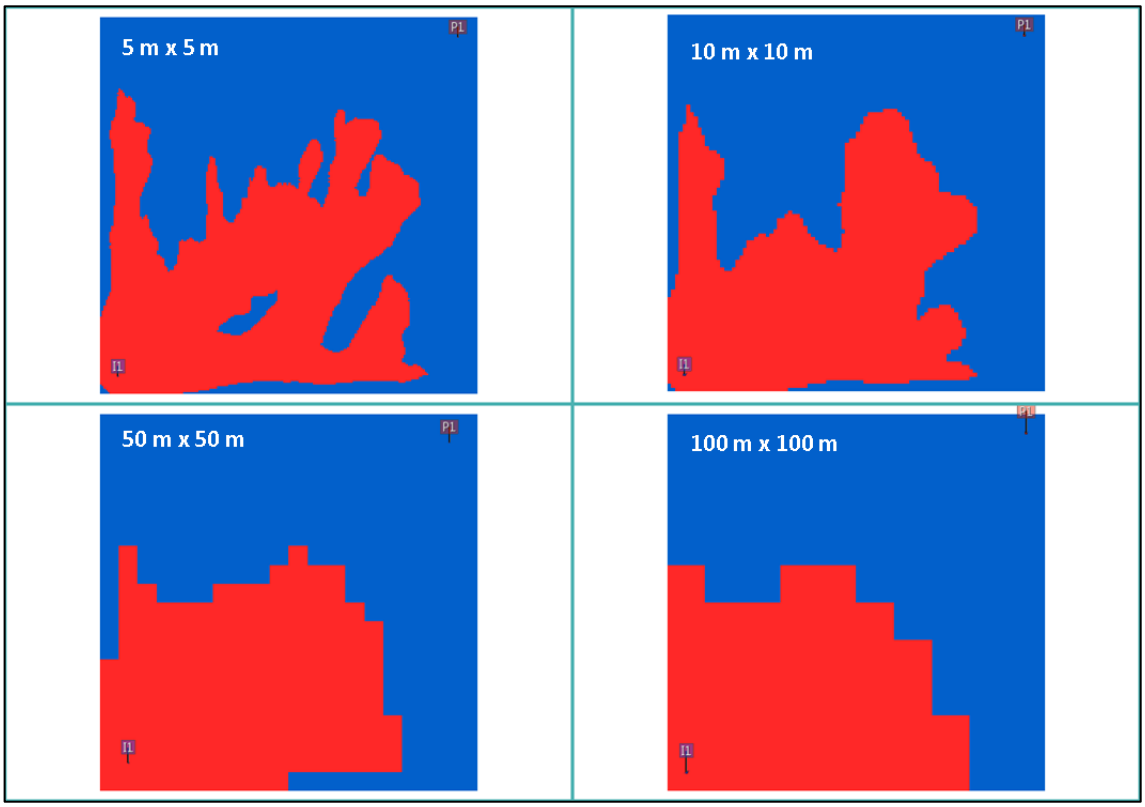

Figure 5. Behavior of the miscible gas front in different refinement levels, at the same simulation time. In red Sg = 1, while in blue, Sg = 0. Rios et al. (2017)

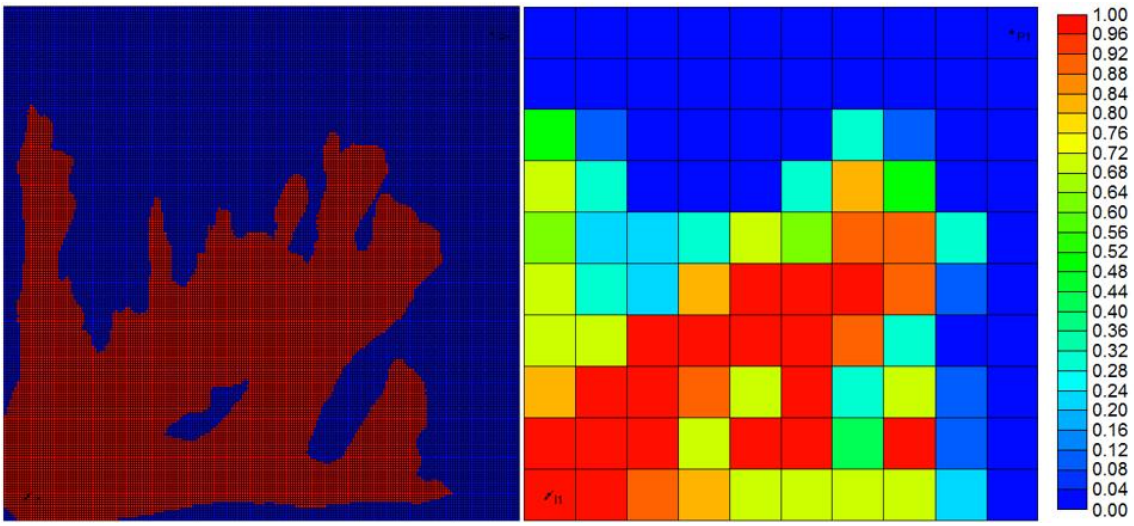

Figure 6. Behavior of the miscible gas front in the fine-scale and its equivalent, averaged over the coarse-scale.

Considering the above discussions, one important step to establish a robust compositional upscaling procedure for miscible gas injection is to reproduce the average immiscible behavior of the gas saturation front. For this purpose, to overcome and compensate the well-known limitations of coarser models, we propose a two-steps technique that allows the improvement of the coarse-scale simulation results, working on an alternative fluid model and on pseudo-relative permeability curves. The two steps are described and the entire procedure summarized in Figure 7:

1. Use of an alternative fluid model with a Pseudo Minimum Miscibility Pressure (PMMP) – Pseudo because it is not an experimentally obtained pressure, but based on a numerical approach - above the experimental values, with the pressure conditions evaluated in the simulations, in order to guarantee an immiscible displacement.
2. Generation of pseudo relative permeability curves (gas-oil in this case) as a history matching task.

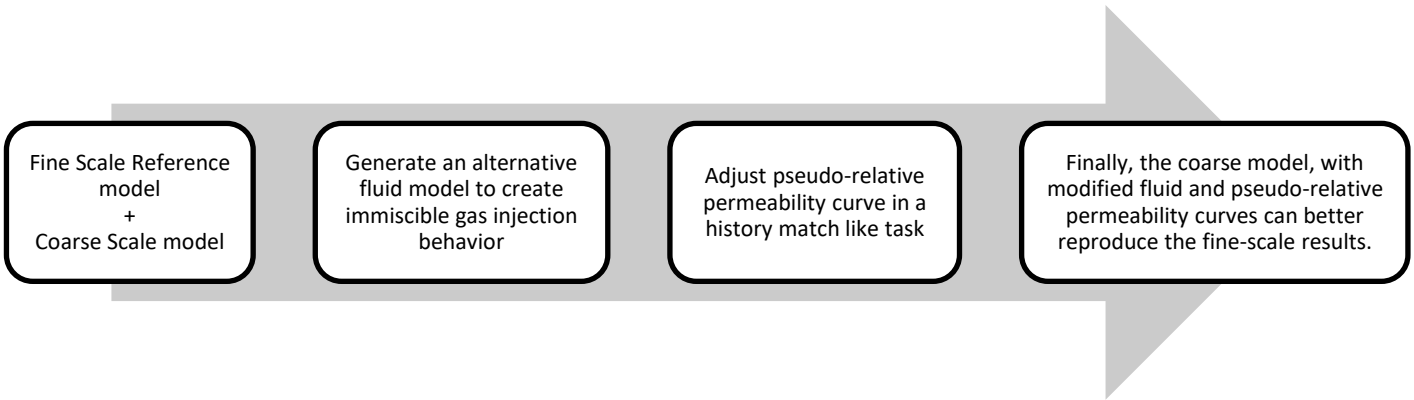

Figure 7. Proposed Methodology for improved coarse-scale simulation in a miscible gas injection process.

The first step of the proposed methodology is an important novelty of this work. When creating an alternative fluid model with immiscible behavior, not only the average gas saturation map physical representation is improved, but also it allows the gas-liquid relative permeability curves to become effective and the generation of pseudo-relative permeability plays an important role to better represent the reference fine scale results using a coarse model. It is also important to highlight that while the first step is unique for a reservoir fluid, the second one can vary depending on the upscaling ratio considered in the simulation model.

In the next sections, the case studies will be presented with the methodology applied to each case.

Case Studies Description

As mentioned earlier, three case studies are discussed in this work. The first one is the same reservoir model used as a motivation case in the previous section, first used by Rios et al. (2017), with a total area of 1000 x 1000 m². However, only two different refinement levels are considered, the 5 x 5 m² grid block size (fine-scale reference model) and the coarser one, which has cell size of 100 x 100 m². This case is referred as Case A and the absolute permeability maps for the two models are shown in Figure 8. One pair of wells is considered, and the injection rate is controlled to keep the pressure close to the original level of approximately 550 kgf/cm².

The second case, also 2D, is similar to the first one, but the reservoir is highly heterogeneous, with some channels in the fine-scale model. Again, the fine-scale reference model has cells with 5 x 5 m² and the coarse-scale model cells are 100 x 100 m². One pair of wells is considered, with the same strategy of Case A. This case is called Case B and Figure 9 shows the permeability maps for both models on this case.

The third case is a classical 3D reservoir model based on SPE10 problem (Christie and Blunt, 2001) and it is referred as Case C. Here, the fine-scale model cells are 6.096 x 3.048 x 0.6096 m³ and the coarse-scale cells have dimension of 30.48 x 15.24 x 3.048 m³. A five spot well scheme is considered with continuous miscible gas injection. Figure 10 shows the permeability maps for both models on this case.

For all the three cases, the original fluid model is the same as presented before, whose EoS parameters were shown in Tables 1 and 2. The injected gas is CO_2-rich with about 60% of CO_2 in molar basis, guaranteeing miscible displacement.

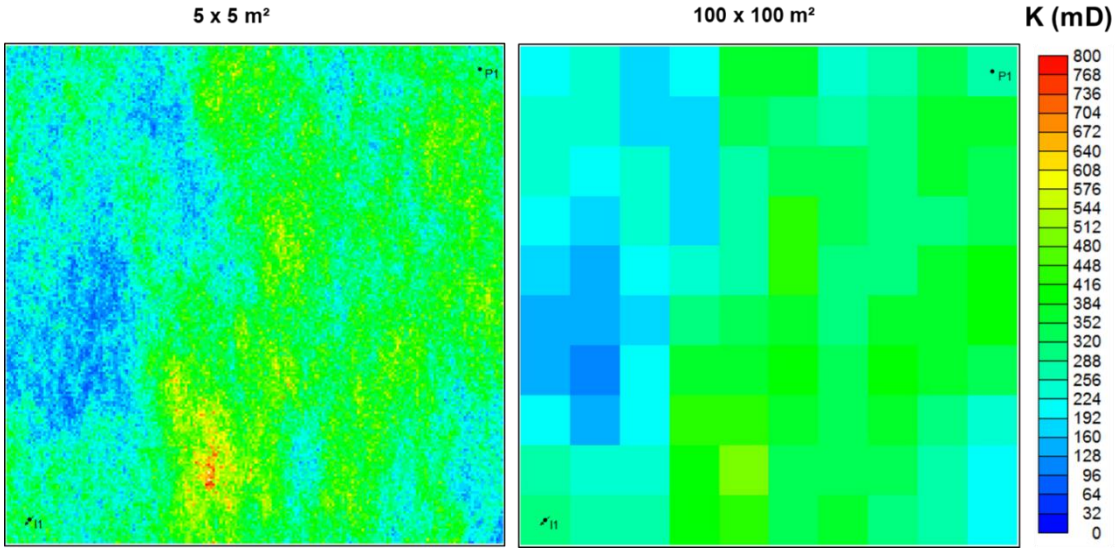

Figure 8. Absolute permeability maps for fine-scale and coarse-scale models in Case A. Rios et al. (2017).

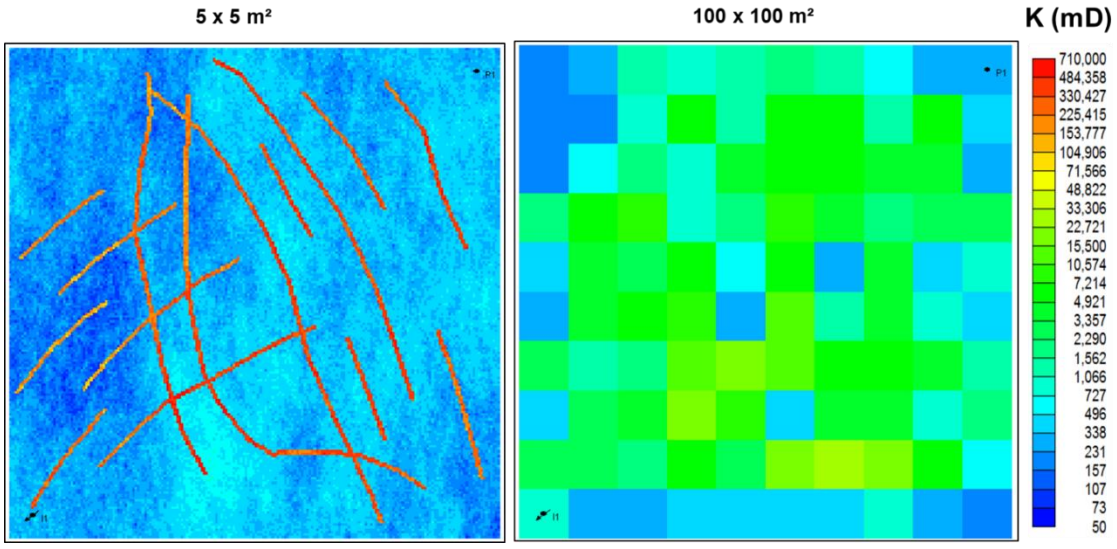

Figure 9. Absolute permeability maps for fine-scale and coarse-scale models in Case B.

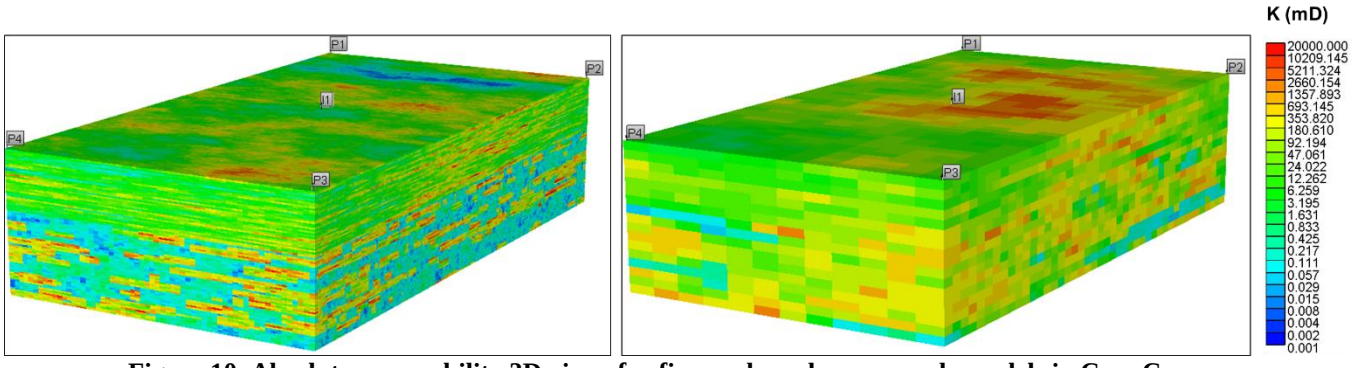

Figure 10. Absolute permeability 3D views for fine-scale and coarse-scale models in Case C.

Results and Discussions

The results are presented in two parts, showing each step of the proposed technique. Initially, the alternative fluid model generation is described. The equivalence between the

alternative fluid model and the original one is shown. Additionally, the desired difference in order to obtain an immiscible displacement behavior on the coarse-scale model is highlighted. This immiscible fluid model is used for all the three case studies in the first step of the technique. Then, the pseudo-relative permeability curves are adjusted, and the results are shown for each case separately.

Step 1 – Alternative Fluid Model Generation

The first stage to perform a robust upscaling of compositional reservoir simulation for miscible gas injection is to make the coarse-scale model reproduce the physical immiscible behavior of the average gas saturation map obtained from the fine-scale reference model (as shown in Figure 6). For that purpose, an alternative equation of state is generated aiming at reproducing an immiscible flow condition for the injected gas in the pressure range operated in the simulation runs. This approach is possible since the EoS adjustment procedure is an inverse problem and different equations can fit the same PVT experiments.

The EoS fitting process is performed with a commercial equation of state multiphase equilibrium and properties determination software package, which allows experimental data to be entered for regression purposes and uses an adaptive least-squares algorithm for the regression procedure. The objective function of the regression involves the solution of complex nonlinear equations such as flash and saturation-pressure calculations. It is possible to enter with a large number of experimental data and control the regression parameters to obtain a representative fit for the EoS.

In order to obtain the alternative immiscible equation, the same fitting procedure used for the original EoS is considered. However, it is recommended to change the binary interaction coefficients between the main gas component (CO_2, in our case) and the heaviest components before the regression. Higher values for these parameters will provide the new equation with an immiscible behavior, since the regression is performed varying the other regression parameters. For better understanding this new fluid model, it is important to check the miscible behavior of the new equation, as proposed by Rios et al., 2016.

Besides the better representation of the averaged reference gas saturation map, this alternative fluid model will allow the presence of gas and oil saturations on the grid block cells. This creates an opportunity to work on relative permeability curves and make the final arrangements to fit the fine-scale simulation results, which will be presented later as step 2. This procedure is commonly used in water injection cases, but cannot be applied directly in the original miscible fluid model due to the absence of two-phase equilibrium in the grid block cells

for these cases. This can be observed qualitatively on Figure 5, which presents only values 0 or 1 for the gas saturation.

Therefore, the proposed alternative fluid model presents a minimum miscibility pressure (MMP) above the experimental values and the pressure conditions evaluated in the simulations, with average of 550 kgf/cm², guaranteeing immiscible displacement behavior.

Under these conditions, there is a formation of two hydrocarbon phases. Thus, the saturations vary smoothly in the porous medium during the simulation period, i.e. the critical point is not achieved. Table 3 shows the parameters of the adjusted EoS to represent immiscible displacement, while Table 4 shows the binary interaction coefficients.

Table 3. Parameters of the state equation for immiscible fit - Peng-Robinson.

	P_c(MPa)	T_c(K)	ω	MW	Vshift
PC1	7.38	304.2	0.23	44.0	-0.0718
PC2	4.59	190.2	0.01	16.1	-0.0553
PC3	4.89	383.8	0.17	33.0	-0.03827
PC4	3.08	621.0	0.36	115.0	-0.01237
PC5	1.99	750.0	0.58	216.4	0.00133
PC6	1.23	780.0	1.21	386.8	0.02593
PC7	0.72	1149.7	1.35	991.5	0.04019

Table 4. Binary interaction coefficients for the immiscible fit.

PC1	0						
PC2	0.20	0					
PC3	0.19	0.01	0				
PC4	0.19	0.03	0	0			
PC5	0.19	0.04	0	0	0		
PC6	0.18	0.06	0	0	0	0	
PC7	0.18	0.09	0	0	0	0	0

The immiscible fluid model must be equivalent to the reference model in terms of the adjustment of the laboratory data, differing only in the miscibility behavior of the injected gas. Figure 11 shows the phase envelopes for the two adjustments of fluid models considered for two distinct compositions of the fluid in the reservoir. It can be seen that the shape and the critical point are very similar in both cases, which shows equivalence for both fitted models. Besides, Figure 12 summarize some PVT experiments and the results obtained with both fluid models. The results are in high accordance, as expected, since both EoS were fitted considering the same set of PVT data.

Additionally, to emphasize the equivalence between the fluid models, a consistency test was performed considering the Case A coarse model. The test consisted on simulating water injection and comparing the results with both fluid models, the original and the alternative one.

Figure 13 shows the total equivalence between the curves, as expected. It is important to highlight that the exact same results observed for the above consistency test are obtained with any other pair of models, changing only the fluid model.

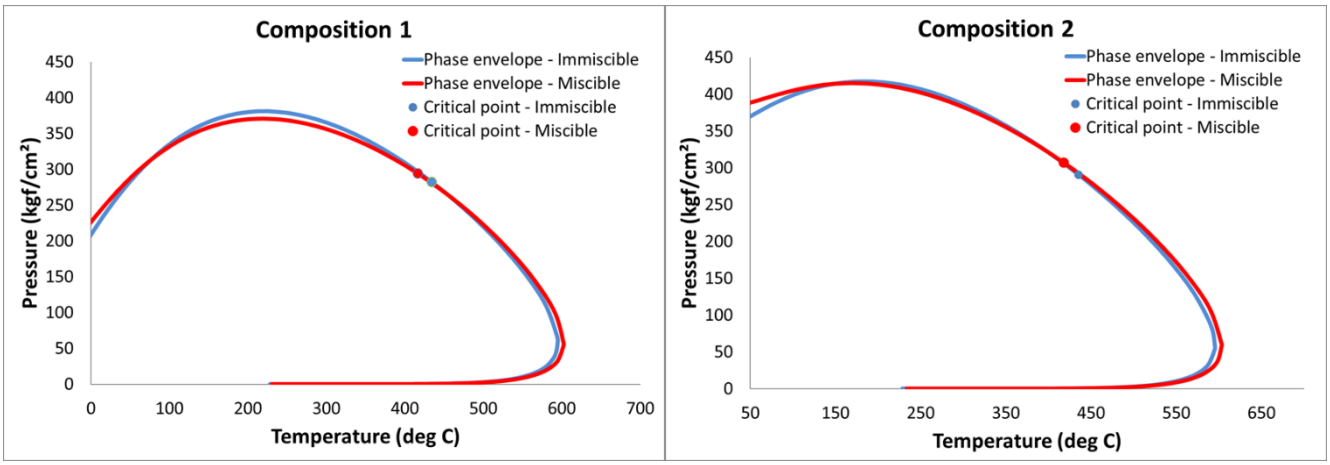

Figure 11. Phase envelope for the two fluid models analyzed with two different global compositions. Data in red refer to the miscible realization, while in blue, the immiscible. Rios et al. (2017).

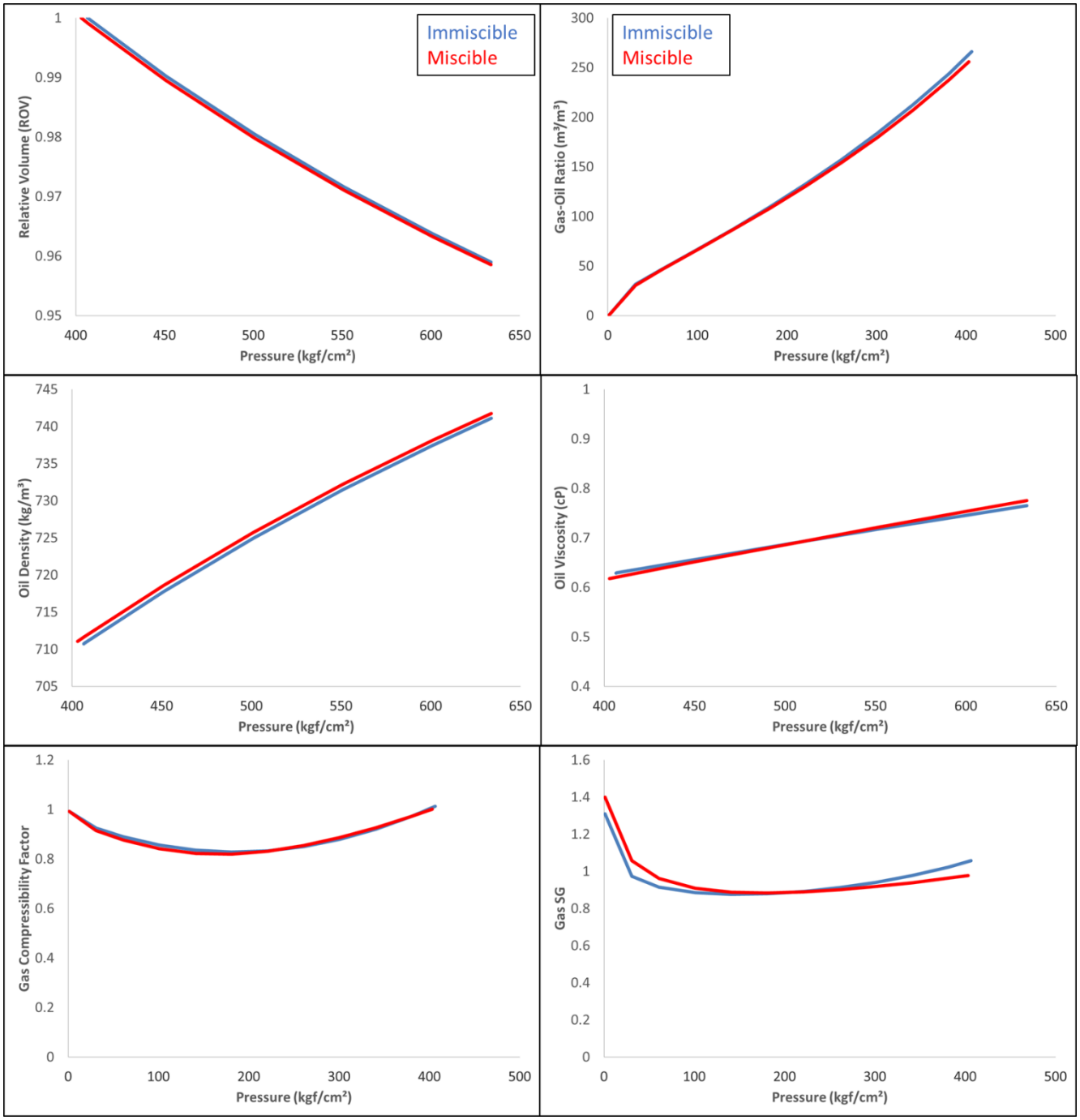

Figure 12. Comparison between original (miscible) and alternative (immiscible) fluid models in some PVT experiment simulations.

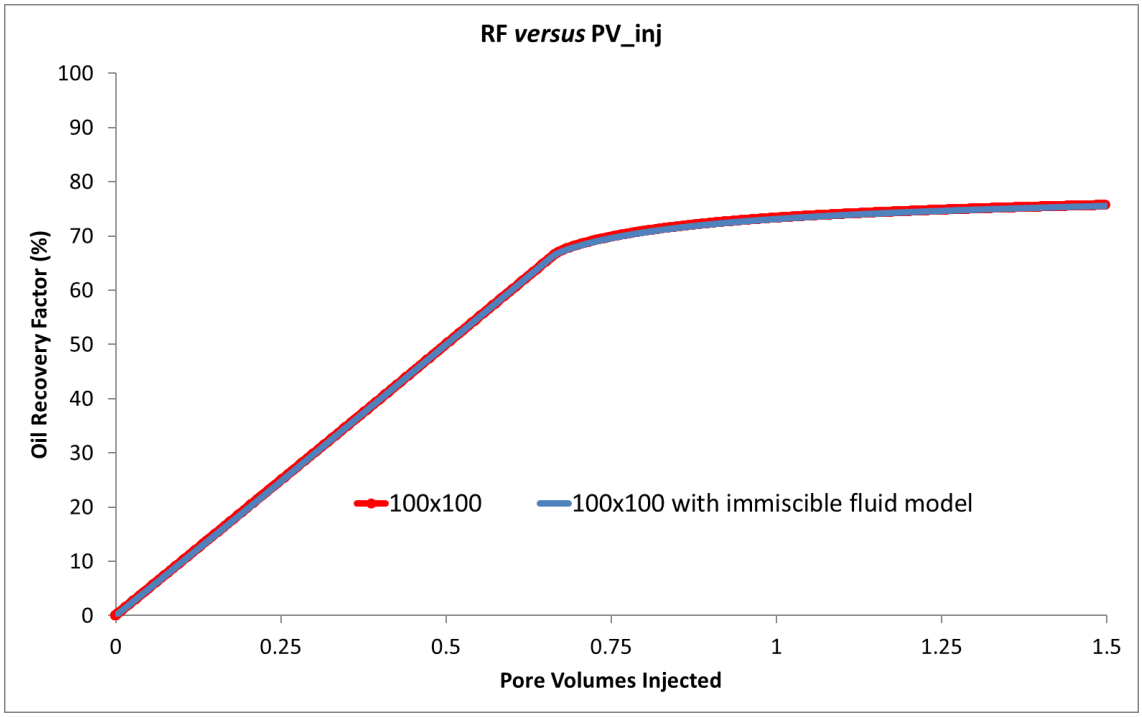

Figure 13. Oil recovery factor against injected pore volume of water for the coarse model in Case A with both, original and alternative (immiscible) fluid models. Adapted from Rios et al. (2017).

As previously mentioned, the fluid model with immiscible characteristics is a realization with the MMP higher than the experimental data and the pressure conditions of the reservoir during the production period. To show this observation, numerical evaluations were carried out reproducing the slimtube experiment, Rios et al. (2016).

There is no universally accepted method to define the MMP from slimtube experiments, but a widely adopted criterion for determining the MMP is the construction of a graph of oil recovery factor after the injection of 1.2 pore volumes (PV) of gas against the injection pressure. The MMP is the pressure value at which oil recovery factor reaches 90 to 95%.

Figures 14 shows the oil recovery factor curves after the injection of 1.2 PV of CO_2-rich gas at different pressures for miscible and immiscible fluid models, respectively.

It is observed that only the original adjustment presents MMP for the investigated pressure range, obtaining a characteristic recovery factor of slimtube miscibility between 430 and 500 kgf/cm². The immiscible case shows no miscible behavior in the evaluated range.

Once the alternative immiscible fluid model is obtained, it is possible to replace the original fluid model in each one of the cases to observe the impact and conclude the first step of the technique. Figures 15.a, 16.a and 17.a show the impact of this change on the fluid model for the cases A, B and C respectively. In these figures, the following oil recovery factor curves

are compared: (i) the coarse models with miscible fluid model (yellow curve), (ii) the coarse model with immiscible fluid model (dashed black curve), and (iii) the fine-scale reference model with miscible fluid model (red curve).

Thus, the alteration of the fluid model has already allowed a greater approximation between the recoveries of the coarse and refined models in all the three case studies. It is observed, however, that there is still a difference subject to improvement. Considering that the coarse case now presents two-phase flow in the reservoir, adjusting the gas-oil relative permeability curve, it is possible to reproduce satisfactorily the recovery behavior observed in the refined reference model. This is the second step of the proposed technique.

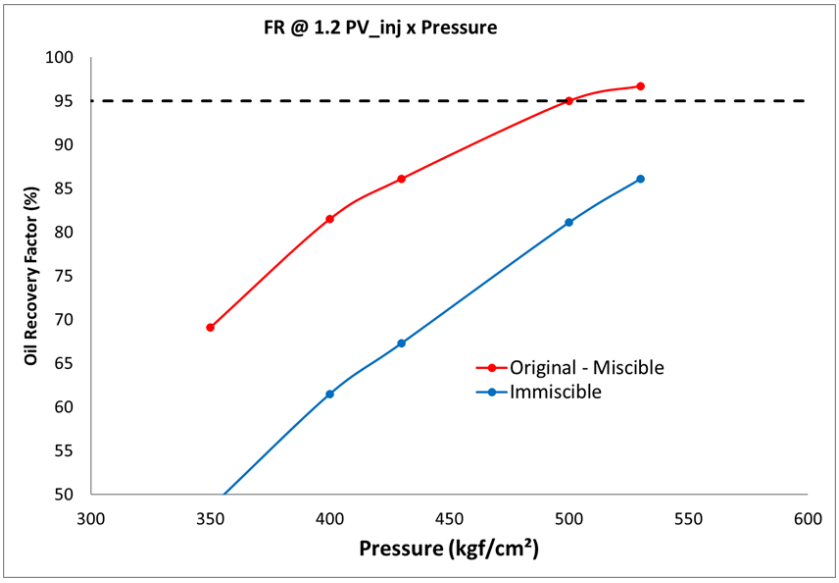

Figure 14. Oil recovery factor versus pressure after 1.2 PV injected gas for miscible gas and immiscible adjustment. Adapted from Rios et al. (2017).

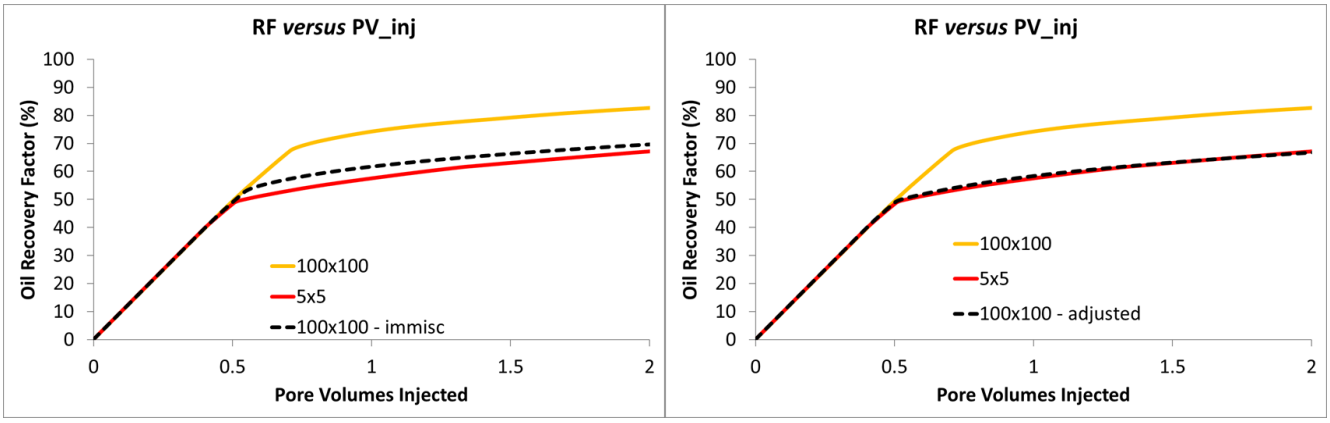

(a) **(b)**

Figure 15. Oil recovery factor versus injected pore volume of gas for Case A with coarse model (miscible and immiscible) and refined model: (a) immiscible without pseudo kr adjustment (b) immiscible adjusted. Adapted from Rios et al. (2017).

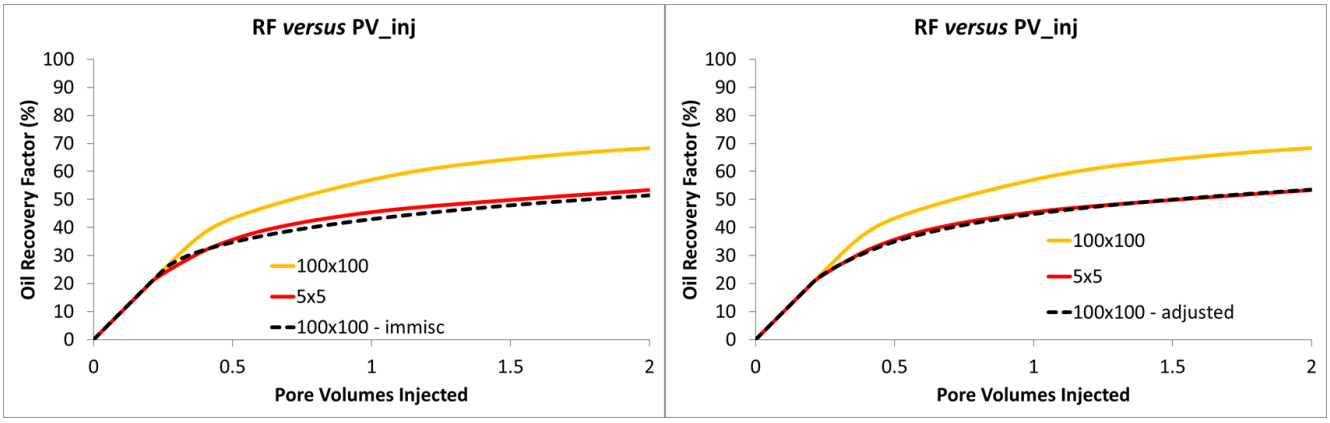

(a) **(b)**

Figure 16. Oil recovery factor versus injected pore volume of gas for Case B with coarse model (miscible and immiscible) and refined model: (a) immiscible without pseudo kr adjustment (b) immiscible adjusted.

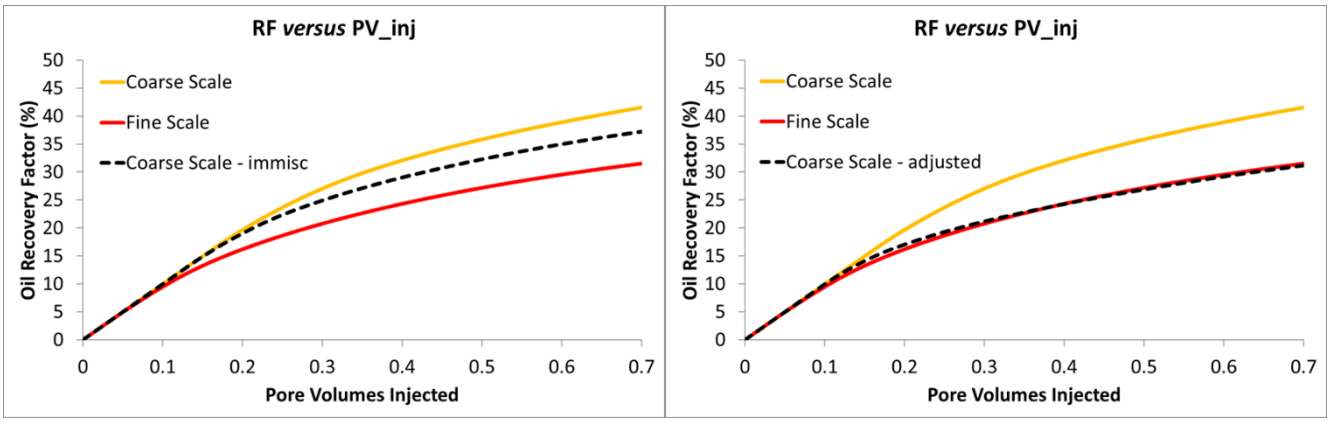

(a) **(b)**

Figure 17. Oil recovery factor versus injected pore volume of gas for Case C with coarse model (miscible and immiscible) and refined model: (a) immiscible without pseudo kr adjustment (b) immiscible adjusted.

Step 2 – Pseudo-Relative Permeability Adjustment

The first step of this new technique presents two important contributions for a robust and effective upscaling procedure in compositional simulation of miscible gas injection cases: it makes the gas saturation behavior more representative of the fine-scale averaged gas saturation map and allows acting on pseudo-relative permeability curves in order to better reproduce production curves using coarse-scale simulation models.

The stage of adjusting pseudo-relative permeability curves (gas-oil in this case because it is only gas injection in oil reservoir) is equivalent to a history matching task. In this work we consider a 3-parameter analytical correlation for relative permeability, proposed by Lomeland et al, 2005. This correlation, known as LET correlation, promotes more flexibility on fitting pseudo-relative permeability curves, since it allows varying three parameters during the history matching procedure to reproduce the fine scale reference curves. To assist this pseudo-relative permeability curves tuning task, we used a commercial software capable of

running the compositional simulator and optimizing the LET parameters to better fit reference curves. Alternatively, usual Corey relative permeability correlation can be used for this step and the same procedure can be done.

In each one of the three case studies, starting from the coarse model, the miscible fluid model was replaced by the immiscible one. After, the relative permeability curve was modified to better adjust the recovery observed in the refined reference model.

Figures 15.b, 16.b and 17.b present the same set of curves in Figures 15.a, 16.a and 17.a, after adjusting the pseudo-relative permeability curves for the coarse models with the immiscible fluid model. It is possible to verify the optimal reproduction of the response obtained in the refined reference model.

The change on the permeability relative curves in each case is shown in Figures 18, 19 and 20. In each graph, two pairs of relative permeability curves are presented: the original curves (continuous lines) and the adjusted curves (dashed lines), which are the pseudo-relative permeability curves.

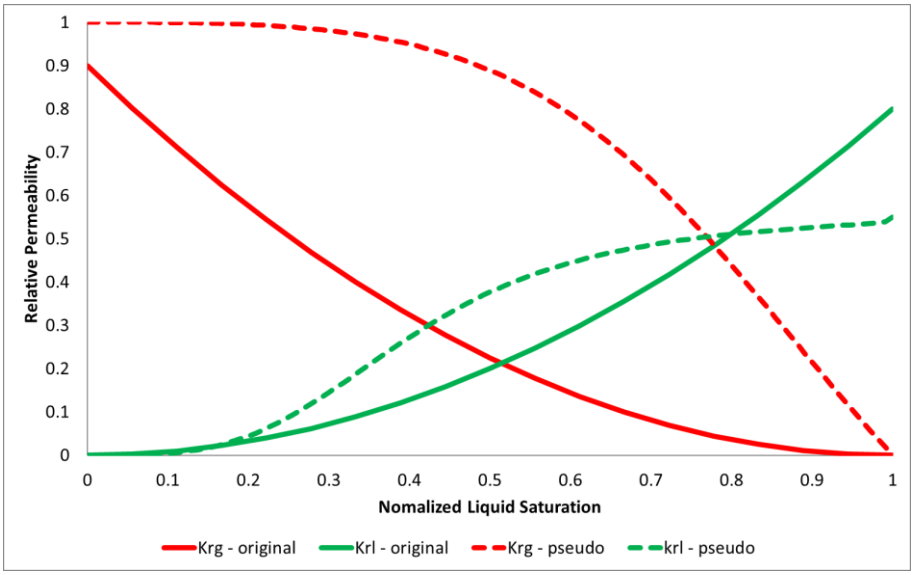

Figure 18. Original and adjusted gas-oil (gas-liquid) relative permeability curves for Case A. Rios et al. (2017).

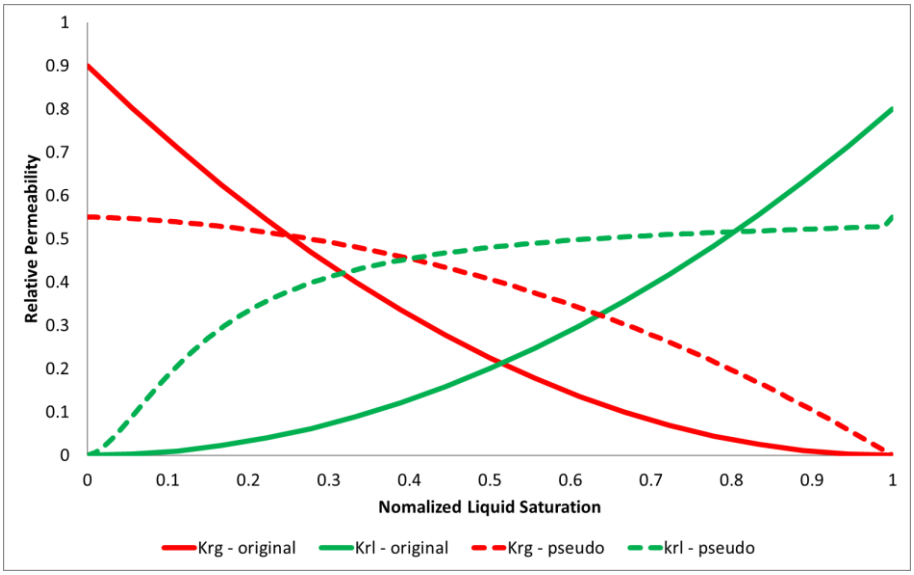

Figure 19. Original and adjusted gas-oil (gas-liquid) relative permeability curves for Case B.

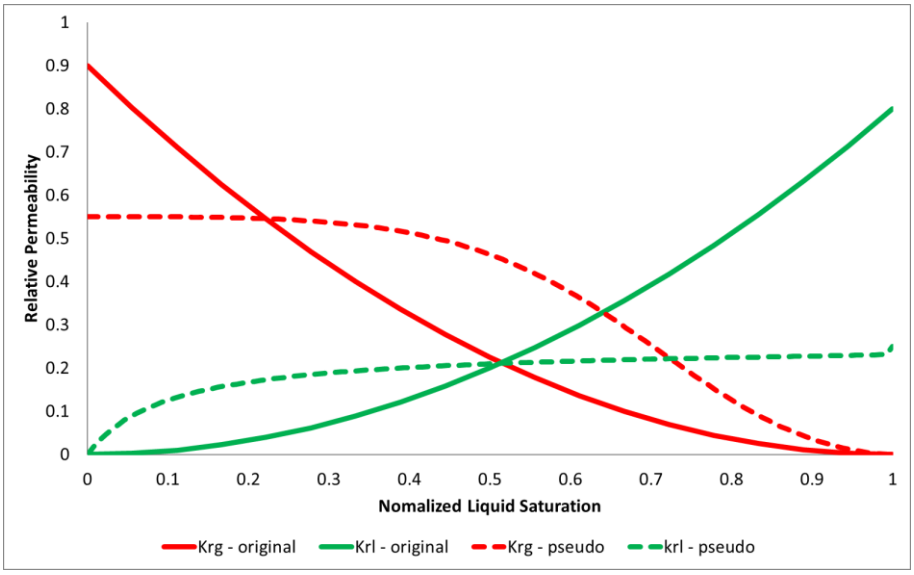

Figure 20. Original and adjusted gas-oil (gas-liquid) relative permeability curves for Case C.

As previously mentioned, besides the significative improvement on the oil recovery factor curves for all the cases, the technique also allowed coarse models to better represent the averaged fine-scale gas saturation map, indicating a closer agreement with the reference results also qualitatively. Case A is considered to illustrate this effect. Figure 21 shows this effect considering the gas breakthrough moment of the reference fine model in case A. Figure 21.a shows the saturation map of the fine-scale model, while Figure 21.b represents the same map averaged to the coarse-scale. This is the reference map to be compared with the coarse-scale runs. Figure 21.c shows, for the same time, the gas saturation simulated with regular static upscaling and original miscible fluid model. The last figure, Figure 21.d, highlights the final gas saturation map after applying the two steps of the proposed technique. It is possible to observe that the overall behavior is much better represented in Figure 21.d, which complement

the best fit of the production curves and emphasize the effectiveness of this upscaling technique for compositional simulations of miscible gas injection. These results can also be seen by the difference saturation maps in Figure 22. In this comparison, it is calculated, for each cell, the difference between the reference gas saturation, Figure 21.b, and the coarse scale gas saturation. Figure 22.a shows the difference the map of Figure 21.c, while Figure 22.b consider the difference related to Figure 21.d. Again, it is possible to verify the improvement after the use of the technique proposed in this work.

Finally, it is worth mentioning that considering the three case studies presented, the final adjusted coarse simulations are around 150 times faster than their reference fine scale simulations for the Cases A and B and more than 600 times faster for the Case C. Even though we did not conduct any numerical optimization for these models, the speed up is significative. Also, to achieve the final pseudo-relative permeability curves, it was necessary, in average, 600 simulation runs. Therefore, the effort associated with the construction of the final upscaled models is equivalent to the time spent on simulating the fine scale models no more than 4 times, which is another important aspect of the proposed methodology.

Additional analyses

In order to prove and verify the robustness and versatility of the technique, additional simulation tests were conducted on case C, which is the most complex among the case studies. Considering the resultant coarse model after the two steps presented above, we performed three different set of simulation runs: first varying the production and injection rates, then changing the 5-spot scheme by inverting the function of each well (i.e. the injector was simulated as a producer and the four producers were simulated as injectors), resulting in four injector wells and one producer at the center. At last, we extrapolated the simulations beyond the matched period, which consisted of 2000 days in the simulation, to evaluate the robustness of the final coarse model on predicting fine scale results. In this task, two new analyses were carried out: (i) simple extrapolation, extending the simulation for more 1000 days after the final period considered for matching the pseudo-relative permeability curves and (ii) new well locations after 2000 days simulating the original 5-spot drainage plan. In this evaluation, all the original wells were shut in the 2000^{th} day and, 30 days later, 3 new wells were opened, one injector and 2 producers, and they operate until day 3000^{th}.

The results considering the above investigations are shown in Figures 23 to 28. First, we considered the rates to be half of the original case and latter, twice higher than the original one. Figures 23 and 24 show that the coarse-scale results after the technique were

almost the same observed with the fine-scale reference model. Also, even when the drainage plan was changed, the methodology proved to be robust with good agreement against the fine-scale results, as shown in Figure 25. Moreover, the extrapolated simulations also show the capability of the final upscaled model to predict fine-scale results starting from a more complex fluid distribution, even when new wells are included in the simulation models, as it can be seen in Figures 26 to 28.

These responses are important to validate the proposed technique in different conditions with no need to change the calibrated relative permeability curves. Thus, reinforcing the capacity of this technique to improve coarse-scale simulation results in compositional simulation of miscible gas injection.

Numerical evaluation

An additional evaluation was performed in this work to emphasize the influence and the behavior of two important small-scale phenomena that are usually lost or severally smoothed due to the upscaling process: viscous fingering and channeling effect related to highly heterogeneous environment.

For this investigation the fine-scale models of cases A and B were analyzed. By the observation of the left images on Figures 8 and 9, it is possible to verify that Case A fine-scale model is much more homogeneous when compared to Case B. Not only considering the permeability distribution but also the existence of high permeability preferential paths. This behavior has an important role considering the impact of different numerical schemes and solutions in the simulations.

In order to evaluate grid orientation effects, minimize numerical dispersion and understand the importance of the heterogeneity level in theses aspects, additional analyses were performed in both cases. Each model was also simulated using 9-point scheme and TVD (Total Variation Diminishing). These solutions were used together and separately and compared with the conventional solution (5-point and *upwind*).

Figures 29 and 30 show the oil recovery factor behavior for cases A and B, respectively, in four configurations: conventional solution, 9-point, TVD and the last two combined. The differences on the results are more prominent in Case A, compared to Case B.

This happens because case A is dominated by viscous fingering and more susceptible to grid orientation effect and numerical dispersion influence. Case B, on the other hand, is dominated by channeling effects due to the heterogeneity and preferential paths, which

diminishes the importance of the numerical effects previously mentioned, since the main dynamic phenomenon is the heterogeneity marked by the channels.

To illustrate the difference among the analyzed cases in relation to the miscible gas front, Figures 31 and 32 show the behavior of the gas front for each of the investigated solutions at an initial time of the simulation. Figure 31 highlights Case A and Figure 32, case B. Also, the same maps are shown again in Figures 33 and 34, but in an advanced simulation time, allowing emphasizing the different impact of the various numerical schemes in both cases.

The analysis of Figures 29 to 34 indicates some important aspects of the investigated cases. Firstly, for case A, it is observed that there is a considerable variation in the behavior of the recovery factor as a function of the solution used. Additionally, it is noticed that the characteristic of the gas miscible front is quite different in each solution.

By analyzing the TVD solution, which reduces the truncation error and decreases numerical dispersion, it can be seen from Figures 31 and 33 that there is a greater emphasis on viscous fingering. On the other hand, the grid orientation effects become even more intense, which justifies the recovery factor slightly higher than that observed in the conventional solution. These results suggest that, while reducing the undesirable effects of numerical dispersion, simulations using high order methods in problems with unstable fronts do not necessarily result in more reliable results. Fernandes et al. (2013) and Fernandes et al. (2015) compared different interpolation functions for TVD in unstructured grids and identified that the results in terms of grid orientation effect vary.

The 9-point solution, in turn, shows a noticeable reduction of the grid orientation effect, which can be verified in Figures 31 and 33. This reduction leads to smaller recovery factors, as it drives the injected gas more directly towards the producing well.

Finally, the combination of the two solutions incorporates the aforementioned effects. The result of this is a miscible gas front with lower numerical dispersion, better defined fingers, and lower grid orientation effect. These factors lead to a lower recovery factor compared to the other configurations.

Considering Case B, on the other hand, all the different approaches lead to close answers, not only in the oil recovery factor curves, but also on the gas saturation profile in two different simulation times. As mentioned before, the reason for this is the dominance of the channeling effect on this problem, with the permeability map playing the most significate role regarding the dynamic effects.

It is worth noting that the above observations are consistent with those reported in the literature. The grid orientation effect tends to be important in cases where viscous fingers

are predominant, not channeling due to heterogeneity. In case A, there was a great reduction of the grid orientation effect with the 9-point solution and, in addition, a better definition of the fingers with the application of TVD. These factors are in agreement with what is observed in the literature and complement each other in the analysis.

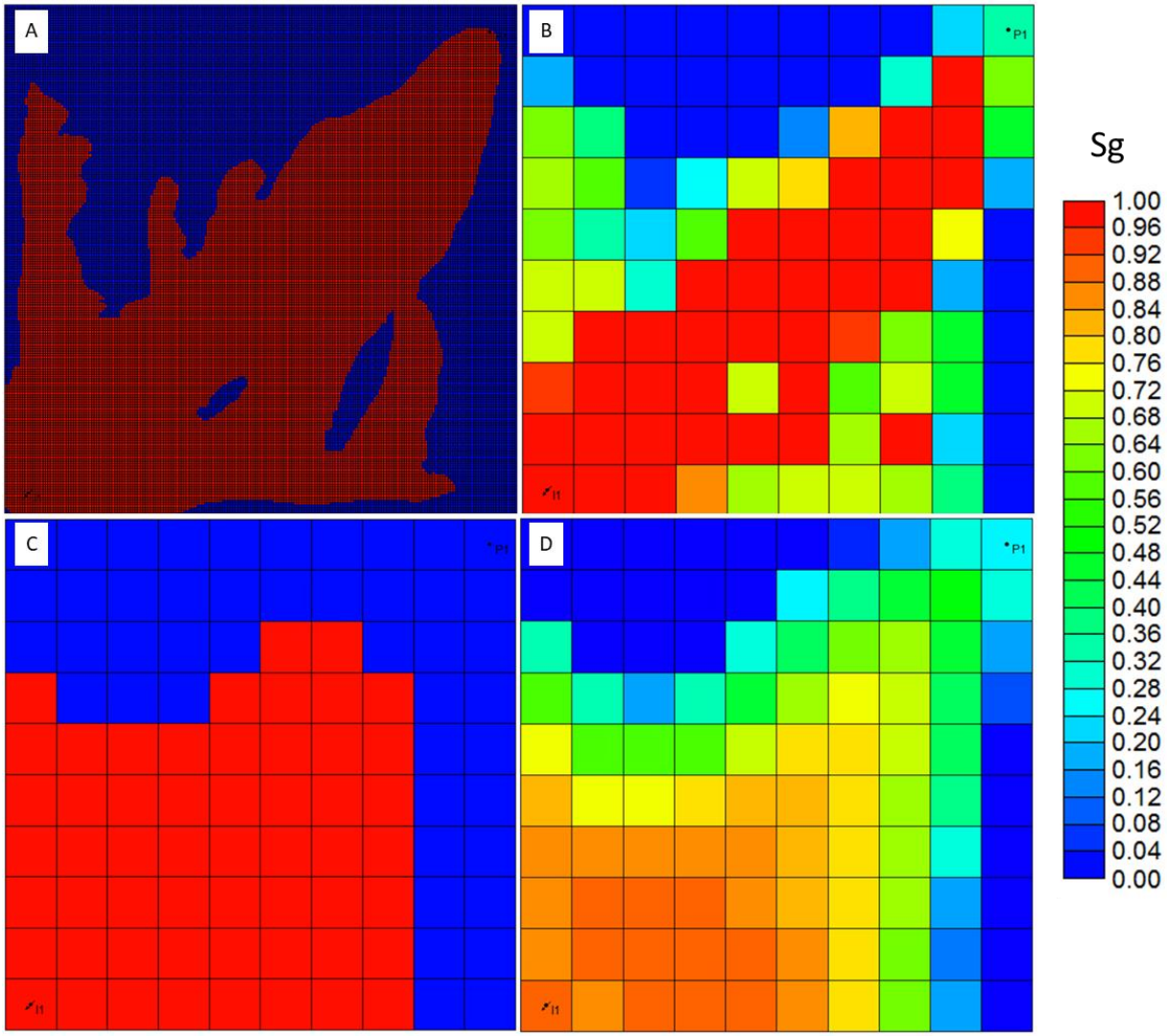

Figure 21. Behavior of the miscible gas front in the fine-scale (A), its equivalent averaged over the coarse-scale (B), coarse-scale with static upscaling and original fluid model (C) and final coarse-scale result after the technique (D).

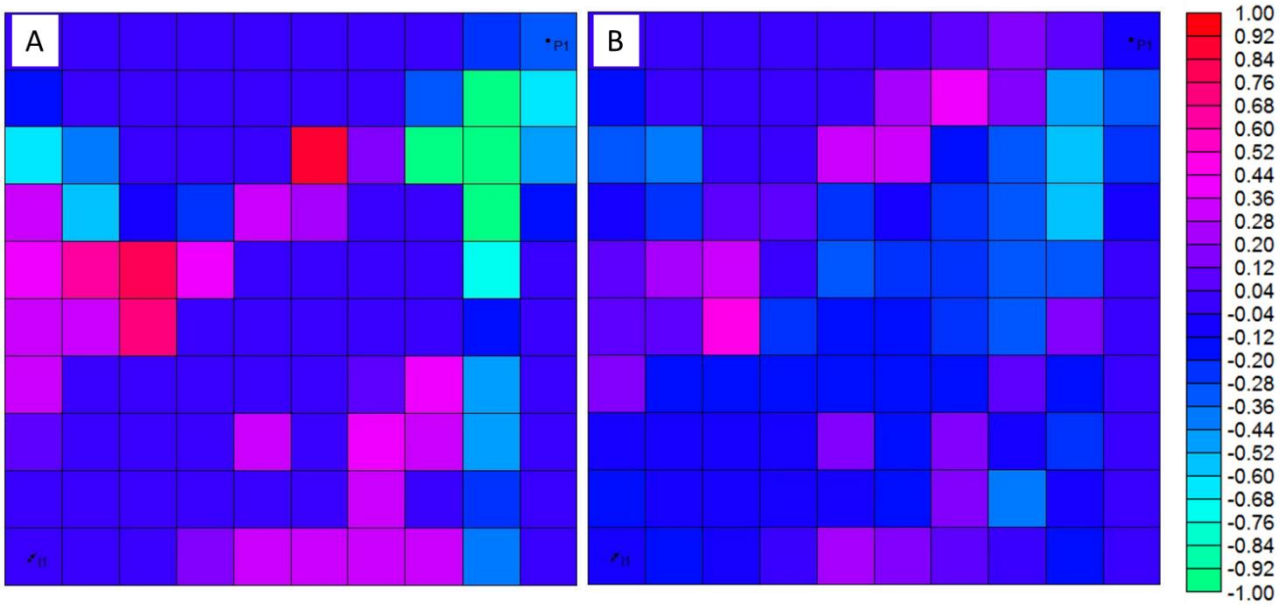

Figure 22. (A) Difference between reference gas saturation map (Figure 21.b) and initial coarse scale saturation map (Figure 21.c). (B) Difference between reference gas saturation map (Figure 21.b) and initial coarse scale saturation map (Figure 21.d).

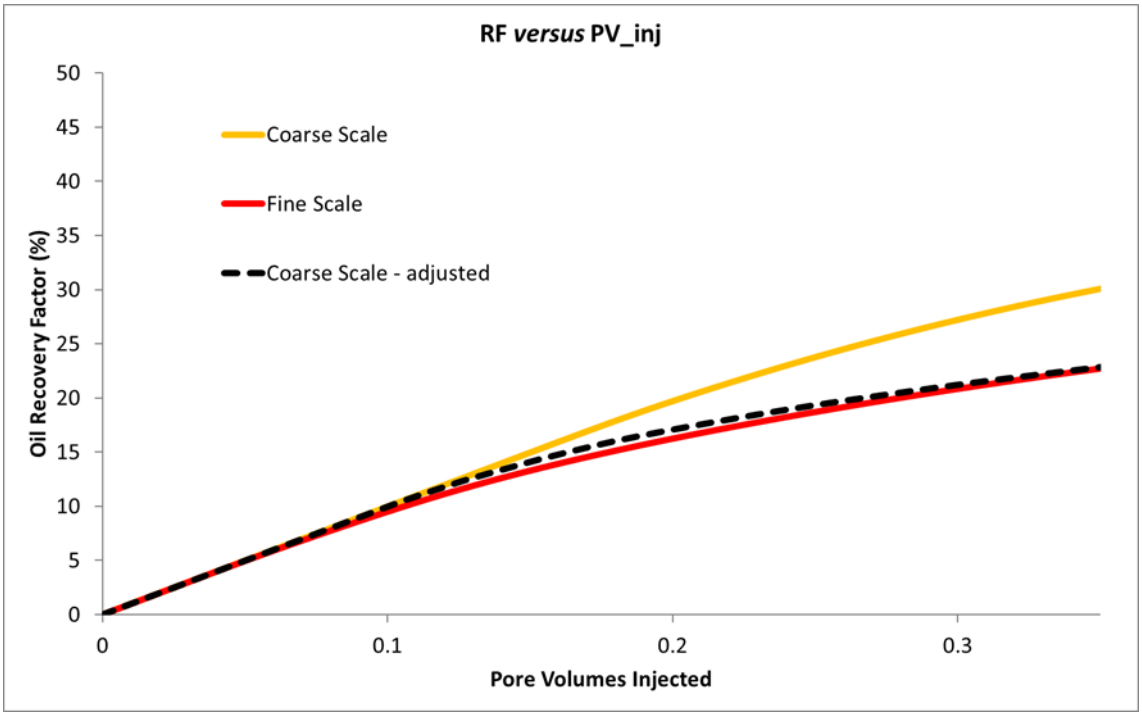

Figure 23. Oil recovery factor versus injected pore volume of gas for additional Case C run with rate divided by two.

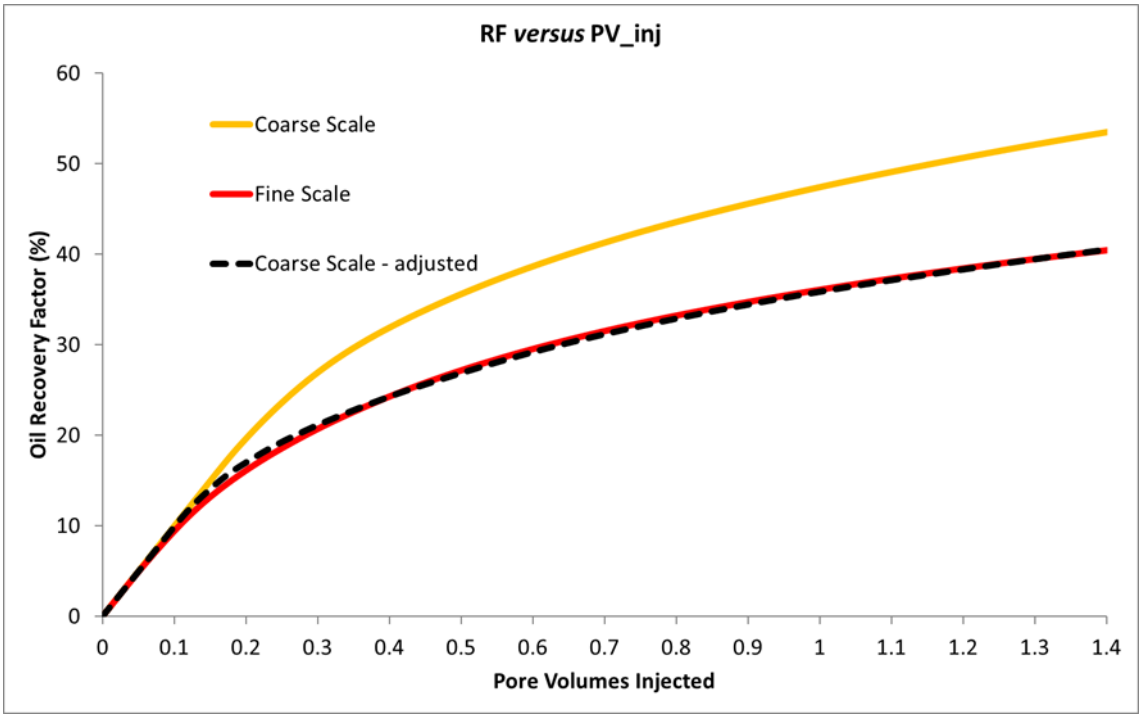

Figure 24. Oil recovery factor versus injected pore volume of gas for additional Case C run with rate times two.

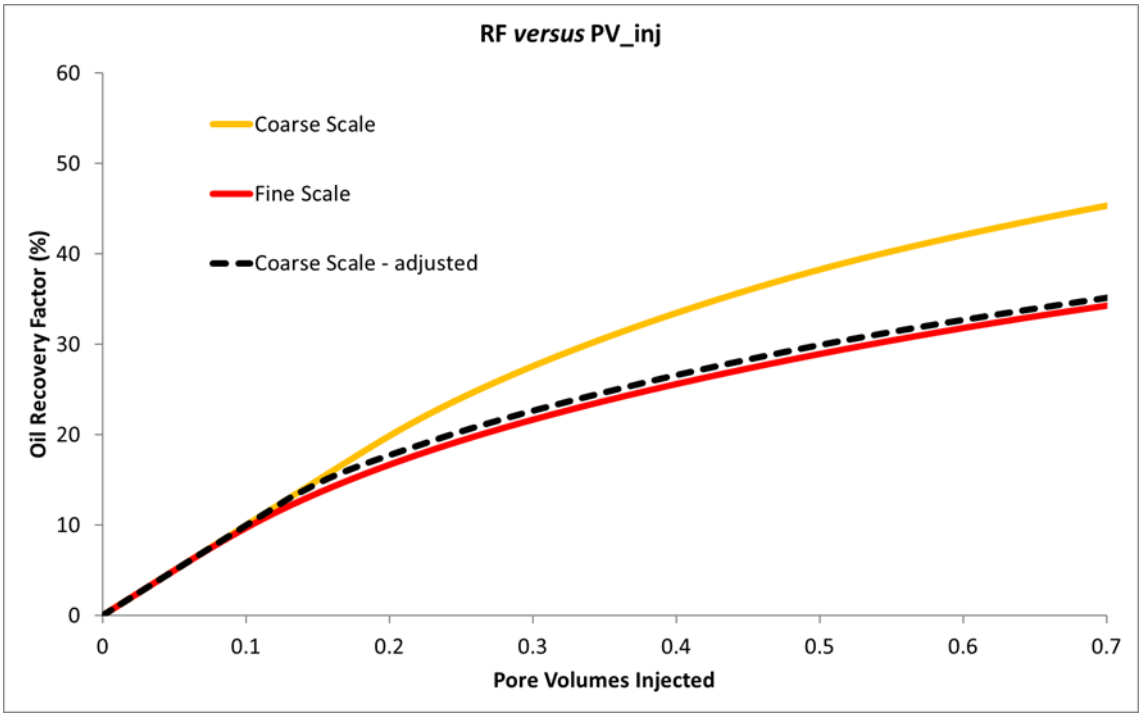

Figure 25. Oil recovery factor versus injected pore volume of gas for additional Case C run with changed well functions.

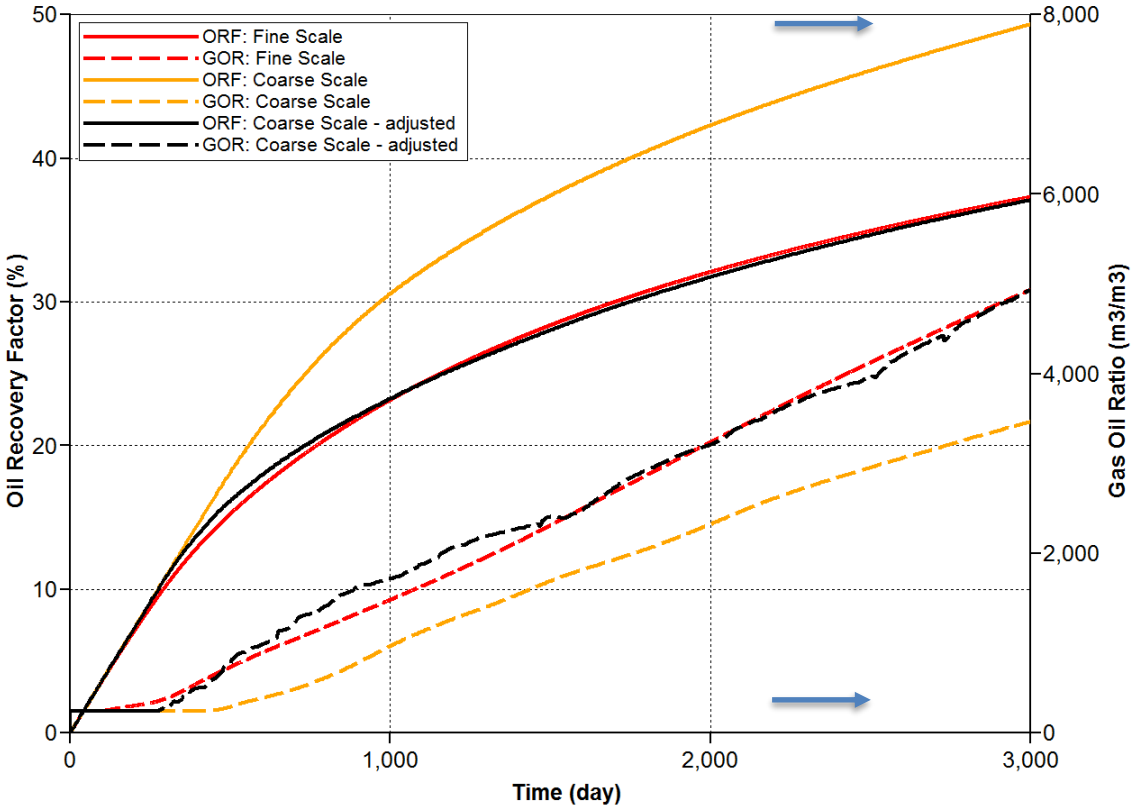

Figure 26. Oil recovery factor versus time for additional Case C run with 1000 days extrapolation.

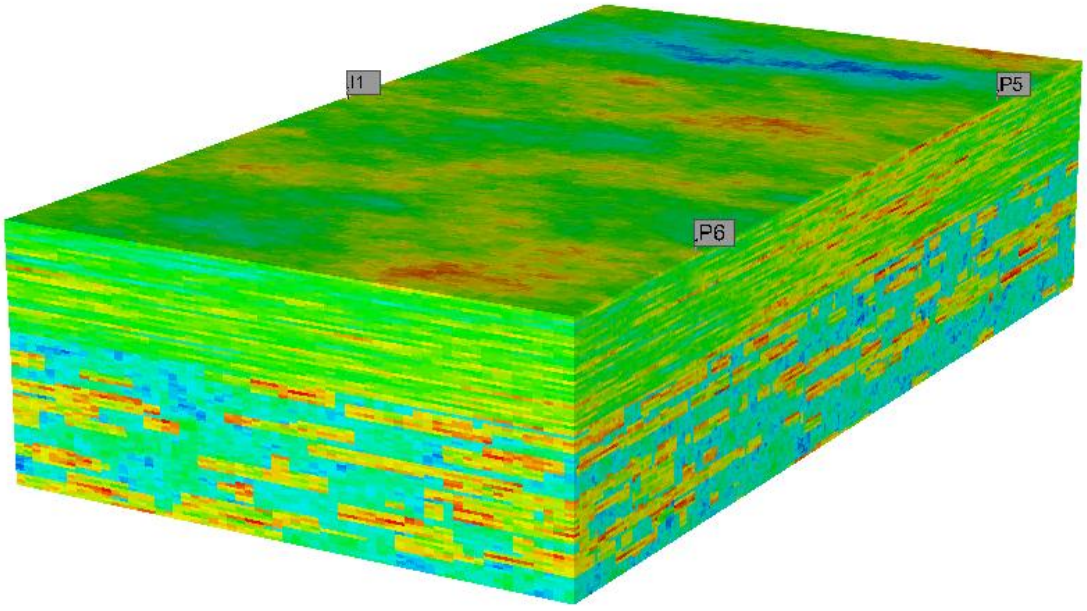

Figure 27. New wells added to extrapolate the results after 2000 days with the original 5-spot drainage plan.

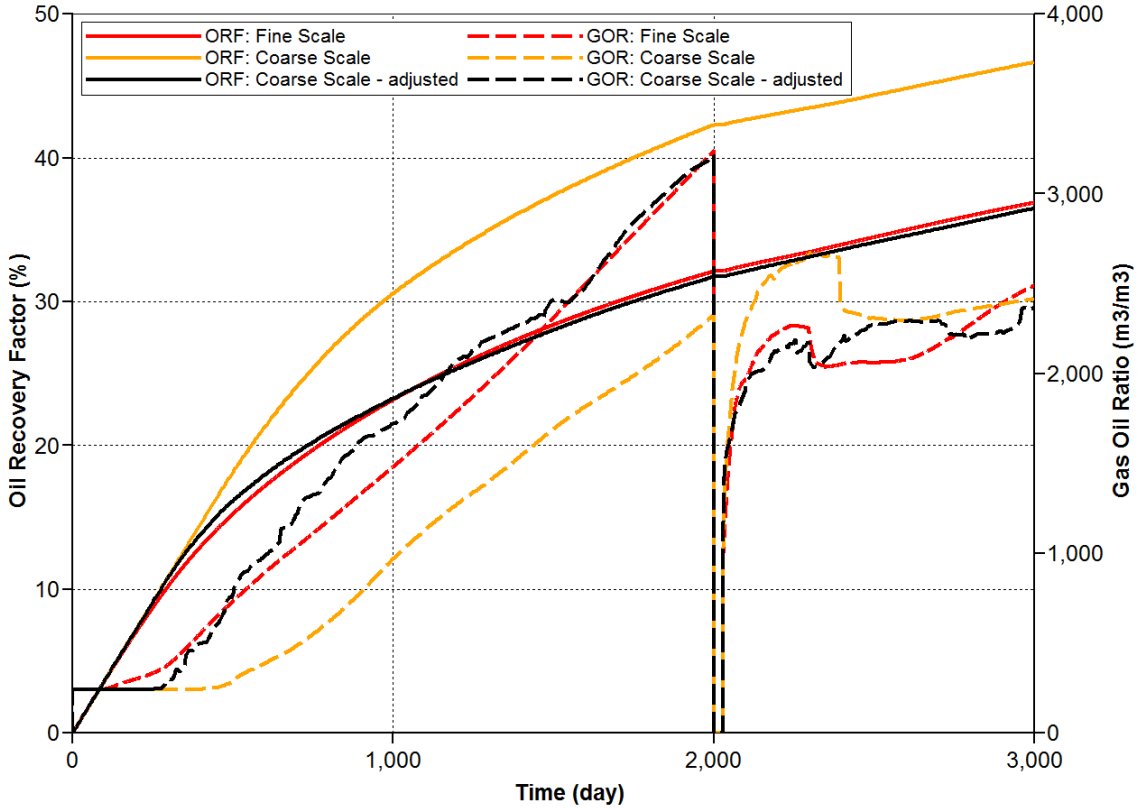

Figure 28. Oil recovery factor versus time for additional Case C run with 1000 days extrapolation and new well included.

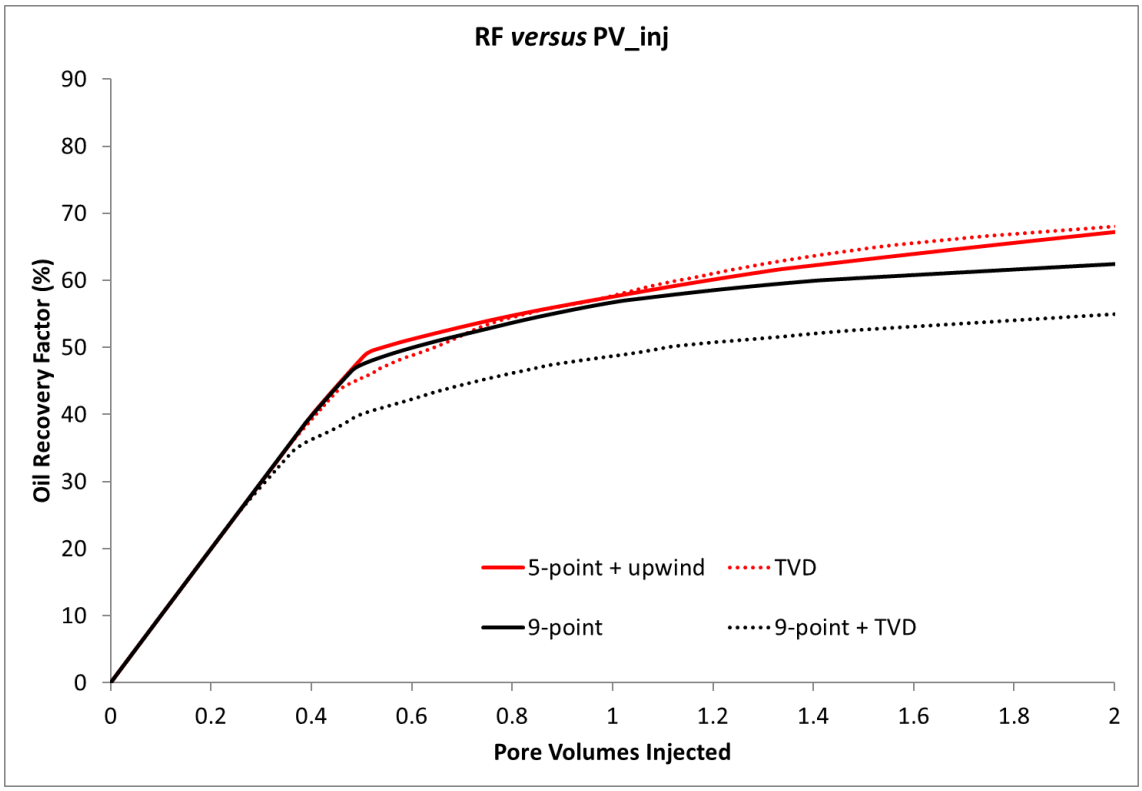

Figure 29. Recovery factor versus pore volumes injected for the fine-scale model (5 x 5 m²) in Case A. Continuous curve, conventional case (upwind + 5-point). Dotted red curve, TVD. Continuous black curve, 9 points. Dotted black curve, 9 points + TVD. Rios et al. (2017).

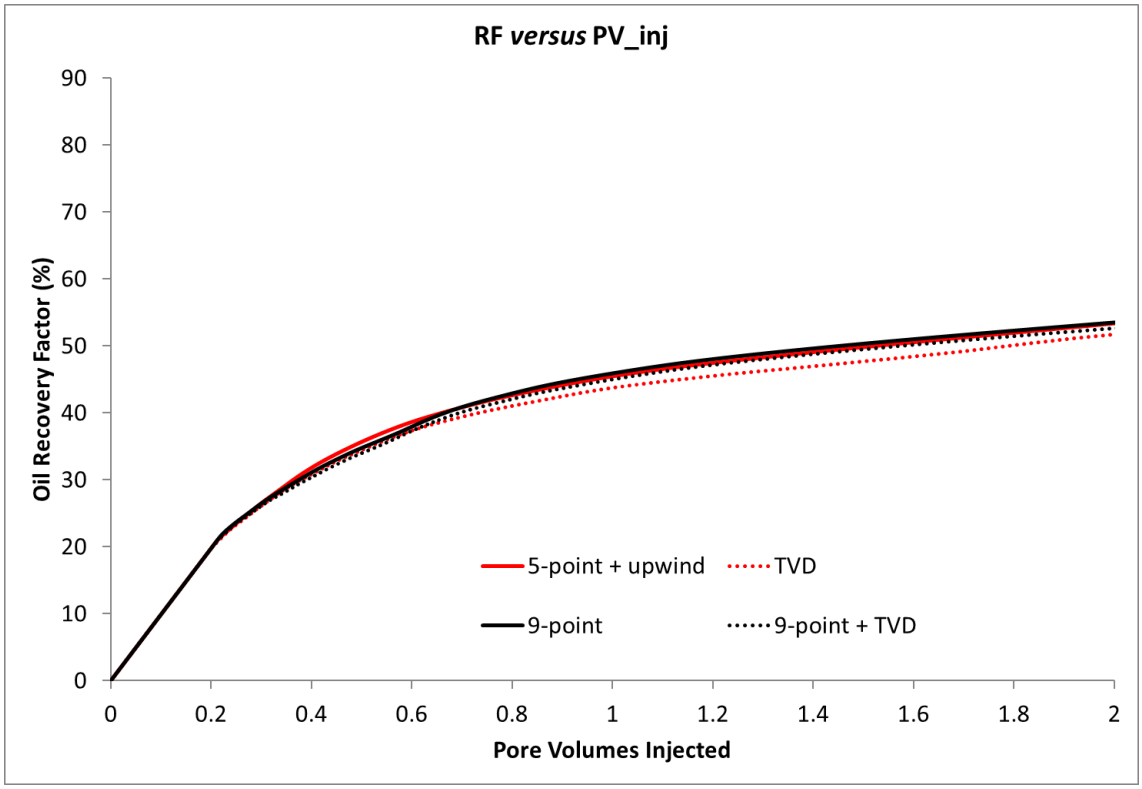

Figure 30. Recovery factor versus pore volumes injected for the fine-scale model (5 x 5 m²) in Case B. Continuous curve, conventional case (upwind + 5-point). Dotted red curve, TVD. Continuous black curve, 9 points. Dotted black curve, 9 points + TVD.

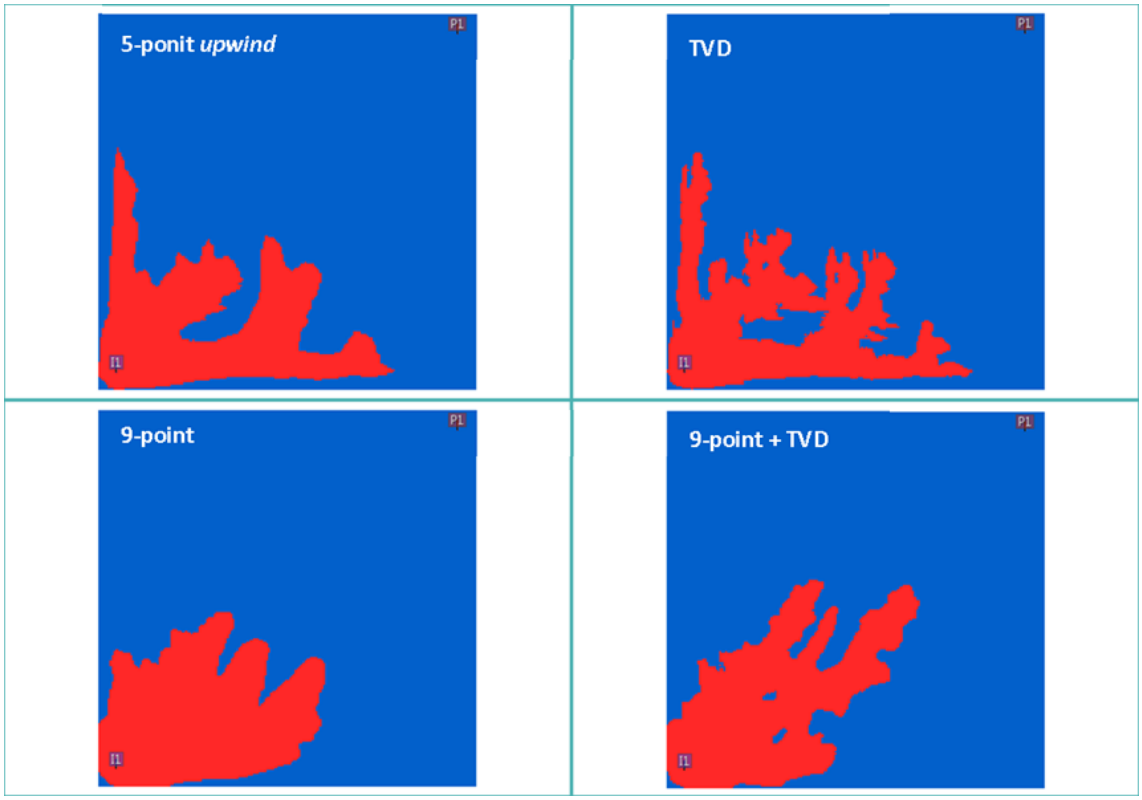

Figure 31. Behavior of the miscible gas front for four different numerical configurations of the fine-scale model in Case A, at an initial time of the gas injection. Rios et al. (2017).

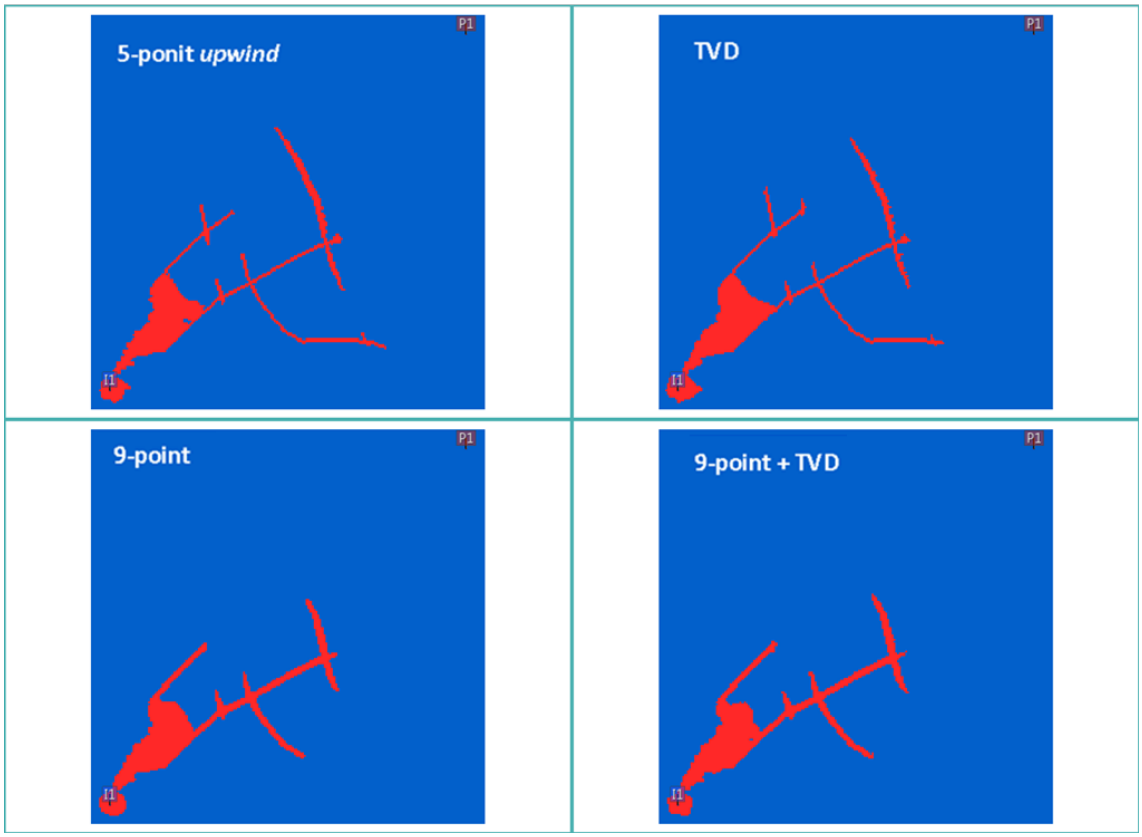

Figure 32. Behavior of the miscible gas front for four different numerical configurations of the fine-scale model in Case B, at an initial time of the gas injection.

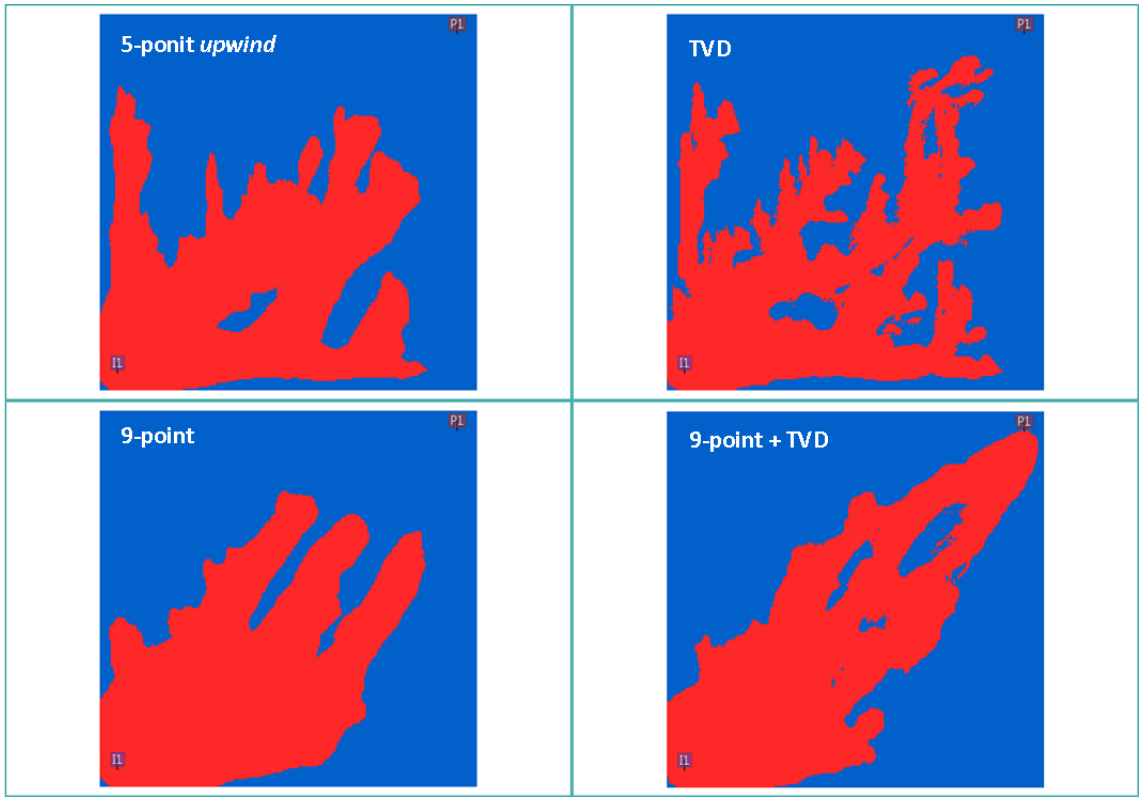

Figure 33. Behavior of the miscible gas front for four different numerical configurations of the fine-scale model in Case A, all solutions on the same date corresponding to the breakthrough of the solution 9-point + TVD. Rios et al. (2017).

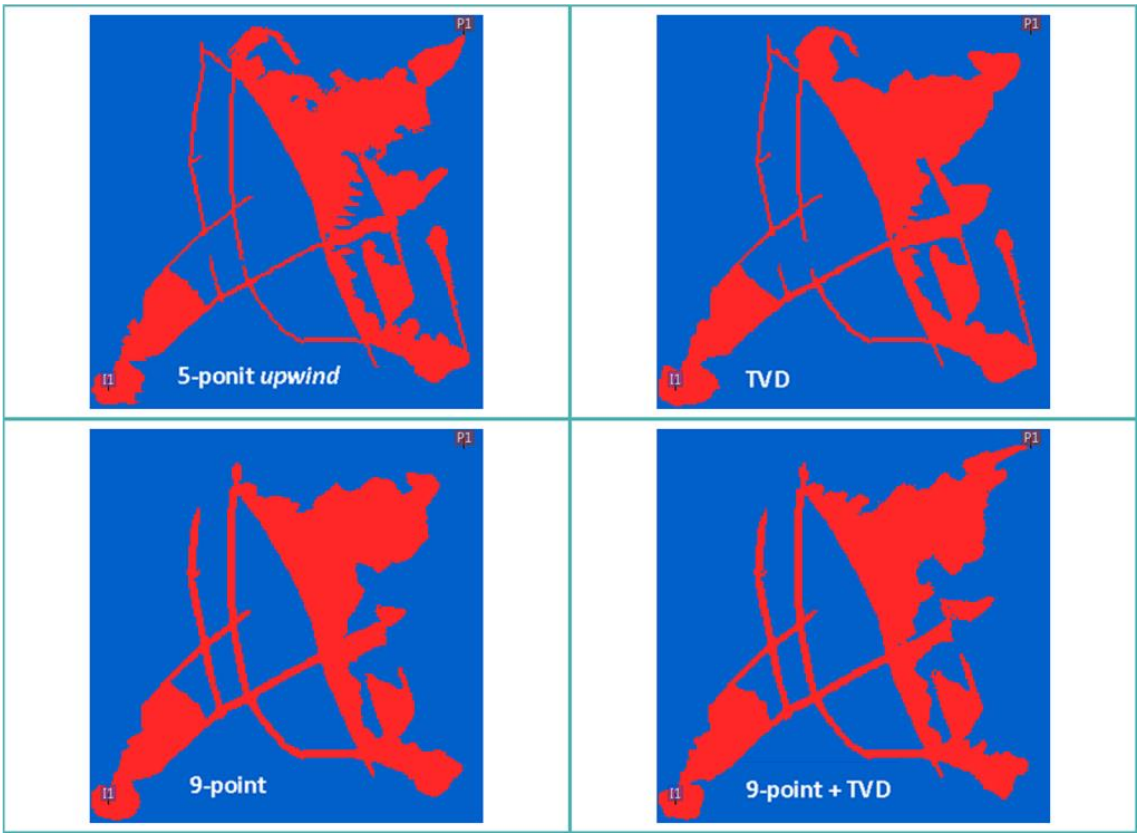

Figure 34. Behavior of the miscible gas front for four different numerical configurations of the fine-scale model in Case B, all solutions on the same date corresponding to the breakthrough of the solution 9-point + TVD.

Conclusions

The problems arising from the grid upscaling process from the geological to flow simulation models considering miscible gas injection were evaluated in this work. It was verified, for the three case studies, that the coarser scale simulations tend to present optimistic oil production results, for miscible gas injection, in comparison to the simulations in a more refined scale.

The main reason relates to the difficulty in representing unstable flow and channeling on a coarse-scale. The involved phenomena tend to disappear with the smoothing of the forward fronts, represented by the numerical dispersion derived from the truncation error.

The proposed technique presents two important contributions for a robust and effective upscaling procedure in compositional simulation of miscible gas injection cases: it makes the gas saturation behavior more representative of the fine-scale averaged gas saturation map and modifies the pseudo-relative permeability curves in order to better reproduce production curves using coarse-scale simulation models.

The use of a 9-point scheme and TVD to mitigate the grid orientation and numerical dispersion effects were evaluated. Viscous fingering dominant cases are more sensitive to different numerical schemes in the simulations. Furthermore, when heterogeneous channels are significant, they tend to dominate the simulation results.

Finally, based on the three case studies presented, it was possible to obtain good results in coarser models with the use of a fluid model that guaranteed the immiscible displacement and consequent formation of two hydrocarbon phases, with subsequent adjustment of pseudo-relative permeability curves. The results were also validated by simulating different operational conditions and drainage plans. These validations were performed for case study C indicating the versatility and robustness of the presented work. Therefore, this technique may be applied to conditions similar to the presented cases.

Acknowledgements

The authors would like to thank Petrobras (Petróleo Brasileiro S.A.), UNISIM, DE-FEM/UNICAMP, CEPETRO, Energi Smulation, ANP, CMG and Dr. Daniel Nunes de Miranda Filho for all the support in this work.

3 ARTICLE 2: UPSCALING TECHNIQUE FOR HIGHLY HETEROGENEOUS RESERVOIRS BASED ON FLOW AND STORAGE CAPACITY, AND LORENZ COEFFICIENT

V.S. Rios, L.O.S. Santos, D.J. Schiozer

SPE Journal, 2020

Abstract

Field-scale representation of highly heterogeneous reservoirs remains a challenge in numerical reservoir simulation. In such reservoirs, detailed geological models are important to properly represent key heterogeneities. However, high computational costs and long simulation run-times make these detailed models unfeasible to use in dynamic evaluations. Therefore, the upscaling of geological models is a key step in reservoir engineering studies to reduce computational time. Upscaling must be carefully performed to maintain integrity; both truncation errors and the smoothing of sub-grid heterogeneities can cause significant errors.

This work evaluates the latter, the effect of averaging small-scale heterogeneities in the upscaling process, and proposes a new upscaling technique to overcome the associated limitations. The technique is based on splitting the porous media into two levels guided by flow and storage capacity analysis, and the Lorenz Coefficient, both calculated with static properties (permeability and porosity) from a fine-scale reference model. This technique allows the adaptation of a fine highly heterogeneous geological model to a coarse-scale simulation model in a dual-porosity, dual-permeability approach and represents the main reservoir heterogeneities and possible preferential paths.

The new upscaling technique is applied to different reservoir simulation models with water injection and immiscible gas injection as recovery methods. We show, in deterministic and probabilistic studies, that the resulting coarse-scale dual-permeability models are more accurate and can better reproduce the fine-scale results in different upscale ratios, without using any simulation results of the reference fine-scale simulation models, as some of the current alternative upscaling methods do.

Introduction

Current advances in geostatistical techniques allow reservoir geological properties to be represented in a highly detailed fine-scale model. This better represents the main reservoir heterogeneities but remains a significant challenge for dynamic reservoir simulations with impractically high computational costs even for single numerical simulation runs. Model sizes can vary significantly depending on the application, but typical fine-scale models may contain up to 10^8 cells, while typical simulation models may contain 10^4 to 10^6 blocks (Chen and Durlofsky, 2006, 2008). Therefore, to evaluate the dynamic behavior, it is usually necessary to upscale a geocellular model, reducing the number of cells to enable a reservoir flow simulation within a time-frame compatible with the needs of the industry.

In practical reservoir simulation studies, single-phase static upscaling strategies are important tools and can be successfully applied to the proper representation of oil production under primary depletion in coarse-scale models. The most frequently used method to upscale porosity from a fine-scale model is the volumetric weighted arithmetic mean because the pore volume is preserved (Durlofsky, 2003). For permeability upscaling, there are three important methods: averaging, which considers horizontal arithmetic average and vertical harmonic average; Cardwell-Parsons directional averaging (Cardwell and Parsons, 1945); and flow-based upscaling with closed boundary conditions (Christie, 1996; Kumar et al., 1997).

Many porosity and permeability upscaling approaches have been developed and applied in reservoir engineering studies. Detailed and comprehensive reviews on several techniques are provided by Wen and Gomez-Hernández (1996), Renard and de Marsily (1997), Farmer (2002), and Durlofsky (2003). In general, flow-based upscaling methods are more widely considered as reference approaches because of their generality and flexibility (Chen and Durlofsky, 2006).

In flow-based upscaling techniques, transmissibility calculation partially captures the effects of heterogeneity on permeability and preferential flow pathways. However, transport calculation can be erroneous because of equilibrium assumptions and uniform displacement at a local level (Jessen and Evazi, 2013). This becomes more challenging in channelized reservoirs and heterogeneous systems with high correlation length (comparable with well spacing).

When fluid is injected into a heterogeneous reservoir, additional effort is usually required for the most effective upscaled model. For water injection or immiscible gas injection simulation processes, a two-phase upscaling procedure is recommended. In this case, pseudo-relative permeability curves are a popular method to improve the results of coarse-scale simulation models when fine-scale simulation results are available.

Several authors proposed methodologies to better represent small-scale results in coarse-scale simulation models. Backer and Fayers (1994) developed the method of transport coefficients (also known as α-factors), which consists of modifiers introduced in the flow terms to relate the compositions of fluids flowing from a large grid block to the average compositions of those fluids within the grid block. In addition to the use of pseudo relative permeability curves, they tested the method for various fluid systems with improved accuracy in the results, especially in terms of component production rates for the cases considered. Barker and Thibeau (1997) reviewed the several existing relative permeability upscaling approaches and noted important limitations when considering pseudo-relative permeability curves while upscaling fine-grid geological models to coarse-scale simulation models. They concluded that pseudo-

relative permeability cannot be used, except in cases where capillary or gravity equilibrium can be assumed at the coarse-scale grid block.

In addition to the α-factor approach, Christie and Clifford (1998) used streamline techniques to generate a fine-scale solution. However, no pseudo-relative curves were used, because they only considered single-phase flow problems.

Chen et al. (2003) developed an upscaling procedure, referred to as a coupled local–global upscaling approach, in which the local boundary conditions (used to compute upscaled properties) are determined from global coarse-scale flows. They showed significant improvement over existing local methods and extended local methods. However, only generic flows were considered in the generation of the coarse-scale properties; specific global flow and well effects, which may affect the upscaling accuracy, were not investigated.

Chen and Durlofsky (2006) proposed an adaptive local–global (ALG) upscaling procedure to generate coarse scale parameters "adapted" for any type of global flow. They included a threshold to update the upscaled properties only in high-flow areas, potentially increasing the efficiency of the upscaling procedure. The authors reported that flow simulation results on highly heterogeneous systems showed improvement over local and coupled local-global upscaling techniques.

Zhang et al. (2008) proposed an upscaling method called Well Drive Upscaling (WDU) that employs global well drive and actual boundary conditions to avoid the problem of using inappropriate boundary conditions in single-phase upscaling. They presented good results, but the methodology can only be applied if a fine-scale pressure solution is available.

Evazi and Jessen (2014) developed a technique for highly heterogeneous reservoirs, in which the pore space is arranged into two levels of porosity based on fine-scale streamline information, and a dual-porosity dual-permeability (DP/DP) flow model is adapted to simulate the coarse-scale model. They demonstrated that DP/DP coarse-models predict the breakthrough time accurately and are less sensitive to the level of upscaling when compared to conventional single-porosity upscaling. However, the overall workflow to obtain the upscaled models can be costly because of the need for streamline simulations for the fine-scale model. Another drawback is the use of fine-scale results to divide the porous media, which can make the strategy strongly dependent on the original well locations and flow rates.

Inspired by the work of Evazi and Jessen (2014), we propose a new dual-porosity dual-permeability (DP/DP) upscaling technique for highly heterogeneous reservoirs. In this work, we use flow and storage capacity analysis, and the Lorenz Coefficient (Lorenz, 1905; Jessen et al., 2000) applied to the static information of a fine-scale model to split the porous

media into two levels: one representing the main flow regions and the other, the secondary flow regions. With the splitting of fine-scale cells, directional upscaling for permeability can be properly performed for each group. We show that the resulting coarse-scale models can adequately reproduce the reference fine-scale results better than traditional static upscaling methods.

The proposed methodology presents two significant improvements over other upscaling techniques. It is 1) less time-consuming to obtain coarse-scale models as no dynamic responses of fine-scale models are used and 2) not dependent on the drainage plan or well flow rates of the fine-scale models.

Another important contribution of the present work is to propose an upscaling procedure that can be applied for multiple permeability realizations. We show that, when compared to the reference results, our methodology can improve the representation of coarse-scale uncertainty curves by mitigating the overestimation of sweep efficiency and oil-recovery factor bias presented when a traditional upscaling procedure is considered. This is a useful tool in current reservoir engineering simulation workflows. Nevertheless, there is limited research reported up to this date on this subject (e.g. Chen and Durlofsky, 2008; Li and Durlofsky, 2016).

In the following sections, this paper presents the problem and motivation for the proposed methodology and the main theoretical concepts. Descriptions of the case studies and applications then follow. We apply the proposed methodology in three ways: (i) a 2D system with heterogeneous permeability log-normal distribution in an immiscible gas injection scheme; (ii) a 2D channelized system with water injection; and (iii) a probabilistic evaluation of the upscaling technique with multiple permeability realizations. Afterwards, the results of each application are discussed. A summary and final remarks conclude this presentation.

The Problem and Motivation

In traditional upscaling procedures, a group of fine-scale cells is averaged to obtain only one cell with uniform properties, corresponding to a coarse-scale cell. Thus, sub-grid heterogeneities tend to be homogenized and each upscaled grid block smooths the behavior of several fine-scale grid cells. Figure 1 illustrates this, showing a heterogeneous fine-scale permeability map, using 5x5 m^2 cells. It highlights the dimension of a coarse-scale grid block to be considered for the upscaled model. Notable, in the expanded, highlighted area, a resulting coarse-scale grid block can average properties of several fine-scale cells whose values can vary as much as four orders of magnitude.

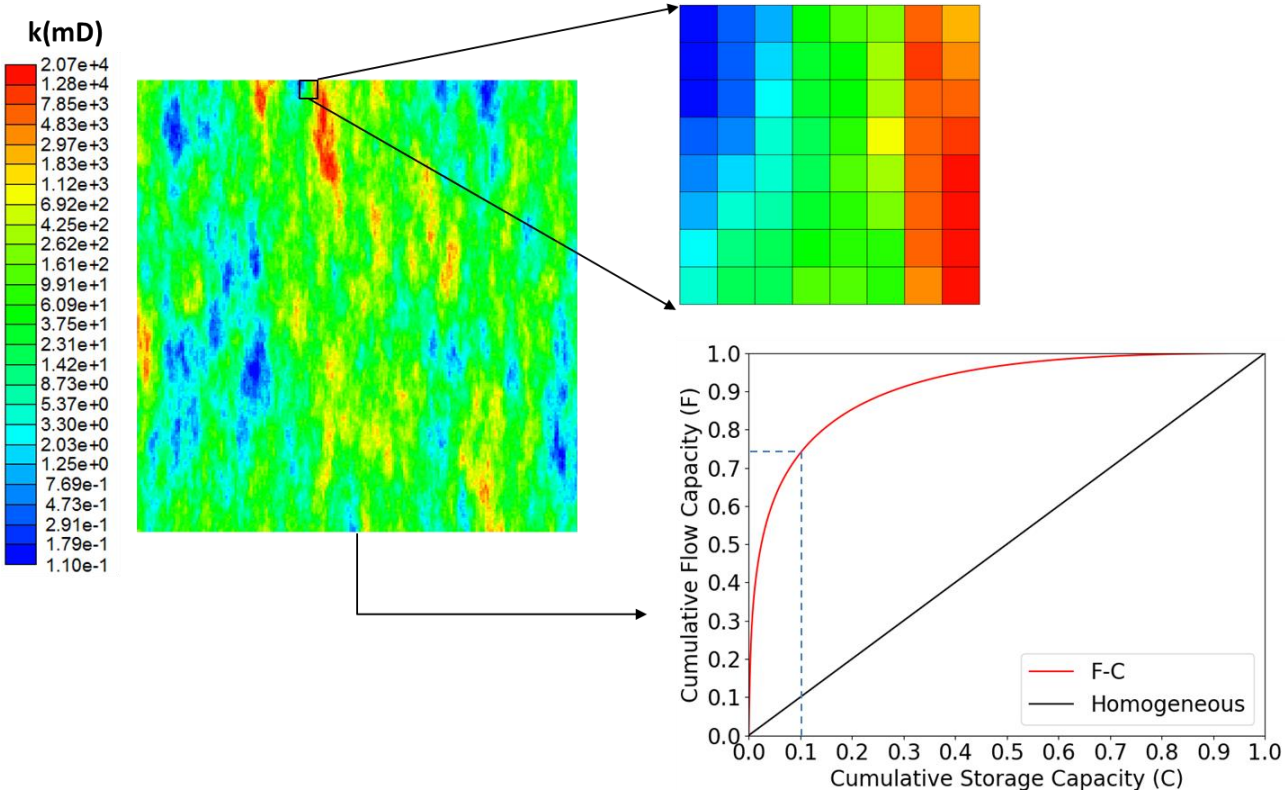

Figure 1. Fine-scale heterogeneous permeability map. A coarse grid block is highlighted taking the average properties of all fine-cells blown up on the right side of the figure. Also, F-C diagram for this reservoir model is shown.

Dynamic evaluations with coarse-scale models in these situations tend to overestimate the sweep efficiency of the injected fluids. This happens mainly because the preferential paths, due to high permeability contrasts, are homogenized in each coarse-scale cell. Depending on the level of heterogeneity and the contrasts between different facies, these preferential paths can behave like fractures, and a traditional single porosity averaging approach is likely to introduce significant upscaling errors (Evazi and Jessen, 2014).

In highly heterogeneous porous media, fluid often flows non-uniformly and the displacement fails to occur evenly in all regions of the reservoir. Areas with high fluid conductivity tend to dominate the flow contribution while regions with lower conductivity have less importance to the viscous flow. This condition is a natural indicator that, in such reservoirs, the porous media can be ranked in at least two levels, based on the potential flow contribution: primary (high contribution) and secondary (low contribution) systems.

Therefore, this work focuses on overcoming the above limitations, proposing a methodology to split the porous media into primary and secondary systems and calculating the upscaled properties for each system. By doing so, each grid block with channeling potential is

modeled with two porosities and two permeabilities and a dual-permeability dual-porosity (DP/DP) simulation for the upscaled model can be performed.

Methodology

The new upscaling technique is divided into two steps. The first divides the fine-scale porous media into two systems, while the second calculates the final properties for each coarse-scale grid block cell.

In the first step, classical flow and storage capacity theory is used as a global guide, based on static data of the fine-scale reference model, to select the fine cells with a higher theoretical contribution for the flow. The Lorenz coefficient is calculated for each group of fine cells that compose a coarse-scale cell. This second criterion is considered a local guide.

In the second step, the coarse-scale properties are calculated. Porosity and permeability are obtained for both primary and secondary systems. The volumetric weighted arithmetic mean is considered for porosity, while directional Cardwell-Parsons upscaling is performed for permeability.

Since the porous media is ranked and divided into two systems, flow and transport need to be modeled in a way that allows two different continua to coexist with interaction between them. To achieve this, the flow in the new upscaled model can be approximated with a DP/DP approach formulation. The dynamic of the fluid flow will have a preferential system (primary system) modeled as “fracture” and a passive system (secondary system), modeled as “matrix”.

In this DP/DP flow model, the primary and secondary systems consist of two distinct continua, with a linear transfer function modeling crossflow between them. The total flow comprises flow through main cells (fracture-fracture), through secondary cells (matrix-matrix), and between the primary system and the secondary system at a certain coarse cell level (matrix-fracture). For mass transfer between primary and secondary systems within a coarse block, Gilman and Kazemi style formulation (Gilman and Kazemi, 1983) is applied for the shape factor, which is uniform throughout the model.

The general workflow proposed for our upscaling technique follows:

1. Construct classical flow (F) and storage capacity (C) diagram (also known as F-C diagram) for fine-scale model;
2. Apply a threshold value for flow capacity (F) to select the primary system fine cells;
3. Select the desired upscaled coarse model size;

4. Calculate Lorenz Coefficient (Lc) for the group of fine cells in each resulting coarse-scale cell;
5. Apply a threshold value for Lc and select additional cells for the primary system;
6. Calculate coarse-scale cell properties.

In the following sections, we detail the above-mentioned steps and show how they combine to complete our upscaling technique. To illustrate the whole procedure, the permeability model of the refined reservoir shown in Figure 1 is considered as a reference and porosity is kept constant.

Two-System Porous Media Division

The division of the fine-scale detailed model into subsystems is guided by two different criteria: one global that considers the classical F-C diagram, and the other using local Lc for each coarse-scale cell.

For the global guide, we first create an F-C diagram for the reference model. The methodology to construct such a diagram is well known in the literature and is described by Lake (1989). This is an important way to establish the reservoir division into two systems while also serving as an indicator of reservoir heterogeneity.

Figure 1shows the F-C diagram for the reference reservoir. Two curves are plotted; the red indicates the actual flow and storage capacity diagram for the model while the black represents the behavior of a homogeneous reservoir. In fact, the further from the homogenous curve, the more heterogeneous the reservoir tends to be. This is the essence of Lorenz coefficient calculation.

As an example of how F-C diagram can guide the division, consider a flow capacity threshold of 0.75. This means that the group of selected cells corresponds to 75% of the total flow capacity. For this reference fine-scale reservoir, only 10% of the system responds to the threshold flow capacity, as seen in Figure 2.

Once the flow capacity threshold is defined, the corresponding fine-scale cells are highlighted and selected for the primary system, that is, the group of cells with most importance for the flow behavior of the reservoir. Figure 2a shows the resulting division, highlighting the primary system cells in white and the secondary in black.

Before concluding the first step of the proposed technique (a general division of the fine porous media into two systems), the local criterion is applied. This step is important, to include as main cells those that, despite not being selected as primary in the global criterion,

can present non-uniform flow behavior due to high heterogeneity. Therefore, they also require special treatment in the coarse-scale model with a two-system division.

For this step, we first define the dimensions of the coarse model cells. Then, Lc is calculated for each group of fine-scale cells. As an example, consider a uniform upscale for a coarse model with 40 x 40 m² grid block cells (upscaling ratio of 64). Figure 2b shows the value of the Lorenz coefficient for each coarse cell in the model. Finally, a threshold value for Lc is chosen and those cells with Lc > threshold also receive special consideration in the upscaling process.

If we consider, for example, an Lc threshold of 0.6, some additional cells are added to the primary system. Therefore, the final upscaled cells that are modeled with the two-system (DP/DP) approach will become more representative of the main reservoir flow contribution and of the heterogeneities. Figure 2 also shows the final coarse-scale model highlighting the DP/DP cells in white and the regular single porosity (SP) cells in black. Figure 2c is the division result after the global criterion and Figure 2d is the final model division after global and local criteria, including some additional heterogeneous cells for the special treatment group.

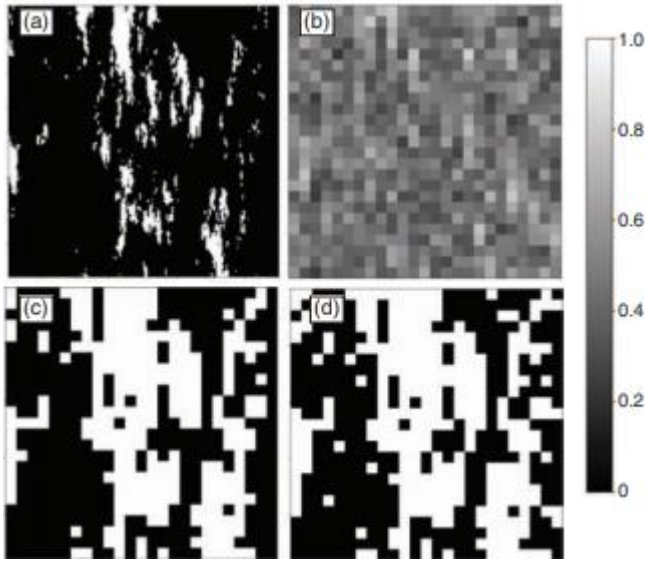

Figure 2. (a) Upper left image: Fine-scale system divided in main (white cells) and secondary (black cells). (b) Upper right image: Lorenz coefficient calculated for each coarse-scale cell with an upscaling ratio of 64. (c) Lower Left image: coarse model division in DPDP cells and single porosity cells after global criterion only. (d) Lower right image: resulting coarse model division after global and local criteria. In both images, white cells represent those with special treatment (DPDP cells) and black, those with a regular upscaling approach

When a coarse cell is marked as DP/DP after the local Lc criterion, this group of fine cells is divided into primary and secondary systems before the next step, which calculates the properties (porosity and permeability). To accomplish this, a local F-C diagram is calculated

for these fine-scale cells, and the same threshold used in the global criterion (0.75 in this example) is applied. With this approach, the volume fraction of each system is obtained, and the porous media division is completed. Figure 3 illustrates this process.

Finally, Figure 4 represents the fraction of the primary system in each coarse-scale cell. All white cells have primary and secondary system properties in the DP/DP upscaled model, while the black cells are modeled as SP cells and treated using a regular upscaling procedure.

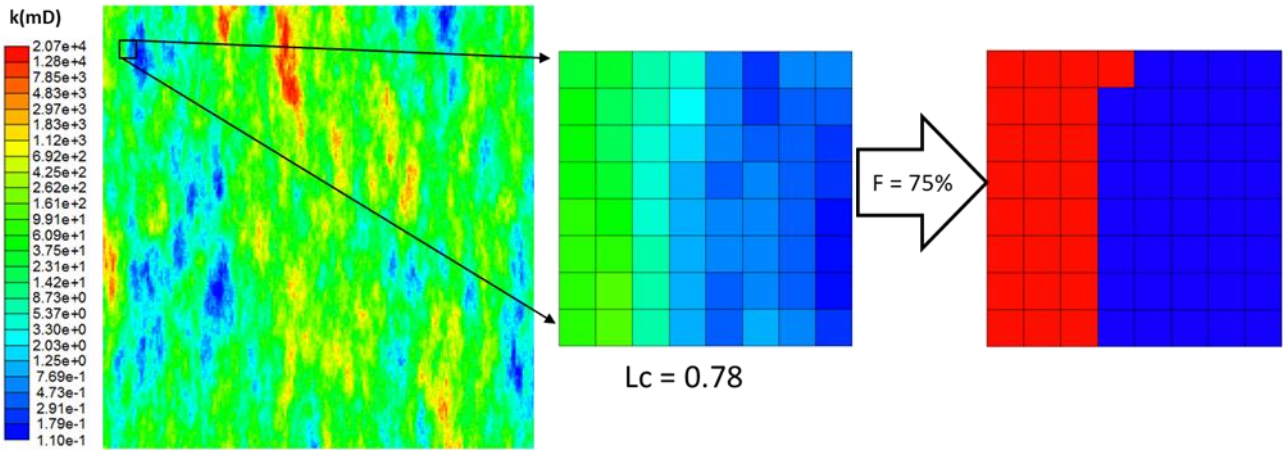

Figure 3. Detail of a group of fine-scale cells of a specific coarse block with Lc > threshold. The permeability value of each fine cell is shown in the second figure. The porous media division into the two systems is shown on the right: cells in blue are part of the secondary system, while the red are part of the main system.

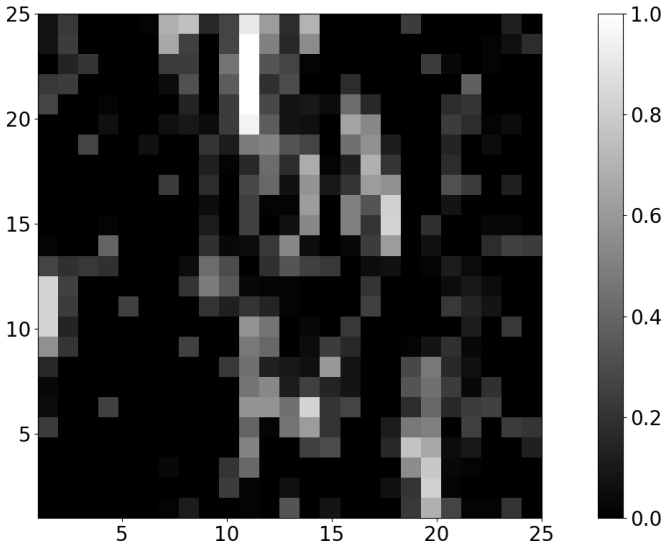

Figure 4. The fraction of the primary system in each coarse-scale cell. Black cells (no main fine-scale cells included) will be treated as regular single porosity cells.

Coarse Scale Properties Calculation

Once the coarse-scale cells are properly divided into primary and secondary systems and the fraction of the primary system contribution is obtained, the second step of the upscaling procedure is performed. In this stage, porosity and permeability are calculated for each coarse grid block cell.

The two possible treatments for the coarse cells are SP or DP/DP. For the first group, regular upscaling is performed, since these cells are exclusively part of the secondary systems. As previously mentioned, porosity is upscaled by the volumetric weighted arithmetic mean procedure and permeability by Cardwell-Parsons directional upscaling. For the second group, the same methods are used but for each system separately.

To illustrate how the upscaling is applied for each system on DP/DP coarse-scale cells, consider the group of fine cells highlighted in Figure 1. After the first step of this methodology, the fine-scale model is divided into subsystems. Therefore, part of the fine cells in this group are treated as the primary system, while the rest is treated as the secondary system. Figure 5 shows in detail how the cells are divided according to their flow importance. Note that, for the future coarse-scale representation, the cells more likely to contribute to flow, in red, less likely, in blue.

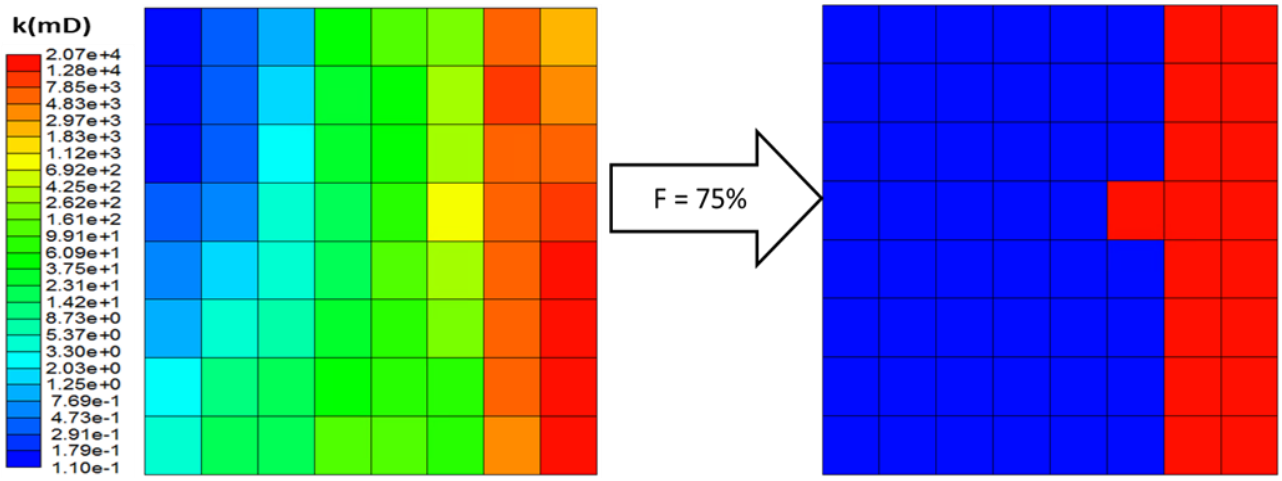

Figure 5. Detail of the group of fine-scale cells highlighted in Figure 1. The permeability value of each fine cell is shown on the left. The porous media division into the two systems is shown on the right: cells in blue are part of the secondary system, while the red are part of the primary system.

The porosity for each system in DP/DP cells can be obtained directly from the porosity of fine-scale cells. A general way to calculate this property for the primary and secondary systems is shown in Equations 1 and 2, respectively.

$$\phi_{I,main} = \frac{\sum_{i=1}^{nx} \sum_{j=1}^{ny} a_{i,j}\phi_{i,j}}{n_x n_y} \quad \text{.....1}$$

$$\phi_{I,secondary} = \frac{\sum_{i=1}^{nx} \sum_{j=1}^{ny} (1-a_{i,j})\phi_{i,j}}{n_x n_y} \quad \text{.....2}$$

In the above equations, $a_{i,j}$ represents the division coefficient and equals 1 when the fine cell belongs to the primary system and 0 to the secondary system. $\phi_{i,j}$ is the fine-scale cell porosity and $n_x\ n_y$ are the total number of fine cells in directions x and y in a coarse-scale cell I.

To proceed with the permeability upscaling calculations for each system independently, first, all the fine-scale permeability values must be filled at a given coarse-scale cell in both systems. In other words, considering Figure 5, the permeability must be assigned for the secondary system cells (blue) when upscaling the primary system and also values for the primary system cells (red) when the secondary system is upscaled.

In the presented method, for the primary system permeability upscaling calculations, we propose the average value of the primary system cells as the value for all secondary fine cells. The same is applied for the secondary system, but replacing the primary system permeability values with the average of secondary cells permeability. This allows the upscaling without adding an external bias to the permeability behavior of either system. Figure 6 schematic illustrates this procedure in a synthetic example.

After the above steps, the permeability assignment of all DP/DP cells in the coarse model is completed. The Cardwell-Parsons permeability upscaling can then be applied directly. According to this approach, the equivalent permeability in a given direction is limited by two values: an upper limit (L_1), given by the harmonic mean of the arithmetic means of the local permeabilities, and a lower limit (L_2) calculated by the arithmetic mean of the harmonic means, in both directions. Figure 7 shows a simplified schematic of this procedure. More details can be seen in Cardwell and Parsons (1945), Renard et al. (2000), and Maschio and Schiozer (2003).

The values of limits L_1 and L_2 for a 3D system can be calculated, for each direction, as follows:

$$L_1^x = \mu_h^x(\mu_h^y(\mu_a^z)) \ , L_2^x = \mu_a^z(\mu_a^y(\mu_h^x)) \quad \text{.....3}$$

$$L_1^y = \mu_h^y(\mu_a^x(\mu_a^z)) \ , \ L_2^y = \mu_a^z(\mu_a^x(\mu_h^y)) \ \text{.....4}$$

$$L_1^z = \mu_h^z(\mu_a^y(\mu_a^x)) \ , L_2^z = \mu_a^x(\mu_a^y(\mu_h^z)) \ \text{.....5}$$

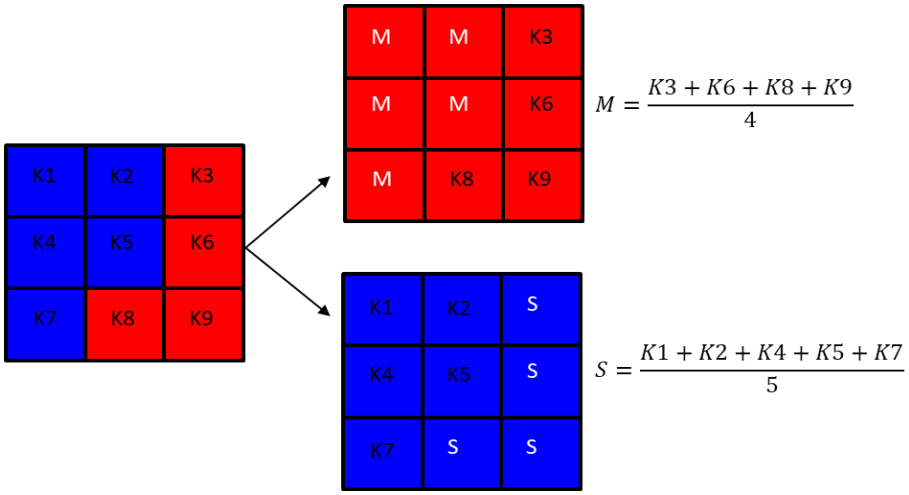

Figure 6. Permeability division before upscaling. Red represents the primary system and blue, the secondary. For the primary system, the original secondary system cells are replaced by the average permeability of the primary system cells. The opposite happens for the secondary system. In this figure, M is the average primary system permeability and S is the average secondary system permeability.

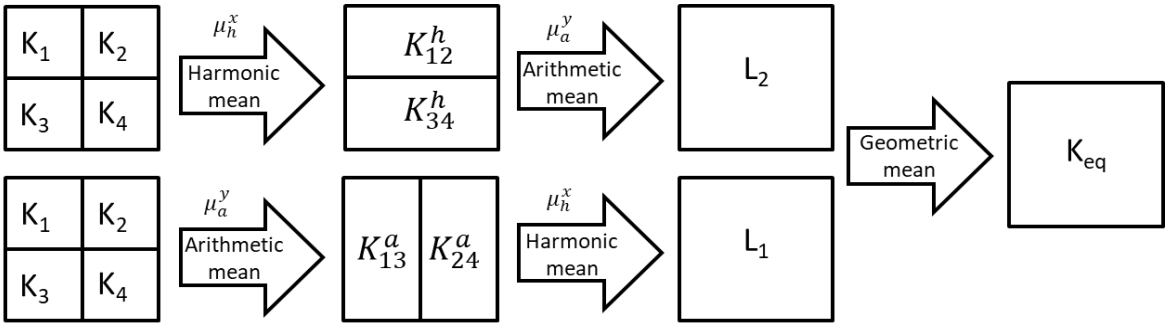

Figure 7. Cardwell-Parsons permeability upscaling approach scheme (adapted from Maschio and Schiozer, 2003).

With coarse-scale porosity and permeability for the primary and secondary systems, the upscaled model can be simulated using a classical dual-permeability approach, and different upscale ratios can be applied considering the same steps mentioned in the previous sections.

Case Studies Description and Applications

The new dual-porosity dual-permeability (DP/DP) upscaling technique is tested in three different applications. Specific evaluations are performed for each application to better test the flexibility and robustness of the proposed methodology.

The first application, A1, uses the same 2D heterogeneous reservoir that was used both to explain the methodology and in the motivation for this work. In this case, different well

configurations are tested to show how the proposed technique behaves for different flow conditions in the reservoir. Four schemes are presented, three different well-pair positions and one 5-spot with a central injector well. In this application, the objective is to emphasize the robustness of the proposed upscaling in different flow and transport situations. The coarse-scale uses 40x40 m² grid block cells, which yields an upscaling ratio of 64, since the reference fine model grid block cells are 5x5 m².

For the second application, A2, the reservoir fine model is the 37th layer of the classical 10th SPE Comparative Solution Project (Christie and Blunt, 2001). This layer is part of the lower portion of the model and is characterized by high heterogeneity and the presence of a channelized fluvial system. Several authors that investigated upscaling approaches (Zhang et al., 2008; Evazi and Jessen, 2014; and Iranshahr et al., 2014; among others) also considered some layers of this benchmark as a case study, as it is challenging to achieve a proper representation in coarse-scale models.

The main objective for the A2 application is to evaluate different upscaling ratios (URs) to verify the sensibility of the coarse-scale results. It is well known that traditional upscaling procedures tend to be highly sensitive to different upscaling levels and this application tests how our technique performs when the fine-scale model is upscaled in three different URs (4, 16, and 50).

The last application, A3, is a probabilistic evaluation. Five hundred fine-scale permeability realizations with the same area and grid block size of the A1 model are considered. These realizations were randomly created, varying permeability mean, standard deviation, anisotropy range and azimuth angle. In this application, we investigate how the proposed methodology can be applied to the global improvement of the coarse model representation, including when multiple permeability realizations are considered.

In all comparisons, the choice for the traditional upscaling method was between Cardwell-Parsons (CP) and flow-based upscaling approaches. In each case, since we simulated the fine-scale models as reference, we could compare CP and flow-based performances to choose the representative single-phase upscaling method. For application 1 and 3, CP and flow-based results were similar, and flow-based was the best option for the models in application 2. However, we understand that fine-scale simulation results are not typically available and, in general, flow-based upscaling tends to be the best single-porosity option for upscaling heterogeneous reservoir models.

General characteristics of each application are summarized in Table 1.

Table 1. General characteristics of the reservoirs for the three applications.

	A1	A2	A3
Fine-scale grid cells	200x200x1 with 5x5x5 m^3	60x220x1 with 6.096x3.048x0.6096 m^3	200x200x1 with 5x5x5 m^3
Permeability	Figure 1	37th layer SPE10	Multiple realizations
Porosity	Constant = 0.15	37th layer SPE10	Constant = 0.15
Fluid Model	See Rios et al. (2017, 2018)	See Christie and Blunt (2001)	See Rios et al. (2017, 2018)
Well scheme	Well pairs/5-spot	5-spot (4P, 1I)	One pair
Injected fluid	Immiscible Gas	Water	Immiscible Gas and Water
Producer bottom hole Pressure (bar)	400	See Christie and Blunt (2001)	400
Initial reservoir Pressure (bar)	640	See Christie and Blunt (2001)	640
Relative Permebility	Corey model: Swi = 0.2 Sor = 0.3 no = 3 nw = 2 Kro(@Swi) = 0.7 Krw(@Sor) = 0.5	See Christie and Blunt (2001)	Corey model: Swi = 0.2 Sor = 0.3 no = 2 nw = 2 Kro(@Swi) = 0.7 Krw(@Sor) = 0.7
Main objective	Robustness to different flow conditions	Evaluate sensibility to different UR	Probabilistic robustness of the technique

Results and Discussions

Next, results and discussions regarding each of the three applications are presented. The performance of the proposed upscaling approach (which we will refer to as DP/DP) is compared with the fine-scale reference models and the traditional single-porosity upscaling (SP).

Application 1

In application 1, continuous immiscible gas injection is applied in a highly heterogeneous reservoir with permeability distribution, shown in Figure 1. The reservoir fluid is a light oil represented by a black oil version of the seven-pseudo-component fluid model presented by Rios et al. (2017, 2018). The initial GOR is 215 m^3/m^3 and the saturation pressure is 400 bar.

The chosen grid block size for the coarse models is 40x40x5 m^3, an upscaling ratio of 64.

Before conducting the gas injection evaluations, however, a basic single-phase test was performed. This is to show the ability of the proposed DP/DP upscaling to reproduce fine-scale well rates at a fixed well bottom-hole pressure, and the pressure drop at a fixed production rate. In this evaluation, we placed a producer well in the center of the reservoir and performed a 400-day test, divided into three parts. First, depletion with a constant well-rate (for 180 days), followed by a static period of 60 days. Finally, for the last 160 days, the well BHP was fixed at 500 bars (saturation pressure).

Following this, four different well configurations are analyzed to effectively test the performance of the proposed upscaling procedure under different flow conditions. Since this technique does not use any dynamic results of the fine-scale model to generate the coarse model, the capability of improving the results (production and injected fluid displacement behavior) of the traditional upscaling methods is a meaningful achievement of this work. As previously mentioned, this is the main objective of application A1. Figure 8 shows all the well configurations investigated in this application. The first one, Pair 1, is a well-pair scheme with an injector located at the upper-right corner and a producer at the lower-left corner. The second scheme, Pair 2, consists of an injector at the upper-left corner and a producer at the lower-right corner. Then, for the last well pair, Pair 3, the injector is located at the same position as Pair 1 and the producer is in the middle of the lower limit of the reservoir. Finally, a 5-spot drainage plan is considered, with one central injector and four producers, one in each corner. In all analyses, the injection was set to keep reservoir pressure at the original value and the minimum bottom hole pressure for the producers were 400 bar, which is the saturation pressure for the reservoir oil.

For the chosen coarse-scale model, the flow-based upscale was performed to obtain the traditional coarse model. To create the upscaled model with the new DP/DP upscaling technique, the two filters mentioned in the described methodology, global flow capacity (F-C) and local Lc can be used as manual fitting parameters for the ranking of the main/secondary systems. For heterogeneous systems, our studies indicate that an initial filter for flow capacity of 70% is a good initial estimate.

This current application yielded good results for the upscaled model considering a flow capacity filter of 65% and an Lc cutoff of 0.8. Figure 9 shows the upscaled permeability for both SP and the new DP/DP coarse models. Note that, the primary system in the new approach has an important role in representing the possible preferential paths that usually are smoothed out when the coarse-scale model is constructed. Thus, the upscaled model in this new approach is more likely to honor breakthrough of the injected fluids and to reduce the usual optimistic bias that standard upscaled models tend to present, due to the loss of sub-grid heterogeneity resolution and the smoothing of small-scale phenomena.

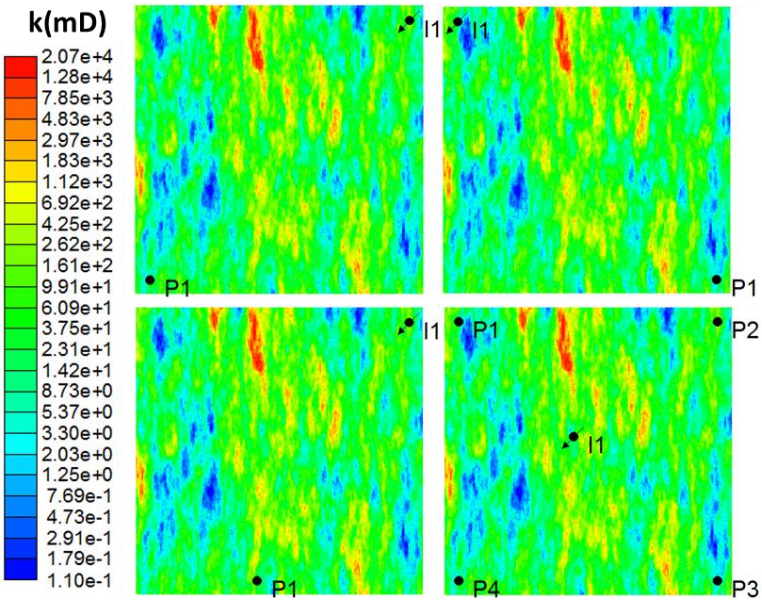

Figure 8. Fine-scale permeability map used as a reference to show the four different well configurations considered in A1. From top to bottom and from left to right, we have Pair 1, Pair 2, Pair 3, and 5-spot.

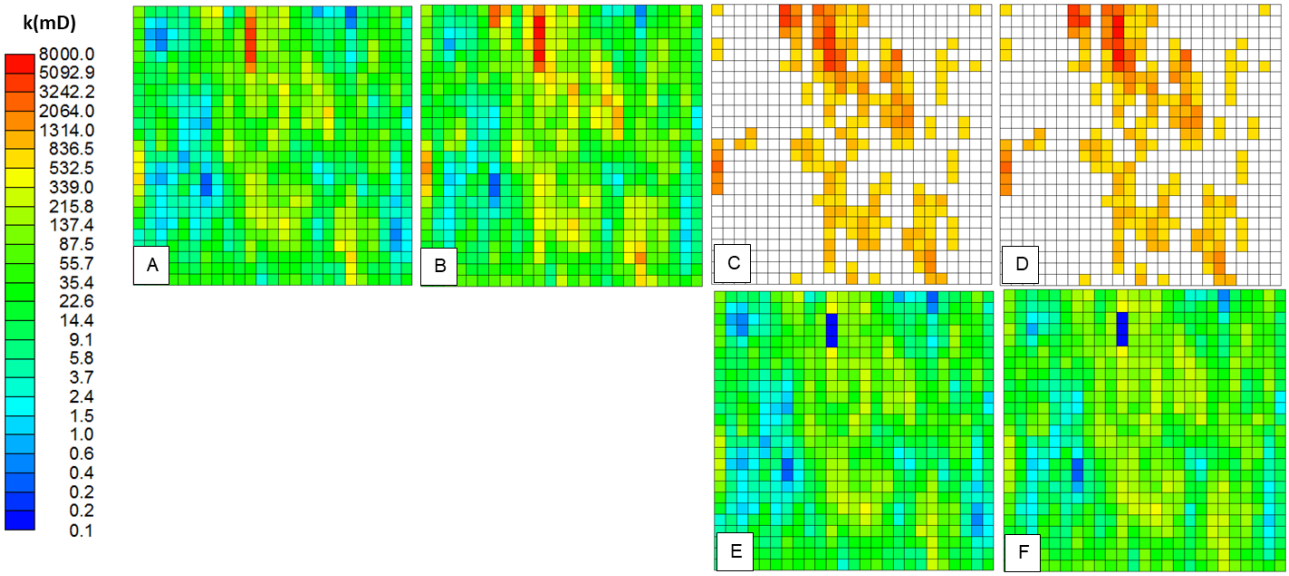

Figure 9. Upscaled permeability maps: permeability in J direction on the right and in I direction on the left. A and B relate to SP upscaling. C and D are primary system permeabilities (white cells are single porosity cells), while E and F are secondary systems final permeabilities.

Figure 10 shows the comparison between fine and coarse-scale DP/DP results for the single-phase evaluations performed with a centralized producer well. Note that, the proposed technique satisfactorily reproduces fine-scale results in this basic test. The coarse-scale DP/DP model was able to reproduce pressure behavior at a fixed well rate and production behavior at a fixed BHP.

Figure 11 compares the production curves for each well configuration of application A1. Notably, the DP/DP upscaling technique improved the coarse-scale simulation results in all cases. Although no dynamic response of fine-scale model was used to calibrate the proposed upscale model, the results are noticeably closer to the reference.

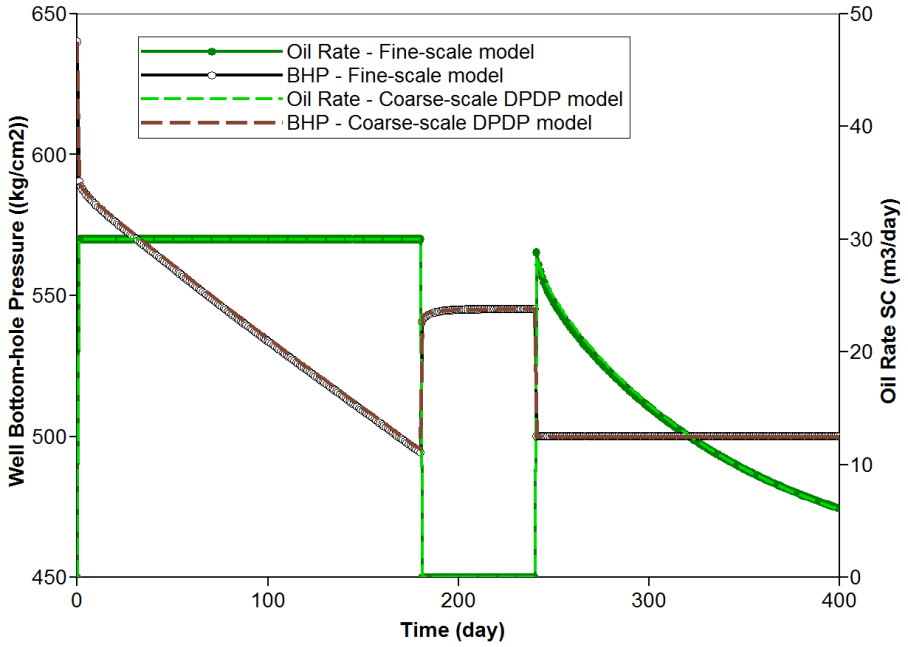

Figure 10. Comparison between fine-scale and DP/DP coarse-scale results. Basic single-phase conditions are tested. First constant well rate and in the end, constant BHP.

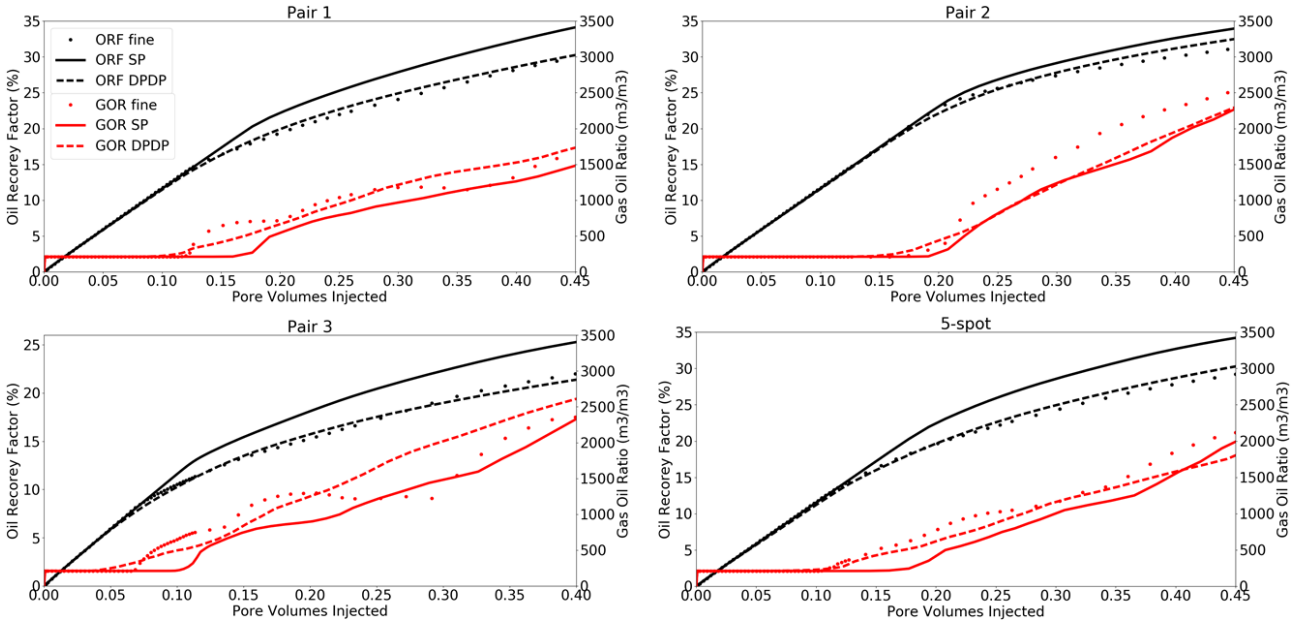

Figure 11. Oil Recovery Factor (black) and Gas-Oil Ratio (red) comparison of the fine reference model (dotted), the SP upscaled model (solid lines) and the new DP/DP upscaling technique (dashed lines) for Pair 1, Pair 2, Pair 3 and 5-spot.

Common limitations of coarse-scale models are the prediction of injected fluid breakthrough and the reproduction of non-uniform sweep behavior in heterogeneous systems. Both effects are visibly better represented by the proposed methodology.

Note that, for Pair 2, the injected gas path was not dominated by the high permeability corpus. Thus, the traditional coarse model presented the closest agreement with the fine model in this configuration. However, even in this case, the new coarse model performed generally better, mainly because of the improved representation of the sub-grid paths in the central part of the reservoir.

Analyzing the results for Pair 1 and Pair 3, close agreement with the fine-scale model is observed for both gas breakthrough and oil recovery factor. This is a natural consequence, as these configurations include the path between injector and producer within most of the regions dominated by the primary system cells.

Finally, the 5-spot scheme is an interesting closure for this application, because the central injected gas can explore most of the reservoir heterogeneities at the same time. As shown in Figure 11, the new upscaling technique compares favorably to the fine-scale reference results.

Besides the comparison of production curves, a qualitative evaluation of the injected fluid toward the front and saturation variation throughout the reservoir is also important to assess the upscaling performance.

For this purpose, we highlight, in Figure 12, the gas saturation map of the four well configurations discussed in this application. In each figure, four images are shown and the fine-scale breakthrough time is considered as a reference for each comparison. The first two images are the references as they result from the fine-scale model. Image A is the fine-scale saturation map and B is the same profile averaged to the coarse-scale in the study. The latter is the reference map for comparison, since it represents the fine-scale map averaged to the same scale of the coarse models, thus making the analysis more straightforward. The last two images are from upscaled coarse models. Image C represents the traditional upscaling approach and D, the proposed DP/DP upscaling technique.

By observing the profiles of the saturation maps, it is possible to distinguish the quality improvement of the coarse-scale results of the new over the traditional methodologies. With our new DP/DP approach, the injected gas front and sweep behavior are consistently closer to the average fine-scale results. This happens for all investigated well configurations and it is an important indicator of the robustness of the new upscaling technique under different flow direction conditions.

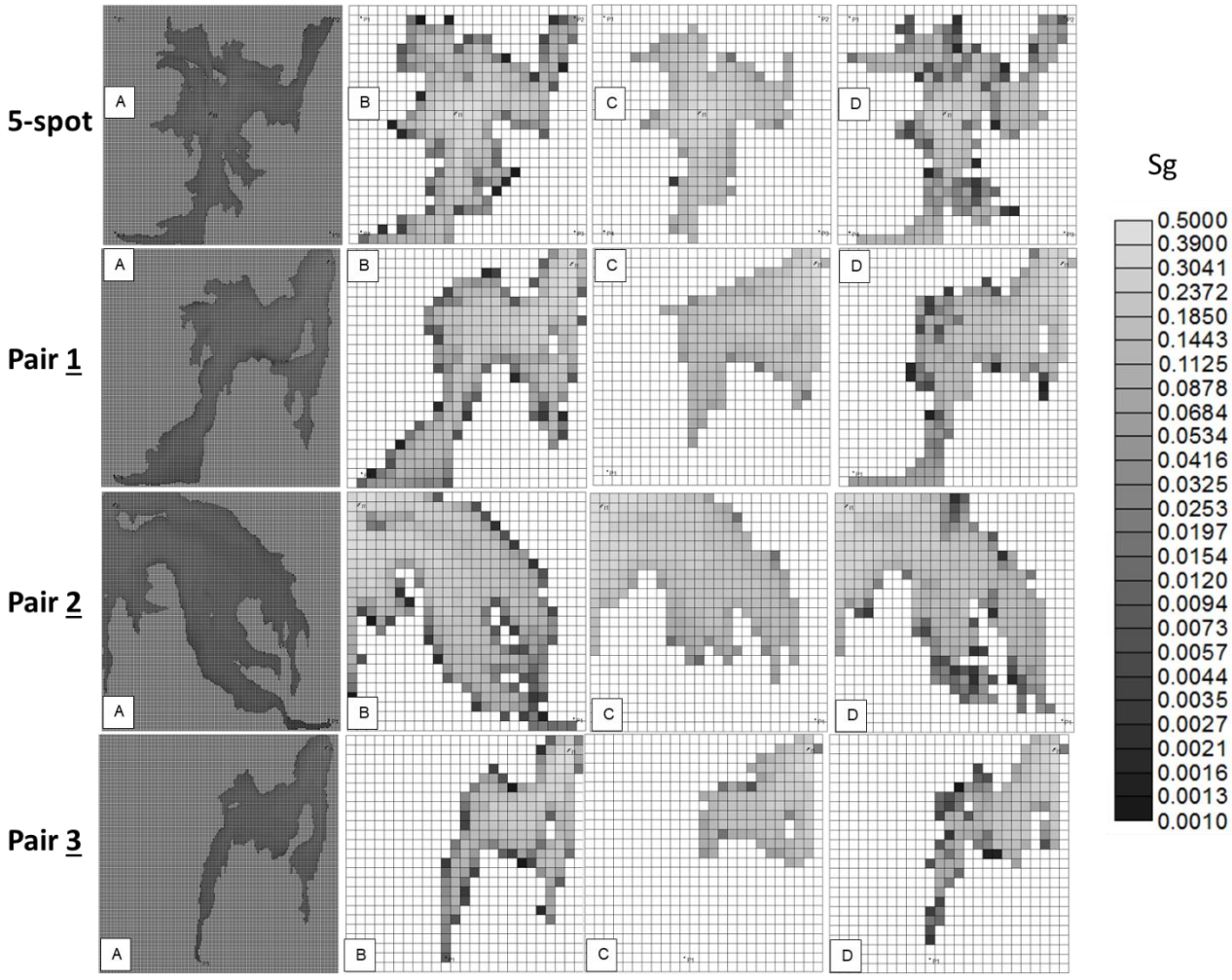

Figure 12. Gas saturation map at breakthrough for the fine-scale model with 5-spot configuration in the first row, Pair 1 in the second row, Pair 2 in the third and Pair 3 in the fourth. A: fine model, B: fine-scale saturation map averaged to the coarse-scale, C: SP upscaled model, and D: DP/DP upscaling technique.

Finally, results from application A1 are crucial to show an important and desirable feature of an effective upscaling procedure; the independence of a specific well configuration. Different from what is observed in most upscaling procedures that used dynamic data from a fine-scale model to obtain the coarse models, our approach used only static information and shows consistency in the improvement of traditional upscaling results.

Application 2

For this application, the main objective is to test the proposed methodology under different upscaling ratios. For this, layer 37 of SPE10 benchmark is considered. The general characteristics of this model and the reference for specific details were previously mentioned in the Case Studies Description and Applications. We adapted the water injection rate to 1.5 m^3/d because of the reduced pore volume of a single layer in the study. Furthermore, we introduced a maximum liquid rate production of 0.8 m^3/d as a constraint for the system, so this application more closely resembles real industry projects.

The original fine-scale reservoir is highly heterogeneous and channelized. This Cartesian system is represented by 60x220 cells, permeability varies from 0.004 to 20 000 mD and porosity from 0.001 to 0.4. To investigate the impact of different coarse-scale models, the original model was upscaled to 30x110, 15x55, and 12x22, which are equivalent to upscaling ratios of 4, 16, and 50, respectively.

Figure 13 shows the permeability map for the original fine-scale model and all upscaled models for this application. Note that as the model gets coarser, the less visible marked heterogeneous channels are. This behavior has an important impact on the simulation results, since coarse models tend to overestimate the sweep efficiency and delay water breakthrough with the smoothing of channelized paths present in the fine-scale.

Because of these aspects, this application is a challenging test to check the robustness of upscaling techniques regarding the capability of honoring the results of the original model in progressively coarser models.

For the three coarse models considered in A2, we used a fixed flow capacity filter of 70% and an Lc cutoff of 0.8. While these filters could have been tuned, the results were satisfactory with the proposed initial estimate.

Figure 14 illustrate the cumulative oil production and water cut for all models. Results for the traditional upscaled models are shown in solid lines, while the new DP/DP technique results are in dashed lines.

Traditional models become more optimistic the coarser they are. This behavior is observed in the higher cumulative oil productions and in the postponed water production breakthrough. Furthermore, the upscaled models are noticeably sensitive to the upscaling ratios.

The results from the coarse models created with the new DP/DP upscaling technique, not only presented a closer agreement with the fine-scale production curves, but also showed to be less sensitive to the upscaling ratio. The coarse models performed significantly better than their equivalent with the traditional upscaling procedure. Additionally, they were close to each other in predicting field production, even with UR varying from 4 to 50.

The challenging analyses in A2 were useful to highlight the capability of the proposed technique. The results indicate that coarse production curves closely match the original fine-scale curves, when the upscaling procedure of the coarse models captures a better representation of the main reservoir heterogeneities, even when they occur on smaller scales. Finally, results from this application suggest that models can be upscaled further, without compromising the overall production results. This is of interest to produce feasible and more reliable simulation results for giant oil fields.

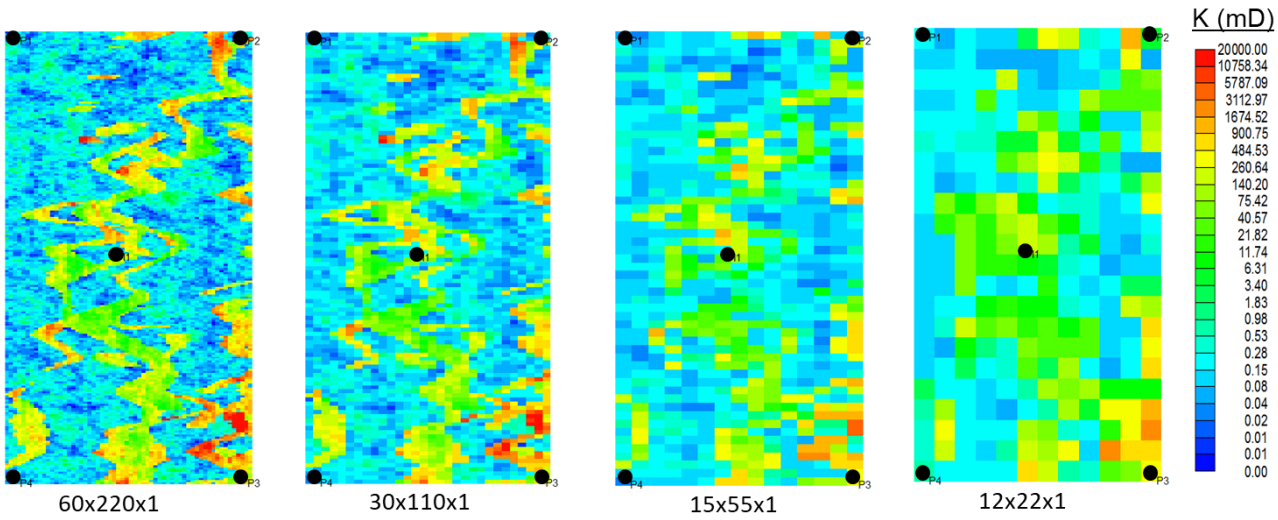

Figure 13. Permeability (I direction) for all models considered in A2.

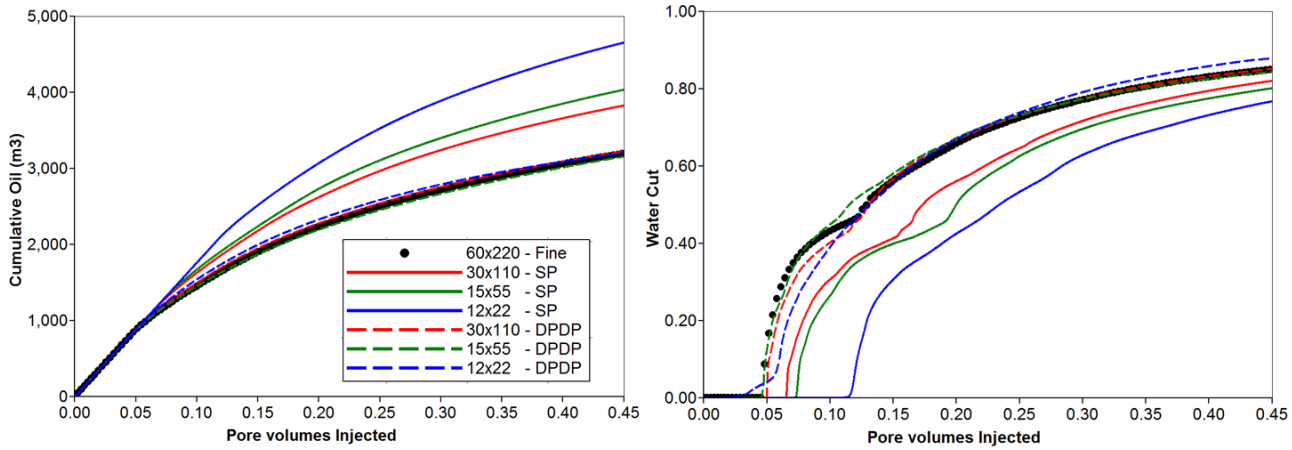

Figure 14. Comparison of Cumulative Oil production (left) and Water Cut (right) between original fine model and coarse models.

The results and discussions presented for the above applications focused on the upscaling technique and its impacts on the simulation results. Another consideration is the speed of simulation runs using coarse-scale models. We showed a noticeable improvement achieved with the coarse model results by applying the proposed methodology. Table 2 summarizes the computational performance for A1 and A2, emphasizing the speed of coarse-scale models compared to fine-scale models, while maintaining good agreement in the production curves.

Note that no numerical optimization was performed on the models, so the results are a relative comparison. Nevertheless, all models can be numerically improved, as shown by Avansi et al. (2019).

Table 2. Simulation time for the models in A1 and A2

	Elapsed time (s)						
	A1				A2		
	Pair 1	Pair 2	Pair 3	5-spot	UR4	UR16	UR50
Fine-Scale	2966	3765	3078	3490	775		
SP upscaling	27	34	36	33	131	56	52
DPDP upscaling	36	44	45	42	220	87	57

Application 3

Applications 1 and 2 focused on testing the robustness of the new upscaling technique under two conditions: variation of well configuration (A1) and performance with different upscaling ratios in a highly heterogeneous system (A2). These studies showed good results and were applied in deterministic simulation models. To complete the evaluation of the DP/DP upscaling technique, application 3 focuses on probabilistic studies, i.e., instead of applying the methodology to a specific reservoir permeability model, multiple permeability realizations are considered, and the final coarse-scale uncertainty curves are compared to those of the fine-scale.

In this study, the reservoir area is 1 km² and the fine model is represented by 200x200x1 Cartesian grid block cells, each measuring 5x5 m². Then, 500 lognormal permeability realizations are randomly created, varying the mean, standard deviation, and anisotropy range properties, as summarized in Table 3. For the dynamic evaluation, the same conditions as applied to A1 were considered, but waterflooding was used as the enhanced recovery method. The well configuration was that of Pair 2, i.e., a well pair with an injector at the upper left corner and a producer at the right lower corner.

Three different coarse model sizes were considered for the coarse-scale evaluations: 50x50x1 (UR 4 with grid-blocks of 20x20 m²), 25x25x1 (UR 64 with grid-blocks of 40x40 m²), and 10x10x1 (UR 400 with grid-blocks of 100x100 m²). All the 500 realizations were upscaled for the three sizes with both traditional and the DP/DP upscaling approaches.

Table 3. Summary of properties for the 500 permeability realizations

	Min	Max
Mean (mD)	2.68	1330
Standard Deviation (mD)	10.14	2017
Major Direction (m)	101	999
Minor Direction (% of major)	10%	90%
Azimuth	-89.8	89.9
Global Lc	0.09	0.94

For multiple models, uncertainty curves (Risk curves, or S curves) for final oil recovery factor are used to compare the general behavior of fine and coarse models. The reference curve is generated by the results of all the realizations in the fine-scale.

The first evaluation performed in this application is the sensitivity to three global flow capacity filters in each coarse-scale model. We aimed to select the best overall behavior for each coarse-scale model to identify any correlation between the global flow capacity filter and the applied upscaling ratio. Figure 15 shows the uncertainty curves for the three coarse-scale models. Each image focuses on one coarse-scale and there are five curves: the fine-scale results, the traditional coarse-scale and the three different filters applied with the new upscaling technique.

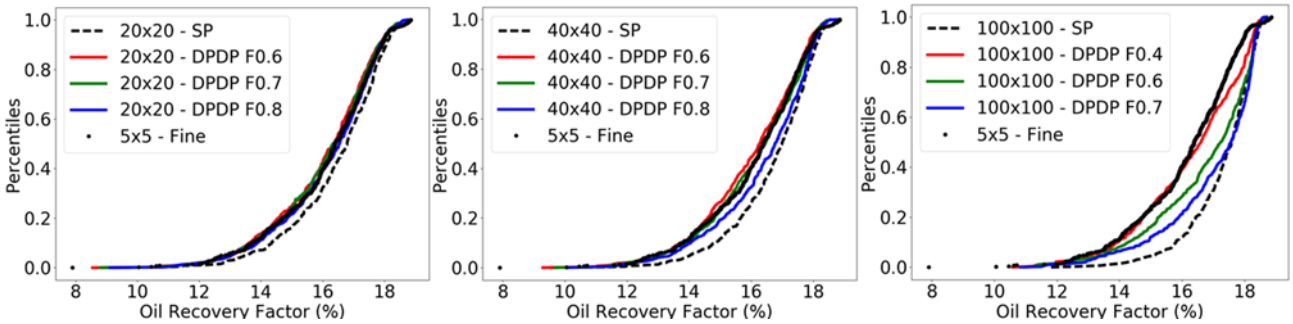

Figure 15. Sensitivity of different flow capacity filters on the uncertainty curves for final oil recovery factor of each coarse model. For the three groups of curves, the black ones represent the fine-scale (solid curves) and the SP coarse-scale (dashed) results.

Initially, only observing the traditional results, it is possible to confirm a general trend, indicating that the coarser the model, the more the results exaggerate those from the fine-scale. Results from the coarse models with 20x20 m² grid-blocks are relatively close to those of the fine-scale but slightly optimistic. This difference is evident in the intermediate coarse model (40x40 m² grid block cells), which is considerably greater than the coarsest model.

The results from the proposed DP/DP technique show consistent improvement on the coarse-scale performance. For the three different filters in each coarse model, the uncertainty curves behave closer to the reference than the traditional upscaling. However, it is possible to indicate the best overall results for each case. For UR 4, the differences are not significant, but the flow capacity filter of 80% (blue curve) has the better fit with the fine-scale results. UR 64 is better represented by a global flow capacity filter of 70% (green curve). Finally, UR 400 was the most challenging, since it is a very coarse model, but reasonably good results can be observed for flow capacity filter at 40% (red curve).

Although more studies and investigations are necessary for an in-depth conclusion, higher upscaling ratios tend to present smaller global flow capacity filters. In our cases, 80% for UR 4, 70% for UR 64, and 40% for UR 400. Furthermore, we fixed the local Lc in all evaluations at 0.8, because this filter works more effectively to improve the results of a specific model, which is difficult to analyze in multiple realization studies.

Figure 16 illustrates, in the upper left image, a summary of all the uncertainty curves for the final oil recovery factor. This illustrates how the traditional upscaling approach is sensitive to UR and how results can be improved with the new method. The new DP/DP upscaling and the equivalent traditional techniques are compared, demonstrating sensitivity to the coarseness of the model.

When working on deterministic cases with the proposed upscaling technique, it is possible to tune the filters for global flow capacity and a local Lorenz coefficient to achieve good agreement with fine-scale results, as shown in A1 and A2. However, for multiple realizations with different levels of heterogeneity, it is unfeasible to individually select the best set of filters for each realization. Despite this, using a fixed set of filters for each coarse-scale, consistently improved the uncertainty curves for the upscaled models, as highlighted in Figure 16.

Nevertheless, note that improving the overall uncertainty curves by improved individual realizations is not the key contribution of this work. Instead, the new DP/DP upscaling technique mitigates the bias in upscaling that traditional approaches generate, which is especially useful in multiple permeability realizations with varying heterogeneity.

To illustrate this aspect, Figure 16 shows histograms of relative error to the fine reference obtained for each coarse model. The error is calculated, for each permeability realization *i*, as shown in Equation 6:

$$Error_i = (ORF_{i,coarse\_model} - ORF_{i,fine\_model})/ORF_{i,fine\_model} \quad \text{..... 6}$$

Analysis of the histograms reveals, in a different way, the optimistic bias generated in traditional upscaling methods, which becomes more noticeable as the level of coarseness increases. The mitigating effect on positive bias of the new DP/DP upscaling technique is apparent in Figure 16 with a normal-like profile centered at zero.

Therefore, the new approach is an important improvement to reservoir engineering workflows, since uncertainty analyses are useful tools for better understanding and estimating oil field production behavior. The new DP/DP upscaling technique also achieves reliable results for large UR, giving flexibility to select a coarser simulation model for specific tasks without losing accuracy in results or creating a bias that can compromise the decision-making process.

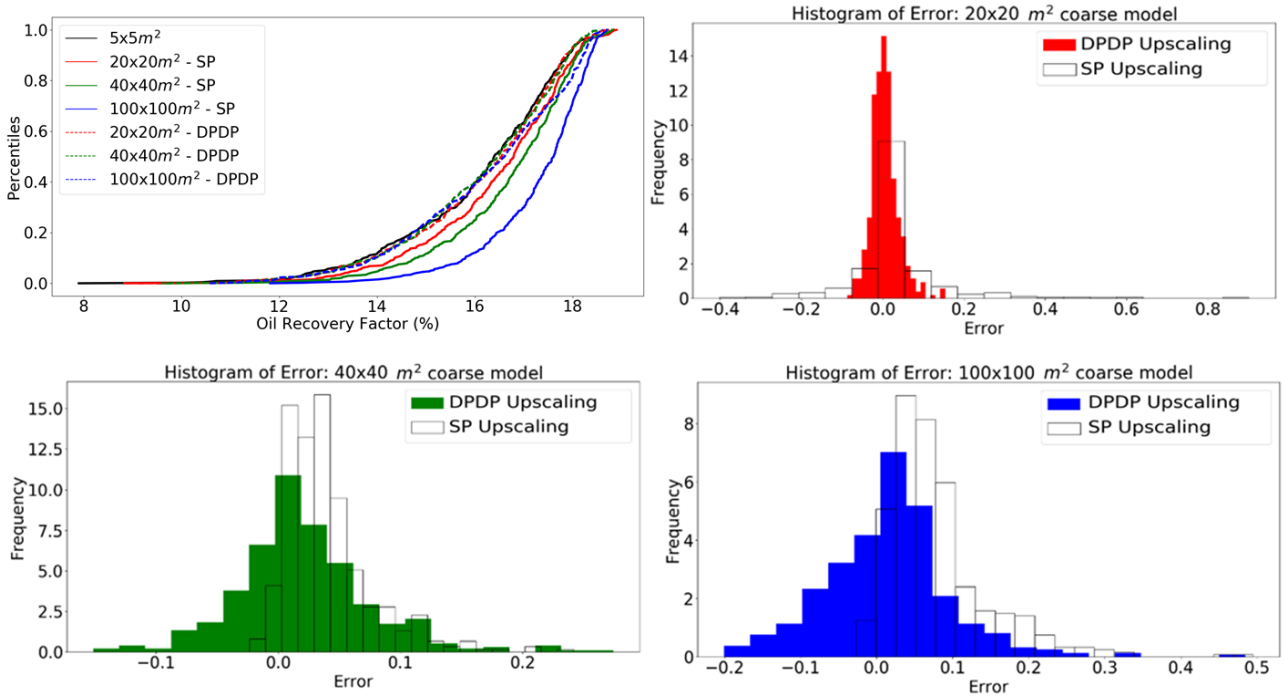

Figure 16. The upper left figure is a summary of all the uncertainty curves for the final oil recovery factor. The black curve is the fine-scale reference. Solid curves are SP upscaled results, while dashed curves are the DP/DP upscaling results. The other three images are histogram of error for each coarse model. In each image, the color histogram relates to the DP/DP upscaling results and the unfilled histograms represent the SP upscaling

Additional Analyses

In reservoir simulation, more significant errors in coarse-scale results are expected in channelized models than in variogram-based systems (Durlofsky, 2003; Chen and Durlofsky, 2006). An additional evaluation of the new DP/DP upscaling technique with a variogram-based permeability field investigates this fact and compares findings with A2.

For this study, we selected layer 12 of the SPE10 model (see Figure 17 for permeability map). The study uses the same coarse-model sizes applied in A2 (UR 4, 16, and 50) and the same dynamic conditions (well pattern and rates).

The results for cumulative oil production and water cut, comparing fine-scale and coarse-scale results are shown in Figure 18. In this figure, the upper graphs highlight the comparison with SP upscaled models. There is an observable link between a high URs and more optimistic coarse-scale results when compared to the reference. Conversely, the DP/DP results (lower graphs) showed to be more robust and less sensitive to the UR, as observed with layer 37 in A2.

However, comparing these results with those from A2 can generate other important observations. For the channelized layer 37, up to 20% error in the final cumulative oil

production was observed with a UR 4. This level of error was only observed for the variogram-based layer 12 with a UR 200 (an extra coarse model with only 6x11 cells). SP results for layer 12 presented less than 10% deviation in final oil production for UR 4, 16, and 50, which is considerably less than observed for the channelized layer 37 (final errors of 20%, 26%, and 45% for UR 4, 16, and 50, respectively).

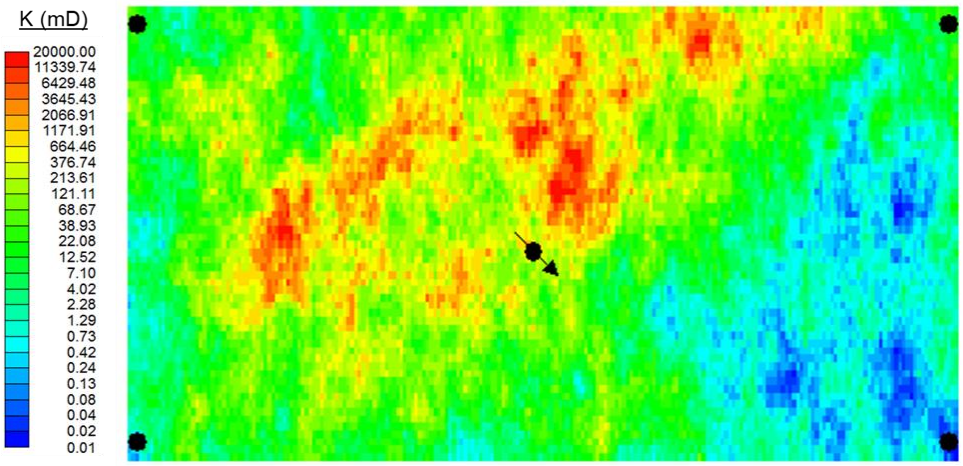

Figure 17. Permeability (I direction) for layer 12th SPE10

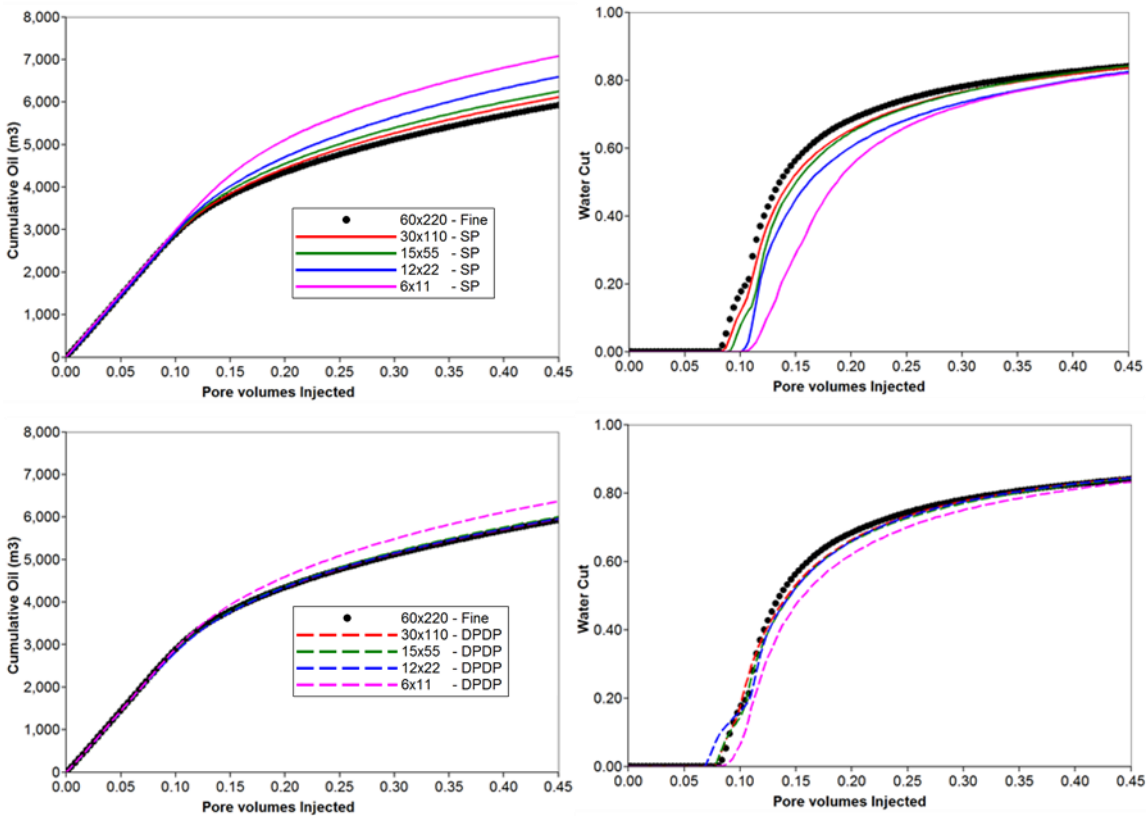

Figure 18. Cumulative oil production and Water Cut for fine-scale model (black) and coarse models (colored). Upper graphs show SP upscaling results and lower dashed curves, DP/DP upscaling results

Despite the lower impact using SP coarse models for layer 12, DP/DP coarse results were significantly better, with improved coarse results in all cases. The results with UR 4, 16, and 50 were almost identical to the fine-scale. Even when a more aggressive UR 200 was considered, the maximum error in oil production was 7.5%, which confirms the capability of the proposed methodology to provide consistently reliable coarse models.

We also evaluate different situations in the multiple permeability realizations study. The results presented in A3 considered water injection and a particular well pair configuration. We also reproduced the same simulation runs for two new conditions: gas injection (same as in A1) and a 5-spot well scheme.

Figure 19 shows that the same trend observed in A3 presented again when changing the injected fluid or the well pattern, i.e., the upscaled models with the proposed DP/DP approach presented a close agreement with the reference results. Therefore, the new upscaling technique is consistently robust enough to improve the coarse-scale results in reservoir simulation runs.

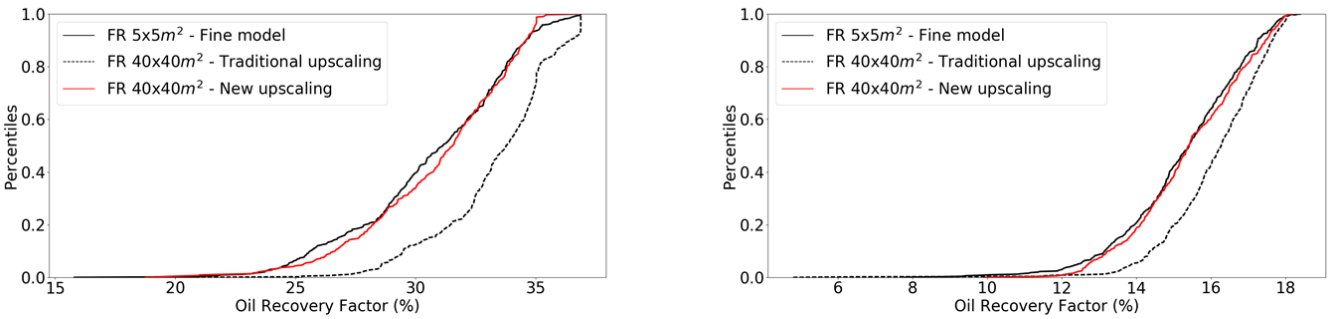

Figure 19. Summary of uncertainty curves for the final oil recovery factor with gas injection (left) and 5-spot pattern (right).

Discussion

In the present work, we introduced a new upscaling technique with a DP/DP approach for highly heterogeneous reservoirs. The methodology is based on two criteria with different, but complementary, objectives. The global guide selects the cells that most influence the flow behavior of the reservoir. It ranks the fine-scale porous media into primary and secondary systems considering the overall heterogeneity and flow capacity. The local Lorenz plot focuses on the group of fine cells in each coarse-scale block of the upscaled model. A coarse cell that presents a local Lorenz coefficient (Lc) above the threshold indicates a high local heterogeneity. Therefore, this criterion is important and useful to select regions with high local property contrast. However, this is insufficient to represent the regions with higher flow tendency in the reservoir.

For example, a group of fine cells in a coarse block can present an Lc below the threshold but still concentrate some of the most conductive cells in the reservoir. In such a scenario, if only local Lorenz is considered, this coarse cell would be treated entirely as secondary (SP), potentially reducing the efficiency of the methodology.

To illustrate this, consider the highlighted group of fine cells in Figure 20. In the upscaling process with a UR 64, these blocks form one coarse-scale cell with a local Lc 0.38, which is a low value. Thus, according to the local Lorenz criterion, no primary system cells would be considered in this group. However, if we observe the gas injection front in application A1 with 5-spot well configuration, shown in Figure 21, the non-homogeneous behavior of the gas pathway in this group of cells becomes notable, highlighted in the image on the right of Figure 21. This behavior would not be represented in the coarse model if the DP/DP approach with global criterion had not been applied, as shown in red in the right image of Figure 20.

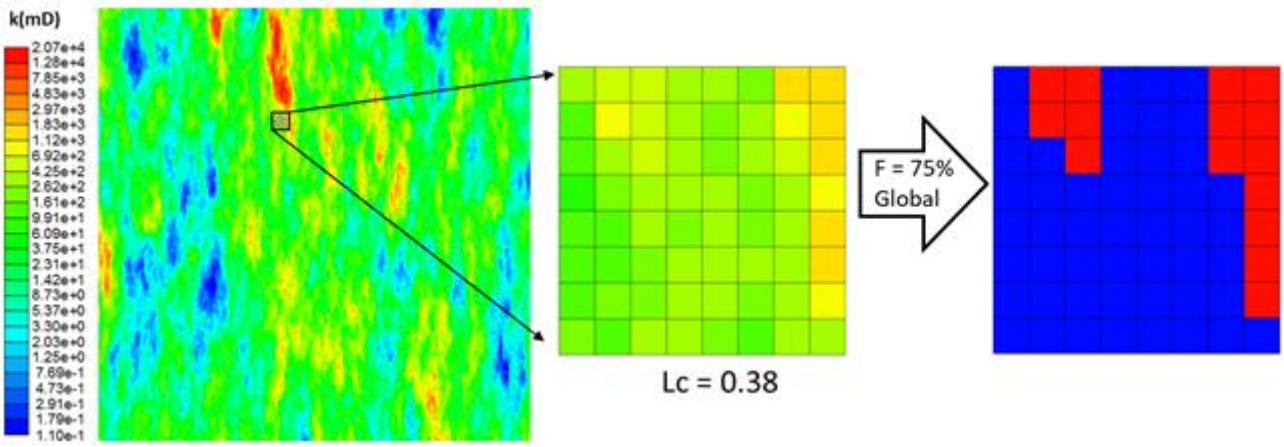

Figure 20. Detail of a group of fine-scale cells of a specific coarse block with low local Lorenz. The permeability value of each fine cell is shown in the second figure. The porous media division into the two systems, from the global guide, is shown on the right: cells in blue are part of the secondary system, while the ones in red are part of the primary system

Similarly, if only the global criterion was considered, coarse cells with high local contrast in the permeability would be treated as SP. This is also undesirable because the relative flow within this coarse cell system tends to occur heterogeneously, thus, splitting this cell into primary and secondary systems may be important. Figure 22 illustrates this through the gas saturation profile for A1 with pair 1 configuration at a certain time, emphasizing the same group of cells highlighted in Figure 3. Again, note the non-homogeneous behavior and, for a coarse cell to reliably represent the flow in this region, a DP/DP cell representing primary and secondary systems must be considered. The global criterion alone would not select any cell in this group as primary because of its relatively lower importance to the flow compared to all the

cells in the system. However, with the local Lorenz criterion, this important local heterogeneity (Lc 0.78) will be captured and this coarse cell will be DP/DP representing primary and secondary systems.

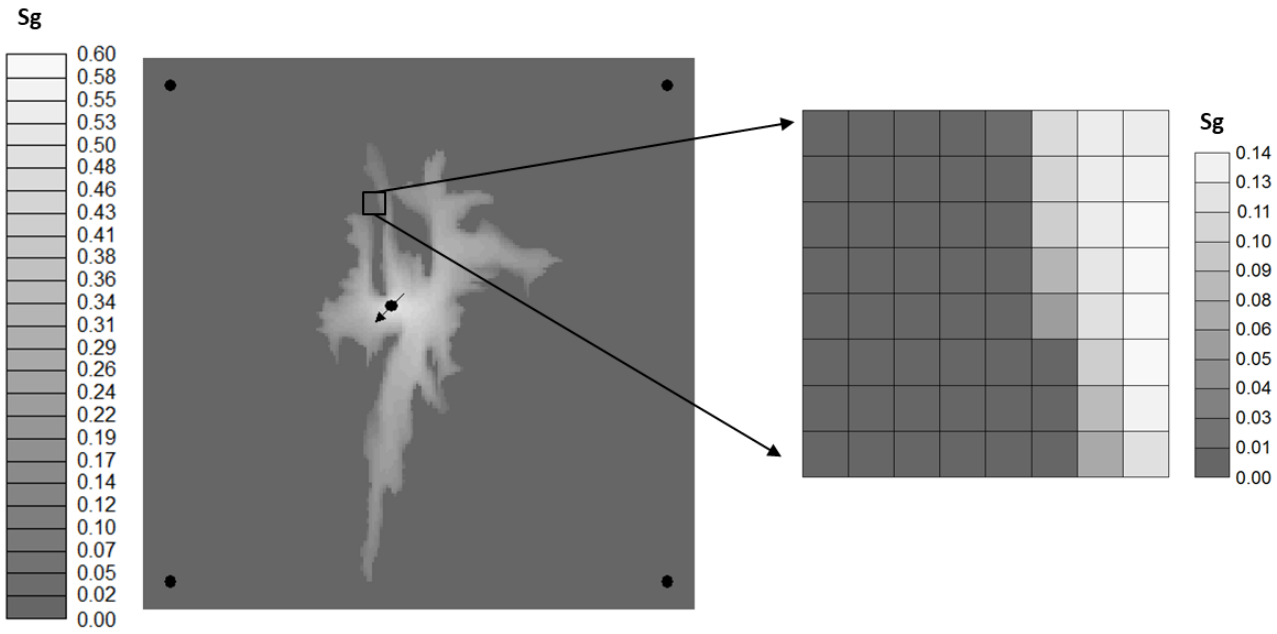

Figure 21. Gas injection map for A1 5-spot with detail for the same group of fine-scale cells shown in Figure 20. Zoom for the highlighted group of cells in the right image.

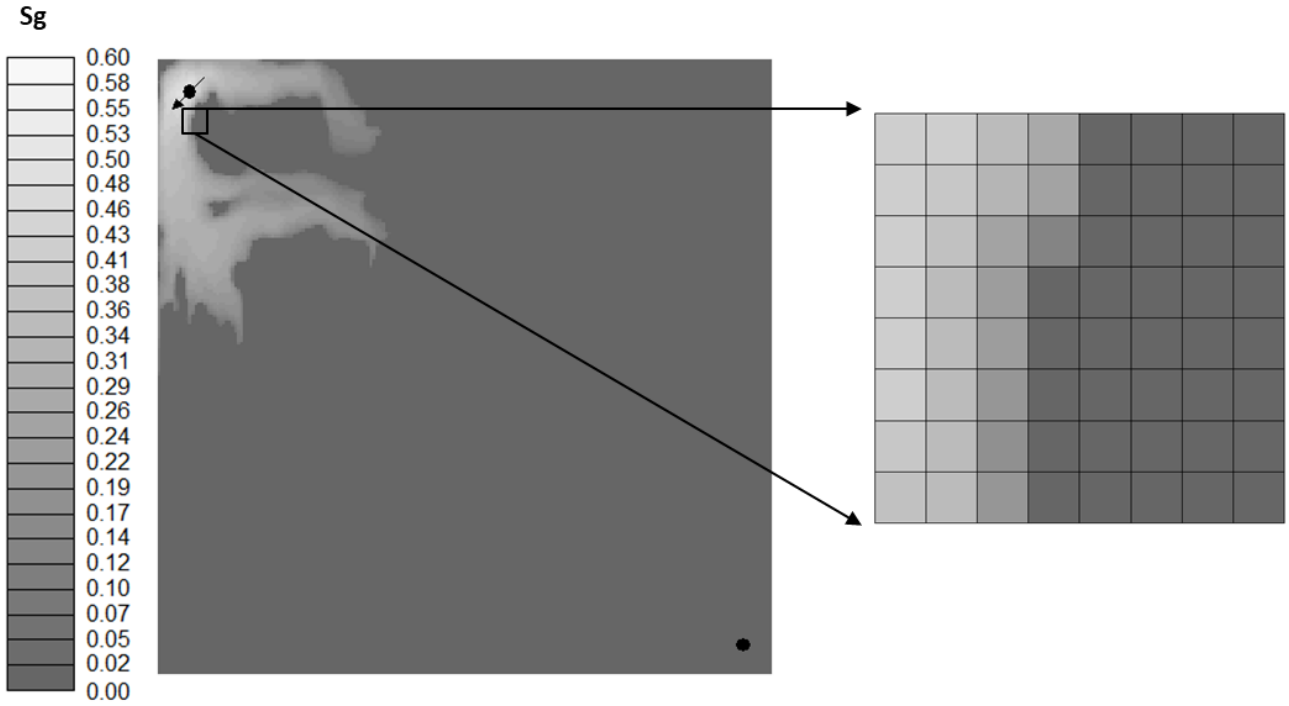

Figure 22. Gas injection map for A1 Pair with detail for the same group of fine-scale cells shown in Figure 3. Zoom for the highlighted group of cells in the right image.

Therefore, as previously mentioned, both criteria are complementary. The most influential flow regions in the reservoir are found through the global criteria. These are complemented by honorary primary cells - those secondary cells with highly heterogeneous behavior highlighted by the local Lorenz criterion.

Despite the difficulty of establishing a quantitative method to define a heterogeneous reservoir, we considered a highly heterogeneous reservoir a system where the fluid flow and transport are often dominated by preferential paths, like channels, or areas with high contrasts in the permeability field. In such conditions, at a local level, fluid tends to flow preferably in the high permeability regions, while lower permeable surrounding may contribute less to flow and transport.

A significant advantage of the new DP/DP upscaling technique is the preservation of large-scale heterogeneities and reliable representation in coarse-scale models. Therefore, the higher the reservoir heterogeneity, the greater the impact of the DP/DP model compared to SP flow-based upscaling procedures, especially for higher UR.

Nevertheless, upscaling of reservoirs with moderate heterogeneity can also be well represented with the DP/DP approach. In these cases, however, the lower contrasts in the permeability field limit the improvement from the DP/DP technique of SP coarse-scale results. Finally, for low heterogeneity systems, the DP/DP approach and SP upscaling tend to present similar results. Thus, SP can be a good option with satisfactory consistency for less effort.

A useful guide as an initial indicative measure of reservoir heterogeneity is the classical Dykstra-Parsons coefficient. As highlighted by Lake and Jensen (1989), lower values (0 to 0.5) represent cases of low heterogeneity, while higher values (0.7 to 1.0) are related to reservoirs with high to extremely high levels of heterogeneity. We extend this classification also considering Lorenz coefficient. Although they are not equivalent, the overall tendency is kept.

In the case studies presented in this work, all models have Lc higher than 0.7, except for the realizations in A3, with Lc varying from 0.1 to 0.8.

The benefits of the new DP/DP approach in channelized reservoirs are more straightforward. First, because SP approaches usually fail to predict these cases and second, because the DP/DP technique can obtain satisfactory simulation results even with large UR.

In variogram-based permeability fields, flow-based SP upscaling presents acceptable results even in heterogeneous systems. However, for a more aggressive UR, the DP/DP approach is indicated. As observed in the results of layer 12, the responses with our approach in a UR200 showed to be equivalent with a UR16 of the SP upscaling.

One important characteristic of the proposed methodology is the potential to work on two simple thresholds in order to improve the coarse-scale results. Based on our investigations in numerous case studies, we recommend the value of 0.7 as an initial starting point for both thresholds.

Ideally, if a full simulation run of the fine-scale model (or part of this model) is available, one could find the most suitable threshold value that improves the upscaled models. In practice, however, the fine model results may not be available, and we still have to make an initial choice. In this case, 0.7 is the value to be used.

From our case studies, we also observed that when a more aggressive upscaling ratio is considered, the global threshold tends to be lower, as shown in application A3, when the coarse model had 100x100 m² grid-block (UR 400).

Finally, it is important to highlight that although the recommended threshold of 0.7 was always a good choice and allowed better representation of the fine-scale results for all our scenarios, we cannot guarantee that this threshold will be suitable for all cases, considering the still limited number of applications in this study. Therefore, for a better definition of the threshold, and to better correlate the threshold selection with the UR, further studies are necessary.

The use of pseudo-relative permeability curves is a common and well-known approach in reservoir engineering studies to improve coarse-scale simulation results of immiscible fluid injection. This technique can considerably improve the performance of upscaled models when fine-scale simulations results are available. However, there are some important limitations related to the pseudo-relative permeability curves, as emphasized by Barker and Thibeau (1997).

One relevant aspect of this technique is its dependence on the fine-scale results. More specifically, the pseudo-relative permeability curves fitted for a certain flow condition of the reference model will not necessarily improve the coarse-scale results when a different well pattern and dynamic evaluation are performed. Besides, the upscaled results with a pseudo-relative permeability curve obtained from a specific dynamic condition of the fine model can lead to a worse coarse-scale response.

We believe that our technique can present more robust results when pseudo-relative permeability curves are required (to obtain coarse models with an aggressive UR), because, as shown in A1, DP/DP upscaling is not dependent on any flow information. This investigation is a promising aspect for future work.

In the present work, we focused on describing and testing the proposed methodology. For this purpose, 2D cases are important tools because they allow isolation of specific features that are desirable to explore, to evaluate the robustness of an upscaling procedure.

Extending the DP/DP upscaling for use in 3D systems is our next step in this line of research. Generally, in 3D applications, capillary and gravity forces tend to have an important influence on multiphase flow dynamics and these forces were not considered in our 2D evaluations. However, we expect that the division of the porous media into primary and secondary systems can improve the averaging of capillary forces and saturation by reducing the typical homogenization that occurs with SP upscaling. The gravity effects are also expected to be better represented with the DP/DP approach, as vertical preferential pathways representation can be better captured by our two systems, compared to SP approaches.

In our current 3D evaluations, we achieved satisfactory results with the full field SPE10 model. We evaluated different URs and, as observed in our 2D cases, the DP/DP methodology presented better results than the flow-based SP approach, not only regarding the capability of reproducing the fine-scale results, but also the potential of less sensitivity to the upscaling level. Figure 23 summarizes the results of cumulative oil production (presented in STB to be aligned with the units of the original paper by Christie and Blunt, 2001) and water cut for the fine reference model and for five different coarse-scale models, upscaled with SP flow-based upscaling technique and the proposed DP/DP approach. Note that DP/DP results are in close agreement with fine results and models with different URs (varying from 25 to 500) have similar results. Figure 24, compares, for the coarse model with UR250, the oil rate and water cut for each producer well, showing the improvement on the coarse-scale results with the use of DP/DP upscaling.

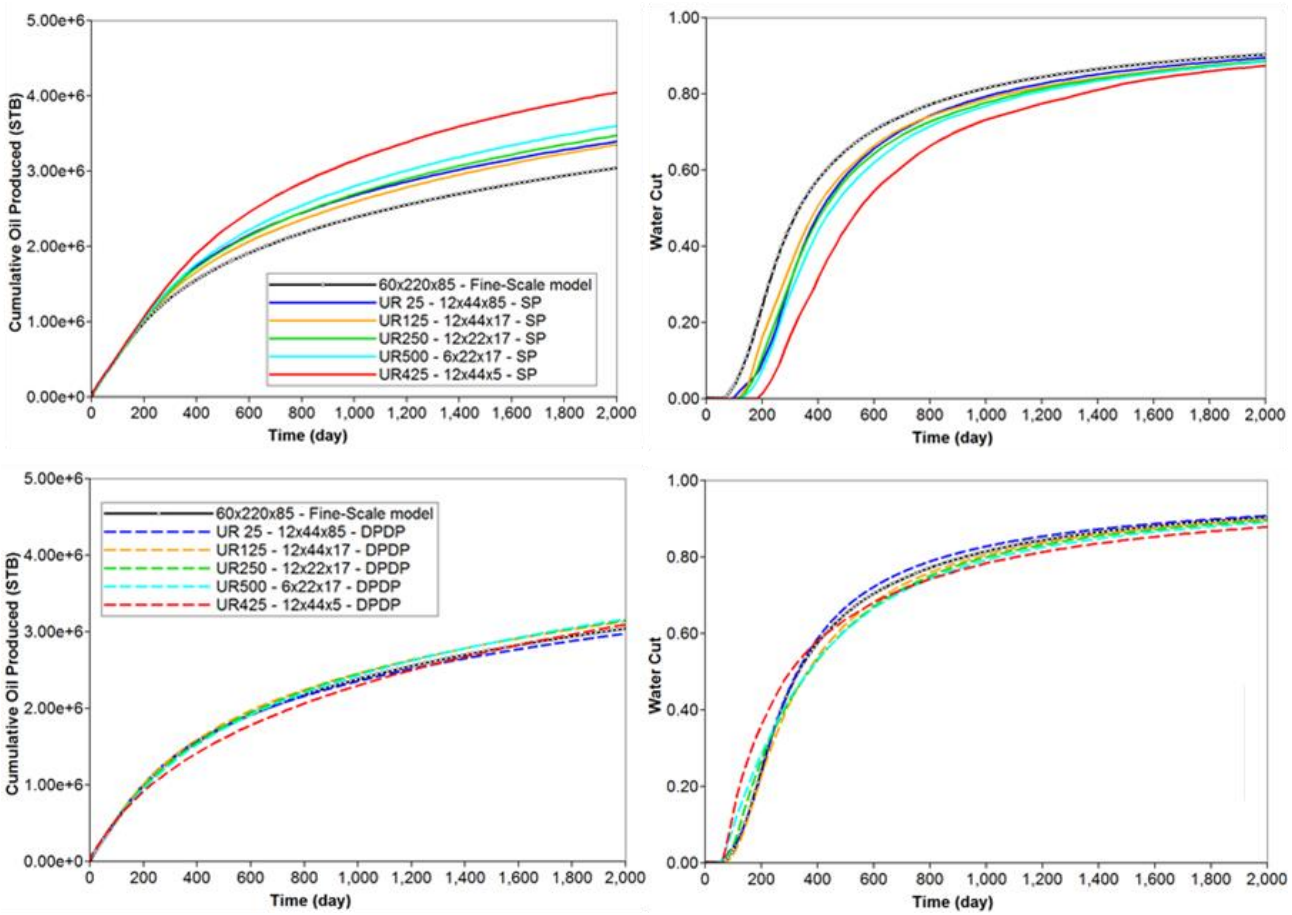

Figure 23. Cumulative Oil production and Water Cut for the Field. Comparison of five coarse models with SP and DP/DP upscaling with the reference fine model.

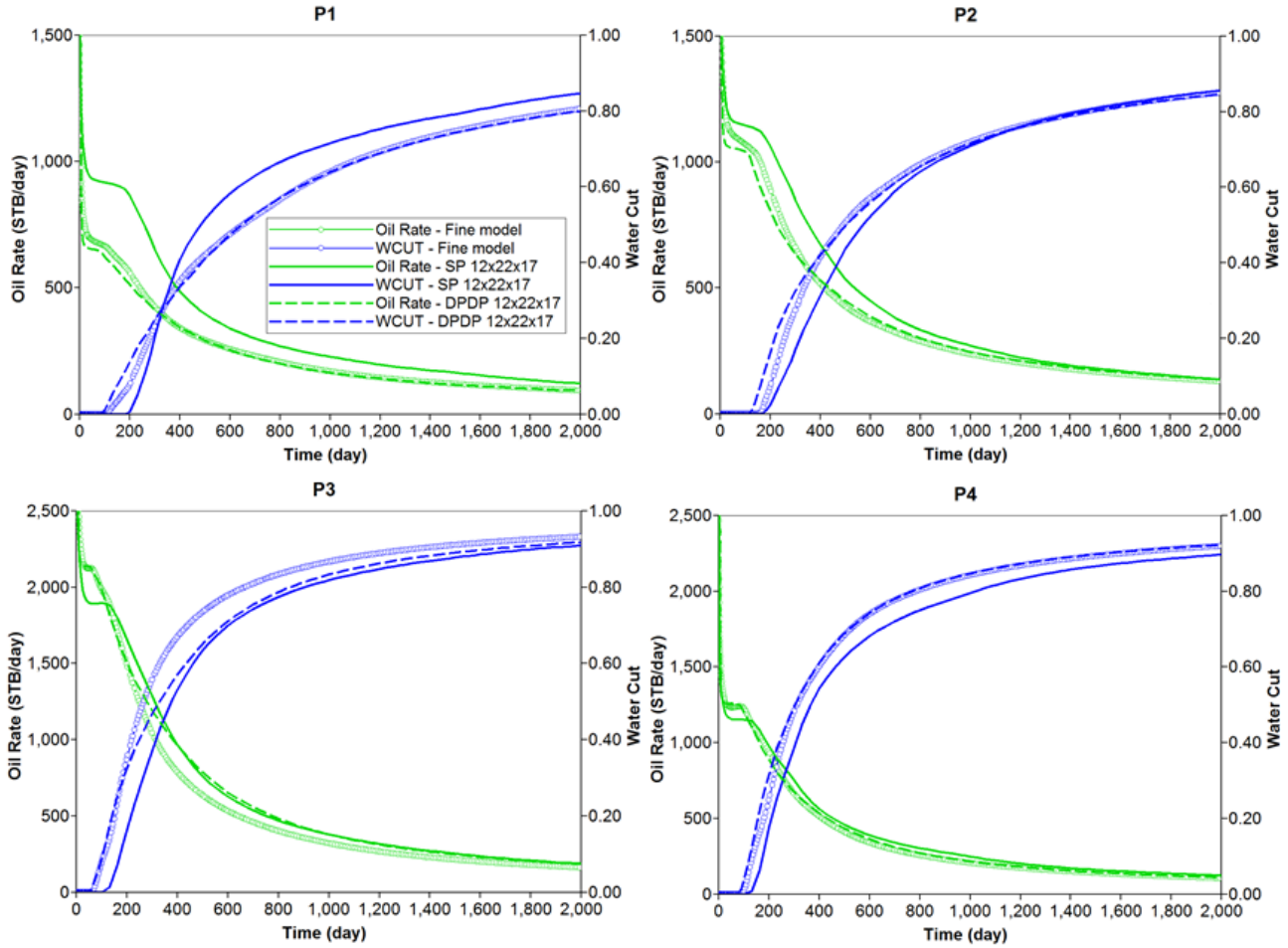

Figure 24. Well rate and WCUT for each well in SPE10 model. Coarse model with UR250 is shown. Continuous curves represent SP upscaling; dashed curves, DP/DP upscaling; and continuous-dotted curves, the fine-scale model.

Conclusions

In reservoir simulation studies, it is always desirable to build fast and accurate numerical models; fast in terms of numerical performance and accurate regarding the capability of reproducing the main reservoir flow dynamics. This is essential even when the search for performance means coarser simulation models. In this work, we proposed a new upscaling technique that combines both aspects, allowing fast coarse-scale models to consistently reproduce fine-scale results.

The results for the new DP/DP methodology support the advantage of the new method over classical approaches, mainly regarding the possibility of creating representative coarse-scale models without requiring the dynamic simulation results of fine-scale models as input. Only static data, classical F-C diagram and the Lorenz coefficient are required to achieve consistent coarse models using our approach.

The presented applications showed the robustness of the technique in several situations. The results in A1 showed that final coarse models behave similarly to the fine models even when the flow conditions are changed. A2 showed that the new upscaled coarse models are less sensitive to the upscaling ratio, presenting results close to others at different upscaling levels and similar to the fine-scale reference model.

Evaluating upscaling techniques considering multiple permeability realizations is uncommon in the published literature. Despite that, we tested our methodology with 500 realizations and it showed remarkable improvement in the uncertainty curves behavior for different upscaling ratios, injected fluid, and well pattern.

We described and tested the proposed technique in 2D evaluations. However, we expect that the division of the porous media into primary and secondary systems will also improve capillary and gravity representation of coarse models in 3D applications. Initial applications in SPE10 benchmark confirm this potential and broader investigation of extending our DP/DP for 3D systems will be the focus of future work.

Finally, based on the presented results and discussions, we conclude that the new DP/DP upscaling technique is an effective and robust tool for creating coarse-scale models and can be used in deterministic and probabilistic reservoir engineering studies.

Acknowledgments

The authors would like to thank Petrobras (Petróleo Brasileiro S.A.), UNISIM, DE-FEM/UNICAMP, CEPETRO, Energi Simulation, ANP, CMG, Dr. Daniel Nunes de Miranda Filho and M.Sc Vinicius de Souza Rios for all the support for this work.

4 ARTICLE 3: A PRACTICAL PROBABILISTIC UPSCALING WORKFLOW FOR COMPOSITIONAL RESERVOIR SIMULATIONS OF MISCIBLE GAS INJECTION

Victor S. Rios, Vinicius S. Rios, L.O.S. Santos, D.J. Schiozer

Presented at the SPE Virtual Europec Conference, 1-3 Dec 2020

Abstract

Numerical reservoir simulation often requires upscaling of fine-scale detailed models and coarse-scale models are necessary to reduce computational time for dynamic evaluations. However, these simplifications may degenerate results due to loss of resolution of the small-scale phenomena, averaging of sub-grid heterogeneity and numerical dispersion, especially in oil fields where miscible gas is injected.

Most of the existing upscaling techniques focus on reproducing the results of a specific geological realization, in a deterministic approach. Nowadays, however, reservoir simulation studies commonly include uncertainty quantifications, which is performed by simulating multiple geological realizations. For that, the use of fine-scale models can be computationally prohibitive and this requires a proper procedure to upscale the coarse-scale simulation models in multiple realizations environment.

In this work, we propose and test an ensemble-level upscaling technique for compositional systems with miscible gas injection. The new approach considers the classical Koval factor, calculated for the fine-scale models, as a guide for selecting representative fine-scale models to train pseudo-functions for the coarse-models. Only a few fine models are simulated (about 1%), and the uncertainty quantification process with coarse-scale models can be significantly improved.

The proposed workflow is guided by ranking the fine-scale models in increasing order of their Koval Factor. We selected representative models and applied a two-step methodology to improve upscaled coarse-scale results for these models. We then propose a consistent procedure to expand the fitted pseudo-functions to all the coarse models, providing an effective ensemble-level upscaling.

The correlation between Koval factor and oil recovery is a useful guide to extrapolate the pseudo-functions obtained for each selected representative model, enabling better coarse-scale simulation results when multiple realizations are considered. This procedure can be applied for continuous miscible gas injection and can be adapted for WAG scheme.

This work was motivated by the lack of practical procedures to improve coarse-scale results at the ensemble-level. With our approach, we can better represent uncertainty quantification using coarse-scale models with reduced computational cost and requiring only a few fine-scale simulation runs.

Introduction

In traditional upscaling procedures, a group of fine-scale cells is averaged to obtain a single cell with uniform properties, which corresponds to a coarse-scale cell. Thus, sub-grid heterogeneities tend to be homogenized and each upscaled grid block smooths out the behavior of several fine-scale grid cells. Dynamic evaluations with coarse-scale models in these situations tend to overestimate the sweep efficiency of the injected fluids. This mainly occurs because the preferential paths, generated by high permeability contrasts, are homogenized in each coarse-scale cell.

When fluid is injected into a heterogeneous reservoir, additional effort is usually required to obtain a more effective upscaled model. For water injection or immiscible gas injection simulation processes, a two-phase upscaling procedure is recommended. In this group, the use of pseudo-relative permeability curves is one of the most used methods to improve the results of coarse-scale simulation models when the corresponding fine-scale simulation results are available. On the other hand, when a miscible gas injection is considered, this strategy cannot be applied directly, and a compositional approach is recommended.

Miscible gas injection is an effective oil recovery method that recently gained special attention in Brazil, especially after the discovery of giant pre-salt oil fields. This method can increase the oil recovery factor due to the formation of a miscible front ahead of the injected fluid. However, its field scale representation is rather challenging, since several small-scale phenomena are smoothed out in coarse simulation grids.

The problems arising from upscaling a geological model from fine-scale to the field-size scale are widely discussed in the literature. However, coarse-scale representation of heterogeneous reservoirs and cases with miscible gas injection, continuous or alternating (WAG), present additional difficulties since traditional single-phase upscaling procedures are not enough to ensure physical consistency or are capable of reproducing the results of fine-scale simulations at a coarser scale.

Some authors proposed methodologies for better representing small-scale results in coarse-scale simulation models. Backer and Fayers (1994) and Christie and Clifford (1998) worked with the method of transport coefficients (also known as α-factors). Coats et al. (2004) considered modeling residual oil saturation in miscible and immiscible gas flooding. Evazi and Jessen (2014) developed a technique, for highly heterogeneous reservoirs, in which the pore space is arranged into two levels of porosity, based on fine-scale streamline information, and a dual-porosity dual-permeability (DP/DP) flow model is adapted to simulate the coarse-scale model.

Li (2014) and Li and Durlofsky (2016) have extended the method of transport coefficient to include treatment of near-well upscaling. Iranshahr et al. (2014) developed a new compositional upscaling formulation, considering the system to be out of thermodynamic equilibrium on the coarse-scale models. They introduced the use of upscaled functions to reproduce this effect. This approach was extended by Salehi et al (2013) and Salehi (2016) with the introduction of a physical non-equilibrium term for the local thermodynamic constraints, which was also converted to a transport coefficient similar to the α-factors. These approaches allowed the coarse-simulation results to better represent the small-scale curves and component rates, but with an impact on the simulation time.

Rios et al. (2017, 2018) proposed a methodology for a robust upscaling of compositional displacements. This procedure enables a better representation of the small-scale results when a miscible gas injection is performed, as in cases in which the produced gas is partially or totally reinjected in the reservoir. It can be applied in any compositional simulator without the need to adapt any transport coefficient, thus providing a flexible and computationally efficient approach. The technique is applied in two steps: first, an alternative fluid model is generated and then pseudo relative permeability curves are used to better fit the simulated fine-scale model production curves. The authors showed that the proposed technique can significantly improve the coarse-scale results – production curves, sweep efficiency and gas saturation map profile – in different scenarios of heterogeneity, with lower simulation time impact, compared to previously mentioned work.

Nevertheless, most of the existing upscaling techniques aim at reproducing fine-scale results of a single geological realization, i.e. deterministically. However, probabilistic approaches and uncertainty quantification studies are a reality in reservoir engineering activities and the simulation of multiple geological realizations is required for these tasks. Since it can be unpractical to use/simulate several highly detailed fine-scale models, coarser models are often necessary. For that, it is essential that the resulting coarse-scale responses correctly reproduce the reference fine-scale solutions.

There is little research reported up to this date on this subject. Chen and Durlofsky (2008) proposed an ensemble-level upscaling approach in which upscaled two-phase functions are numerically generated for a portion of the coarse-scale blocks and statistically estimated for the others. The results showed a good agreement between fine and coarse-scale flow models at the ensemble-level, rather than realization-by-realization agreement. However, they do not show how the coarse-scale models would respond if different well positioning or well rates are applied. Since the proposed methodology considers fine-scale velocities, the dependence on a

specific condition can be important. Li and Durlofsky (2016) also developed an ensemble level upscaling (EnLU) procedure, but for compositional systems, enabling efficient generation of multiple coarse models for use in uncertainty quantification. Although a close match between fine and coarse P10, P50 and P90 production rate curves was achieved, it was required that 10% of the fine-scale models were simulated in order to calibrate the data, which can be prohibitive when these reference/fine models require several hours or days to conclude a single run.

Inspired by the aforementioned work, and motivated by the lack of practical procedures to improve coarse-scale results at the ensemble-level, we propose and test a new approach to better represent uncertainty quantification using coarse-scale models with reduced computational cost and requiring only a few fine-scale simulation runs.

The present work extends the two-step methodology proposed by Rios et al. (2018) applied to multiple geological realizations. The new approach considers the classical Koval (Koval, 1963) factor calculated for each fine-scale model as a guide for selecting few representative fine-scale models to train pseudo-relative permeability curves (step 2 of the upscaling technique presented in Rios et al.,2018) for the coarse-models. The outcome is an ensemble of coarse-models whose simulation results' statistics are unbiased related to the fine-scale ensemble.

This paper proceeds as follows: after describing the problem and motivation for this work, we present details of the proposed methodology and the main theoretical concepts. Then, we describe the case studies and applications. We consider two applications for the proposed technique in this work: (i) 100 realizations in a 2D evaluation with heterogeneous Gaussian permeability fields, randomly generated with spherical variogram, where we only vary the heterogeneity level but keep the permeability mean and seed in all models; (ii) 500 realizations in a 2D evaluation with heterogeneous Gaussian permeability fields, randomly generated with spherical variogram, where we vary the heterogeneity level, permeability mean and seed in all models. We then discuss the results of each application and provide additional analyses. We conclude with a summary and some final remarks.

The Problem and Motivation

Uncertainty quantification is an important and useful tool to assist the decision-making process in reservoir engineering studies. To perform this procedure, multiple geological realizations are generated, and multiple simulation runs are required. This task usually demands the use of coarse-scale models due to the high computational cost associated with the simulation of highly detailed fine-scale models. This is a challenge for probabilistic studies of miscible gas

injection because the flow statistics can differ substantially between fine and coarse models when traditional upscaling techniques are used.

To illustrate this problem, we generated 500 geological realizations representing one layer of part of a reservoir with an area of 1 km². The heterogeneity level of the permeability field varies considerably throughout the realizations, while keeping a constant porosity of 15%. Figure 1 shows the permeability maps for three different realizations and it is useful to highlight (visually) the variability in the heterogeneity level among the realizations.

In the fine-scale model, the cells have 5 x 5 m² of area and the wells are located according to a five-spot well scheme, with a central injector well and four producers in each corner. CO_2-rich miscible gas is continuously injected, and the system has a maximum production oil rate and gas rate as constraints, so this application more accurately resembles actual industry projects. The reservoir fluid is a light oil represented by seven-pseudo-components, as presented by Rios et al. (2017, 2018). The initial GOR is 215 m³/m³ and the saturation pressure is 400 bar.

For the dynamic evaluations, the fine model was upscaled to a coarser system with 40 x 40 m² grid block cells, resulting in an upscaling ratio (UR) of 64. Traditional permeability upscaling techniques, such as averaging, which considers horizontal arithmetic average and vertical harmonic average; Cardwell-Parsons directional averaging (Cardwell and Parsons, 1945); and flow-based upscaling with closed boundary conditions (Christie, 1996, Kumar et al., 1997) were evaluated and Cardwell-Parsons' approach was chosen as reference due to its good balance between results and computational cost. Following, we summarize the main static and dynamic characteristics for this problem:

- 500 fine-scale geological realizations
- Fine-scale model with 5 x 5 m² grid block cells
- Gaussian permeability fields with spherical variogram
- Heterogeneity variation: Dykstra-Parsons' coefficients from 0.1 to 0.84
- Coarse models with 40 x 40 m² grid block cells (UR 64)
- 5-spot well pattern configuration
- Continuous CO_2-rich miscible gas injection
- Group constraints: maximum oil rate and maximum gas rate
- Well constraints:
    - Producers: minimum well bottom hole pressure and maximum oil rate;
    - Injector: maximum well bottom hole pressure and maximum injection rate.

Once the coarse-scale models were obtained, compositional simulation was performed for the 500 realizations. Since it is unpractical to show the time-series results for all simulation runs, we built uncertainty curves for oil recovery factor after the injection of 0.2, 0.3, and 0.4 pore volumes of gas (representing initial, intermediate and final stages of the oil recovery). The results are shown in the red curves of Figure 2. The shape of these red curves indicates that most of the models present close recovery factor, suggesting a homogeneous group of realizations from the dynamic point of view. However, this is not in accordance with what was expected, since the heterogeneity level is considerably varying in this group of reservoirs (Vdp values from 0.1 to 0.84, illustrated by Figure 1).

To obtain a reference uncertainty curve, we also simulated all the fine-scale models. This step is not practical in real cases and this is the reason why we propose the methodology discussed in this work. The step was only performed for a more effective comparison and discussion. By observing Figure 2, in which black curves represent the fine-scale realizations, an important difference between fine and coarse models can be highlighted. Fine-scale results present a higher variability in the results, which is in accordance with the heterogeneity variation in these realizations. Coarse-scale models, on the other hand, provided a more homogeneous flow behavior and cannot be considered useful in the decision-making process since an important bias is imposed on the results.

A different and more continuous way to discuss the optimistic behavior of the coarse models is by comparing the full-time representative P10, P50 and P90 oil recovery factor curves, shown in Figure 3. In this figure, dotted curves represent fine-scale results, while continuous curves represent the coarse models. This result is particularly critical because it emphasizes how poorly the reference (fine) results are represented by the coarse models, with traditional upscaling approach in numerical simulation of miscible gas injection.

This limitation of the use of coarse models in compositional simulation was broadly discussed for deterministic cases (Salehi et al (2013), Evazi and Jessen (2014), Iranshahr et al. (2014), Li (2014), Li and Durlofsky (2016), Salehi (2016), Rios et al. (2017, 2018), and others). However, practical approaches to improve coarse model representation for multiple realizations are still a problem with limited discussion. This is the main motivation for the present work, which provides a practical methodology to allow the use of coarse models in multiple realizations studies of miscible gas injection. The proposed approach is guided by classical reservoir engineering concepts and it will be detailed and discussed in the next section.

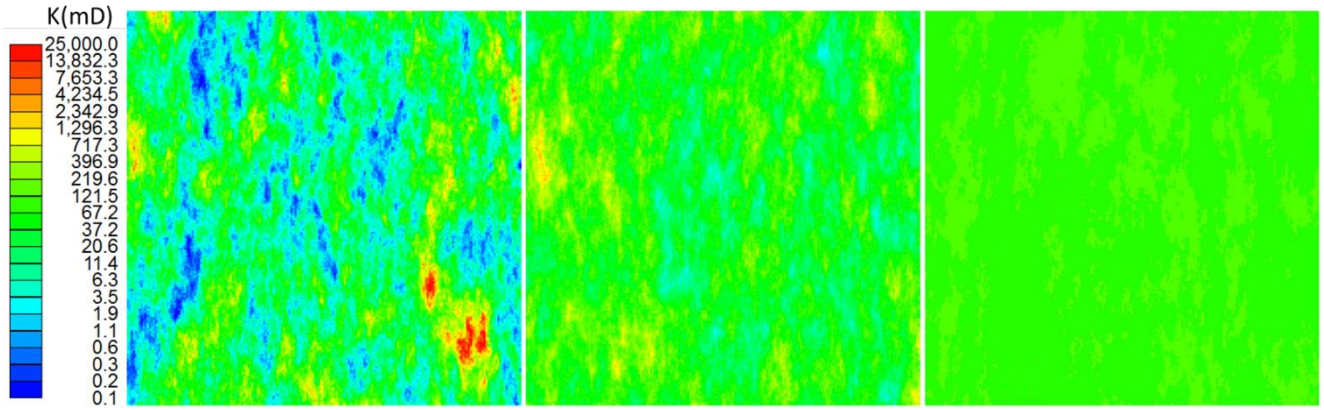

Figure 1. Permeability maps for three realizations with Dyskstra-Parsons coefficient of 0.84, 0.6 and 0.1 (from left to right)

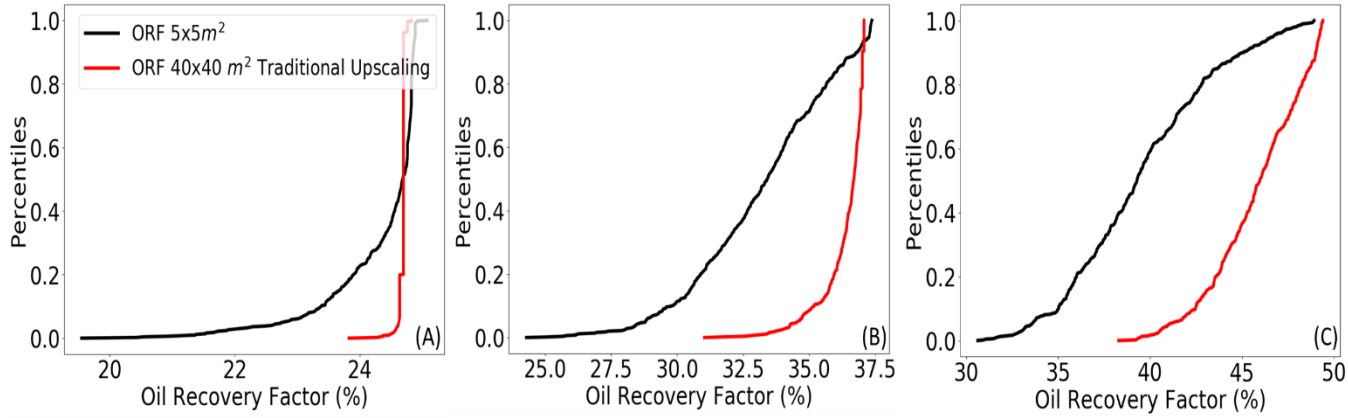

Figure 2. Oil recovery factor uncertainty curve after 0.2 (A), 0.3 (B) and 0.4 (C) PV injected of miscible gas. Coarse models in red and reference fine models in black.

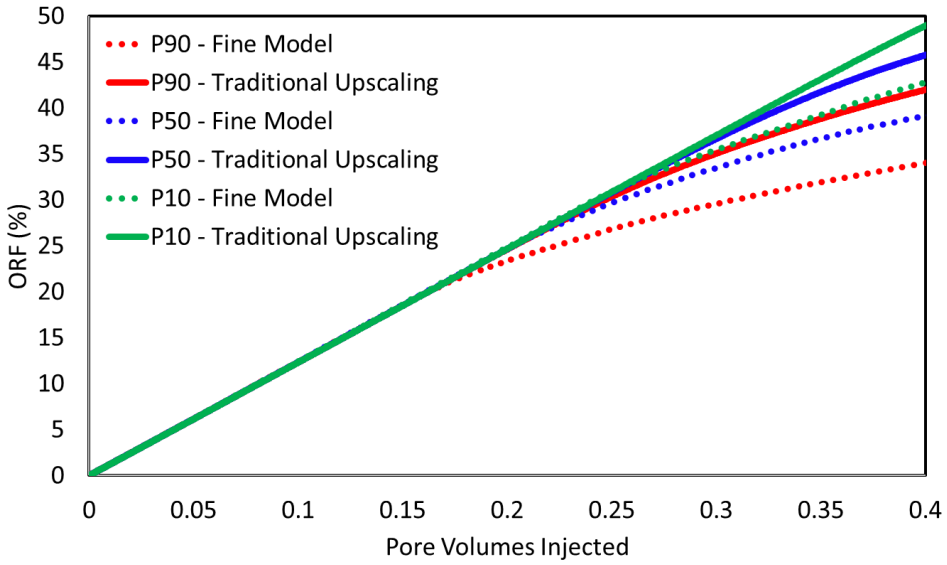

Figure 3. Comparison of representatives P10, P50 and P90 oil recovery factor curves.

Methodology

The task of improving coarse-scale simulation results in compositional simulation of miscible gas, for multiple permeability realizations, is a challenge that requires two key

procedures, namely: a robust upscaling technique and a general law to extend this technique for multiple realizations with cost-effective computational resources.

As a reference compositional upscaling, we consider the two-step methodology proposed by Rios et al. (2018). This technique was robust and effective to improve deterministic coarse-scale simulation results for miscible gas injection scenarios. It was applied in three different case studies and the results of coarse-scale models accurately reproduced the fine responses, even when varying the well configuration and the flow behavior.

Once we have chosen the upscaling technique, we must extend it to multiple realizations. This task is important and it is the key contribution of this work. Our objective in this matter is to establish a general law using only a few fine-scale simulation runs to improve the coarse-scale results of an ensemble of realizations.

The effectiveness of this process is guaranteed if we appropriately choose the few representative fine scale models to run, and we understand how to properly extend this to the remaining models, by identifying possible correlations between the (geostatistical realizations) heterogeneity and the dynamic simulation results.

In reservoir engineering studies, there are some classic and well-known indexes to measure the reservoir heterogeneity. Among the static measures, Dykstra-Parsons and Lorenz Coefficient are two of the most important and frequently used coefficients, since they offer a good balance between required cost in the calculations and effectiveness in representing the heterogeneity. For miscible gas injection, the Koval factor (K) is a widely used parameter. It is the product of a heterogeneity factor (H_k) and an effective viscosity ratio (E), and it was proposed to predict the interaction of micro (longitudinal dispersion) and macro (channeling) heterogeneity on viscous fingering. A detailed review of the above-mentioned heterogeneity measures, and others, can be found in Lake and Jensen (1989).

In general, strong contributions of viscous fingering and channeling effects (commonly present in miscible gas injection in heterogeneous reservoirs) tend to result in poor oil recovery, with premature breakthrough of the injected fluids. In other words, the stronger the channeling and viscous fingerind effects, the lower the oil recovery factor (ORF) at the breakthrough time (BT).

Considering this, we used our simulated 500 fine-scale models and evaluated the behavior of the oil recovery factor at the breakthrough of the miscible gas injected against the three heterogeneity measures highlighted above. The main idea was to investigate if any of them could represent a well-established general trend when correlated with oil recovery.

Figure 4 presents the relation between oil recovery factor in the moment of gas breakthrough against Dykstra-Parsons (left image), Lorenz Coefficient (central image) and Koval factor (right image) for all the 500 realizations considered in the motivation section of this work. Generally, it is possible to observe that there is a correlation between the oil recovery (at BT) and the heterogeneity indexes. In each of the analyzed heterogeneity factors, there is a negative trend, where the oil recovery decreases with the increase in the heterogeneity index value.

By inspection, the correlation with Koval factor is likely to follow a potential law, while with Dykstra-Parsons and Lorenz Coefficient, a nearly linear behavior can be seen. However, for the two static indexes, in the highest heterogeneity zone (higher than 0.7, highlighted in the oval red area), a large group of realizations is concentrated and the correlation with ORF is weaker. This behavior can make it hard to establish a procedure to distinguish models in this important zone, which can be a problem when considering using these measurements to extend the upscaling technique.

The Koval factor, on the other hand, does not present this collapsed and concentrated effect in the highest heterogeneous models. Instead, the correlation between oil recovery at breakthrough and this factor is smoother, evenly distributed and, despite not being a perfect correlation, the overall trend is kept, which can be an important ally for the purposes of this work.

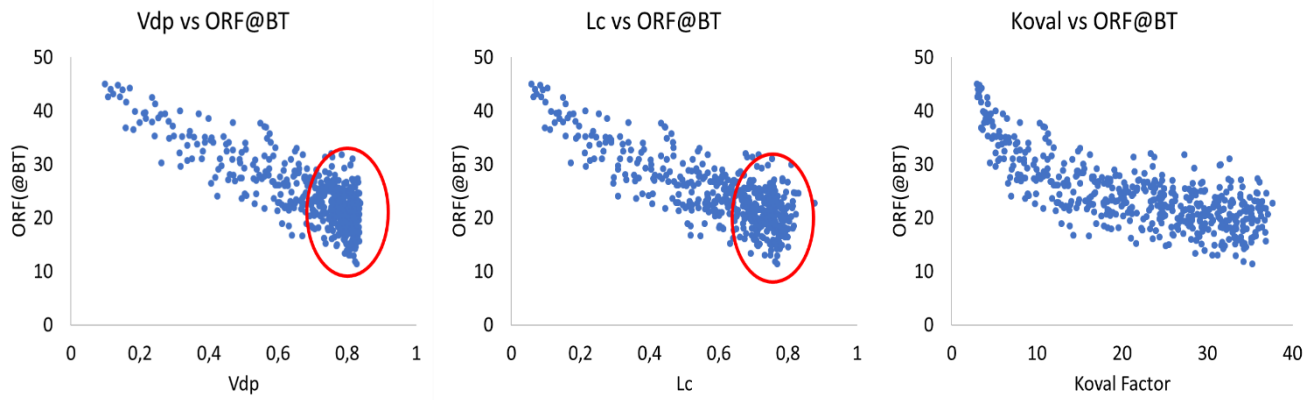

Figure 4. Oil Recovery Factor at BT against Koval factor, Dykstra-Parsons and Lorenz Coefficient for the 500 realizations.

At this point, we hypothesize that a promising extending law could be obtained using the potential correlation between oil recovery factor at the breakthrough and Koval factor. In order to validate this hypothesis, we created a new set of fine-scale realizations, named “control group”, with the same reservoir size and dynamic conditions considered for the previous 500 realizations. This group is formed by 100 models, all modeled with a fixed seed

and the same average permeability of approximately 100 mD, but varying the heterogeneity level with Dykstra-Parsons coefficient between 0.05 and 0.83. Figure 5 shows the permeability maps for three different realizations and it is useful to highlight (visually) the variability in the heterogeneity level among the realizations.

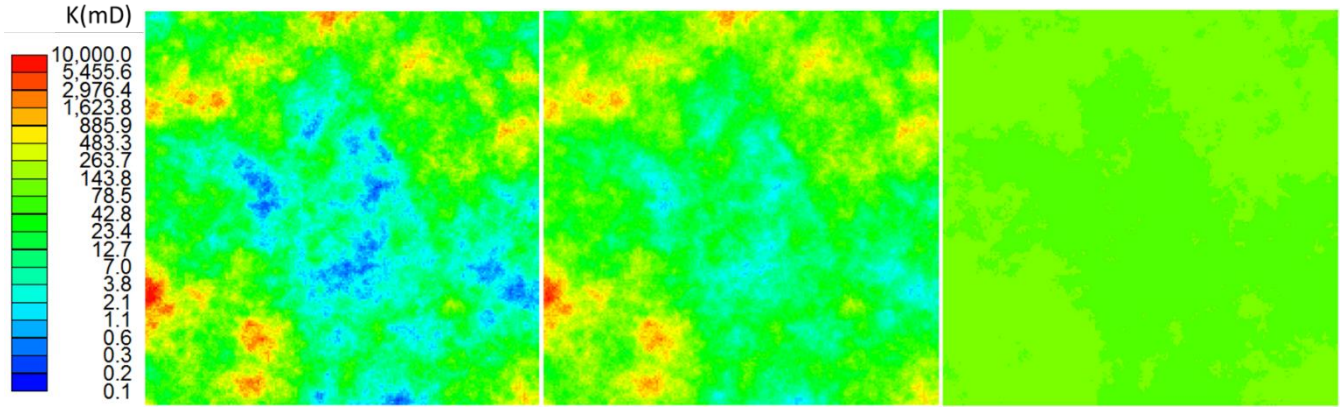

Figure 5. Permeability maps for three realizations in the "control group" with Dyskstra-Parsons coefficient of 0.83, 0.5 and 0.05 (from left to right)

The objective of this evaluation is to isolate the heterogeneity effect in the oil recovery with miscible gas injection. By doing this, if the above-observed potential-law correlation between Koval factor and the oil recovery factor at the breakthrough is well-established, it should be clearer. This would happen because, within the "control group", the heterogeneity effect is isolated from others, such as the anisotropy range and main heterogeneity direction.

Thereby, we simulated all the "control group" realizations and their respective upscaled models (using the Cardwell-Parsons approach again). The left image of Figure 6 highlights the oil recovery factor uncertainty curve in a final moment of the simulations (after 0.4 PV injected of gas). As expected, it shows that coarse models with traditional single-phase upscaling procedure are not able to capture the behavior of the fine-scale results. The right image in Figure 6 shows the correlation between the Koval factor and oil recovery at the breakthrough for all the 100 models in the "control group". This graph shows a clear potential-law correlation between these properties and confirms the hypothesis we proposed after analyzing the results from the 500 realizations. Furthermore, this correlation will be considered as an important basis for our practical probabilistic upscaling workflow for compositional simulations of miscible gas injection.

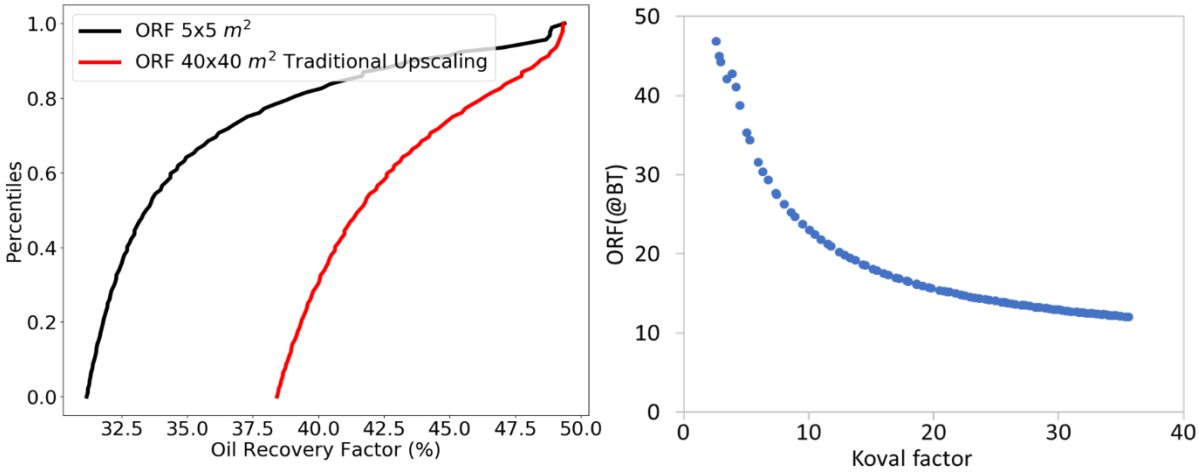

Figure 6. *Left*: Oil recovery factor uncertainty curve after 0.4 PV injected of miscible gas. Coarse models in red and reference fine models in black. *Right*: Oil Recovery Factor at BT against the Koval factor for the "control group".

Proposed workflow

Once the correlation is verified, we now have the desired tools for an effective multiple realizations upscaling workflow in miscible gas injection scenarios: a robust upscaling technique – by Rios et al. (2018) – and a general law to guide us in extending this technique for multiple realizations, based on the correlation between the Koval factor and oil recovery factor.

Furthermore, we propose a methodology with the following steps:

1. Sort the fine-scale models in increasing order of the Koval factor
2. Select 5 representative models according to a rank of fine-scale Koval factor: minimum Koval, maximum Koval, P10, P50 and P90.
3. Simulate the 5-representative fine-scale selected models and plot a Koval vs ORF (at BT) graph with the results.
4. Fit a potential-law correlation (regression) to estimate ORF as a function of Koval.
5. Calculate the estimated ORF using the correlation for each fine model. This ORF is named "synthetic ORF" because it is not the result of a numerical reservoir simulation.
6. Divide the models into three groups with evenly-spaced synthetic ORF range.
7. For each group, one of the following can happen:
    a. If there is only one representative model in the group, this model will be the reference for expanding the pseudo-relative permeability curves for the remaining models in that group.
    b. If there is no representative model in the group. A model in the middle of this ORF synthetic interval is selected as a representative candidate of this group. Steps 3 to 6 are repeated.

   c. If there is more than one representative model in a group, the most centralized model can be the reference for this interval. Yet all models can be used to expand their results according to a Koval interval within each model.
8. Apply the methodology proposed by Rios et al. (2018) for each of the representative models selected in step 7.
9. Apply the representative pseudo-relative permeability curves obtained in the previous step to all remaining models in their respective groups.
10. All the coarse models will be simulated with the alternative fluid model (step 1 of the methodology presented in Rios et al. (2018)) and their corresponding pseudo-relative permeability curves from the representative models.

Case Studies Description and Applications

We test the proposed workflow in two different applications. In the first application, A1, we apply the procedure for the "control group" of realizations and show, step by step, the improvements on representing the fine-scale results with coarse-models in a UR of 64 (cells with 40 x 40 m²). Then, in the second application, A2, we apply the workflow for the 500 realizations, which represents a more challenging scenario. We compare the fine and coarse-scale results according to the uncertainty curves and P10, P50 and P90 oil recovery factor curves.

Results and Discussions

We present below the results and discussions regarding the two applications. We compare the performance of the proposed upscaling with the fine-scale reference models and the traditional upscaling approach.

Application 1

In application 1, we apply the proposed workflow and highlight the results of each step described in the "Proposed workflow" section. As mentioned previously, miscible CO2-rich gas is injected in all 100 realizations of the "control group", and the coarse-scale results with traditional upscaling technique fail to reproduce the ORF uncertainty curve behavior of the fine-scale models, as shown in Figure 6. We then show how our proposed workflow can make the same set of coarse models to become useful in the decision-making process by satisfactorily representing the fine-scale reference results.

For the first two steps, we calculate the Koval factor for each fine-scale realization, rank them in increasing order and select the 5-representative fine-scale models. These steps are summarized in the left graph of Figure 7.

These 5 models are important for the process because they allow us to cover the maximum theoretical range (by including maximum and minimum Koval) of oil recovery within the realizations, and these provide data for establishing the potential-law regression. For that, initially the 5 fine models are simulated and the ORF at BT is plotted against their Koval factors, as shown in the right graph of Figure 7. With these points, and with numerical regression, we obtain the equation that correlates ORF and the Koval factor, as shown in the left image of Figure 8. Also, by applying this equation for all models (using their corresponding Koval factor), we can create the full synthetic ORF curve. These procedures correspond to Steps 3 to 5.

For Step 6, it is necessary to divide the entire ORF(at BT) versus Koval factor into three evenly spaced intervals of ORF, as illustrated in the right image of Figure 8. This division is the guide for the selection performed in Step 7.

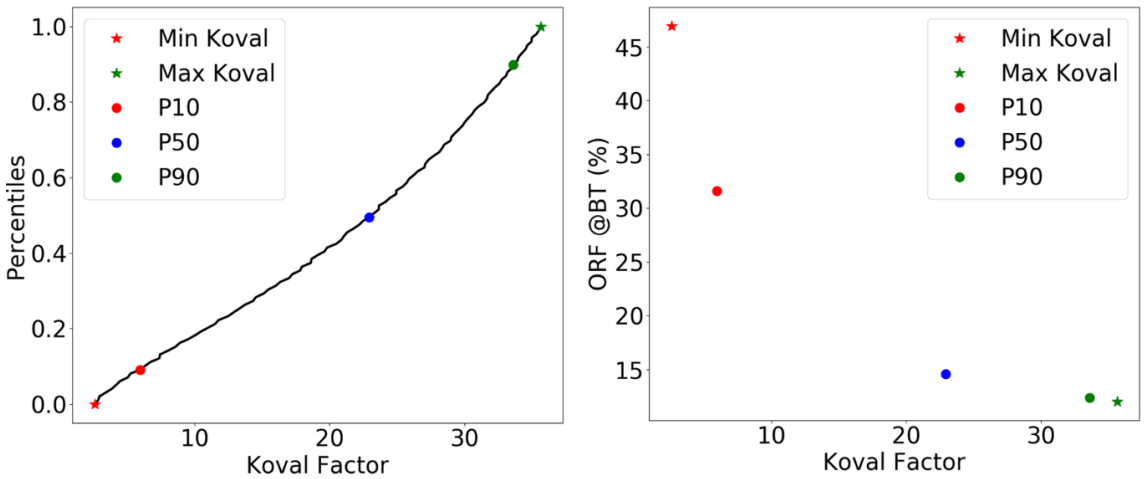

Figure 7. *Left*: Ranked Koval factor of each fine-scale model with the 5-representative models in highlight. *Right*: Oil Recovery Factor at BT against Koval factor for each representative model.

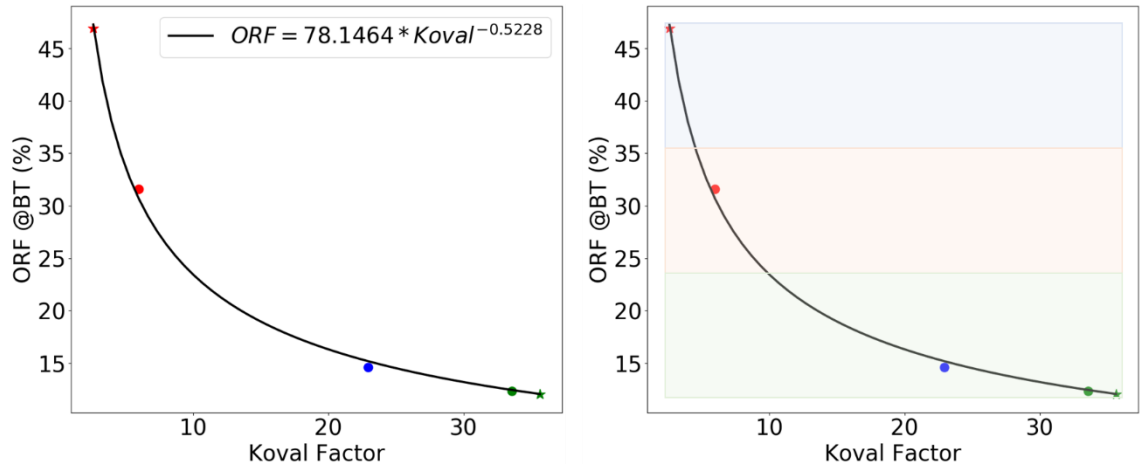

Figure 8. *Left*: Fitted potential-law correlation (regression) to estimate ORF as function of Koval. *Right*: Dividing the models into three groups, with evenly-spaced synthetic ORF range.

Figure 9 illustrates two possible situations that can happen after the division performed in Step 6. The upper and the intermediate intervals only have one representative model each. Therefore, they correspond to the scenario described in Step 7.a. The lower interval, however, includes three representative models, which is a situation described in Step 7.c. In this case, two options can be chosen: The first and simpler one involves electing the most centralized model (in terms of Koval for the given ORF limited interval) as the representative one for this interval (blue dot in the left image of Figure 9). Another possibility is to subdivide this interval into three regions, this time in terms of Koval, where each model would represent its corresponding subdivision, as shown in the right image in Figure 9. For this application, we proceed with the work using the first option, i.e., left image of Figure 9.

After Step 7, we now have three representative models as a reference to extend their upscaling results to the three equivalent groups: The first group has the model with maximum Koval as representative, the second has the P10 Koval and the third, the P50. For each of these three models, we performed the 2-steps of compositional upscaling proposed by Rios et al. (2018).

The application of this 2-step methodology to the representative models is our Step 8. Since the procedure is the same for each model, we show the results for only a single procedure, the P50-Koval model, to illustrate the effectiveness of this upscaling technique for miscible gas injection compositional simulation.

According to this upscaling technique, we first replace the fluid model by an alternative one which mimics the immiscible behavior, commonly observed in coarse-scale cells, but not possible to represent with the original fluid model due to the averaging of small-scale phenomena (Rios et al., 2018). Then, we perform the second step, where we fit pseudo-relative permeability curves to improve the coarse-scale results, compared to the fine case. At this point, we also borrow the concept of splitting the porous media into primary and secondary systems, presented by Rios et al. (in press), and adapt this idea to the generation of pseudo-curves. With this approach, we work on different pseudo-curves for each system - a primary and a secondary. Figure 10a-b show the fine and coarse-scale permeability map for the realization P50-Koval and, in Figure 10c, we highlight the porous media divided into two systems.

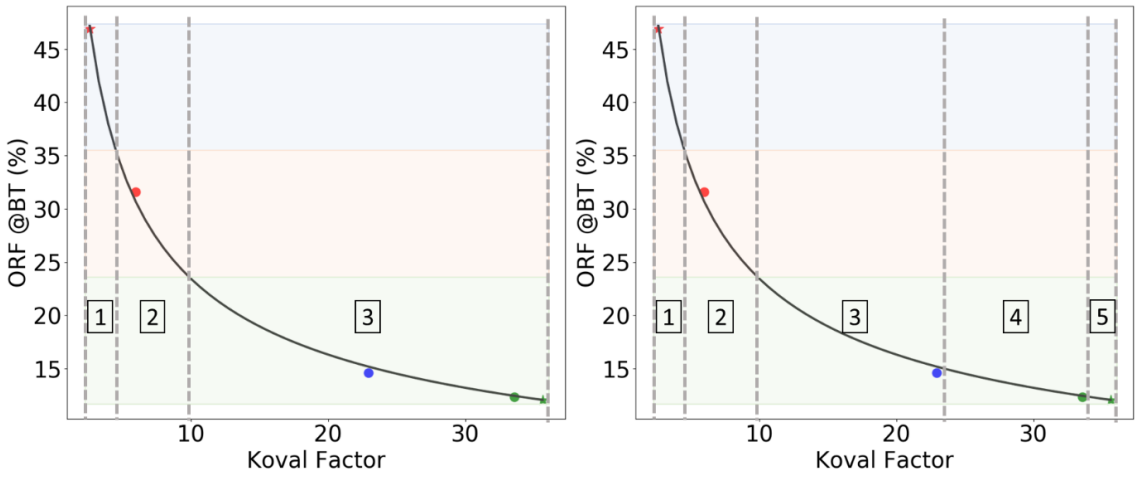

Figure 9. *Left*: Division of the models into three groups, according to criterion 7.a. *Right*: Division of the models into five groups, according criterion 7.c.

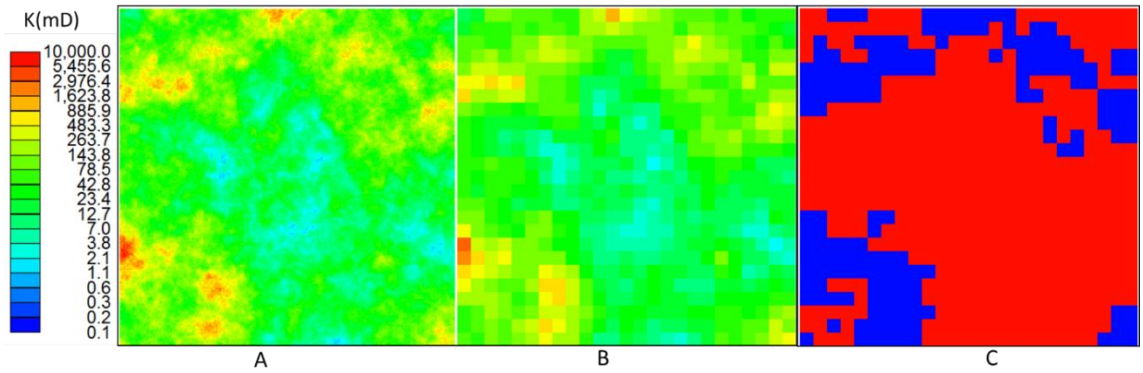

Figure 10. Permeability map for (A) fine-scale and (B) coarse-scale P50-Koval representative models. And (C) coarse model divided into two systems, primary (blue) and secondary (red).

After applying the procedure mentioned above, we obtain a coarse model with considerably better results compared to the traditional upscaling, and a satisfactory reproduction of the fine-scale responses. We confirm this by the results in Figure 11, which shows oil ORF and GOR curves and ratifies the capability of the considered upscaling technique in improving coarse-scale simulation results. It is worth mentioning that the fine-scale GOR curve presents important variations throughout the gas injection because our system is limited in maximum oil and gas production. Therefore, since the gas breakthrough happens at a different time for each of the four producer wells, the overall GOR curve presents these changes due to the gas production constraints at the platform level.

Once we repeat this process for the three representative models, we conclude Step 8 and begin Step 9. In this step, having generated the representative pseudo-curves, we apply them to all coarse models in each respective group. We highlight that each model is also divided into two systems to allow the use of two different pairs of pseudo-curves generated for the representative models.

To complete the workflow, all coarse models are simulated with the alternative fluid model and the respective pseudo-relative permeability curves provided by their representative model.

Finally, the proposed workflow provided tools to upgrade the uncertainty quantification of the coarse-scale multiple realizations. We summarize the result in Figure 12, showing the oil recovery factor uncertainty curve after 0.4 pore volumes injected of miscible gas. It is remarkable that the new workflow consistently improved the upscaled models' results at the ensemble-level, with only 5 fine-scale simulation runs required.

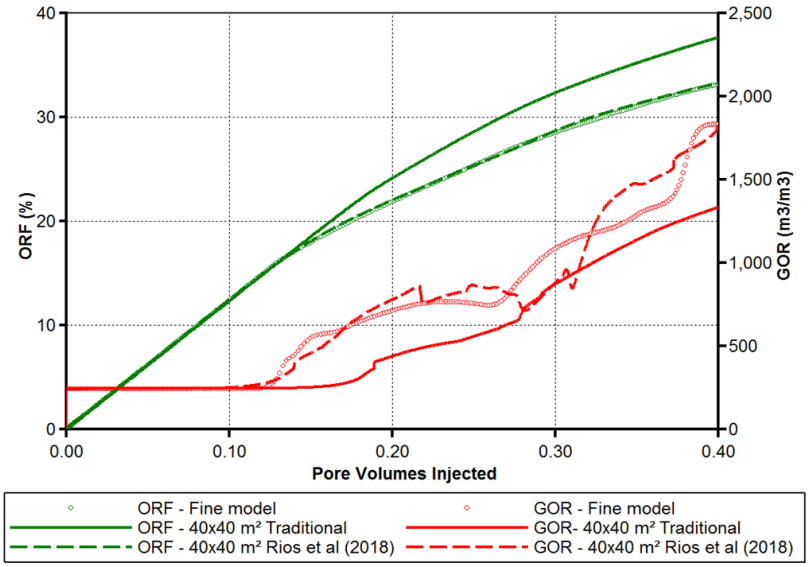

Figure 11. Comparison of ORF and GOR between fine-scale (dotted curves), traditional coarse-scale (continuous curves) and coarse-scale with adapted Rios et al. (2018) methodology, applied to the model P50-Koval.

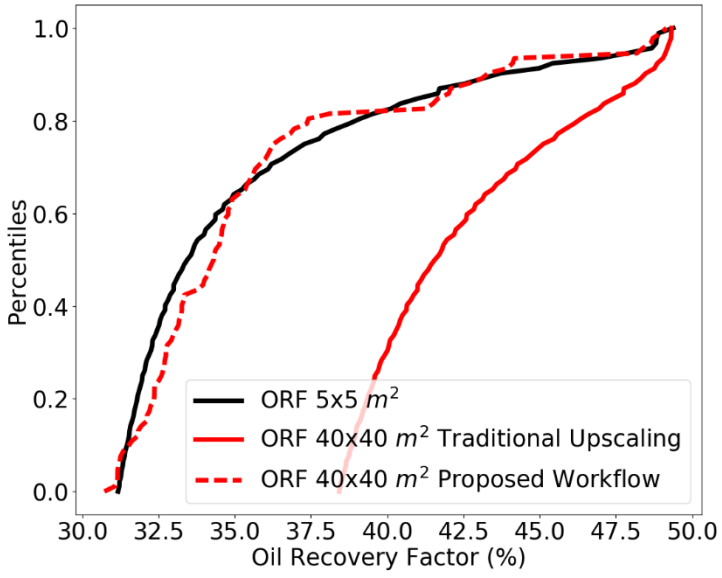

Figure 12. Oil recovery factor uncertainty curve after 0.4 PV injected of miscible gas. Coarse models in red and reference fine models in black. Traditional upscaling in continuous curve and proposed workflow in dashed curve.

Application 2

The second application considers the 500 permeability realizations described in the "The Problem and Motivation" section of this work. It represents a more challenging scenario, since the permeability variations among the models are not controlled, as was the case in A1.

All the steps of the proposed workflow are again applied in A2, and some are highlighted in the following figures. Initially, we rank the Koval factor of the fine-scale realizations into increasing order and select the 5-representative models. Afterwards, we simulate these 5 models and plot the ORF (at BT) against their Koval factors. With these points, we obtain the equation that correlates ORF and Koval factor, then, applying this equation for all the models (each calculated Koval factor), we can create the full synthetic ORF curve. Figure 13 summarizes these steps.

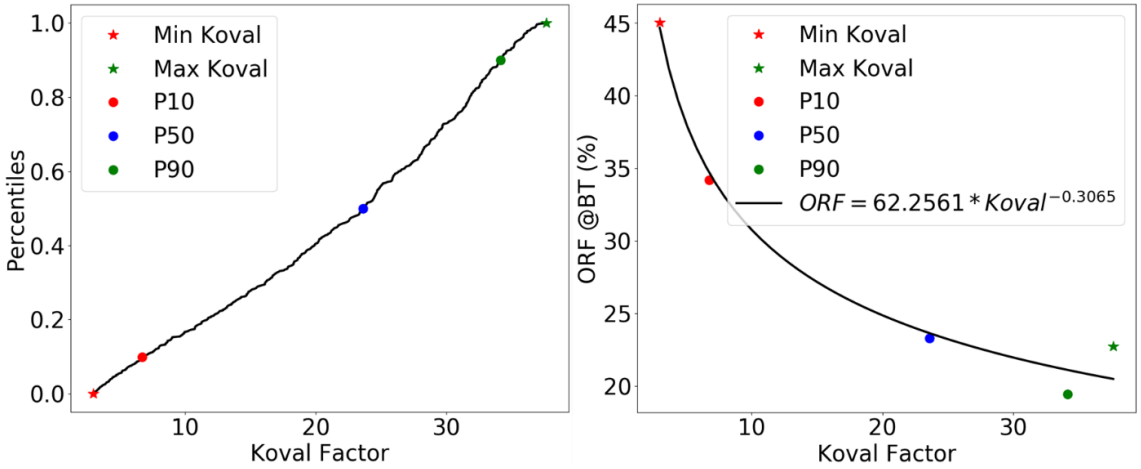

Figure 13. *Left*: Ranked Koval factor of each fine-scale model with the 5-representative models in highlight. *Right*: Oil Recovery Factor at BT, against Koval factor, for each representative model with the regressed potential-law equation and synthetic ORF calculated in the black curve.

Following the workflow, Figure 14 (left) shows the division of the ORF (at BT) versus Koval factor curve into three evenly-spaced intervals of ORF, which is the basis for selecting the representative models. As occurred in the previous application, the upper and the intermediate intervals of ORF presented only one model each, while the lower interval, three models. This time, however, instead of using the most centralized model (as in A1), we decided to further divide the lower interval into three groups, which means that all the fine models simulated in the initial steps will be used as a reference for a set of realizations. Figure 14 (right) illustrates this selection and the groups' division.

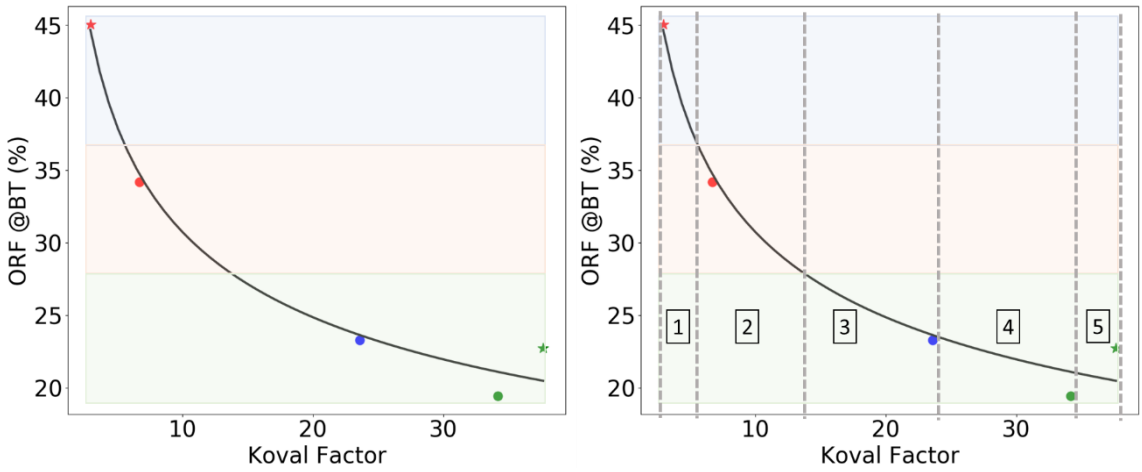

Figure 14. *Left*: Division of the models into three groups with evenly spaced synthetic ORF range. *Right*: Division of the models in five groups, according criterion 7.c.

We now have five representative models for use as reference to extend their upscaling results to the five respective groups: The first group has the model with maximum Koval as the representative, the second has the P10 Koval, the third: P50, the fourth: P90, and the fifth: minimum Koval. For each of these models, we again apply the adapted version of Rios et al. (2018) 2-step compositional upscaling.

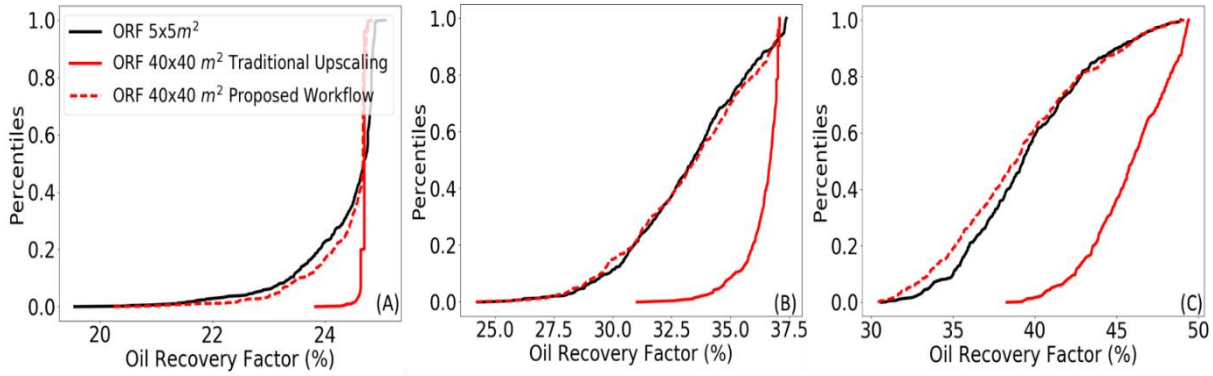

Figure 15. Oil recovery factor uncertainty curve after 0.2 (A), 0.3 (B) and 0.4 (C) PV injected of miscible gas. Coarse models in red and reference fine models in black. Continuous red curves refer to Traditional upscaling, while dashed curves relate to the proposed workflow

Finally, after accomplishing the steps of the proposed workflow, we were able to upgrade the uncertainty quantification of the 500 coarse-scale realizations. We summarize the results in Figure 15 and Figure 16. The first reproduces the uncertainty curves presented in Figure 2, including the results after applying the new workflow. The latter compares the fine and new coarse-scale representative P10, P50 and P90 oil recovery factor curves (in contrast with Figure 3). Both results show noticeable improvements provided by the proposed workflow. With this approach, we were able to remove the bias, maintaining the global fine-scale variability and making the same set of coarse-scale models closely reproduce the fine-

scale results. More importantly, only 1% of the fine-scale models were simulated, which renders a relatively low computational cost for the achieved improvement in the results.

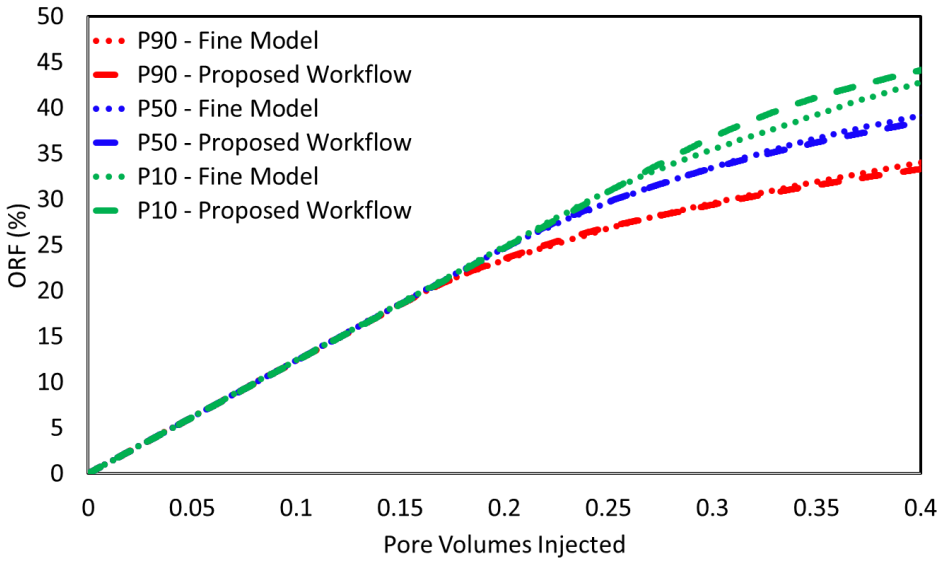

Figure 16. Representative comparison of P10, P50 and P90 oil recovery factor curves. Dotted curves: fine-scale results. Dashed curves: coarse-scale results with the proposed workflow.

Additional Analyses

After presenting and testing a new and practical methodology in two applications to allow the use of coarse models in multiple realizations studies of miscible gas injection, we performed additional evaluations to stress test our workflow and illustrate its robustness under various conditions.

We divided these evaluations into three groups:

- G1: sensitivity to UR – for both A1 and A2, we show that the same methodology can be applied to different coarse-scale models and the results can be improved, even for large UR.
- G2: evaluating different well configuration – it is well-known that the use of pseudo-curves can make the coarse models dependent on the original fine-scale flow conditions. Rios et al. (2018) showed that their upscaling technique was not highly dependent on the original well configuration and here we reinforce this result. We changed the dynamic evaluation from 5-spot to well pair and compared the uncertainty quantification results.
- G3: application with different EOR methods – we tested the workflow with miscible WAG injection. Application A2 was adapted to this end and this was a challenging test for the flexibility of the proposed workflow.

The results and discussions of each group will be presented separately in the next sub-sections.

Sensitivity to UR (G1)

The results for A1 and A2 showed in "Results and Discussions" section focused on a coarse-model with grid-blocks of 40x40 m². However, the same workflow can be applied to different coarse models. To perform this, we only need to work on different pseudo-curves for each representative model when changing the coarse scale.

To illustrate this, we first present the results for A1 with an additional coarse model with 20x20 m². As can be observed with the uncertainty curves shown in Figure 17 , the proposed workflow satisfactorily improved the coarse-scale representation, also in this additional UR of 16.

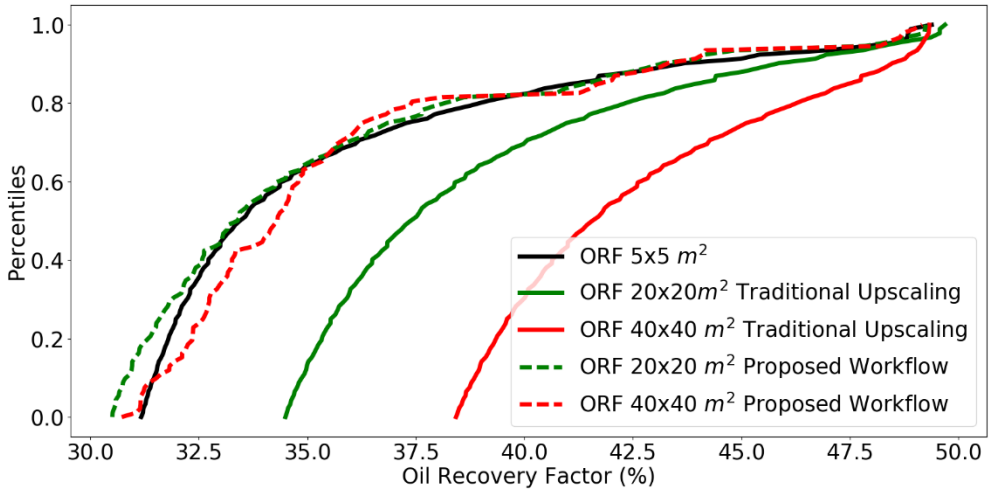

Figure 17. Oil recovery factor uncertainty curve after 0.4 PV injected of miscible gas. Coarse models with UR 64 in red, UR 16 in green and reference fine models in black. Traditional upscaling in continuous curve and proposed workflow in dashed curve.

For application A2, due to its challenging nature, we tested not only coarse models with 20x20 m², but also a more aggressive 100x100 m², representing an UR of 400. Again, we followed the same steps of the proposed workflow and obtained remarkable improvements, as summarized in Figure 18.

The additional studies to evaluate how the proposed workflow behaves for different coarse grid-block sizes confirmed the capability of the new procedure of improving the uncertainty quantification using coarse models.

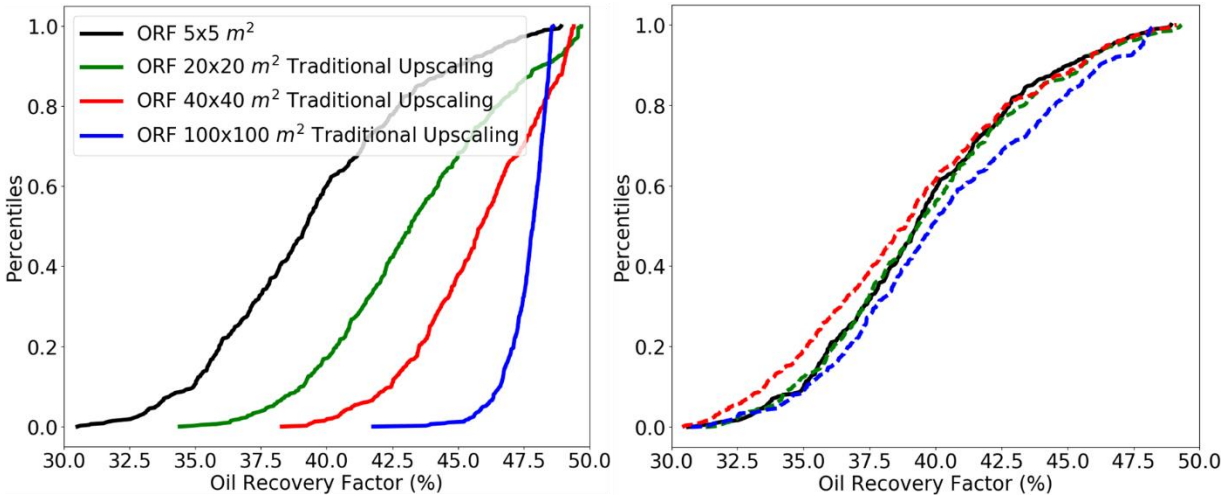

Figure 18. Oil recovery factor uncertainty curve after 0.4 PV injected of miscible gas. Coarse models with UR400 in blue, UR64 in red, UR16 in green and reference fine models in black. Traditional upscaling in continuous curve (*left)* and proposed workflow in dashed curve *(right)*.

Different well configuration (G2)

For this group, the objective is to verify how the same set of pseudo-curves generated, based on a 5-spot well scheme from fine-simulation results of the representative models, would behave in a different flow condition. For that, we re-run the models used in A2 considering a well pair configuration with the injector located on the upper left corner and the producer on the lower right corner.

Figure 19 shows the oil recovery factor uncertainty curves for this evaluation after 0.3 PV of miscible gas was injected. Again, coarse-scale results with the proposed workflow presented a close agreement with fine-scale results.

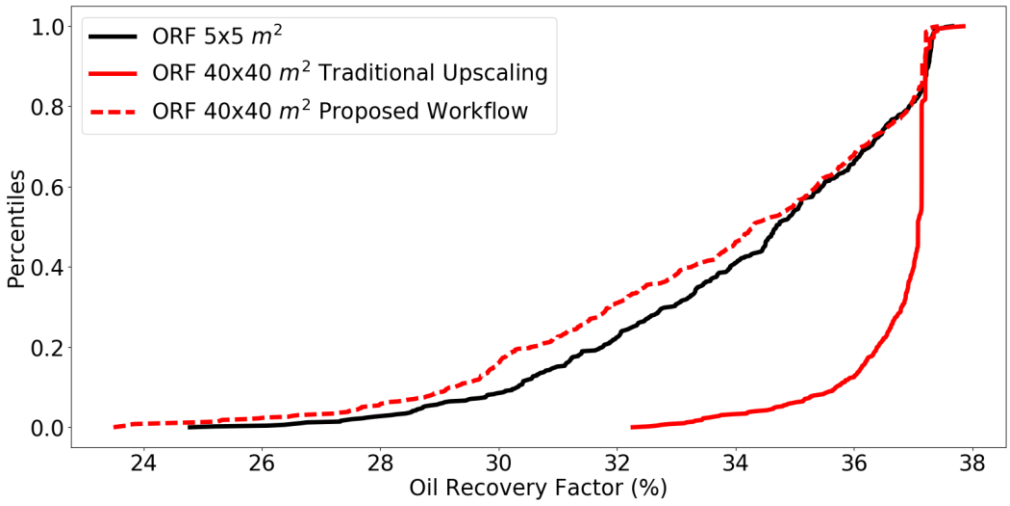

Figure 19. Oil recovery factor uncertainty curve after 0.3 PV injected of miscible gas. Coarse models in red and reference fine models in black. Traditional upscaling in continuous curve and proposed workflow in dashed curve.

Different EOR method (G3)

Our last study in Additional Analyses is to investigate the performance of our workflow when miscible WAG is the chosen EOR. In this case, since one more phase (water) is added to the system, we must adapt Step 7 of this workflow. When working on pseudo-curves, we now consider pseudo-relative permeability for both water-oil and gas-liquid curves. Apart from this particularity, all the steps of our workflow can be followed as proposed in this work.

Finally, this last result again shows the consistency of the proposed workflow. Even when water is also injected with miscible gas, we were able to improve the uncertainty quantification using coarse-scale models. We present the results of this application in Figure 20.

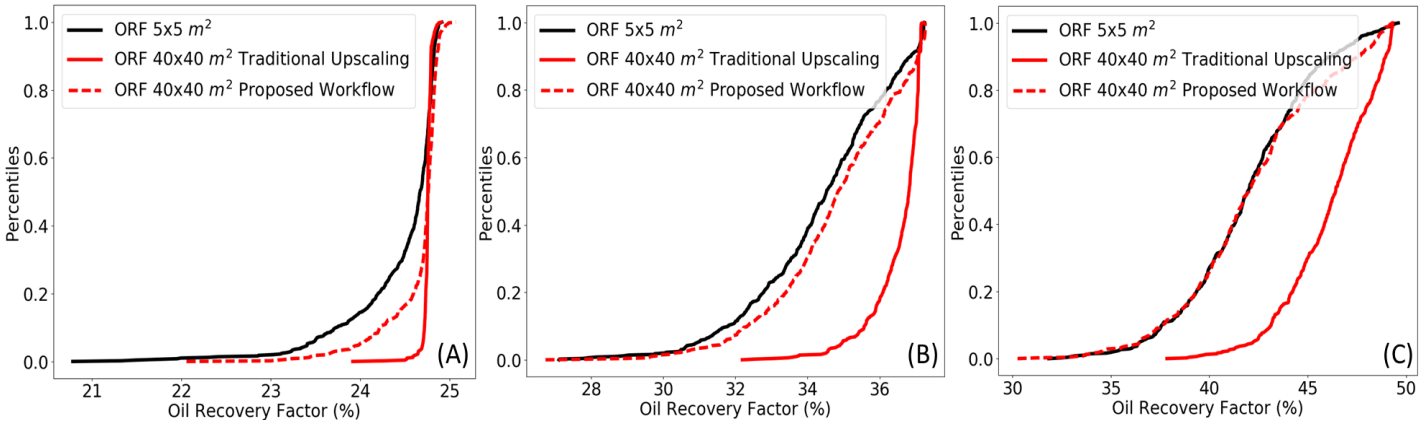

Figure 20. Oil recovery factor uncertainty curve after 0.2 (A), 0.3 (B) and 0.4 (C) injected of water and miscible gas. Coarse models in red and reference fine models in black. Traditional upscaling in continuous curve and proposed workflow in dashed curve.

Final comments, conclusions, and future works

The proposed workflow was effective in making coarse-scale models properly reproduce fine-scale results when multiple realizations are considered in a probabilistic study. Based on this work, we provide final comments below and describe ideas which we are considering for the sequence of this work:

- Our Step 6 proposes a division of three evenly spaced groups, but for more aggressive upscaling ratios, more than three Intervals may be necessary for improved results.
- To generate pseudo-relative permeability curves, the Corey model is usually considered. However, LET correlation (Lomeland et al, 2005) promotes more flexibility on fitting pseudo-relative permeability curves since it allows the variation of three parameters during the history-matching procedure to reproduce the fine scale reference curves, therefore it was used in Step 8 of the proposed methodology for the presented studies.

- In this work, we used ORF and the identified correlation with Koval as a general law to extend the representative model's upscaling characteristics to the remaining models. Although ORF adequately summarizes the global behavior of the simulation model result, other dynamic function outputs such as the cumulative production of fluids and injection could also be assessed.
- The use of multiple dynamic functions and the identification of their correlation with static functions (such as Koval) could be achieved in a more automated manner, using machine learning and clustering techniques, and this will be the subject of future work.

Finally, after the results and discussions provided by the analyzed applications, a number of important remarks must be highlighted:

- The proposed workflow can improve coarse-scale simulation results when multiple realizations are considered. The simulation results removed bias and maintained global fine-scale variability, essential to probabilistic studies and decision-making process.
- The correlation between the Koval factor and oil recovery is a useful guide to extrapolate the pseudo-curves obtained for each selected representative model.
- The methodology was applied to different upscaling ratios, flow conditions, and recovery method, which shows its robustness in better representing coarse-scale simulation results in multiple realization scenarios.
- The proposed workflow is very cost-effective, since it only requires a few fine models to be simulated (roughly 1%) to improve the entire ensemble of coarse-scale models simulation results.

Acknowledgments

The authors would like to thank Petrobras (Petróleo Brasileiro S.A.), Libra Consortium (Petrobras, Shell Brasil, Total, CNOOC, CNPC and PPSA), UNISIM, DE-FEM/UNICAMP, CEPETRO, Energi Simulation, ANP andCMG for all the support in this work.

5 ARTICLE 4: IMPROVING COARSE-SCALE SIMULATION MODELS WITH A DUAL-POROSITY DUAL-PERMEABILITY UPSCALING TECHNIQUE AND A NEAR-WELL APPROACH

Victor de Souza Rios, Denis José Schiozer, Luiz O. S. dos Santos, Arne Skauge
Journal of Petroleum Science and Engineering, v. 198, March 2021, p. 108-132

Abstract

In the management of an oil field, the creation of a highly detailed fine-scale model to properly represent the key reservoir heterogeneities is important. This model better represents the main reservoir features but remains a significant challenge for dynamic reservoir simulations with impractically high computational costs, even for single numerical simulation runs. Therefore, the scaling up of a highly detailed model is a crucial step in reservoir engineering studies to enable field-scale simulation runs within a time-frame compatible with the needs of the industry. Upscaling must be carefully performed because it can introduce significant errors and bias to the numerical models due to truncation errors and the smoothing of sub-grid heterogeneities.

This work focuses on improving the representation of small-scale heterogeneities in coarse models. It expands the dual-porosity and dual-permeability upscaling technique proposed (Rios et al., 2020) to be applied to 3D highly heterogeneous systems. Specific near-well treatment is considered to improve the overall flow distribution in the wells; with this procedure, the coarse model better represents the production and injection profiles throughout the wells. Therefore, the final coarse-scale model can represent the main reservoir heterogeneities and possible preferential pathways, while improving the definition of the wells' productivity and injectivity indices.

The proposed upscaling technique is applied to different reservoir simulation models with immiscible water flooding in 3D evaluations. Our approach was validated by two case studies: SPE-10 and a field-case heterogeneous reservoir with karst structures. The focus is to demonstrate that the division of the porous media into primary and secondary systems improves capillary and gravity representation of coarse models in 3D applications, while the near-well upscaling makes the flow distribution in the wells in agreement with the fine-scale solution. The resulting coarse-scale dual-permeability models are much faster than the reference fine models (between 0.025% and 1.5% of the fine-scale simulation time), more accurate than the traditional flow-based upscaling results, and can better reproduce the fine-scale responses in different upscale ratios (from 25 up to 1 700)

Introduction

In traditional upscaling procedures, a group of fine-scale cells is averaged to obtain a single cell with uniform properties, which corresponds to a coarse-scale cell. Consequently, sub-grid heterogeneities tend to be homogenized, and each upscaled grid block smooths out the behavior of several fine-scale grid cells. Dynamic evaluations with coarse-scale models in these

situations tend to overestimate the sweep efficiency of the injected fluids. This effect mainly occurs because the preferential paths, generated by high permeability contrasts, are homogenized in each coarse-scale cell.

Upscaling fine-scale detailed models to a coarser system with improved performance is a frequent need in practical reservoir simulation studies. For this purpose, various techniques were proposed throughout the years with an increasing level of complexity, depending on the static and dynamic challenges represented by each reservoir and production strategy. Detailed and comprehensive reviews on several techniques are provided by Wen and Gomez-Hernández (1996), Renard and de Marsily (1997), Farmer (2002), and Durlofsky (2003).

In practical reservoir simulation studies, single-phase static upscaling strategies are valuable tools. They can be successfully applied to the proper representation of oil production under primary depletion in coarse-scale models. The most frequently used method to upscale porosity from a fine-scale model is the volumetric weighted arithmetic mean, because the pore volume is preserved (Durlofsky, 2003). For permeability upscaling, there are three important methods: averaging, which considers horizontal arithmetic average and vertical harmonic average; Cardwell-Parsons directional averaging (Cardwell and Parsons, 1945); and flow-based upscaling with closed boundary conditions (Christie, 1996; Kumar et al., 1997). In general, flow-based upscaling methods are more widely considered as reference approaches because of their generality and flexibility (Chen and Durlofsky, 2006).

In flow-based upscaling techniques, transmissibility calculation partially captures the effects of heterogeneity on permeability and preferential flow pathways. However, transport calculation can be erroneous due to the equilibrium assumptions and uniform displacement at a local level (Jessen and Evazi, 2013). This challenge increases in channelized reservoirs and heterogeneous systems with high correlation length (comparable to well spacing).

When fluid is injected into a heterogeneous reservoir, a more complex flow-distribution occurs and additional effort is usually required for the most effective upscaled model. For water flooding or immiscible gas injection simulation processes, a two-phase upscaling procedure is recommended. In this case, pseudo-relative permeability curves are a popular method to improve the results of coarse-scale simulation models when fine-scale simulation results are available.

Barker and Thibeau (1997) reviewed several existing relative permeability upscaling approaches. They noted significant limitations when considering pseudo-relative permeability curves while upscaling fine-grid geological models to coarse-scale simulation

models. It is worth highlighting that the various pseudoization approaches require that one must either be able to run the fine grid or select a representative section of the fine grid, and assert that the pseudo functions are appropriate for use elsewhere in the model (Fayazi et al., 2016). This limitation is well known when applying pseudo-relative permeability curves to reproduce fine-scale results using coarse models.

Several authors have proposed methodologies to improve the representation of small-scale results in coarse-scale simulation models. Backer and Fayers (1994) developed the method of transport coefficients (also known as α-factors), which consists of modifiers introduced in the flow terms to relate the compositions of fluids flowing from a large grid block to the average compositions of those fluids within the grid block. Together with the use of pseudo relative permeability curves, they tested the method for various fluid systems with improved accuracy in the results, especially in terms of component production rates for the cases considered. Christie and Clifford (1998) also used the α-factor approach, but they considered streamline techniques to generate a fine-scale solution. However, no pseudo-relative curves were used because the authors only considered single-phase flow problems.

Chen et al. (2003) developed an upscaling procedure, referred to as a coupled local-global upscaling approach, in which the local boundary conditions (used to compute upscaled properties) are determined from global coarse-scale flows. The authors showed significant improvement over existing and extended local methods. However, only generic flows were considered in the generation of the coarse-scale properties; specific global flow and well effects, which may affect the upscaling accuracy, were not investigated.

Chen and Durlofsky (2006) proposed an adaptive local-global (ALG) upscaling procedure to generate coarse-scale parameters “adapted” for any type of global flow. They included a threshold to update the upscaled properties only in high-flow areas, potentially increasing the efficiency of the upscaling procedure. The authors reported that flow simulation results on highly heterogeneous systems showed improvement over local and coupled local-global upscaling techniques.

Zhang et al. (2008) developed an upscaling method called Well Drive Upscaling (WDU) that employs global well drive and actual boundary conditions to avoid using inappropriate boundary conditions in single-phase upscaling. The authors presented good results, but the methodology can only be applied if a fine-scale pressure solution is available.

Evazi and Jessen (2014) developed a technique for highly heterogeneous reservoirs, in which the pore space is split into two levels of porosity. The division is based on fine-scale streamline information, and a dual-porosity dual-permeability (DP/DP) flow model is adapted

to represent the coarse-scale model. They demonstrated that DP/DP coarse-models predict the breakthrough time accurately and are less sensitive to the level of upscaling when compared to traditional single-porosity upscaling. However, the overall workflow to obtain the upscaled models can be costly because streamline simulations for the fine-scale model are needed. Another drawback is the use of fine-scale results to divide the porous media, which can make the strategy strongly dependent on the original well locations and flow rates.

Correia et al. (2019) investigated the specificities of the upscaling problem for karst reservoirs. Their work is an extension of the embedded discrete-fracture model (EDMF) developed by Li and Lee (2008), later extended by Monfair et al. (2014), and stress-tested by de Sousa et al. (2016) and others. The authors proposed an approach, named EDKM (embedded discrete-karst model) in which they considered special connections between matrix and karst media to represent karst reservoir systems. The authors applied the methodology to a carbonate reservoir with megakarst structures. They obtained a coarse model with a good dynamic match compared with the reference results and an important time reduction (about 95%). Despite the remarkable improvements shown by the authors, the final coarse model still consumed three hours to complete a simulation, mainly because the karst representation had the same block size as the refined grid.

Rios et al. (2020) proposed a new dual-porosity dual-permeability (DP/DP) upscaling technique for highly heterogeneous reservoirs. They used the flow and storage capacity analysis, and the Lorenz Coefficient (Lorenz, 1905; Jessen et al., 2000) applied to the static information of a fine-scale model to split the porous media into two levels: one representing the main flow regions and the other, the secondary flow regions. With the splitting of fine-scale cells, directional upscaling for permeability is performed for each group. They showed, in deterministic and probabilistic evaluations, that the resulting coarse-scale models can adequately reproduce the reference fine-scale results better than traditional static upscaling methods with two significant improvements over other upscaling techniques. It is 1) less time-consuming to obtain coarse-scale models since no dynamic responses of fine-scale models are used and 2) not dependent on the drainage plan or well flow rates of the fine-scale models.

This work extends the DP/DP upscaling technique for 3D highly heterogeneous systems. For this purpose, the proposed general upscaling procedure provides a workflow to divide the porous media into two systems through all layers of the fine scale model. Then, vertical upscaling is performed, which enables the final coarse-scale model to represent the main sub-grid heterogeneities areal and vertically. This approach improves capillary and gravity representation of coarse models in 3D applications. The DP/DP approach with a near-

well treatment is combined to enhance the overall flow distribution in the wells. The improved coarse-scale representation of the small-scale heterogeneities in 3D systems in association with a near-well upscaling procedure are the main contributions of this work.

In the following sections, after highlighting the objective of our work, the methodology is described and the steps and procedures are given. In sequence, the case studies and applications are shown. Then, the proposed methodology is applied to two case studies with water flooding: (i) classic SPE-10 benchmark, and (ii) a carbonate reservoir with kart structures. The study continues with additional evaluations and discussions. Lastly, a summary and final remarks are given to conclude this presentation.

Methodology

The proposed methodology for our DP/DP upscaling technique is divided into two parts: (i) DP/DP workflow and (ii) near-well approach.

The first is an extension of the procedure described by Rios et al. (2020). For each layer in the model, the porous media is split into primary and secondary systems according to the classical flow and storage capacity theory (as a global guide) and the Lorenz coefficient for each group of fine cells that compose a coarse-scale cell (as a local guide). The coarse-scale properties are then calculated for both systems. The volumetric weighted arithmetic mean is considered for porosity, while directional Cardwell-Parsons upscaling is performed for permeability.

With the porous media ranked and divided into two systems, flow and transport need to be modeled in a way that allows two different continua to coexist with interaction between them. To accomplish this, the flow in the new upscaled model can be approximated with a DP/DP approach formulation (Rios et al., 2020).

In this DP/DP flow model, the primary and secondary systems consist of two distinct continua, with a linear transfer function modeling crossflow between them. The preferential system (primary system) is modeled as “fracture,” and the passive system (secondary system) as “matrix.” The total flow includes flow through primary cells (fracture-fracture), through secondary cells (matrix-matrix), and between the primary system and the secondary system at a certain coarse cell level (matrix-fracture). For the mass transfer between primary and secondary systems within a coarse block, the style formulation of Gilman and Kazemi (Gilman and Kazemi, 1983) was applied for the shape factor, which is uniform throughout the model (Rios et al., 2020).

The well-blocks are not split into systems, so they are treated as single-porosity. For these well-blocks, a near-well upscaling is considered to improve the well-index calculations and enable a better representation of the production/injection profile throughout the well, which is the second part of our upscaling process.

The main steps of the proposed methodology are described below and summarized in Figure 1.

DP/DP upscaling workflow:

This part of our methodology expands the concepts and procedures detailed by Rios et al. (2020) in a 2D setting. The main difference in the extension is regarding the application of the porous media splitting into two systems throughout the layers in a 3D model. The following steps summarize the extended DP/DP upscaling workflow for a chosen coarse-scale model size:

1. For each layer in the fine-scale model:
    a. Construct classical flow (F) and storage capacity (C) diagram (also known as F-C diagram) for the fine-scale model;
    b. Apply a threshold value for flow capacity (F) to select the primary system fine cells. One can consider different threshold values for each layer depending on the heterogeneity level;
    c. Calculate Lorenz Coefficient (Lc) for the group of fine cells in each resulting coarse-scale cell;
    d. Apply a threshold value for Lc and select additional cells for the primary system;
    e. Calculate coarse-scale cell properties for both systems: weighted arithmetic mean for porosity, and directional Cardwell-Parsons upscaling for permeability.

    Rios et al. (2020) present a complete description of this part of our methodology and provide details about each step and calculations.

2. Uplayer (vertical upscaling) the resulting coarse model with harmonic average to achieve the final coarse-scale.

It is important to highlight that, if the reservoir heterogeneity presents a uniform vertical distribution, i.e., not layered, but continuous vertical structures, it is possible to apply the uplayer of the fine model, and then follow to the DP/DP procedure. Therefore, steps 2 and 1 are inverted. With this change, time can be saved with the upscaling calculations without jeopardizing the coarse-scale results for this type of reservoir.

Near-well upscaling procedure:

After the DP/DP upscaling, special treatment was given to all the coarse-scale cells, and these present an increased capability of representing sub-grid heterogeneities. However, the well-blocks in the DP/DP upscaling were not included, and a specific near-well upscaling was performed to improve the coarse-scale well-indices. Nevertheless, the well-blocks are considered as secondary system cells.

An upscaling procedure is proposed in the near-well region, based on the approach presented by Ding (1995), and described by Durlofsky (2003). The pressure and flow rate information of a group of fine-scale cells within a coarse-scale block are considered to calculate the coarse-scale upscaled well-index. The steps to accomplish this procedure are as follows:

1. Run a single-phase simulation for the fine-scale model controlling all wells with constant bottom-hole pressure ($P^w{}_{I,J,K}$). Note that only near-wells regions need to be activated for this purpose*;

   It is worth mentioning that an area corresponding to the coarse-scale well-blocks and one neighbor cell in each direction is satisfactory to be considered the near-well region. Additionally, only one day of the fine-scale single-phase simulation run is necessary to provide the required data for the next steps.
2. Extract the well flow rate information along the entire well path;
3. Extract the fine-blocks' pressure within a coarse-scale region;
4. Calculate the well flow rate for each coarse-scale block using the well flow rate information collected for the corresponding fine-blocks:

$$\boldsymbol{Q^w{}_{I,J,K}} = \sum_{l=1}^{N_w} \boldsymbol{q^w{}_l} \qquad \textbf{(1)}$$

   where $Q^w{}_{I,J,K}$ is the well flow rate for the coarse block (I, J, K); $q^w{}_l$ is the well flow rate for each fine-scale well-block within a coarse block; and N_w is the number of fine well-blocks corresponding to a single coarse block (I, J, K).
5. Calculate the volume-averaged pressures $P_{I,J,K}$ for each coarse-scale block regions using the corresponding fine-blocks' pressure and bulk volume information:

$$\boldsymbol{P_{I,J,K}} = \frac{1}{V_t}\sum_{l=1}^{N_t} \boldsymbol{p_l V_l} \qquad \textbf{(2)}$$

*in this case, only flow inside the selected ear-well area is considered.

where N_t is the number of fine blocks corresponding to the single coarse block (I, J, K); p_l and V_l are the fine-scale pressures and cell bulk volumes; and V_t is the total bulk volume of the coarse block.

6. Calculate the upscaled coarse-scale well-index $WI^*_{I,J,K}$:

$$WI^*_{I,J,K} = \frac{Q^w_{I,J,K}}{P_{I,J,K} - P^w_{I,J,K}} \quad (3)$$

In our methodology, the well-blocks' transmissibilities are not calculated during the near-well upscaling. For this, our DP/DP technique, combined with the upscaled well-indices, provided accurate results without any further improvement in the near-well transmissibilities.

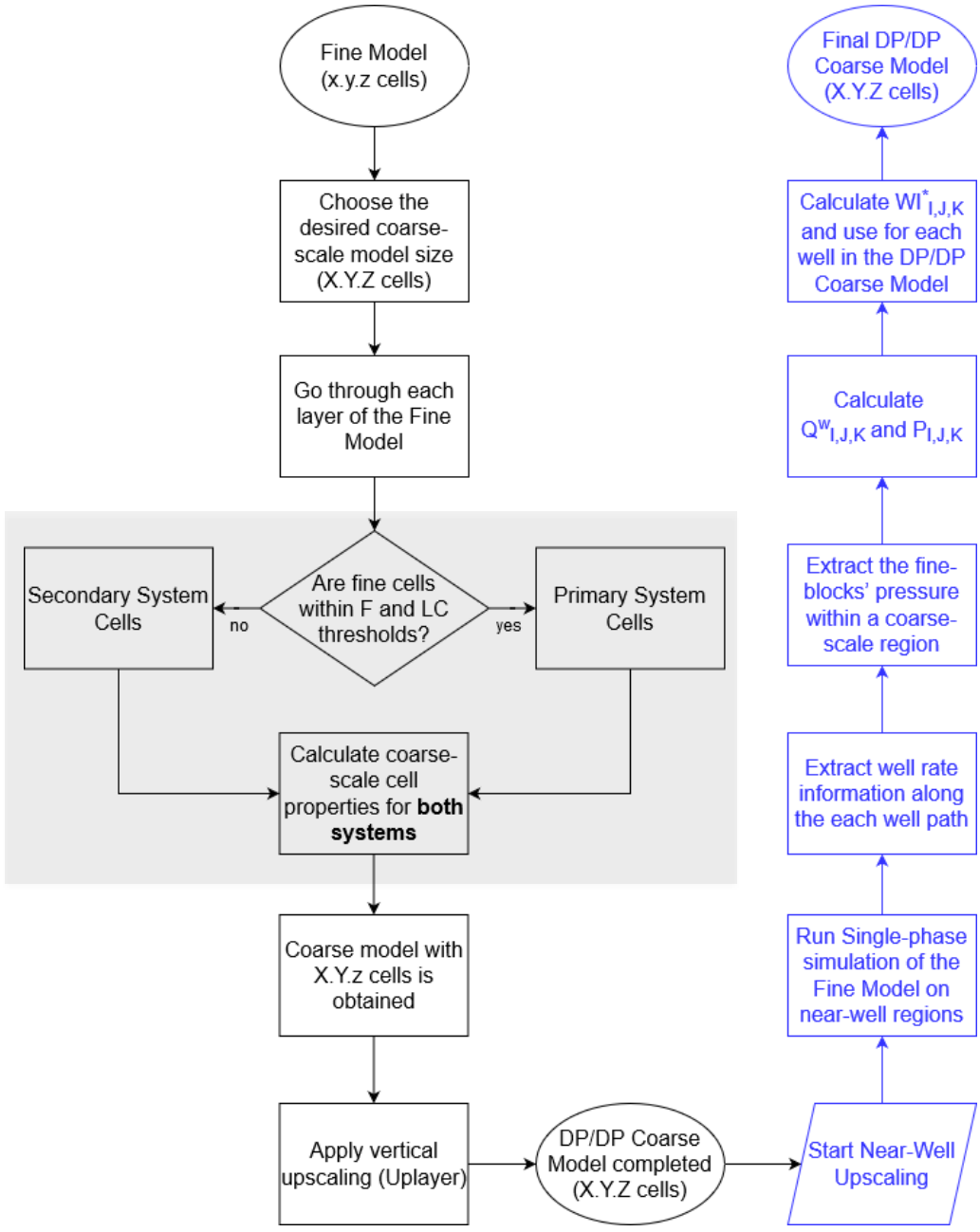

Figure 1. Flowchat summarizing the steps of the proposed general DP/DP upscaling procedure. The highlighted steps are detailed in Rios et. al. (2020)

Description and Applications of Case Studies

The proposed methodology is tested in two different 3D case studies. For each case, specific evaluations are conducted to stress-test the new upscaling approach. With the chosen case studies, a number of critical upscaling limitations are addressed and these show the performance of this DP/DP technique in challenging scenarios.

Case A: SPE 10th model

The first case study, Case A, is the classical 10th SPE Comparative Solution Project (Christie and Blunt, 2001), and it is used to evaluate the sensibility of our DP/DP upscaling to different upscaling ratios (URs). It is well known that traditional single-porosity upscaling procedures tend to be highly sensitive to different upscaling levels. Rios et al. (2020) showed, in 2D applications, that the DP/DP approach presents accurate and consistent results in three different URs (4, 16, and 50). In this work, a further investigation is made possible in that the URs are tested from 25 up to 1700.

The SPE 10th model is a highly heterogeneous and channelized fluvial system with 60 x 220 x 85 Cartesian grid block cells. The permeability values vary from 0.001 to 20 000 mD, while the porosity ranges from 0 to 0.4. The reservoir presents two different zones. The upper 35 layers of the model present a variogram-based permeability distribution, while the 50 lower layers are the result of fluvial depositions, with marked high-permeability channels. These characteristics make this model very challenging to upscale and a good test for evaluating our DP/DP upscaling technique. Figure 2 shows the permeability field and highlights both zones mentioned above.

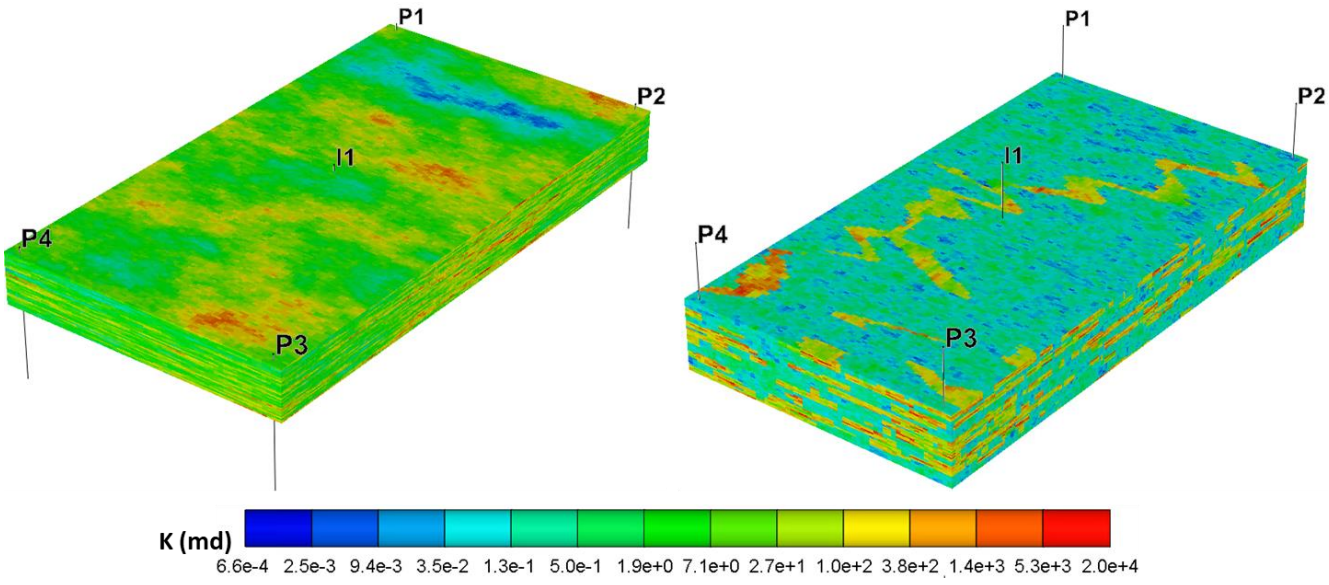

Figure 2. SPE 10th model. Permeability field with highlight to both zones. The upper, with variogram-based distribution, and the lower, with high-permeability channels.

Case B: Field case study

The second case study, Case B, is a field-scale heterogeneous reservoir with karst structure. The presence of karst, explicitly modeled in the fine-scale, adds complexity to the upscaling problem. Such structures present high permeability, high porosity, and a different flow behavior compared with the regular matrix regions. Representing these sub-grid features in coarse-scale models is a difficult task, and traditional single-porosity approaches usually fail. Details about the geological model are provided by Chaves (2018) and Correia et al. (2019).

Case B is a complex reservoir system modeled with 400 x 700 x 40 grid block cells, of which more than 5 million are active. The reference fine-scale model presents grid blocks with 10 x 10 x 1 m3. The permeability varies from 0.003 to 11 000 mD, and porosity ranges between 0 and 0.84. Figure 3 (a) and (b) show the 3D porosity and permeability maps for this reservoir. Here we observe the overall heterogeneous distribution and some marked areas in which porosity and permeability values are consistently higher. These areas are the karst structures, highlighted in red in Figure 3 (c), using layer 8th as reference.

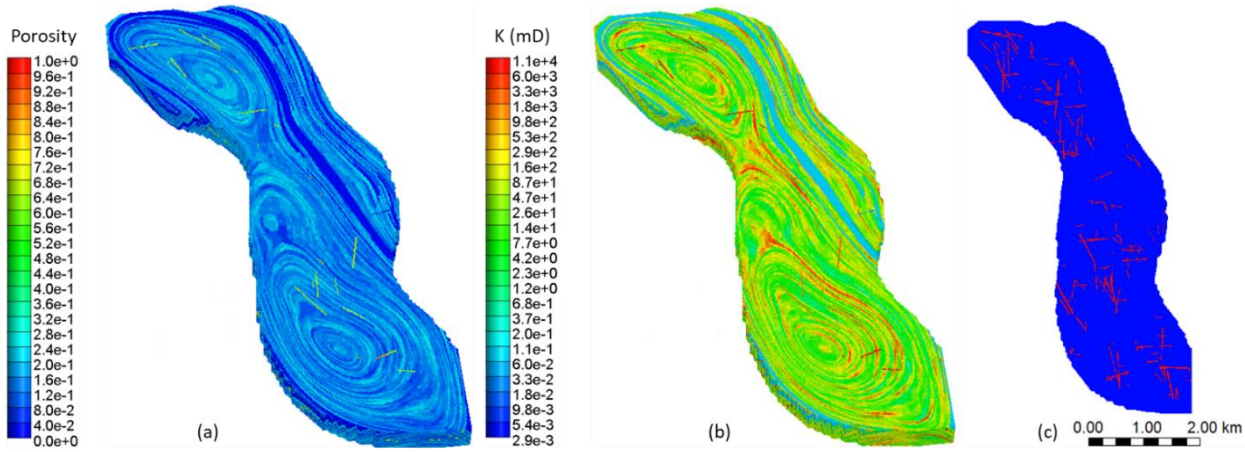

Figure 3. Case B: heterogeneous carbonate reservoir with karst structures. (a) porosity, (b) permeability, and (c) layer 8th of the reference model: the matrix cells are in blue and the karst structure cells are in red.

Results and Discussions

Next, the results and discussions regarding both case studies are presented. The performance of the DP/DP upscaling approach is compared with the fine-scale reference models and the traditional single-porosity upscaling (SP). In all comparisons, the flow-based upscaling is considered as the reference for SP upscaling, since it tends to be the best option for heterogeneous reservoir models (Chen and Durlofsky, 2006).

Case A

For the first case study, the dynamic evaluations are performed with the same conditions outlined for the 10th SPE Comparative Solution Project (Christie and Blunt, 2001).

The central injector well injects water at a constant rate of 5000 bbl/day and a maximum bottom hole pressure of 10 000 psi. There are four producer wells in the corners of the model; each produces at a constant bottom hole pressure of 4 000 psi. The viscosity ratio (oil/water) is 10, which implies an unstable water flooding process. Fluid properties and relative permeability curves are detailed by (Christie and Blunt, 2001). The Field units for Case A are used for alignment with the units of the original paper.

The five different coarse model sizes are considered for evaluating our upscaling technique. For this purpose, the fine-scale reference model (60 x 220 x 85 cells) is upscaled uniformly to 12 x 44 x 85, 12 x 44 x 17, 12 x 22 x 17, 6 x 22 x 17, and 6 x 22 x 5. Which corresponds to URs of 25, 125, 250, 500, and 1700, respectively. Figure 4 shows the permeability field for the reference model and the five coarse-scale upscaled models. It is noteworthy that the coarsening process progressively averages the heterogeneity representation, and the upscaled models are more likely to smooth preferential pathways and high permeability channels. This process can lead to an overestimated sweep efficiency of the water flooding process and result in delayed water breakthrough and artificially high oil production.

To evaluate the performance of the traditional flow-based upscaling technique for Case A, the fine-scale simulation results are compared with all the upscaled models. The comparisons for cumulative oil production and water cut are given in Figure 5. Also, the coarse models' results are systematically optimistic, with higher cumulative oil production and postponed water breakthrough. More importantly; the higher the UR:(i), the higher the overestimation of the sweep efficiency will be;(ii) the more optimistic the oil production will be; and (iii) the later the water breakthrough will be.

As previously discussed, these limitations of traditional SP upscaling techniques are well-known, and they were crucial motivations for Rios et al. (2020) to propose their DP/DP upscaling, which is extended in this work. To appraise the performance of our methodology, the upscaling procedure proposed in this work is then applied to generate the coarse models with the five URs mentioned earlier.

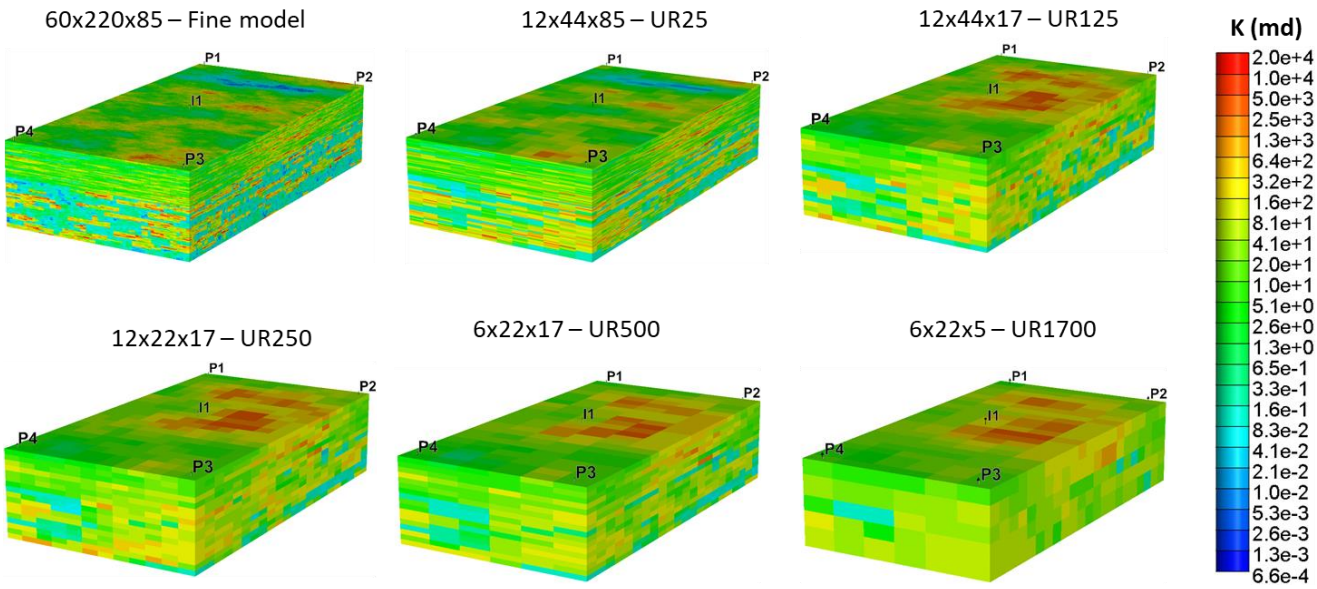

Figure 4. Permeability field for all models in Case A.

Figure 6 shows the results and comparison between fine-scale model and DP/DP coarse models. By preserving the main reservoir heterogeneities and sub-grid features, the DP/DP upscaled m odels present accurate results compared with the reference model. It is also important to mention that all DP/DP coarse models are capable of reproducing the cumulative oil production and water cut from fine-scale. The breakthrough time is well captured even for a UR of 1 700. Again, as stated by Rios et al. (2020), for 2D evaluations, the DP/DP coarse-scale results not only present a close agreement with the reference response, but they are close to each other. This result is a remarkable achievement from our upscaling technique since the coarse model results' are significantly less sensitive to the level of upscaling as compared to traditional SP upscaling.

Apart from analyzing the results for the entire field, the responses for each producer well is also evaluated.

Figure 7 shows the comparison between the fine model and the SP coarse-scale models for cumulative oil production.

Figure 8 shows the same comparison but considers DP/DP upscaled models. As observed for full-fiel d responses, traditional SP upscaling results are more optimistic and highly sensitive to the level of upscaling. At the same time, the DP/DP approach provides a good agreement between fine and coarse results, even when each producer well is compared.

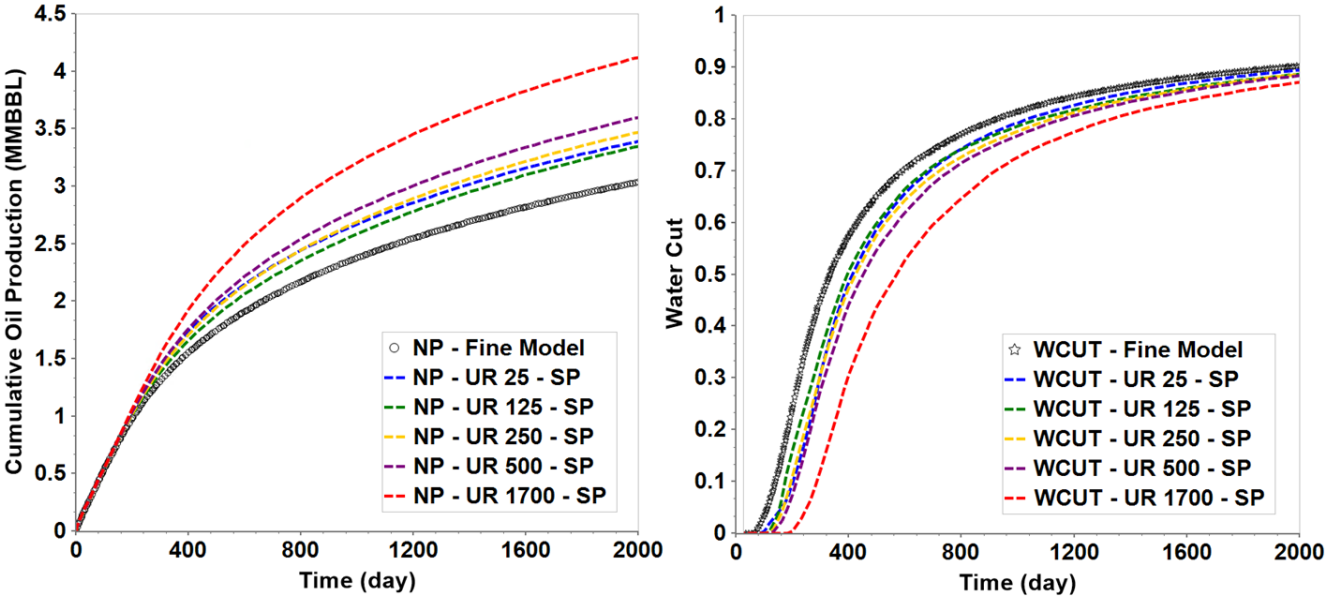

Figure 5. Comparison between fine model and SP coarse models for cumulative oil production (left) and water cut (right).

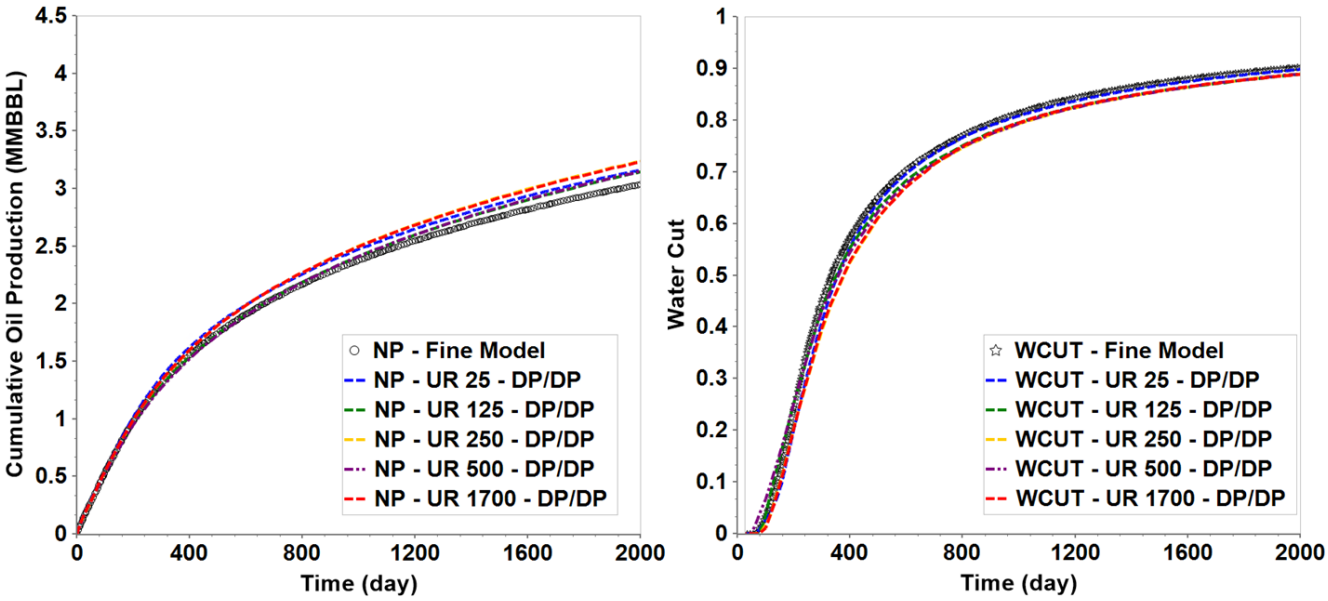

Figure 6. Comparison between fine model and DP/DP coarse models for cumulative oil production (left) and water cut (right).

After presenting a general performance evaluation of our DP/DP upscaling for various URs, the intermediate UR of 250 is selected to further explore the main improvements that the proposed methodology provides. Firstly, the porous medium division is illustrated in Figure 9, which shows the permeability field for both systems of the DP/DP coarse model. The concentration of the highest permeability values is observed in the primary system, which brings an improved representation of the main reservoir heterogeneities to the coarse model.

Following this, the dynamic results are compared, first for full-field evaluation, then for well-by-well performance.

Figure 10 shows the full-field comparison between the fine model and both coarse models, SP and DP/DP. The results of average field pressure, oil rate, and water cut are shown. From the presented curves, it is possible to observe the improvements obtained with the use of our DP/DP approach. For all the compared curves, the DP/DP coarse-model closely reproduces the reference responses.

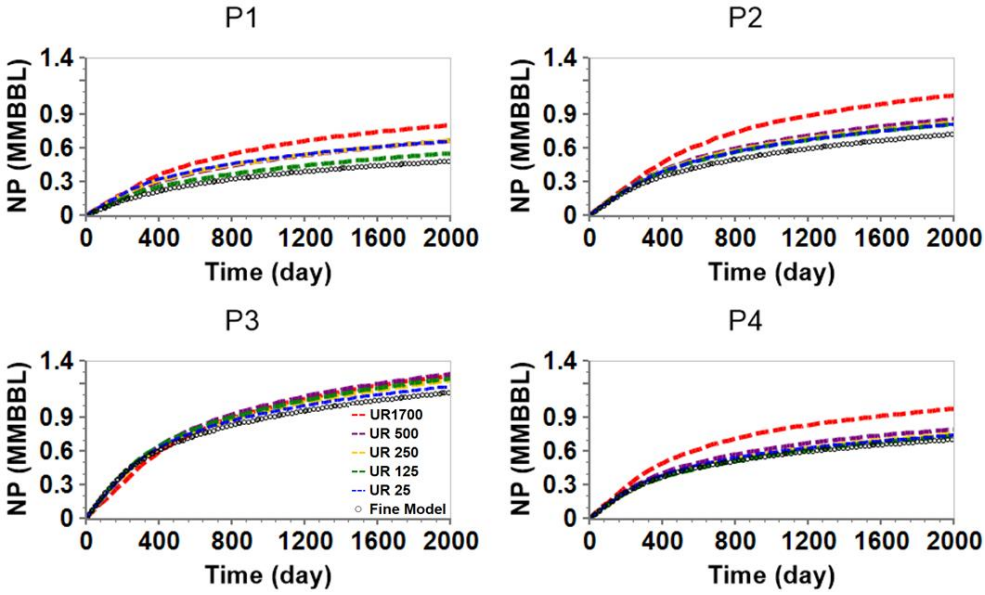

Figure 7. Well-by-well comparison between fine model and SP coarse models for cumulative oil production.

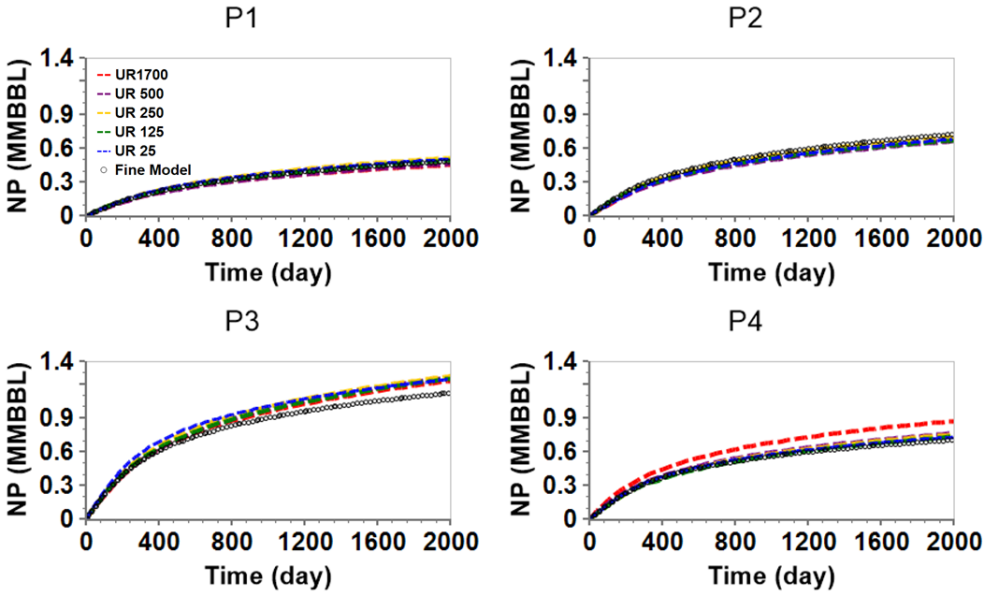

Figure 8. Well-by-well comparison between fine model and DP/DP coarse models for cumulative oil production.

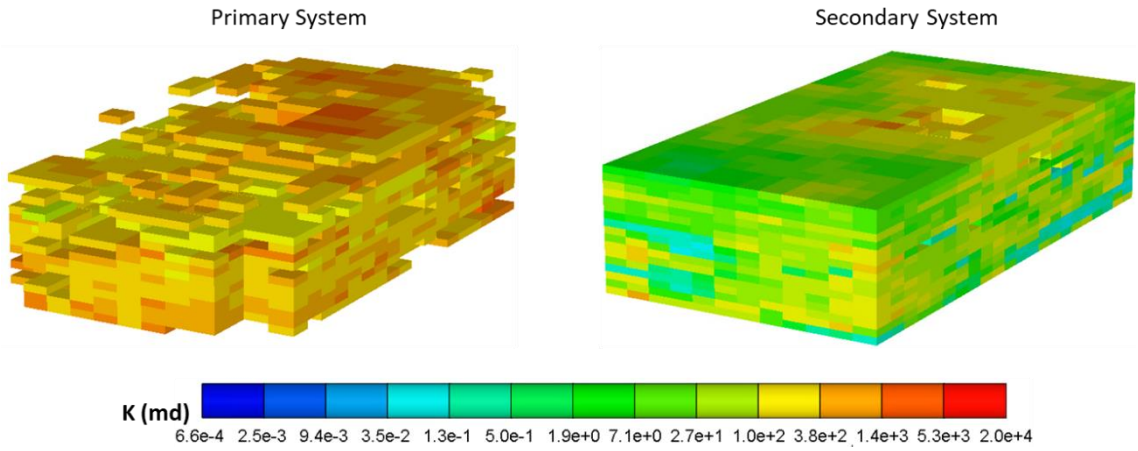

Figure 9. Permeability field, I direction, for DP/DP upscaled model with UR 250.

These results are noticeable since the SPE-10 problem has low compressibility; thus, the water and oil rate predictions are almost independent of the quality of the field average pressure prediction. However, average field pressure is sensitive to the correct estimation of the wells' productivity indices (PIs) (Christie and Blunt, 2001). Therefore, the fact that our DP/DP upscaled model can satisfactorily reproduce production rates and the average field pressure is a consequence of two key factors: (1) a better representation of the sub-grid heterogeneities and preferential pathways, and (2) a proper estimation of the well PI.

To highlight the second-mentioned factor, Figure 11 shows, for each producer well, the oil rate production and water cut. Again, the DP/DP results are consistently better than the SP ones. Also, if the initial oil rate for all wells is observed, it is fair to say that the DP/DP coarse model correctly predicts the PI. This result is a critical contribution from our near-well upscaling treatment.

Lastly, as a particular way to present the contribution of the near-well upscaling procedure, Figure 12 shows the bottom-hole fluid rate profile for all the wells, for each of the five wells in Case A, after 30 days of simulation. These results are a complementary way to show the improvements from the near-well procedure coupled with our DP/DP upscaling technique.

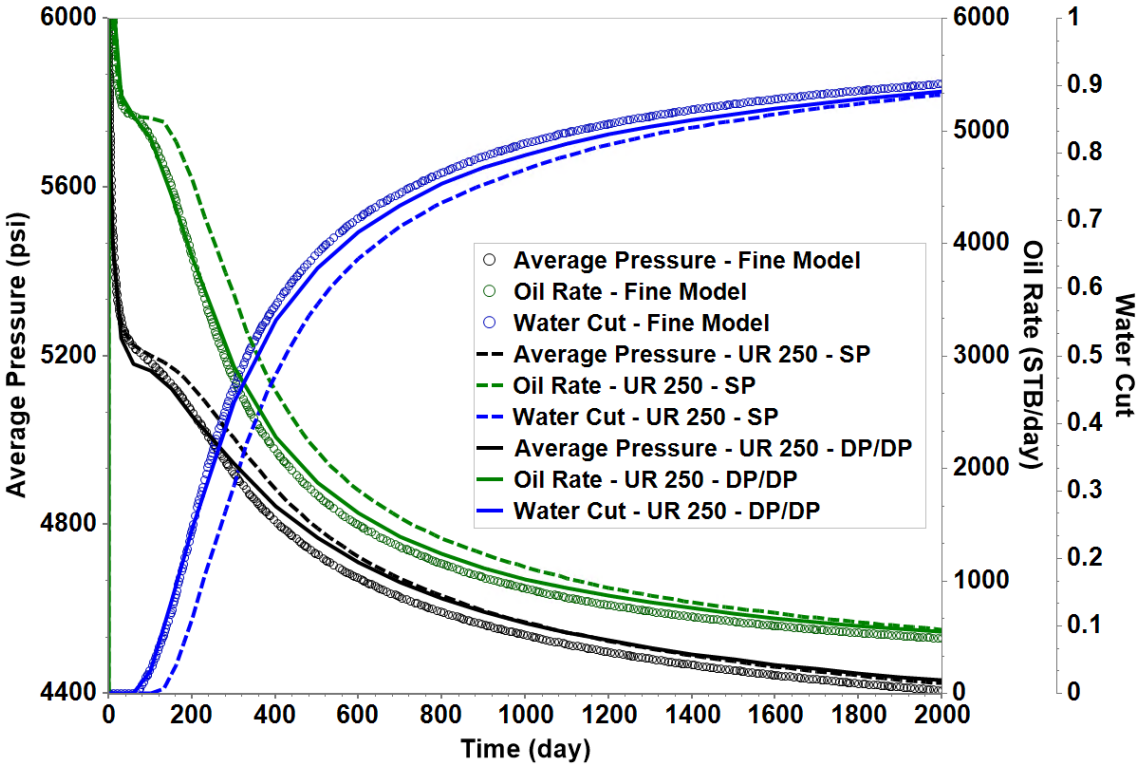

Figure 10. Average Field Pressure, Oil rate, and WCUT for the full-field in Case A. Coarse model with UR250 is shown. The continuous curves represent DP/DP upscaling; the dashed curves, SP upscaling; and the dotted curves, the fine-scale model

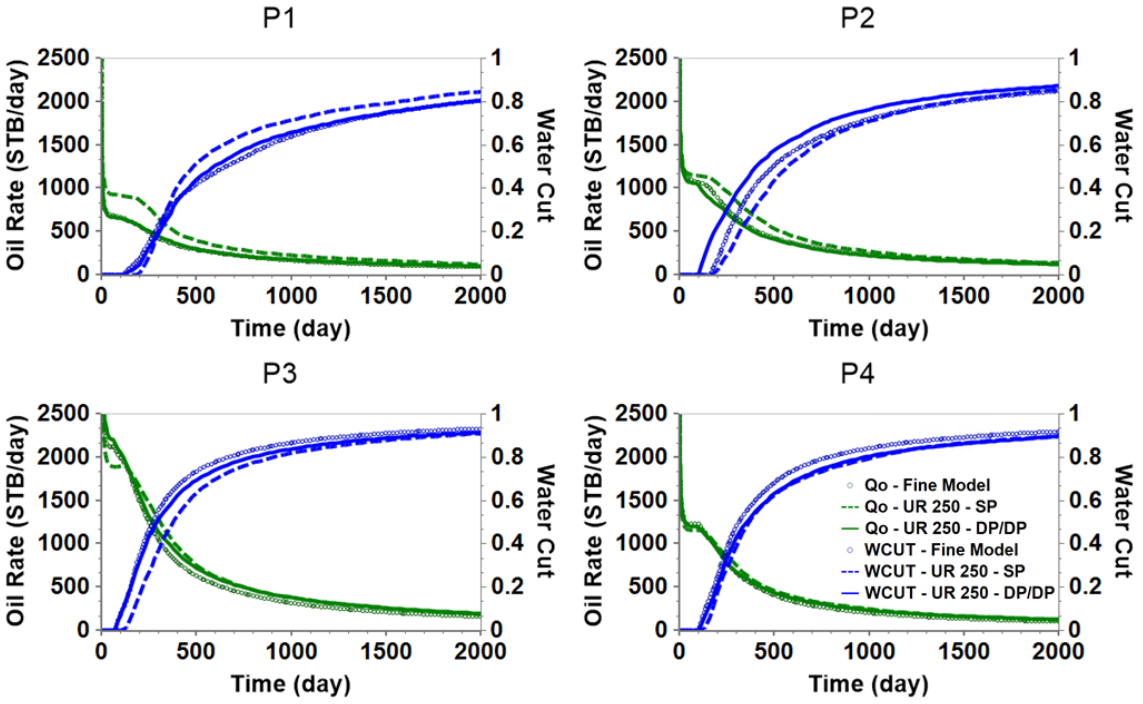

Figure 11. Oil rate and WCUT for each well in Case A. Coarse model with UR250 is shown. The continuous curves represent DP/DP upscaling; the dashed curves, SP upscaling; and the dotted curves, the fine-scale model.

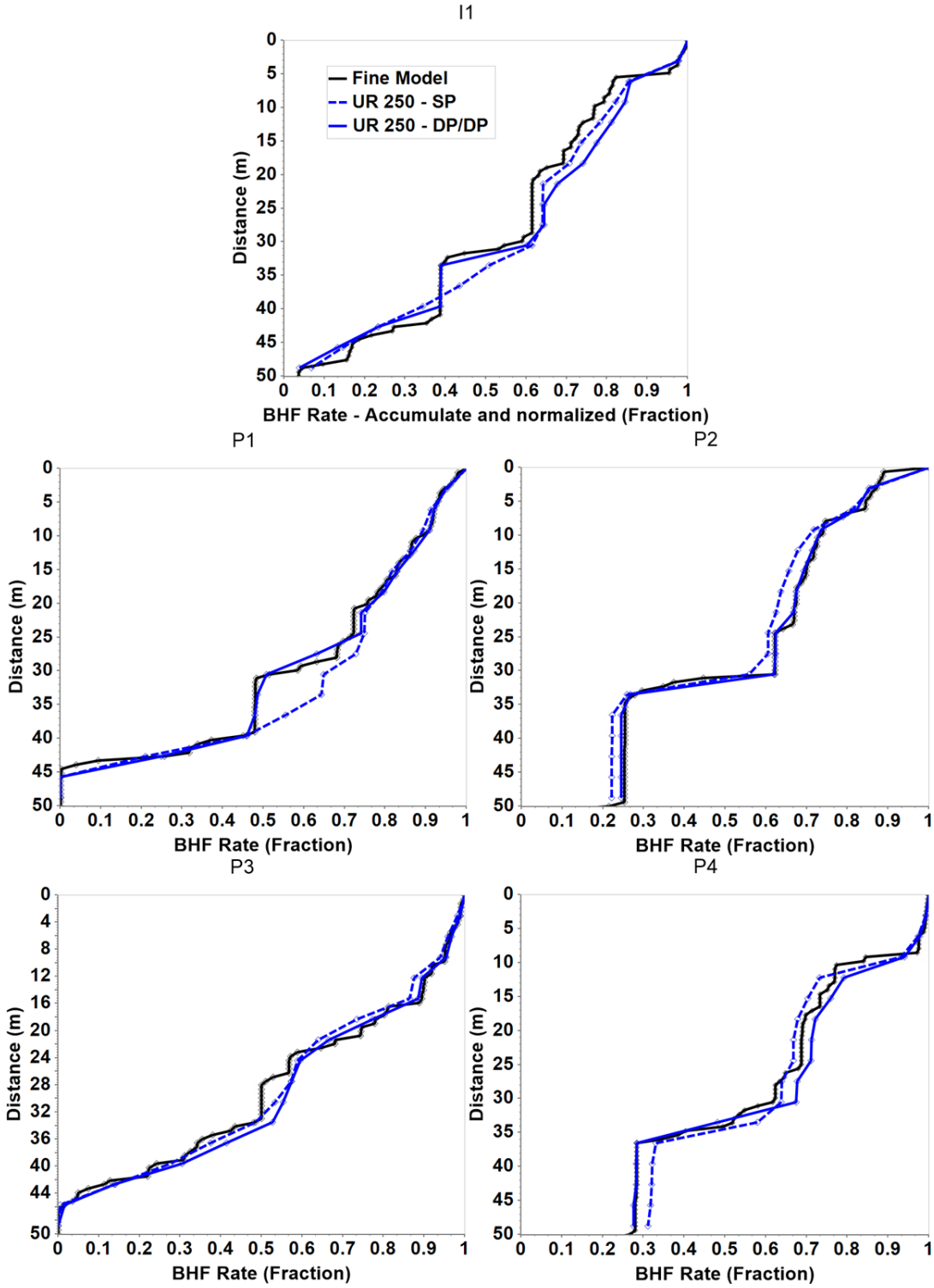

Figure 12. Accumulated and normalized well bottom hole fluid rate along the wells for each well in Case A after 30 days. The coarse model with UR250 is shown. The continuous curves represent DP/DP upscaling; the dashed curves, SP upscaling; and the black-marked curves, the fine-scale model

Case B

For the second case study, the reservoir static-properties (permeability, porosity, and rock types) are applied based on the works of Correia et al. (2019) and Chaves (2018).

Since this case will be considered in a future publication, to evaluate miscible gas injection, a different fluid model is implemented and a compositional simulation is conducted. For this purpose, the seven pseudo-component Peng-Robinson equation of state presented by Rios et al. (2017, 2018) is used. The initial gas-oil ratio (GOR) is 240 m^3/m^3, the saturation pressure is 400 bar, and the oil viscosity at the initial conditions is 0.75 cP.

For the dynamic evaluations, the water flooding production-strategy presented by Correia et al. (2019) is initially considered. There are three injectors and six producers, distributed in the reservoir according to the drainage plan shown in Figure 13. Figure 13 (right) also presents the relative permeability curves for matrix cells and karst structures. Note that the curves for the karst medium are two-straight-line functions with endpoints at the initial water saturation (0.18) and 100% saturation.

All injector wells operate under a maximum bottom hole pressure of 800 bar and a constant water injection rate of 2 000 std m3/day. The producer wells are controlled by a minimum bottom hole pressure of 500 bar, which is above the saturation pressure and about 140 bar below the initial reservoir pressure. All the wells operate from the start of the simulation until the final date, 40 years later.

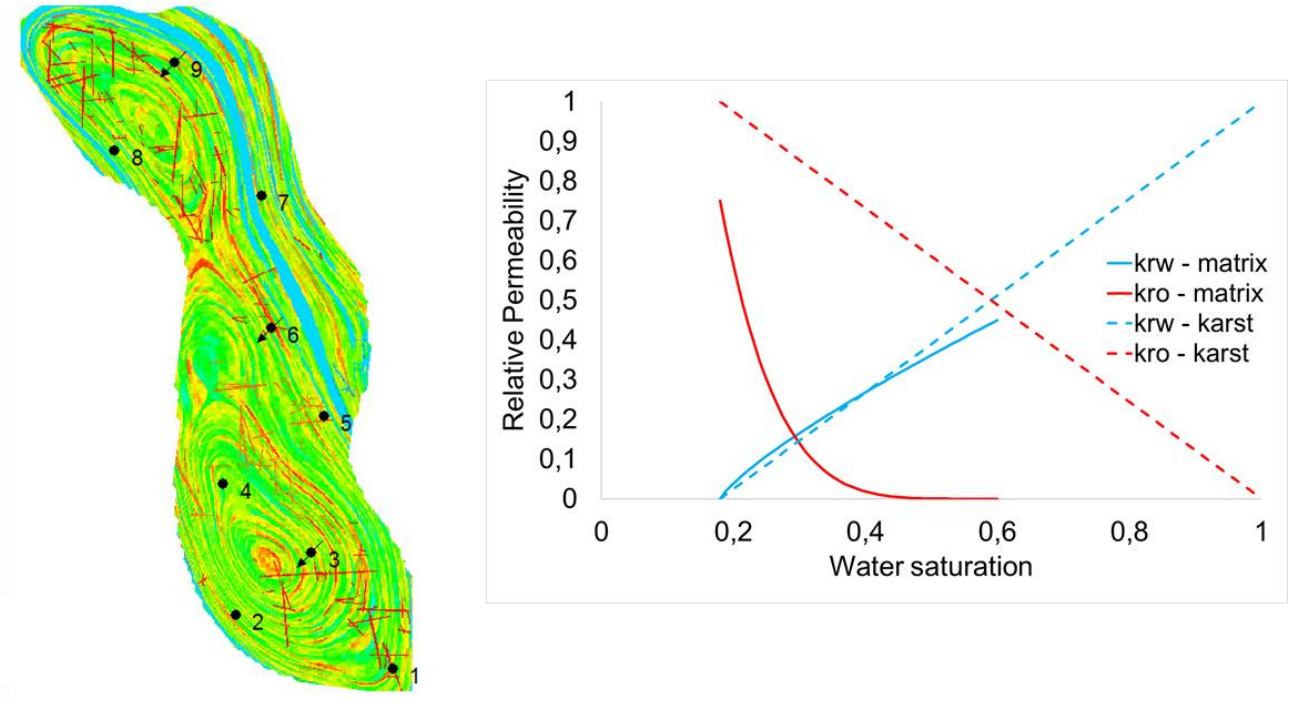

Figure 13. Left: Top view of the permeability field with the production strategy. Wells 3, 6, and 9 are injectors, and wells 1, 2, 4, 5, 7, and 8 are producers. Right: relative permeability curves, continuous curves for matrix, and dashed curves for the karsts.

The fine model is upscaled to a coarse system with a grid block size of 100 x 100 x 5 m3, resulting in a UR of 500. The flow-based technique is applied to generate the traditional SP coarse model and our DP/DP upscaling approach to evaluate its performance in such a challenging reservoir in the field-scale. In the SP coarse model, a cell is considered karst when a karst structure is present. For the DP/DP model, karst structures are part of the primary system, and their representation is more straightforward. However, since the primary system comprehends karst structures and other highly heterogeneous regions, the same criterion used for the SP model is applied to classify the karsts within the primary system.

Figure 14 shows the permeability field for both coarse models. (a) and (b) relate to the DP/DP upscaled model, while (c) represents the SP coarse model. It is possible to see that the primary system captures the highest permeability values and enables the coarse DP/DP model to better describe the main reservoir heterogeneities and non-uniform flow behavior.

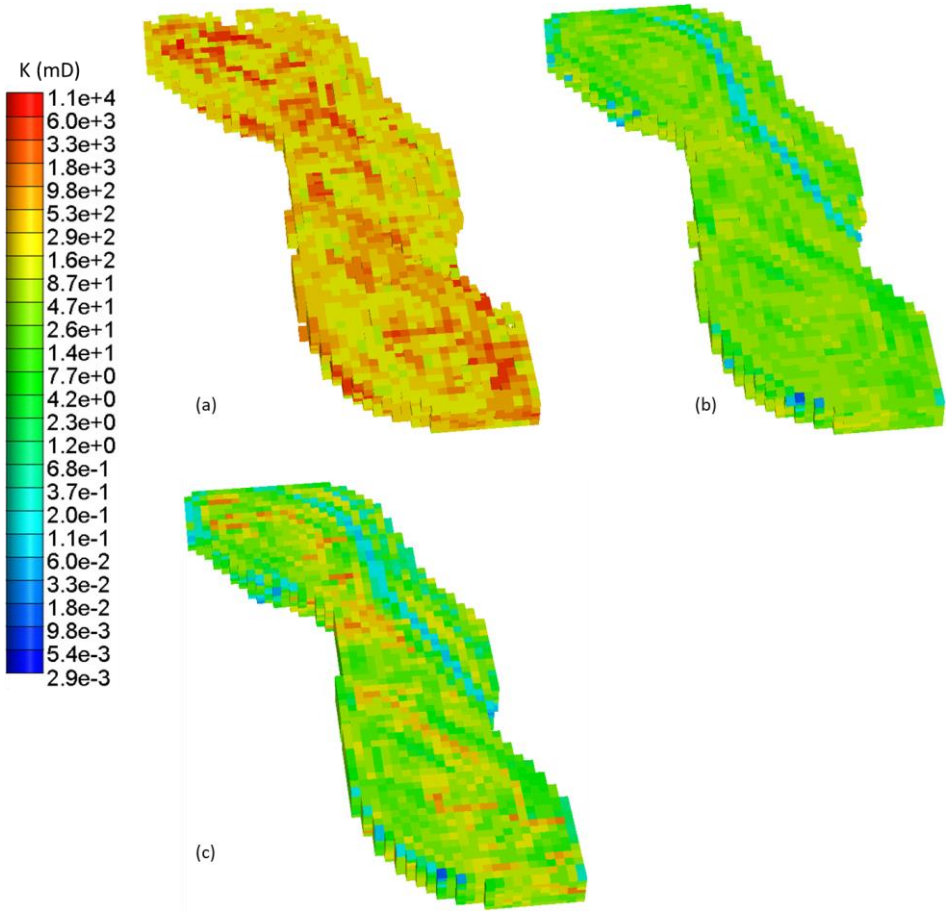

Figure 14. Coarse-scale permeability field. (a) DP/DP coarse model: primary system; (b) DP/DP coarse model: secondary system; and (c) SP coarse model.

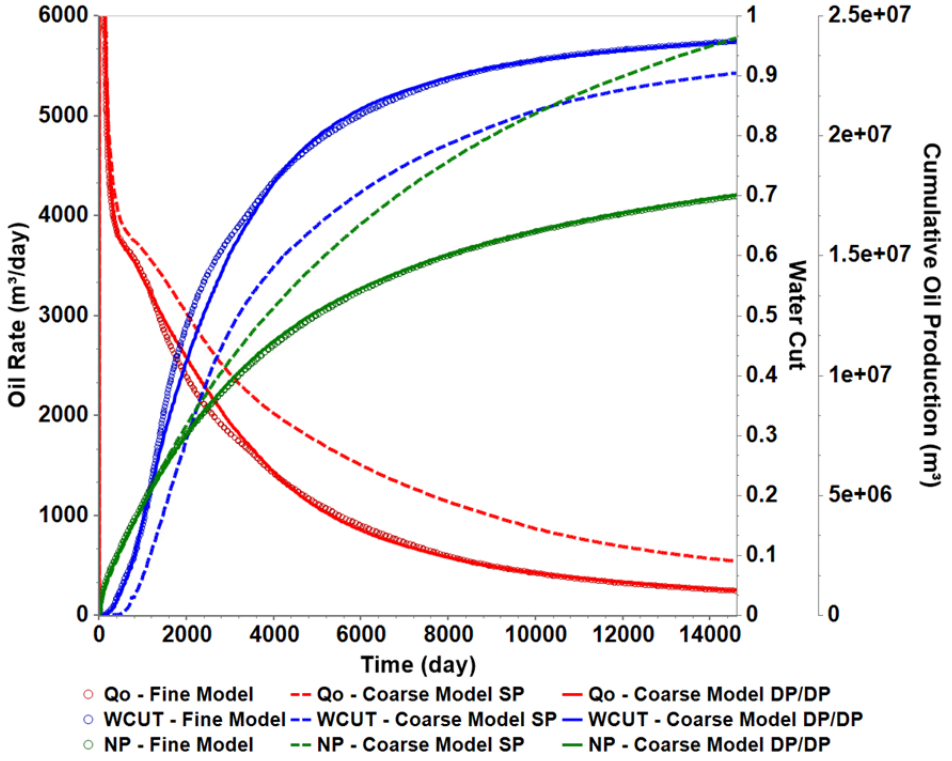

Figure 15. Cumulative Oil Production, Oil rate, and WCUT for the full-field in Case B. Continuous curves represent DP/DP upscaling; dashed curves, SP upscaling; and dotted curves, the fine-scale model

The numerical simulations are performed with the fine model and both coarse models. The fine-scale results are the reference, and the coarse models must reproduce them as closely as possible. In this case study, a high UR is applied, in which each coarse block averages the properties of 500 fine-scale blocks. This fact is particularly more challenging in the presence of karsts that appear in a sub-grid domain. Figure 15 shows the full-field results. The cumulative oil production, oil rate, and water cut is compared. One must note that the coarse model with traditional SP upscaling presents a highly optimistic behavior. The oil production is overestimated while the water breakthrough is postponed. This result is a consequence of the smoothed sub-grid features and an inefficient description of the karst structures. The DP/DP coarse model, on the other hand, performs in close agreement with the fine-scale model. The water breakthrough time and water cut behavior are coherent with the reference results, as is the oil production.

A qualitative way to evaluate the improvements provided by our DP/DP upscaling procedure is to analyze the water saturation maps. Figure 16 shows the water saturation for the three models after four years in the simulation. In (a) the fine-scale results are presented, which shows that the water has achieved the entire reservoir in area, already reaching Producer 1. In (b), it is possible to see the result for the traditional SP approach. It is important to mention that the water is more confined throughout the reservoir and has not yet reached Producer 1. In fact,

it is still far from this well after four years. Lastly, (c) and (d) show the secondary and primary system results from our DP/DP upscaling. The primary system, (d), which is responsible for representing the cells with the highest importance for the flow, presents a close saturation profile compared with the fine model. Combined with the secondary system, (c), the final result is an improved reproduction of the fine-scale model's behavior. This outcome is a remarkable accomplishment for such a coarse model.

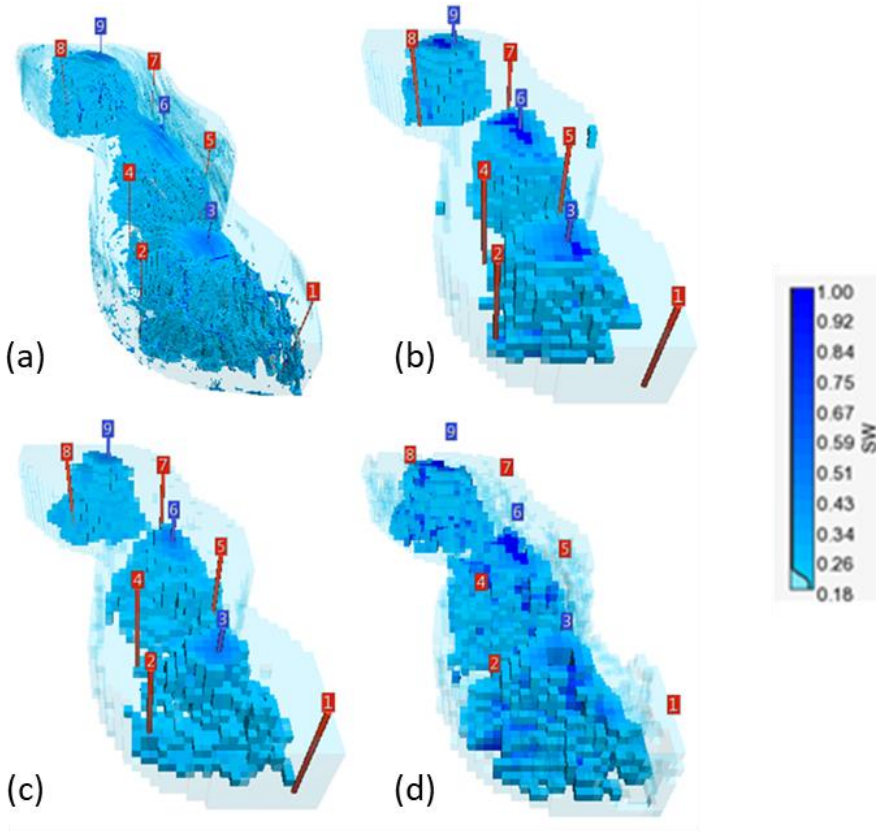

Figure 16. Water Saturation after four years of continuous water flooding. (a) Fine model. (b) SP Coarse model. (c) Secondary system of the DP/DP coarse model. (d) Primary system of the DP/DP coarse model.

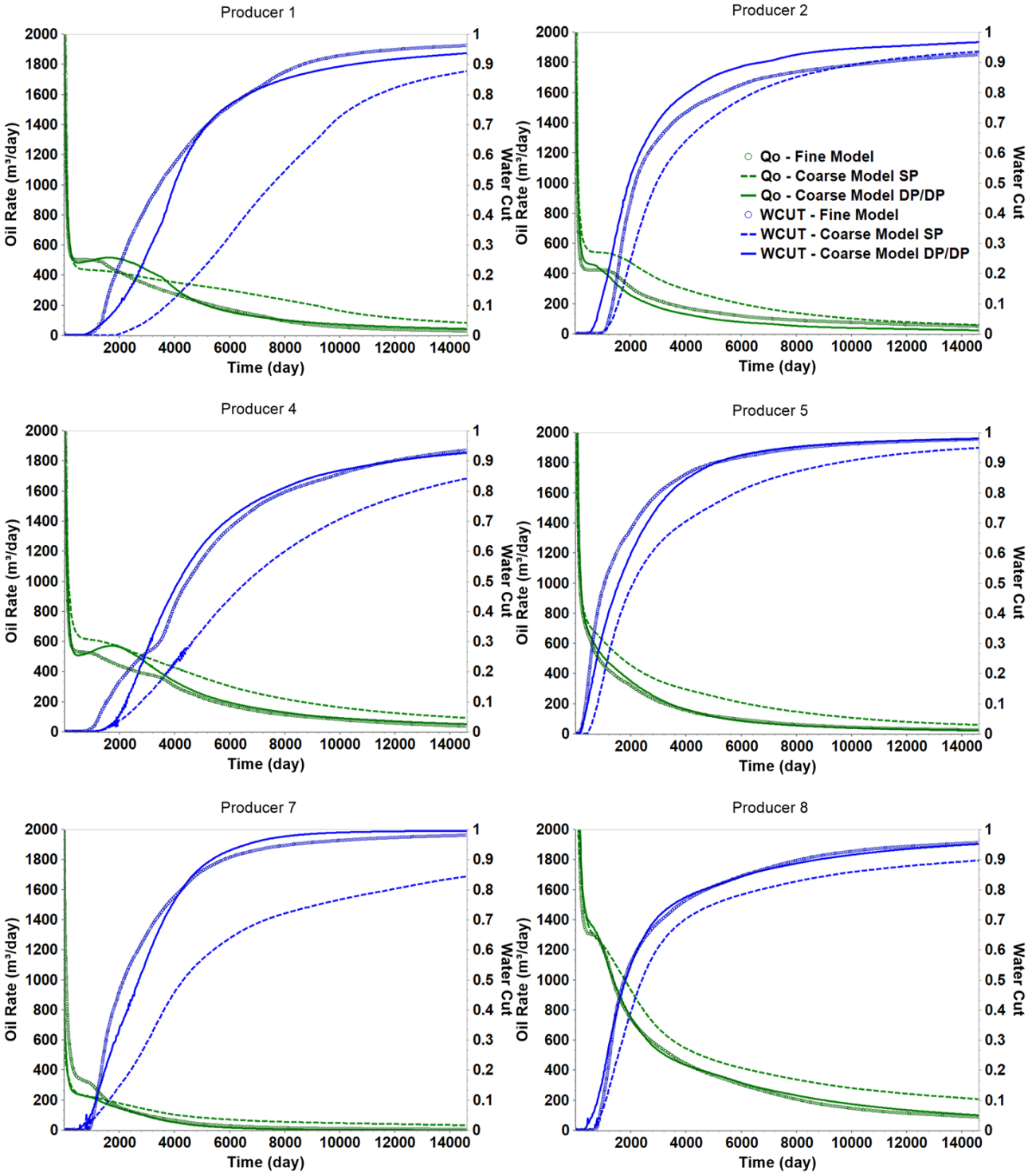

Figure 17. Oil rate and WCUT for each well in Case B. The continuous curves represent DP/DP upscaling; the dashed curves, SP upscaling; and the dotted curves, the fine-scale model.

To conclude the studies for Case B, the well-by-well comparisons between fine- and coarse-scale models are given in Figure 17.It is again possible to observe the enhancement provided by the use of our DP/DP approach. Apart from the better reproduction of the reference

results over time, we also highlight the short-time well-rate improvement achieved from the near-well treatment that composes the methodology.

The results and discussions presented for the above case studies focused on the upscaling technique and its impacts on the simulation results. Another important consideration concerns the speed of simulation runs using coarse-scale models. When compared with the fine-scale, coarse models require only a fraction of the run-time. Table 1 summarizes the computational performance for Case A and Case B, emphasizing the speed of DP/DP coarse-scale models compared to fine-scale models, while maintaining good agreement in the production curves.

Note that no numerical optimization was performed on the models; therefore, the results are a relative comparison. Nevertheless, all models can be numerically improved, as shown by Avansi et al. (2019).

Table 1. Simulation time for the models in Cases A and B

	Case A					Case B
	UR25	**UR125**	**UR250**	**UR500**	**UR1700**	**UR500**
Fine-scale	3.3 h					76 h
DP/DP coarse-scale	16 min	70 s	15 s	9 s	3 s	3 min
SP coarse-scale	3 min	30 s	5	4 s	3 s	1 min

Additional Analyses

In the previous sections, the two case studies were presented and the behavior of the DP/DP upscaling technique was tested in each of them. Case A was used to evaluate the performance of our DP/DP approach under different levels of upscaling, and Case B to stress-test the methodology in a field case study with karst structures. In this section, a number of additional investigations are performed to verify the robustness and versatility of our technique.

Initially, Case A is considered and the same set of simulations is evaluated with different viscosity ratios. As previously mentioned, the original viscosity ratio is 10. Then, the performance of our DP/DP coarse models are tested in a matched viscosity water flooding and with a viscosity ratio of 50. These additional tests are important because, the higher the viscosity ratio, the more unstable the displacement becomes and the more significant the channeling effect triggered by the permeability heterogeneity tends to be.

Figure 18 shows the comparison between fine model and coarse-scale models for a matched viscosity evaluation, while Figure 19 presents the results for viscosity ratio of 50. As observed for the original investigations in Case A, DP/DP results show a close agreement with

the reference response for both of the new viscosity ratios. It is also possible to highlight that this upscaling technique is less sensitive for different levels of upscaling and robust when submitted to different viscosity ratios.

As the last analysis using Case A, a varied flow pattern was considered. For this purpose, the function of all five wells is inverted, i.e., the four injectors in the corners and one central producer is evaluated. The same constraints as the original case are kept. Again, the results with our DP/DP upscaling procedure are accurate for all the evaluated URs, as shown in Figure 20. This performance is achieved because our technique improves the representation of the main reservoir heterogeneities without applying any changes to the relative permeability curves between fine and coarse models.

After the new studies with Case A, a final additional exploration of Case B is conducted. For this exercise, the numerical evaluations previously accomplished are repeated, but these assume a different well strategy. The new drainage plan comprises five injectors and five producers distributed in the reservoir in a peripheral-like flood scheme, as shown in the left image of Figure 21. The simulation results of this analysis are presented in Figure 21 (right). The same discussions performed for the original case are valid in the new configuration. The DP/DP coarse-scale results accurately reproduce the reference curves for all the comparisons, while the SP results are highly optimistic.

It is possible to qualitatively confirm these conclusions by observing the water saturation profile for all three models after two years, as shown in Figure 22. In (a), the fine-scale results are presented; it is possible to observe the water moving throughout the reservoir, already reaching P1. However, there is no direct communication between I5 and P3. In (b), it is possible to see the result for the traditional SP approach. The water has not yet achieved P1 and there is clear communication between I5 and P3. In fact, this behavior is very different from the reference. Lastly, (c) and (d) show the secondary and primary system results from our DP/DP upscaling. The porous medium division into two systems provided an improved reproduction of fine-scale behavior with our DP/DP technique. Notably, with quantitative and qualitatively criteria, the proposed upscaling approach achieves reliable and robust results. Moreover, consistent results for different well strategies, which is also a remarkable contribution of this work.

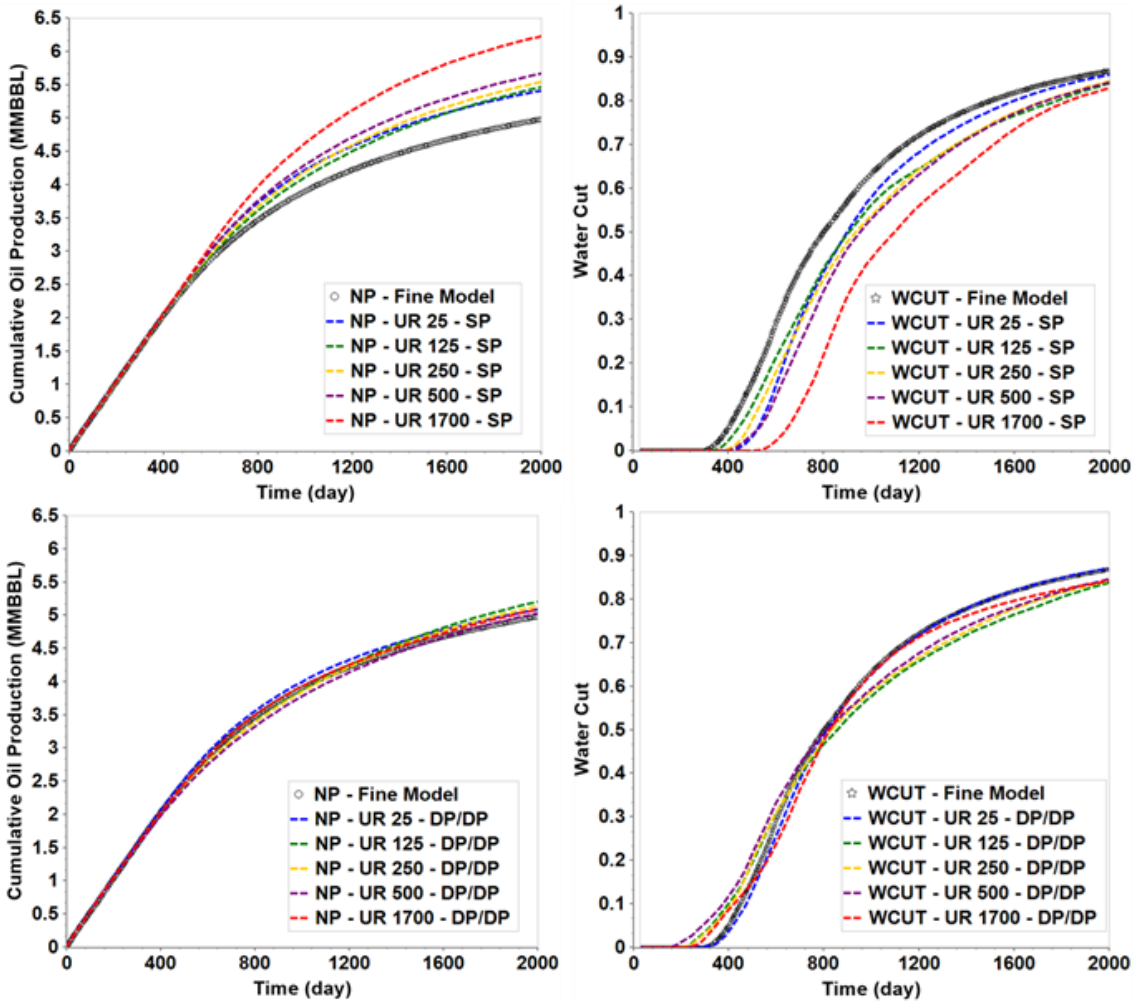

Figure 18. Comparison between fine model and coarse models for a viscosity ratio of 1. The above images are SP and the lower are DP/DP. Cumulative oil production (left) and water cut (right).

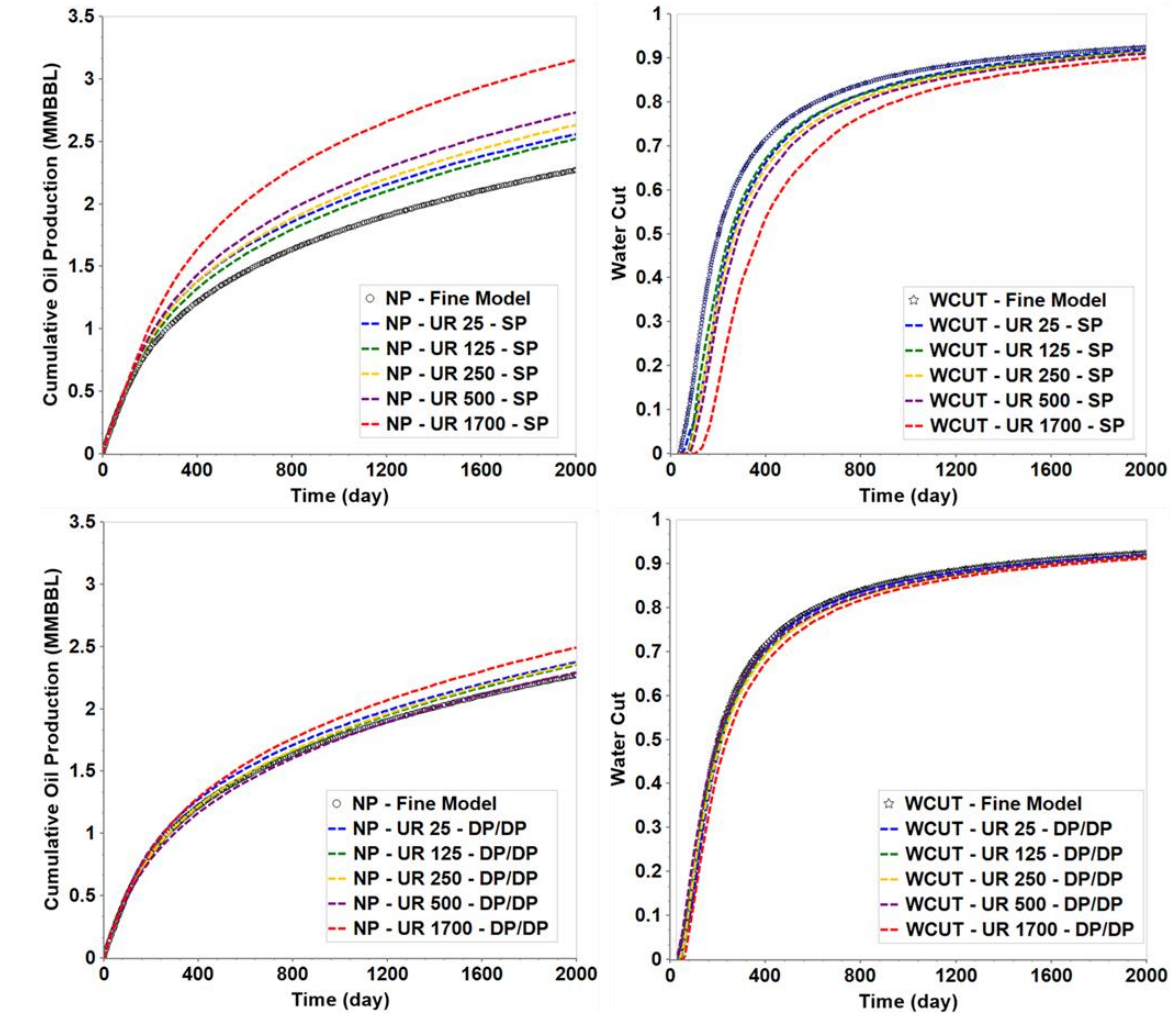

Figure 19. Comparison between fine model and coarse models for a viscosity ratio of 50. The above images are SP and the lower are DP/DP. Cumulative oil production (left) and water cut (right).

.

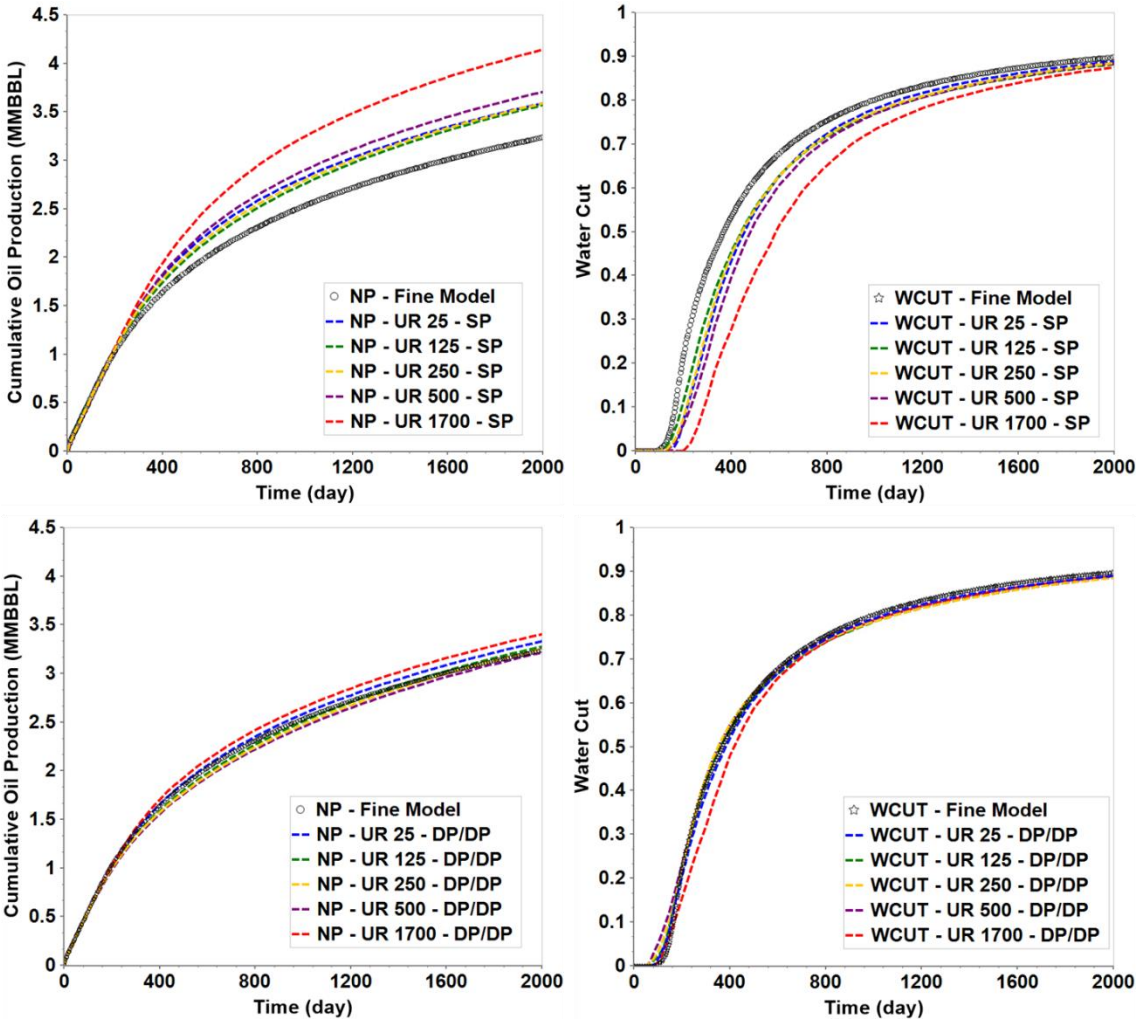

Figure 20. Comparison between fine model and coarse models with inverted well functions. The above images are SP and the lower are DP/DP. Cumulative oil production (left) and water cut (right).

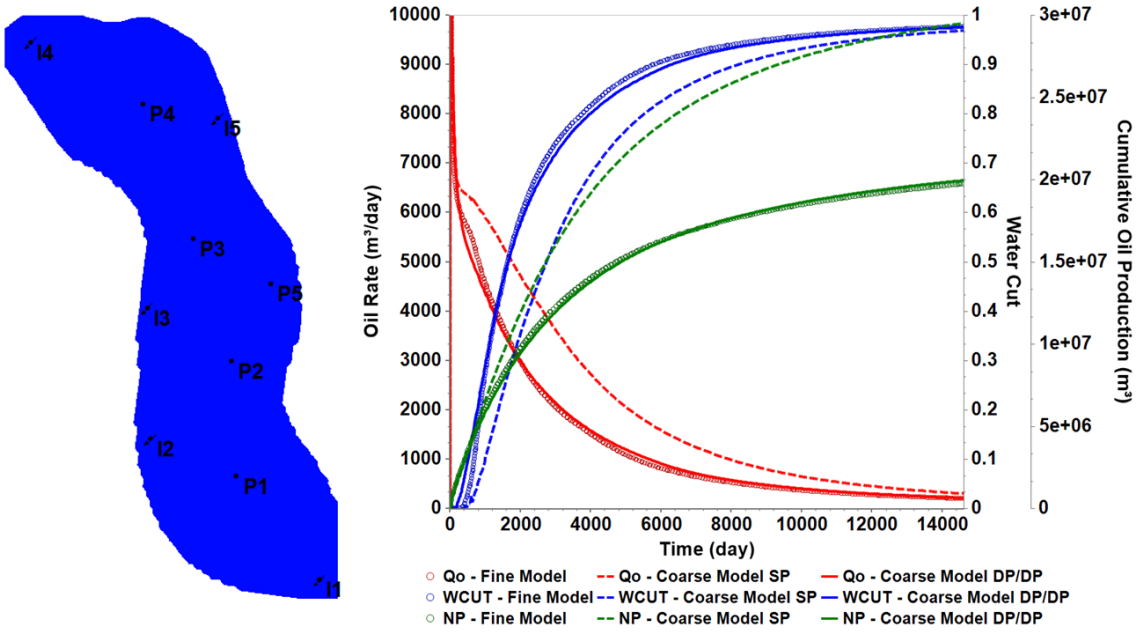

Figure 21. Left: Top view of the new well strategy. Right: Cumulative Oil Production, Oil rate, and WCUT for the full-field in Case B (new strategy). The continuous curves represent DP/DP upscaling; the dashed curves, SP upscaling; and the dotted curves, the fine-scale model

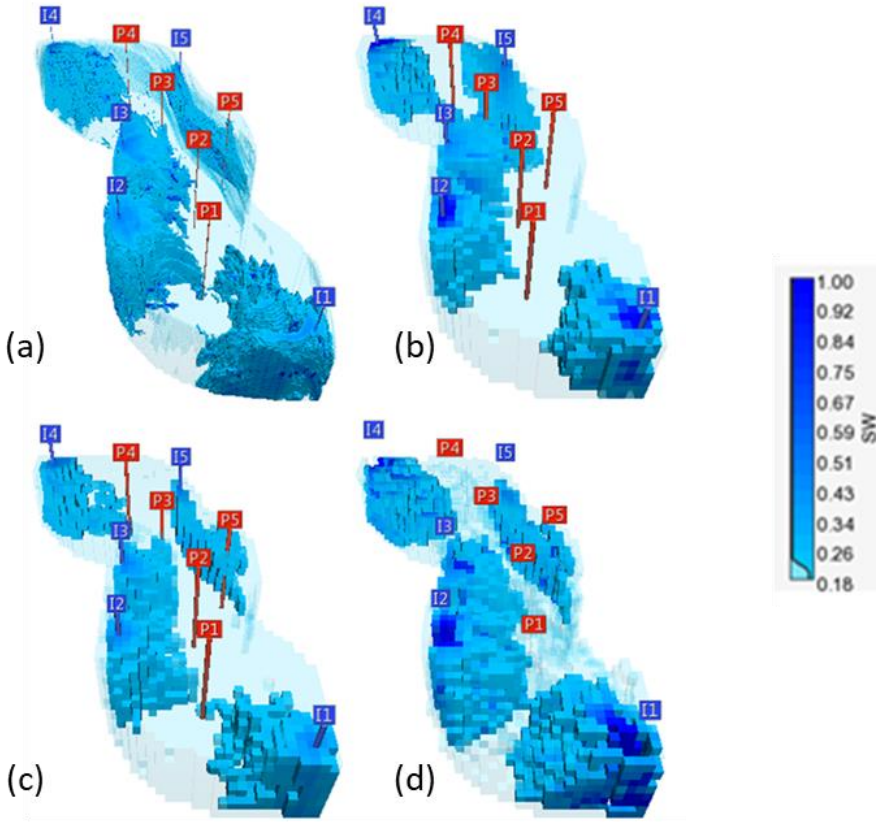

Figure 22. Water Saturation after two years of continuous water flooding with the new well strategy. (a) Fine model. (b) SP Coarse model. (c) Secondary system of the DP/DP coarse model. (d) Primary system of the DP/DP coarse model.

Final comments and conclusions

In the presented study, the DP/DP upscaling technique proposed by Rios et al. (2020) was extended and tested for 3D systems. The new methodology was divided into two parts. Initially, the porous medium was split into primary and secondary systems to improve the representation of the main reservoir heterogeneities and sub-grid features. Then, a near-well upscaling procedure was employed to enable a better description of the flow distribution in the wells.

The presented case studies demonstrated the accuracy and robustness of our technique in critical situations. The results for Case A showed that the DP/DP coarse models are less sensitive to the upscaling ratio, presenting accurate results at different upscaling levels. Also, the additional analysis verified that even for different viscosity ratios and flow behavior, the DP/DP coarse models present consistent results and a reliable capability of reproducing the reference responses.

The evaluations with Case B presented a different type of challenge for the upscaling procedure. The main reason is because it was a field-scale model with complex permeability field and karst structures. It was possible to demonstrate that the DP/DP coarse models with a UR of 500 presented results in close agreement with the reference, not only regarding the full-field production curves but also well-by-well comparison and water saturation map behavior. To stress-test this evaluation, the well strategy and flow pattern were changed and consistent results were still obtained from our DP/DP model.

Based on our investigations, the main contributions of our DP/DP methodology are highlighted below:

- The porous medium division, based on the static properties of the fine-scale model, is a crucial step to provide a better representation of the sub-grid heterogeneities and preferential pathways.
- The DP/DP coarse models are consistently less sensitive to the level of upscale. This characteristic enabled a more aggressive upscaling procedure without jeopardizing the decision-making process guided by simulation results.
- Since dynamic responses from fine-scale full-field simulation are not used, this methodology provides improved coarse-scale results even when different well-strategies and flow patterns are considered.
- Consistent results are achieved with our DP/DP coarse models for different viscosity ratios.

- The computational time for the resulting coarse models is only a fraction of the fine-scale models.

Finally, based on the presented results and discussions, we can conclude that the new DP/DP upscaling technique is a useful and robust tool for creating coarse-scale models, and we recommend its use in reservoir engineering studies of highly heterogeneous systems.

Acknowledgements

The authors would like to thank Petrobras (Petróleo Brasileiro S.A.), UNISIM, DE-FEM/UNICAMP, CEPETRO, Energi Simulation, ANP, CMG, Dr. Daniel Nunes de Miranda Filho and M.Sc Vinicius de Souza Rios for their support for this work.

6 ARTICLE 5: A GENERAL UPSCALING WORKFLOW APPLIED TO HIGHLY DETAILED HETEROGENEOUS RESERVOIRS UNDER NEAR-MISCIBLE WAG FLOOD

Victor de Souza Rios, Arne Skauge, Ken Sorbie, Gang Wang, Denis José Schiozer, Luiz O. S. dos Santos

To be submitted to a peer-reviewed journal

Abstract

Simulation of water flooding on field scale models is well established. However, it is more challenging to model gas injection and combination of water and gas (WAG), especially when injected gas is near-miscible with strong compositional mass exchanges.

The paper address solutions for effective field simulations of near-miscible WAG in highly heterogeneous reservoirs. We have made use of extreme fine-scale reservoir simulation models as the "true" solution. The team have proposed and tested a general upscaling workflow to guide the necessary grid coarsening process. A new approach was needed and required to split the problem into two groups, static and dynamic upscaling. The final coarse-scale dynamic responses presented a close agreement with the fine-scale production results and required less than 0.005% of the total time used for a single fine-scale simulation run.

Introduction

Upscaling fine-scale detailed models to a coarser system with improved numerical performance is a frequent need in practical reservoir simulation studies. For this purpose, various techniques have been proposed throughout the years with an increasing level of complexity, depending on the static and dynamic challenges represented by each reservoir and production strategy. Detailed and comprehensive reviews on several techniques are provided by Wen and Gomez-Hernández (1996), Renard and de Marsily (1997), Farmer (2002), and Durlofsky (2003).

When fluid is injected into a heterogeneous reservoir, additional effort is usually required to achieve a useful upscaled model. For water injection or immiscible gas injection simulation processes, a two-phase upscaling procedure is generally recommended. In this case, pseudo-relative permeability curves are a popular method to improve the results of coarse-scale simulation models when fine-scale simulation results are available.

Barker and Thibeau (1997) reviewed several existing relative permeability upscaling approaches. They noted significant limitations when considering pseudo-relative permeability curves while upscaling fine-grid geological models to coarse-scale simulation models. It is worth highlighting that the various pseudoization approaches require that one must either be able to run the fine grid, or select a representative section of the fine grid, and assert that the pseudo functions are appropriate for use elsewhere in the model (Fayazi et al., 2016). This limitation is one that is well-known when applying pseudo-relative permeability curves to reproduce fine-scale results using coarse models.

Several authors have proposed methodologies to improve the representation of small-scale results in coarse-scale simulation models. Chen et al. (2003) developed an upscaling procedure, referred to as a coupled local-global upscaling approach, in which the local boundary conditions (used to compute upscaled properties) are determined from global coarse-scale flows. They showed significant improvement over existing local methods and extended local methods. However, only generic flows were considered in the generation of the coarse-scale properties; specific global flow and well effects, which may affect the upscaling accuracy, were not investigated.

Chen and Durlofsky (2006) proposed an adaptive local-global (ALG) upscaling procedure to generate coarse-scale parameters "adapted" for any type of global flow. They included a threshold to update the upscaled properties only in high-flow areas, potentially increasing the efficiency of the upscaling procedure. The authors reported that flow simulation results on highly heterogeneous systems showed improvement over local and coupled local-global upscaling techniques.

Evazi and Jessen (2014) developed a technique for highly heterogeneous reservoirs, in which the pore space is arranged into two levels of porosity. The division is based on fine-scale streamline information, and a dual-porosity dual-permeability (DP/DP) flow model is adapted to simulate the coarse-scale model. They demonstrated that DP/DP coarse-models predict the breakthrough time accurately and are less sensitive to the level of upscaling when compared to conventional single-porosity upscaling. However, the overall workflow to obtain the upscaled models can be costly because of the need for streamline simulations for the fine-scale model. Another drawback is the use of fine-scale dynamic results to divide the porous media, which can make the strategy strongly dependent on the original well locations and flow rates.

Rios et al. (2020) proposed a new dual-porosity dual-permeability (DP/DP) upscaling technique for highly heterogeneous reservoirs. They used flow and storage capacity analysis and the Lorenz Coefficient (Lorenz, 1905; Jensen et al., 2000) applied to the static information of a fine-scale model to split the porous media into two levels: one representing the main flow regions and the other, the secondary flow regions. With the splitting of fine-scale cells, directional upscaling for permeability is performed for each group. They showed, in deterministic and probabilistic evaluations, that the resulting coarse-scale models can adequately reproduce the reference fine-scale results better than traditional static upscaling methods with two significant improvements over other upscaling techniques. It is (1) less time-

consuming to obtain coarse-scale models as no dynamic responses of fine-scale models are used and (2) not dependent on the drainage plan or well flow rates of the fine-scale models.

Despite the numerous published upscaling techniques, there is not a universal approach to generate reliable coarse-scale simulation models. The main reason is that the upscaling problem averages a complex combination of static properties and dynamic phenomena. Therefore, it requires prior knowledge and understanding of the problem to enable an adequate choice of the most appropriate upscaling technique or group of approaches.

In this context, a detailed fine-scale model representing the main reservoir heterogeneities and preferential pathways is a crucial step to guide the proper selection of the permeability upscaling method. In general, flow-based methods can be used. However, for highly heterogeneous systems, the use of DP/DP upscaling technique proposed by Rios et al. (2020) to better represent the sub-grid heterogeneities and non-homogeneous flow behavior within a coarse grid block must provide a better solution.

Besides, the previous familiarity with the dynamic evaluations to be considered in the development plan of an oil field is also mandatory. Immiscible displacements are more likely to be well modeled with traditional upscaling techniques, while near-miscible and miscible gas injection processes still represent an enormous challenge. The difficulty arises due to the smoothing of small-scale phenomena and the intense compositional exchange and mass transfer between gas and oil (Rios et al., 2017, 2019).

Therefore, the upscaling process to create a useful (for decision-making) and efficient (computational cost) simulation model involves a combination of techniques to overcome the different consequences of the use of coarser grid block cells. Thus, considering the nature of the effects, we generically divide the upscaling problem into two groups that requires different approaches: static modeling limitations (Group 1) and flow-dynamics specificities (Group 2).

From the static modeling side, the smoothing of subgrid heterogeneities tends to overestimate the sweep efficiency of the injected fluids, leading the simulation to give an artificially higher oil recovery factor. Also, from the dynamic point of view, the behavior of compositional effects related to near-miscible gas injection is unlikely to be reproduced within coarse-scale models. This is mainly because of the homogenization of small-scale phenomena such as viscous-fingering and complex mass transfer between oil and gas phases.

In practical situations, the generation of a coarse model can be dominated by one of the above-mentioned groups or a combination of both. Working on Group 1 alone may be enough when immiscible fluid is injected in a highly heterogeneous reservoir, where the

preferential pathways concentrate the overall flow dynamics. Group 2 tends to be the focus when a near-miscible or miscible gas injection is performed (continuously or WAG) in a low heterogeneous reservoir. Lastly, both groups are important when a combination of the earlier scenarios occurs.

In this work, we propose and test a general upscaling workflow that provides a practical stepwise procedure. This new workflow presents two important features that represent a novelty in terms of how to deal with upscaling problems. It (1) guides the upscaling process by enabling the selection of the proper approach according to the problem's limitations - Group 1 or Group 2. Also, it (2) enables a better understanding of the upscaling problem as a whole, resulting in improved and robust coarse-scale simulation models.

We evaluate the proposed workflow on the upscaling of two 2D highly detailed geological models with different heterogeneity behavior, which have been used to model near-miscible CO_2 WAG injection. These fine models were introduced and described by Wang et al. (2019a) in an analysis of compositional effects on different heterogeneous systems in near-miscible displacements. The authors also considered one of the models in a sequence of detailed small-scale evaluations of near-miscible WAG injection process (Wang et al., 2019a, 2019b, 2020a, 2020b).

The models represent a sector of a reservoir with an area of 50 x 10 m^2 and present a highly refined set of grid block cells, with a 5 x 5 cm^2 area, which consists in a great challenge for the upscaling work. Indeed, these models are close to the size of just one grid block that might appear in a conventional reservoir simulation. We upscaled the models to coarser systems with grid block cells of 8 x 10 m^2, which is compatible with a refined geological model in reservoir engineering studies. This results in an upscaling ratio (UR) of 32 000 and the proposed workflow was applied to achieve improved coarse-scale models.

The remainder of the text is organized as follows. In the next section, we present the problem and motivation for the proposed methodology, highlighting the importance of a procedure to better understand the upscaling problem and its specifics. We then present the methodology and detail the steps of the proposed workflow. Description of the case studies then follows. We apply the proposed methodology for two highly detailed models with near-miscible WAG injection. Following this, the results of each case are discussed and a summary and final remarks conclude this presentation.

Methodology

In this section, we first present an illustration about the problem we aim to solve in this work, followed by the proposed workflow to achieve this goal and the description of the case studies we considered to test the methodology.

The Problem and Motivation

To illustrate the problems arising from the use of traditional upscaling techniques in heterogeneous systems, we consider the 2D highly detailed models presented by Wang et al. (2019a). They introduced two heterogeneous reservoirs, named Model A and Model B, which were considered to investigate full-physics simulations of near-miscible CO_2 WAG injection. They generated both models with the same Dykstra-Parsons (Dykstra and Parsons, 1950) coefficient ($V_{DP} = 0.7$) and different dimensionless correlation ranges (RL). Model A presents a short correlation length ($R_L = 0.1$) with the idea of triggering possible fingering flow. Model B is characterized by a long correlation length ($R_L = 1$) to enable a channelized flow pattern. Figure 1 shows the permeability field for both models.

Models A and B are highly refined, and each cell has a 5 x 5 cm^2 area. This refinement level is important for a more detailed investigation of small-scale compositional oil stripping effects and interfacial tension (IFT) effects. These evaluations were described and discussed in detail by Wang et al. (2019a, 2019b, 2020a, 2020b). However, for practical reservoir simulation activities, such fine-scale models are nearly impossible to be used.

Therefore, it is necessary to create reliable coarse models for dynamic evaluations of these systems. This task is a challenge, especially because near-miscible CO_2-WAG displacement is the chosen recovery method, since it presents some complex physical interactions between the compositional and IFT effects, as related by Wang et al. (2019a, 2019b, 2020a, 2020b).

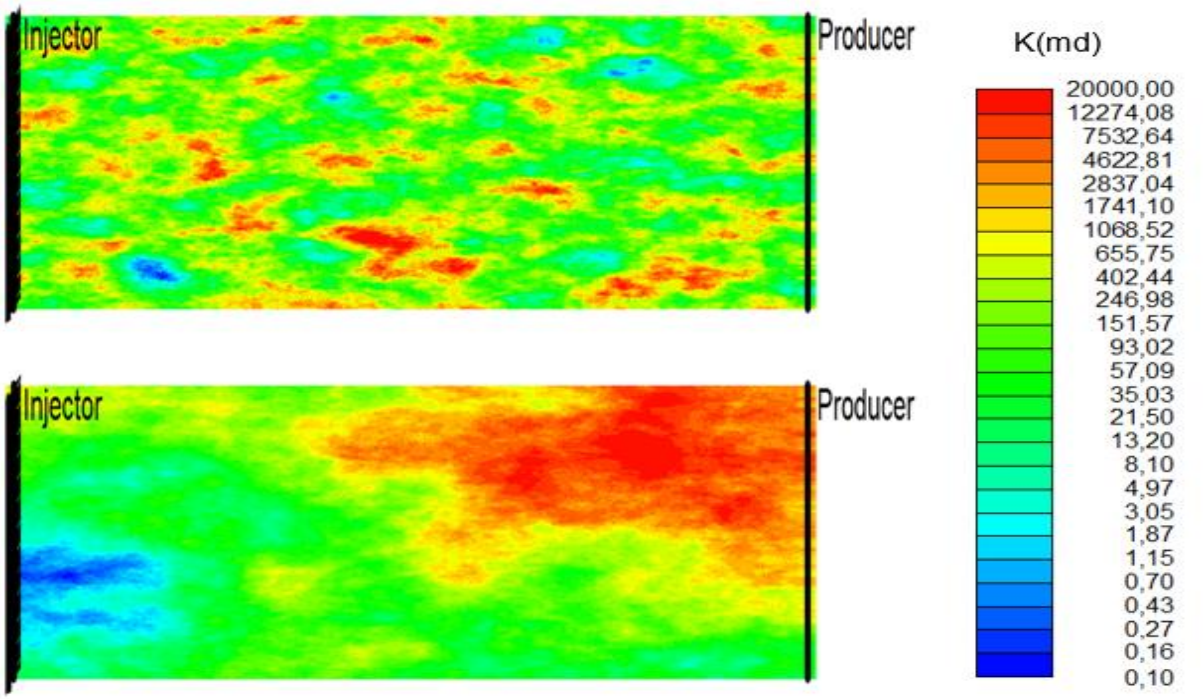

Figure 1. Permeability Field for Models A (upper image) and B (lower image)

Although models A and B were modeled on the same scale, they represent different challenges for the upscaling process. By analyzing the permeability fields in Figure 1, we note that Model A presents a heterogeneity distribution with a repeated pattern throughout the reservoir. Model B, however, has a high permeability concentration in the upper area, which tends to concentrate and dominate the flow, leading to a channelized flow behavior. Therefore, an upscaled version of the Model A is more likely to capture the average behavior of the fine model than an upscaled Model B.

To investigate the impact of the coarsening in both systems, we upscaled the models to coarser systems with grid block cells of 8 x 10 m2, resulting in a UR of 32 000. In this configuration, the coarse models present six cells between injector and producer wells, which is still acceptable from the numerical point of view. This grid block size is compatible with a refined geological model in practical reservoir engineering studies. Note that these models are usually upscaled to even coarser systems to obtain the simulation models used in the decision-making process. Figure 2 shows the permeability field for both upscaled models.

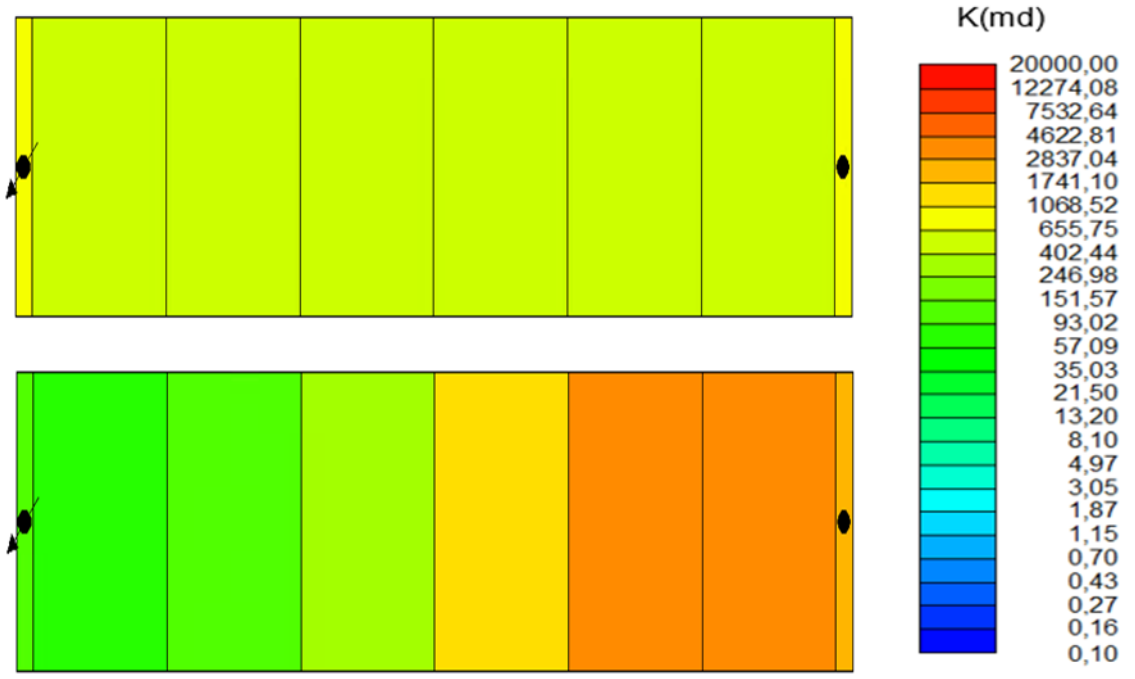

Figure 2. Permeability Field for UR 3200 Models A (upper image) and B (lower image)

For the dynamic evaluations, we consider CO_2-WAG displacement in both models. The injection strategy and details about reservoir properties, fluid model, and relative permeability curves were described by Wang et al. (2019a, 2019b), and we summarize in Table 1 and Table 2. We performed all the simulations using the compositional simulator GEM from CMG (Computer Modelling Group Ltd., 2018).

Table 1 - Summary of Model A and Model B properties. (PVI is pore volume injected, W is water and G is gas)

	Porosity	**Average K (mD)**	**V_{dp}**	**R_L**	**WAG Injection**
Model A	0.1	1000	0.7	0.1	2 PVI = WGWGW (0.4 PVI each leg)
Model B	0.1	1800	0.7	1	2 PVI = WGWGW (0.4 PVI each leg)

Table 2 – Additional information about the numerical models (MR is mobility ratio, BHP is bottom hole pressure and EoS is equation of state)

Number of cells	Fine-Scale = 192400 Coarse-Scale = 20
Simulator type	Compositional
Fluid Model	EoS with 7 components (see Wang et al. 2019a)
Water/Oil MR	0.2
Gas/Oil MR	4.3
Producer BHP	120 bar
Injection Rate	0.4 PV/day
Relative Permeability curves	Corey type (see Wang et al. 2019a)

Initially, we generated the coarse models with the traditional flow-based upscaling technique. We, then, simulate fine and coarse models with the near-miscible CO_2-WAG displacement. This first evaluation is essential to show the behavior of each coarse model and its limitations on representing the respective fine-scale response with a widely used upscaling method. The comparison for the oil recovery factor between fine and coarse models is shown in Figure 3.

From these initial results, we can make some important considerations: (i) for both models, coarse-scale results deviate from the reference fine-scale response; (ii) fine Model B, as expected, presents a notably worse recovery factor that fine Model A due to its permeability distribution enabling a channelized flow; (iii) fine Model A, with a fairly well-distributed heterogeneity, presents a high oil recovery factor; and (iv) coarse Model B presents a highly overestimated recovery factor.

One way to explain the latter is by observing the coarse cells close to the producer well. These cells average fine blocks with high permeability variation (up to five orders of magnitude) with a clear preferential pathway been smoothed. Indeed, when we observe the fine-scale remaining oil saturation at the end of the simulation, Figure 4, it is possible to confirm that Model B (lower image) presents a non-uniform behavior, and the final oil saturation is considerably lower in the upper area of the reservoir. A different scenario is observed for Model A, in which the remaining oil saturation is not concentrated. Thus, considering the representation of these behaviors with the coarse-scale models, it is expected that the highly

non-uniform behavior presented by Model B represents a different type of challenge compared to Model A.

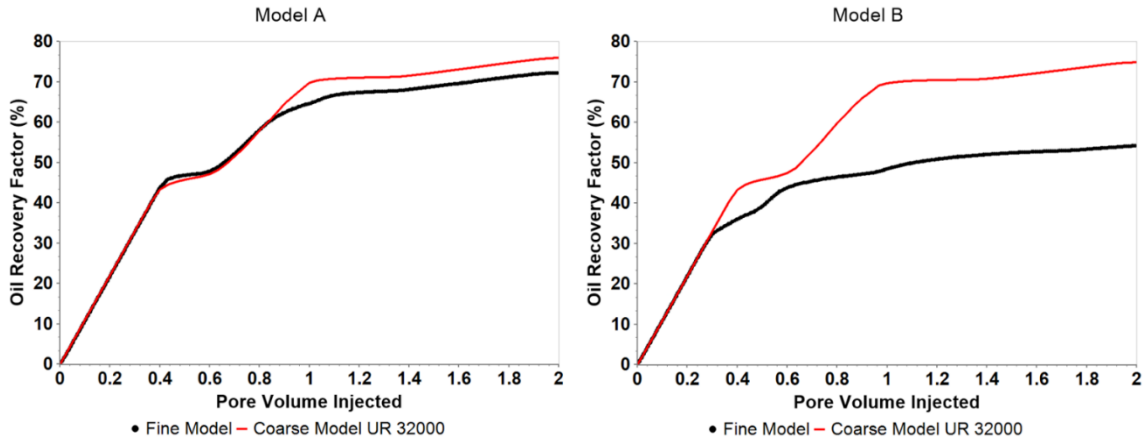

Figure 3. Oil Recovery Factor comparison between Fine and Coarse model for CO_2-WAG displacement. Models A on the left and Model B on the right

Therefore, the selected case studies provide different types of challenges for establishing an improved upscaled model with the proposed UR. Moreover, these models represent an opportunity to discuss in detail the specificities of the upscaling process. We use them to illustrate the proposed general workflow for upscaling reservoir simulation models to reliable and consistent coarse-scale models.

Accordingly, in the next sections, we aim to address the following questions:

1) When are traditional single-phase and single-porosity upscaling techniques recommended?
2) When is it important to work on Group 1 (G1) techniques?
3) When is it necessary to work on Group 2 (G2) techniques?

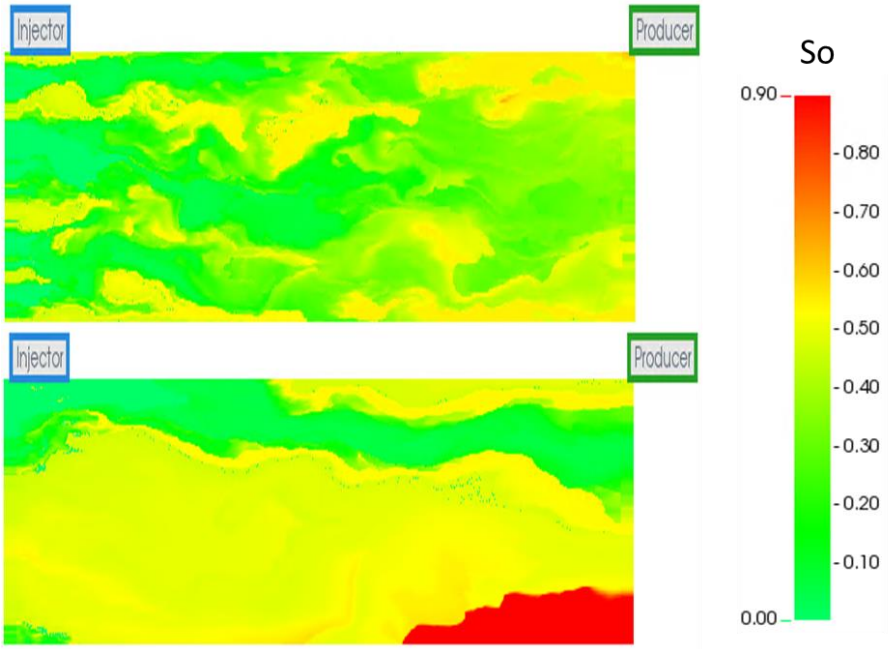

Figure 4. Oil Saturation after 2 PVI for Models A (upper image) and B (lower image)

Proposed Workflow

We divide the new general upscaling workflow into three main parts, as follows: (i) check if the traditional single-phase upscaling is useful and sufficient for the problem; (ii) verify whether the problem is G1 or G2 type; and (iii) evaluate the need for applying G2 solutions after working on G1.

In the first part, we generate the coarse model with a traditional flow-based upscaling methodology. Following this, we simulate coarse and fine-scale models with the desired recovery method. If the fine model is too time-consuming to simulate even a single run, we recommend the use of representative sectors for this evaluation. Then, we compare the results and verify if the coarse model is acceptable to be used. If not, the next step is required.

In the second part, we propose a test to investigate whether it is the averaging of the permeability field and the smoothing of sub-grid heterogeneities that are compromising the coarse-scale results (G1 type of problem). If this is so, then traditional single-phase and single-porosity upscaling techniques are not sufficient, and the DP/DP upscaling proposed by Rios et al. (2020) is recommended, given its capability for improving upscaling results for highly heterogeneous reservoirs has been demonstrated. If no, then the problem is of G2 type; therefore, we generate pseudo-relative permeability curves to improve the upscaled model results.

The third part is a final inspection after the G1 solution, in case that it is applied. At this point, we can also apply G2 solutions to conclude the upscaling process, if required.

The proposed general upscaling workflow is described in the flowchart presented in Figure 5 and can be summarized stepwise, as follows:

1) Choose the desired coarse grid size and generate the coarse model with the traditional flow-based upscaling technique.
2) Simulate the coarse model to compare with the fine-scale results. Note that, if the full-field simulation of the fine model is not practical, one must extract a sector model to perform this evaluation.
3) Compare fine and coarse-scale results.
4) If the results are close, the traditional upscaling approach is sufficient, and the coarse model is ready to be used. If not, further improvements are necessary.
5) Evaluate stable flow injection to better isolate the impact of permeability upscaling and verify if the DP/DP technique is recommended to improve sub-grid heterogeneity representation. In this step, highlighted in blue in Figure 5, the injected fluid to be considered depends on the original recovery method:
    a. If water flooding, we only need to make the flow stable with unit viscosity ratio;
    b. If gas flooding, we adapt the injected gas to provide an immiscible injection with unit viscosity ratio;
    c. If WAG, both abovementioned evaluations are recommended. It enables the investigation of possible differences in the permeability influence when combined with gravitational effects.

    This step is crucial because once we promote stable flooding (unit viscosity ratio) and prevent the system of compositional exchanges (immiscible displacement), the impact of the permeability can be highlighted. More importantly, by comparing coarse and fine-scale results in these conditions, we can determine if the permeability upscaling method needs to be improved.
6) Compare fine and coarse results with the stable flow flooding:
    a. If they are similar, the upscaling problem is a G2 type. Therefore, we keep the flow-based permeability upscaling and work on pseudo-relative permeability curves to improve the original deviations in the response. Then, the coarse model is ready.
    b. If there are discrepancies in the results, we have a G1 problem, and the permeability upscaling must be improved. We then apply the DP/DP technique, as presented by Rios et al. (2020).

7) Compare the fine and new coarse-scale results with the original recovery strategy:
    a. If they are similar, the new coarse model with DP/DP upscaling is ready.
    b. If there is a deviation in the results, the problem is now G2, and we can work on pseudo-relative permeability curves and, then, the coarse model is ready.

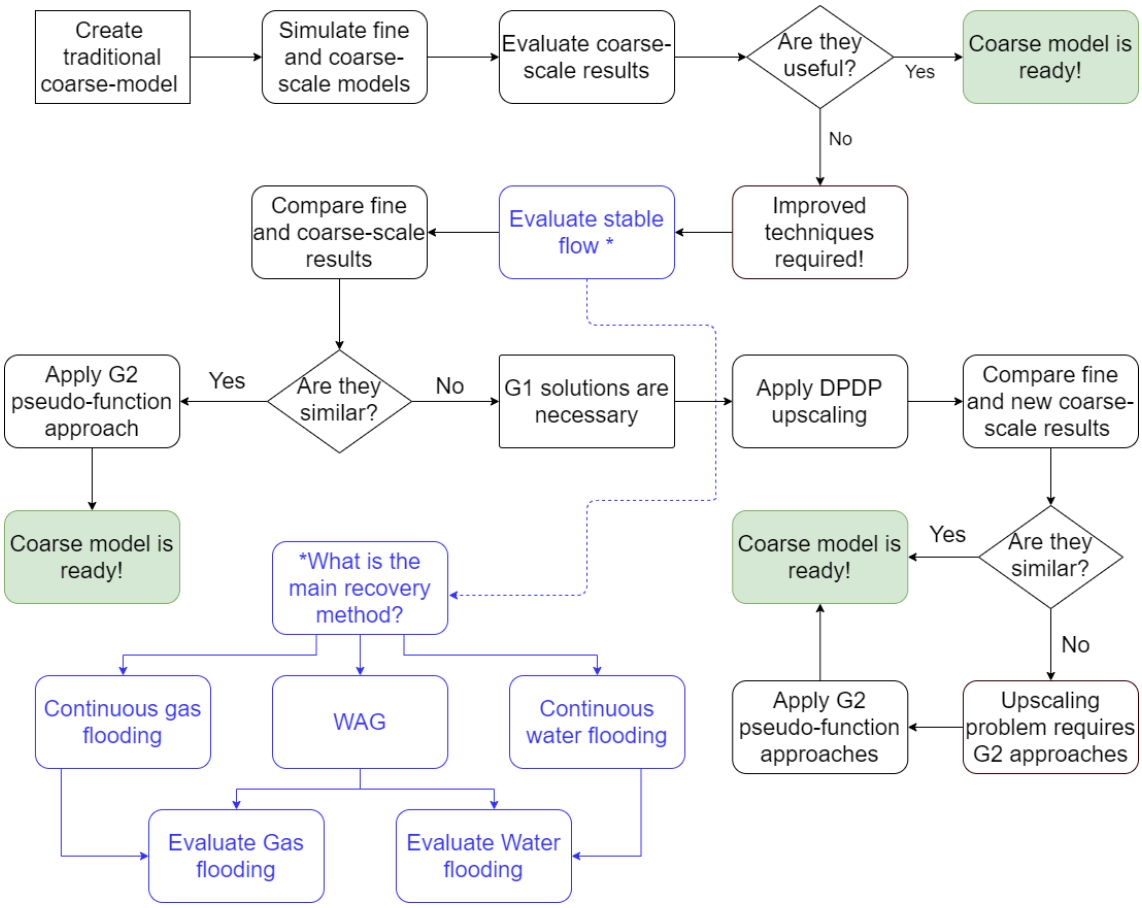

Figure 5. Flowchart to guide a general upscaling procedure.

Case Studies Description

We test the proposed general upscaling workflow in two highly detailed heterogeneous case studies, both with near-miscible CO_2-WAG displacement. In the fine-scale, Model A and Model B are 2D areal models described on a regular Cartesian grid with dimensions of 50 x 10 x 0.1 m^3. The size of all the grid-blocks is 0.05 x 0.05 x 0.1 m^3, except in the first and last columns, with 1 x 0.05 x 0.1 m^3 . A horizontal injector is completed along the entire length of the first column, and a horizontal producer is completed along the entire length of the last column. Therefore, there are 192 400 cells in total (962 x 200 x 1).

The initial reservoir temperature and pressure are set at 53 °C and 120 bar, respectively, at the top of the reservoir, which is 1 000 m. The rock compressibility is 5e-007 1/KPa at a reference pressure of 101.325 KPa. There is no free gas, and the initial water

saturation is 0.1. More information about the numerical models is summarized in Table 1 and Table 2, and details are provided by Wang et al. (2019a, 2019b).

As previously mentioned, Model A and Model B represent different heterogeneity and flow behavior, and are significant challenges to stress-test the proposed workflow. We apply each step of our workflow for both models and show the differences between them as an upscaling problem. As described in "The Problem and Motivation" section, both models are upscaled to coarse models with a UR of 32 000. The high level of coarsening (the fine model is a highly refined 2D system, while the coarse model is 1D) combined with the near-miscible CO_2-WAG injection make these upscaling problems more complex and complete for discussing all the proposed steps of our workflow.

Results

Next, we present results regarding the upscaling process on models A and B. We follow the steps of the proposed general upscaling workflow and discuss each of them until an improved coarse-scale model is obtained for both cases. First, we show the results for Model A and, then, for Model B. We conclude with an additional evaluation to complement the discussions on the proposed methodology.

Model A

Model A is a highly heterogeneous system with a nearly homogeneous distribution of the permeability field (Figure 1). This characteristic tends to make the upscaling problem less severe since the averaging process is less likely to change the overall flow behavior. We investigate this idea more deeply as we pass through the proposed upscaling workflow. To enable a direct tracking of the steps, we will follow the same steps proposed in the "Methodology and Proposed Workflow" section.

1) Initially, a coarse-scale model with UR 32 000 was created with a traditional flow-based approach, and the upscaled permeability field is shown in Figure 2.
2) Both coarse and fine-scale models were simulated.
3) Figure 3, the left graph, shows the comparison between fine and coarse models for the oil recovery factor.
4) We see in Figure 3 (left) and Figure 6 (left) that the coarse model presents deviations comparing with the reference fine-scale responses. Figure 3 compares the oil recovery factor, while Figure 6 shows cumulative gas production (GP) and cumulative water production (WP). The differences are not severe, and gas production shows the highest discrepancies. This effect is probably due to the near-miscible compositional effects

combined with the unfavorable mobility ratio between gas and oil that are highly smoothed in the coarse-scale. This happens because the compositional exchange in the surroundings of the gas front is highly overestimated in the coarse-scale cells. In addition, the viscous fingering instabilities are impossible to be reproduced in the upscaled models. Therefore, we will keep following the workflow to improve these results.

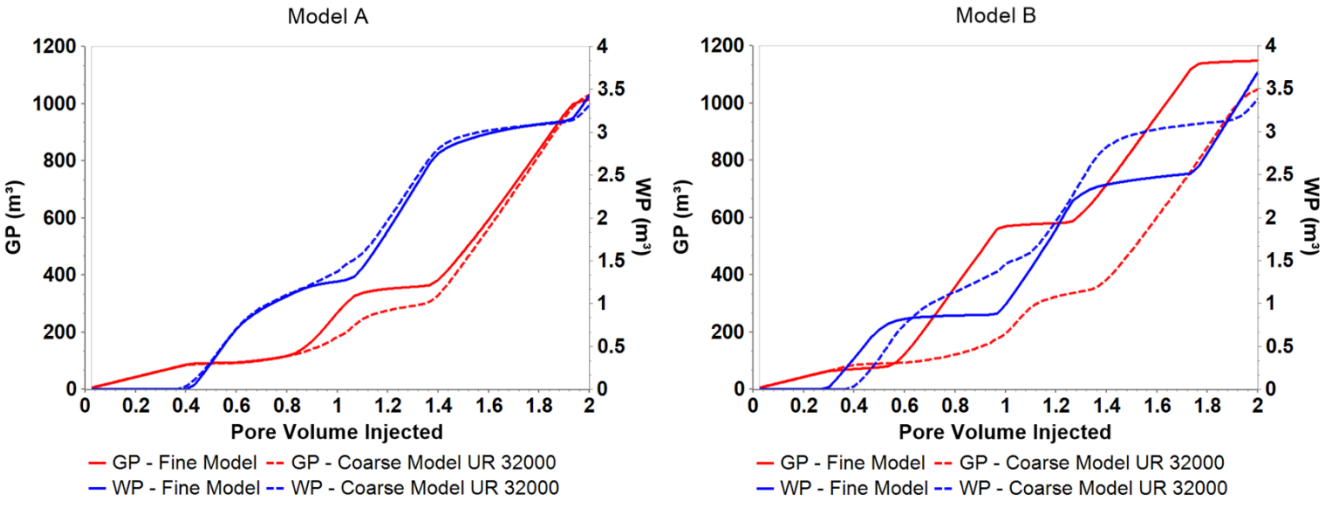

Figure 6. Cumulative gas (GP) and water (WP) production comparison between Fine and Coarse model for CO_2-WAG displacement. Models A on the left, and Model B on the right. Continuous lines represent Fine-scale results and dashed lines, coarse model results.

5) Since WAG is the recovery method, we must evaluate stable flow with continuous water and immiscible gas with matched viscosity. This step enables isolating effects of averaging the permeability and, therefore, the need for DP/DP upscaling. We summarize the comparison between fine and coarse-scale results for both stable flow investigations in Figure 7. In this figure, we show the results for continuous water flooding in the left and continuous gas flooding on the right. The continuous curves relate to the fine-scale results, while dashed curves represent the coarse-scale responses. Note that, for the case studies presented in this work, stable water flooding evaluation should be enough for the purposes of this step, because no gravitational effect is present in these 2D areal models.

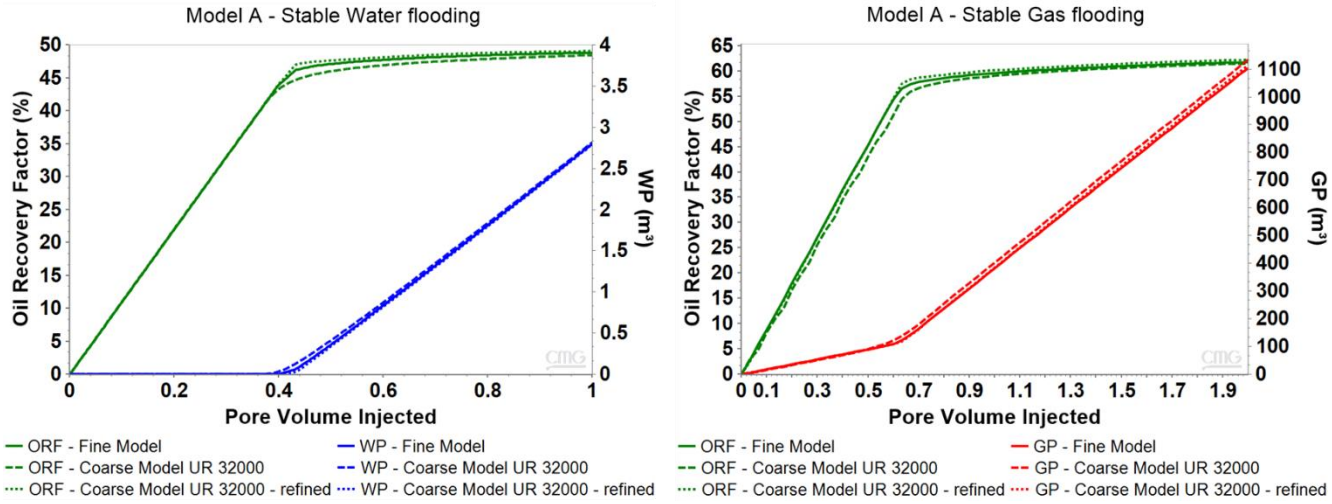

Figure 7. Stable flow evaluations. Left, water flooding, comparing oil recovery factor and WP. Right, gas flooding, comparing oil recovery factor and GP.

6) Notably, the upscaled model is capable of representing the fine-scale responses in these investigations, and it is possible to observe in Figure 7 that the coarse-scale results presented a close agreement with the fine-scale ones. Nevertheless, we note a slight difference in the curves, with little anticipation of the breakthrough of the injected fluids. This effect is a consequence of the higher numerical dispersion in the upscaled model (fine-scale has 960 blocks between the injector and produces wells, while coarse-scale only six). To prove this assumption, we promoted a grid refinement on the coarse model in which we divided each coarse cell into eight (in the flow direction), all with the same properties. The simulation results of this investigation are shown in the dotted curves of Figure 7. With this numerical exercise, the numerical dispersion effect is diminished, and the coarse-scale results become even more similar to the reference.

Therefore, the averaged permeability field and smoothing in the sub-grid heterogeneities are not mandatory issues for this model. As earlier discussed, this is a consequence of the “homogenous” distribution of the permeability field in Model A. Thus, this is a G2 type of problem.

Furthermore, the traditional flow-based permeability upscaling is useful for this problem, and we must work on pseudo-relative permeability curves to improve the coarse-scale results.

There are several published approaches to generate pseudo-curves (Barker and Thibeau, 1997). In this work, we consider a history-matching process with fine-scale results as responses to be matched. For this task, we use the software CMOST from

CMG (Computer Modelling Group Ltd., 2018). Since we are evaluating a WAG displacement, we consider three objective-functions in our history-matching procedure: oil recovery factor, cumulative water production, and cumulative gas production.

To obtain the pseudo-relative permeability curves, we consider a 3-parameter analytical correlation proposed by Lomeland et al., 2005. This correlation, known as LET correlation, promotes more flexibility in fitting pseudo-relative permeability curves. This happens because it allows varying three parameters – for water-oil curve and three more for the gas-liquid curve - during the history matching procedure to reproduce the fine-scale reference curves. Alternatively, the usual Corey relative permeability correlation can be used for this step, and the same procedure can be performed.

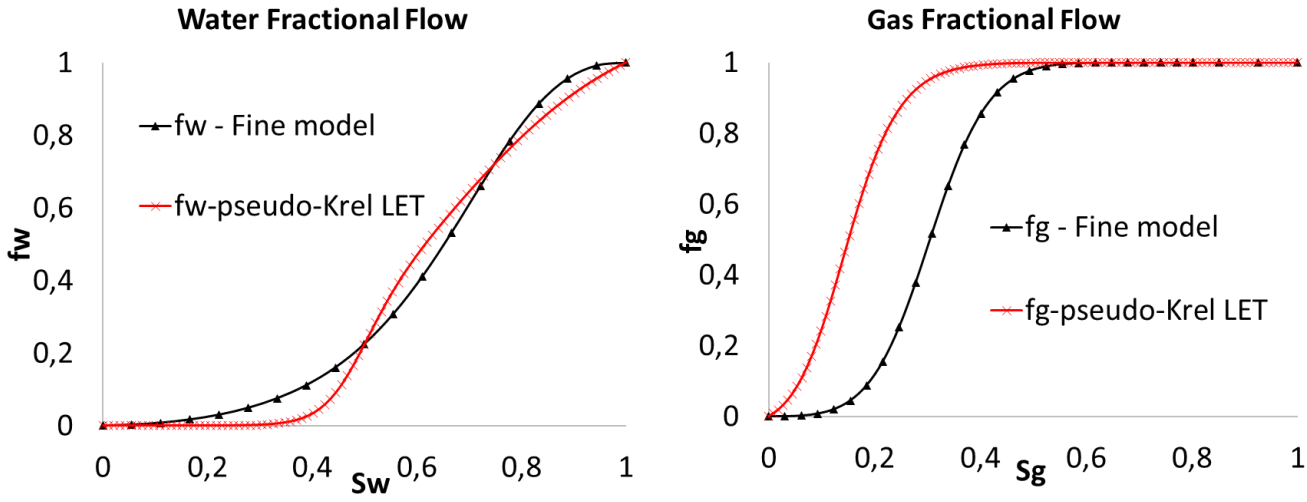

Figure 8. Fractional flow curves for original relative permeability curves and pseudo-relative permeability curves with LET type.

After the history matching process, pseudo-relative permeability curves were developed to improve the coarse model results. The comparison between original and pseudo fractional flow curves for gas and water is shown in Figure 8. As expected, more significant changes are observed for the gas curve, since the smoothing of compositional effects caused the major differences in the results for this case. The pseudo-relative permeability curves increased the gas mobility, which balanced the overestimated compositional effects in the coarse cells. The final results obtained with the upscaled model are shown in Figure 9. In green are the results for oil recovery factor, in blue for cumulative water production and in red for cumulative gas production. Continuous curves represent fine-scale results, while dotted curves are the final coarse-scale

responses. It may be noted that the coarse model with UR 32 000 showed close agreement with the fine-scale model for all the production curves and diminished the important differences in the cumulative gas production between 0.8 and 1.4 PVI (see left image in Figure 6).

Finally, the proposed workflow properly guided the upscaling procedure for Model A, which is a G2 type problem, and we obtained an improved coarse model with traditional flow-based upscaling for permeability and pseudo-relative permeability curves. Moreover, we highlight that our focus is to show a comprehensive workflow to enable better coarse-scale results. The method we used to generate pseudo-curves is only illustrative, and one can use different techniques for this purpose.

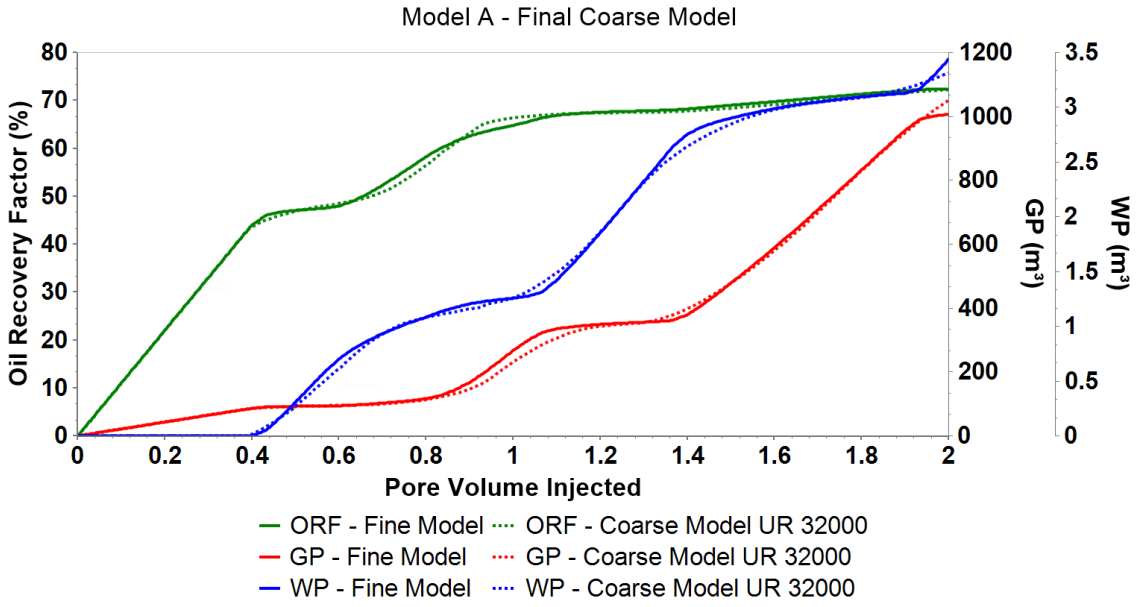

Figure 9. Final comparison between fine and coarse-scale models for Model A. The upscaling procedure indicated that this is a G2 type of problem, and the use of pseudo-curves provided improved results for the UR 32000.

Model B

Model B is a highly heterogeneous system with a channelized permeability field, in which the highest permeability values are concentrated in the upper area (Figure 1). This characteristic tends to increase the difficulty of the upscaling problem, especially for the 1D coarse model considered in this evaluation. Again, we will follow the same steps proposed in the "Methodology and Proposed Workflow" section to illustrate the improvement of the coarse-scale results for Model B.

1) Initially, a coarse-scale model with UR 32 000 was created with a traditional flow-based approach, and the upscaled permeability field is shown in Figure 2.

2) Both coarse and fine-scale models were simulated.
3) Figure 3, the right graph, shows the comparison between fine and coarse models for the oil recovery factor.
4) We see in Figure 3 (right) and Figure 6 (right) that the coarse model shows high deviations compared with the reference fine-scale responses. Again, Figure 3 compares the oil recovery factor, while Figure 6 shows cumulative gas production (GP) and cumulative water production (WP). In this case, not only is the oil recovery factor highly overpredicted, but the cumulative production of water and gas are also showing very optimistic behavior. This result is a consequence of the smoothing of sub-grid heterogeneity combined with the loss of resolution in the compositional effects. Following the proposed workflow, we isolate both problems to overcome the limitations and provide an improved coarse-scale mode.
5) In this step, we perform stable water/gas injection to investigate the need for DP/DP upscaling to represent the reservoir heterogeneities better. As mentioned for Model A, since we consider WAG displacement, we should evaluate water and gas stable flooding. However, these models do not have acting gravitational forces, therefore, for Model B, we focus the evaluations of this step on stable water flooding, because the same behavior is expected for stable immiscible gas flooding. Figure 10 compiles the results and comparisons between fine and coarse-scale models. In green are the oil recovery factor curves and in blue the cumulative water production curves.

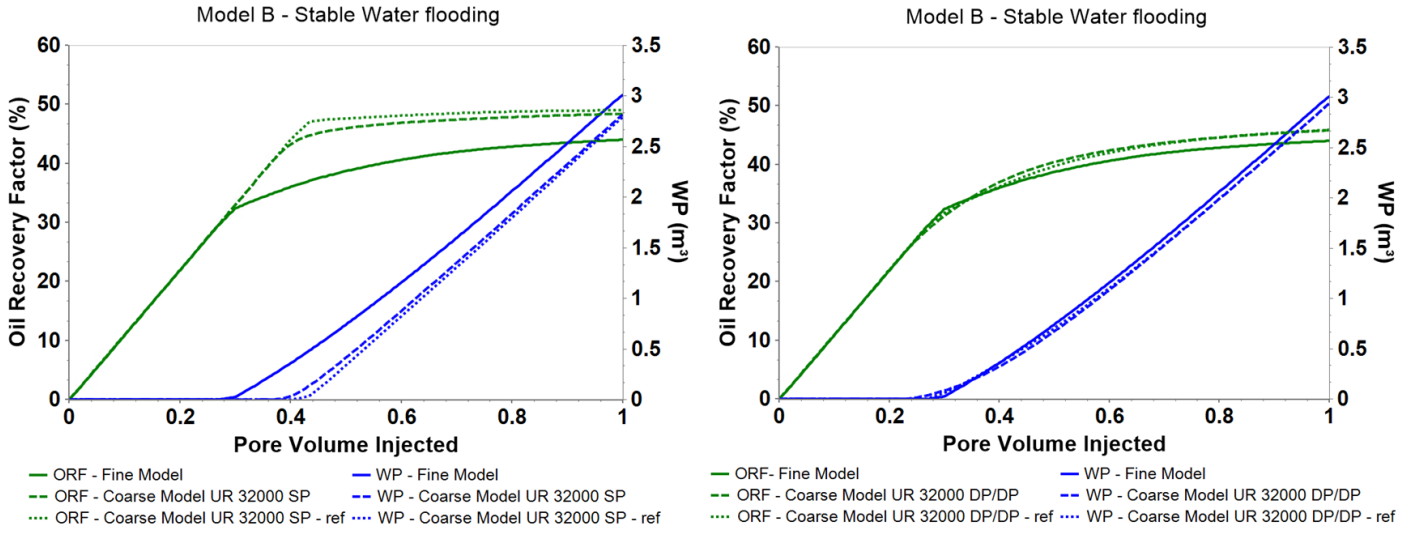

Figure 10. Stable water flooding evaluation comparing oil recovery factor and WP. Left: the initial coarse-scale model with traditional flow-based upscaling. Right: the coarse model with DP/DP upscaling proposed by (Rios et al., 2020)

6) The left graph in Figure 10 shows the comparison between fine-scale and traditional coarse-scale results. We note that the coarse model is not properly reproducing the fine-scale responses for stable water flooding evaluation. The oil recovery factor is highly overestimated and the water production is delayed. This behavior is a consequence of the non-uniform flow behavior due to the heterogeneity, which is lost in the coarse-scale representation.

In addition to the curves regarding fine and upscaled models, we present an additional simulation-run with the refined coarse model. As we did for Model A, the idea with this evaluation is to diminish numerical dispersion. However, since the numerical dispersion tends to anticipate the water breakthrough, we observe that, for Model B, the refined model responses are even more optimistic.

With this result, we conclude that the traditional flow-based upscaling is not a good solution for upscaling this permeability field. Furthermore, we recommend DP/DP upscaling, which can improve the sub-grid heterogeneities representation and the non-uniform flow behavior. Thus, this a G1 type of problem at this point.

According to Rios et al. (2020), the first step of the DP/DP upscaling technique is to divide the fine-scale porous medium into two systems – primary and secondary -, and the second is to calculate the final properties for each coarse-scale grid block cell.

In the first step, classical flow and storage capacity theory is used as a global guide, based on static data of the fine-scale reference model, to select the fine cells with a higher theoretical contribution for the flow. The Lorenz coefficient is calculated for each group of fine cells that compose a coarse-scale cell. This second criterion is considered a local guide.

In the second step, the coarse-scale properties are calculated. Porosity and permeability are obtained for both primary and secondary systems. The volumetric weighted arithmetic mean is considered for porosity, while directional Cardwell-Parsons upscaling (Cardwell and Parsons, 1945) is performed for permeability.

Since the porous media is ranked and divided into two systems, flow and transport need to be modeled in a way that allows two different continua to coexist with interaction between them. To achieve this, the flow in the new upscaled model can be approximated with a DP/DP approach formulation. The dynamic of the fluid flow will have a preferential system (primary system) modeled as “fracture” and a passive system (secondary system), modeled as “matrix”.

Following the workflow proposed by Rios et al. (2020), we generate the DP/DP coarse model with a UR 32 000 for Model B. Figure 11 summarizes the final permeability upscaling.

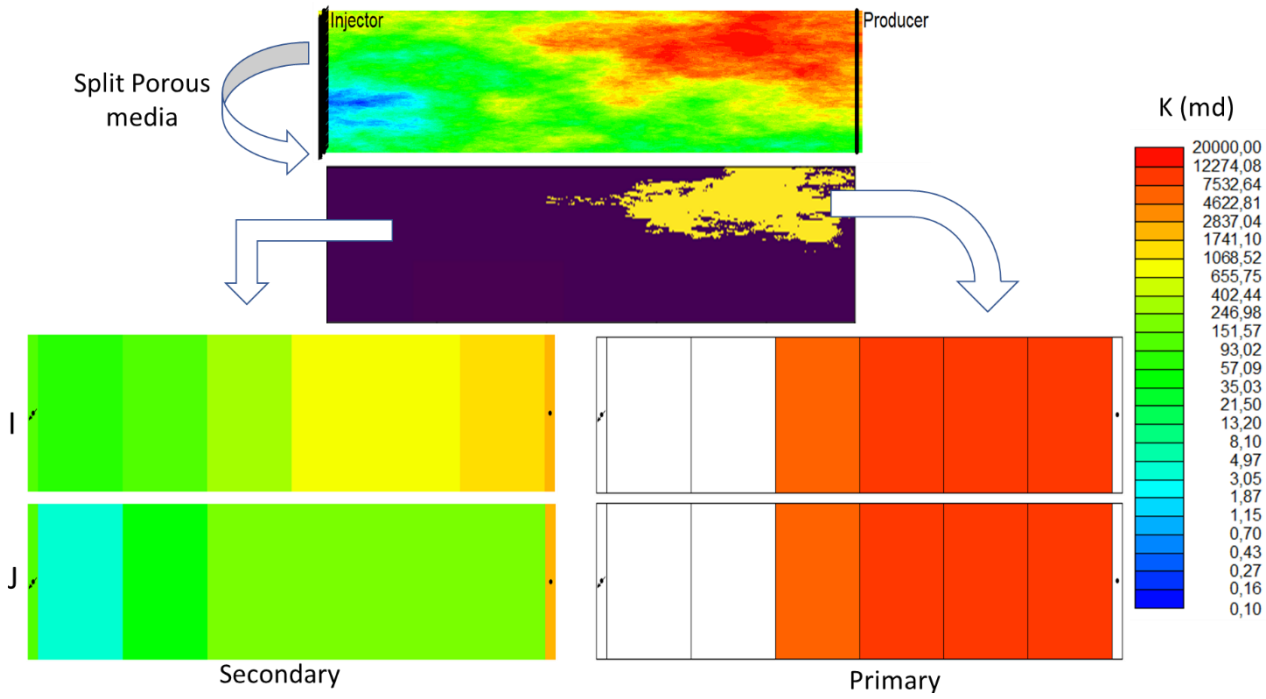

Figure 11. Summary of DP/DP upscaling for Model B. The Coarse-scale model with UR 32 000 now can represent sub-grid heterogeneities.

With the DP/DP upscaled model, we perform the stable water flooding evaluation again. Now, since the coarse model can represent sub-grid heterogeneities due to the porous media division promoted by the DP/DP technique, the results are improved. The primary system can better represent the high heterogeneous regions and enables a non-uniform flow in the coarse-scale cells. Figure 10 (right) shows that coarse model results are in close agreement with the fine-scale curves: the oil recovery factor is not overestimated and the water breakthrough is well reproduced. Hence, this step is completed, and, with the DP/DP upscaled Model B, we move to the next.

7) If the objective of this work were to evaluate water flooding, the coarse model would be ready. However, near-miscible WAG is the goal, and we need to verify if the results are already satisfactory or not.

To continue evaluating the new upscaled model, we simulate this model with near-miscible CO_2-WAG displacement. A comparison between DP/DP coarse and fine model results are shown in Figure 12. The left figure shows the oil recovery factor results and the right compares cumulative production of water and gas. Note that,

compared with traditional flow-based upscaling (Figure 3 (right) and Figure 6 (right)), there was an improvement in the results, but a high deviation is still observed.

Observing the curves in Figure 12, we note that the coarse model results start to deviate from the fine after the first water injection leg (first 0.4 PVI). At this point, the first near-miscible gas injection leg starts, and the coarse model fails on reproducing the small-scale compositional effects. The oil recovery factor results (left graph in Figure 12) indicate this increasing difference between coarse and fine models when the gas becomes part of the system. Moreover, in the right graph of Figure 12, we note that cumulative water production results were in close agreement up to the point where gas participation in the reservoir became more important (around 0.6 PVI).

Therefore, the problem is now of G2 type, and we can work on pseudo-relative permeability curves to improve the coarse model results and achieve a useful final upscaled model.

The same approach presented for Model A to generate pseudo-curves is performed in this case. The only difference is that, since the DP/DP model presents two systems (primary and secondary), we can fit pseudo-curves for each system to improve the final results.

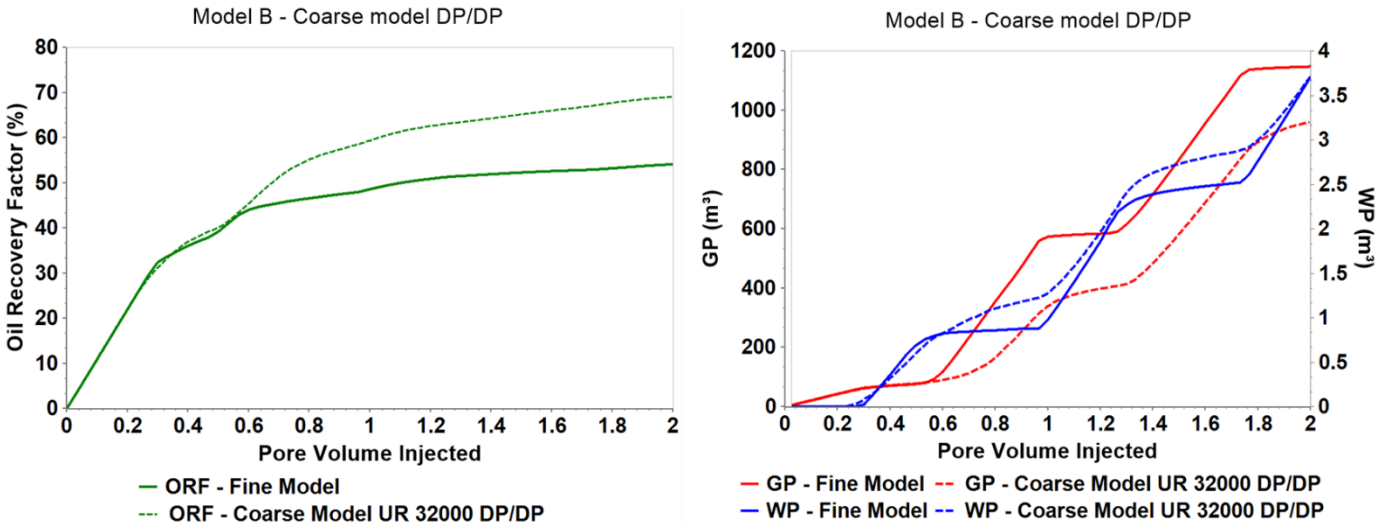

Figure 12. CO_2-WAG displacement results. Left: Oil Recovery Factor comparison between Fine and Coarse DP/DP. Right: Cumulative gas (GP) and water (WP) production comparison between Fine and Coarse DP/DP model. Continuous lines represent Fine-scale results and dashed lines, coarse DP/DP model results.

Figure 13 shows the final results after the generation of pseudo-curves for both systems in the DP/DP upscaled model B. Continuous curves represent the fine-scale results, and dotted curves represent the final coarse-scale model. The left graph presents a comparison between the final coarse model and fine model for the oil recovery factor, cumulative production of gas and water. Note that the results are highly equivalent, and the coarse model with DP/DP permeability upscaling and pseudo-relative permeability curve is now useful and equivalent to the fine-scale responses. The right graph shows the gas and water saturation in the reservoir throughout the simulation. Again, the final coarse model presents a close agreement with the fine model and a notable improvement when compared with the traditional single-phase (and single-porosity) flow-based upscaling.

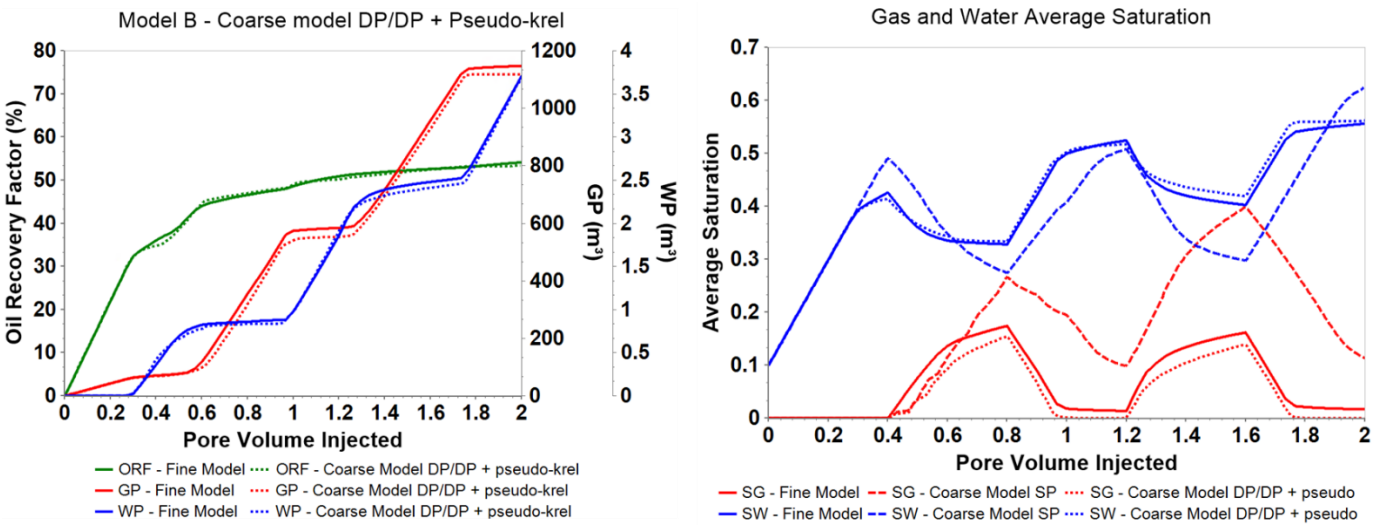

Figure 13. CO_2-WAG displacement results. Left: ORF, GP, and WP comparison between Fine and Coarse DP/DP with pseudo-relative permeability curves. Right: Average water and gas saturation throughout the simulation. Continuous lines represent Fine-scale results, dashed lines traditional coarse model, and dotted lines, coarse DP/DP model with pseudo-curves results

Lastly, Model B was a more challenging upscaling problem, since the 1D coarse model fails on representing the sub-grid heterogeneities using a traditional permeability upscaling approach. Besides, compositional effects representation added complexity to the process. This case is a G1 type for water flooding, but G1 and G2 types for near-miscible WAG displacement.

Nevertheless, the general upscaling workflow proposed in this work properly guided the upscaling procedure. By following the steps, we first noted the importance of applying DP/DP upscaling for this case. Then, we observed the need for additional improvement in the results

with pseudo-curves. Finally, a useful and effective coarse model was obtained, and the proposed workflow showed to be valid.

It is worth mentioning the results and discussions presented for the above case studies focused on the general upscaling workflow and its impacts on the simulation results. Another important consideration is regarding the speed of the simulation runs using coarse-scale models. When compared with the fine-scale, coarse models require only a fraction of the run-time. For both models, the final coarse models require less than 0.005 % of the total time used for a single fine-scale simulation run.

Note that no numerical optimization was performed on the models; therefore, the results are a relative comparison. Nevertheless, all models can be numerically improved, as shown by Avansi et al. (2019).

Additional Analysis

In the previous sections, we proposed and tested the general upscaling workflow for two highly detailed reservoir models. For both models, improved coarse-scale models with a UR 32 000 were obtained with a sound reproduction of the respective fine-scale results. We now propose an additional evaluation to stress-test the final coarse models. For this exercise, we focus on Model B, because it was, as previously discussed, more challenging to enable a satisfactory upscaled model.

This additional analysis consists in creating a new fine model by repeating the same pattern of Model B four times. All the dynamic conditions, recovery method, fluid properties, and relative permeability curves were the same as for the original Model B. The permeability field of this new model, named “Expanded Model B”, is shown in Figure 14. Note that the second and fourth patterns were inverted to keep the continuity of the high permeability zones in the top area of the model and trigger channelized flow.

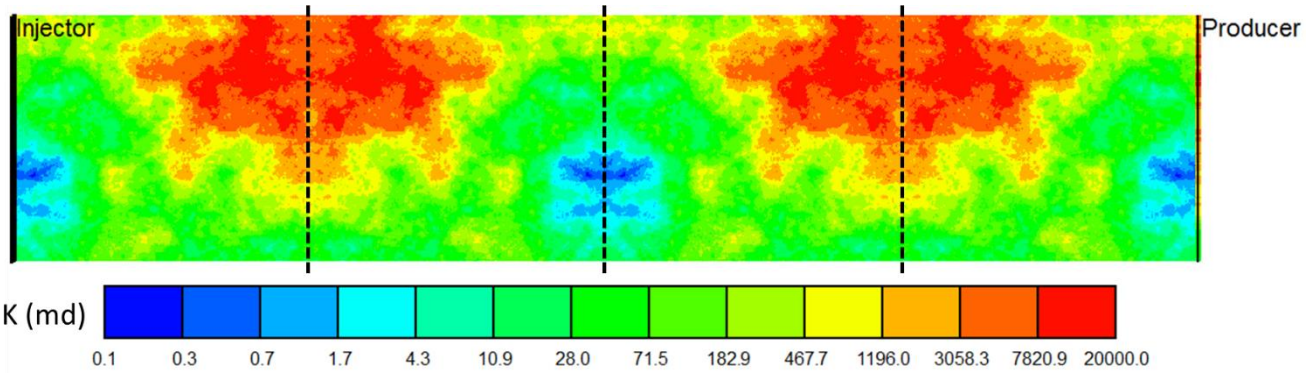

Figure 14. Permeability Field for Expanded Model B

In this study, the coarse model with a UR 32 000 is again considered. We compare the fine-scale results with the coarse model generated with traditional flow-based upscaling and the new upscaled model obtained for Model B. This investigation is important to test the improved coarse model under an even more challenging condition.

Figure 15 shows the final results. Note that the coarse model with DP/DP upscaling and pseudo-curves generated for Model B shows good agreement with fine-scale results in all the comparisons. The only exception is for water production in the last WAG cycle. However, the deviation occurs in a condition where the oil production is already close to its maximum. This result is remarkable since no new treatment was performed for this case; we simply extended the results from Model B. More importantly, these results indicate that our general upscaling workflow can be applied to refined sector-models of complex giant reservoirs, and the improvements on coarse models can be effectively expanded to full-field studies.

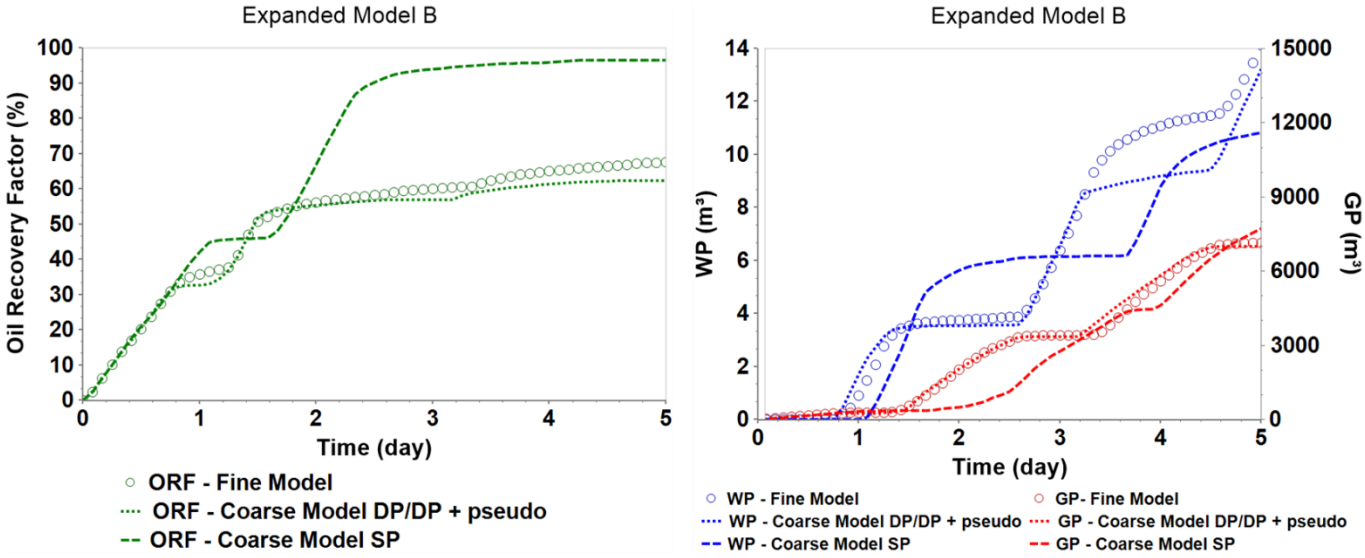

Figure 15. CO_2-WAG displacement results. Left: Oil Recovery Factor comparison between Fine, Traditional Coarse, and Coarse DP/DP + pseudo-krel. Right: GP and WP comparison between Fine, Traditional Coarse, and Coarse DP/DP + pseudo-krel. Continuous lines represent Fine-scale results, dashed lines traditional coarse model, and dotted lines, coarse DP/DP model with pseudo-curves results.

Discussions

In the present work, we introduced a new upscaling workflow to provide a better understanding of the coarsening problem and its main limitations. With a stepwise procedure, we showed that it is possible to evaluate when the coarse model needs improvements on G1, G2, or both, and suitable techniques are suggested for each group. This result is an important contribution because coarse models can fail to represent the reference results for different

reasons, and the current upscaling published library is more dedicated to presenting specific techniques, rather than providing a global workflow.

With a structured procedure, it is possible to deal with the upscaling problem more efficiently, focusing on the real limitations that prevent the coarse model from being useful for the decision-making process. In two highly detailed case studies, we showed that different strategies might be recommended according to the nature of the reservoir heterogeneity and the chosen recovery method.

For Model A, the challenges for a consistent upscaled model were more related to the dynamic specifics of the problem. Two main aspects were not possible to be properly represented in the coarse model and lead to an optimistic behavior: the compositional effects associated with the near-miscible gas front and the viscous instabilities, resultant from the unfavorable gas/oil mobility ratio. Besides, there is also the effect of the numerical dispersion, which, in this case, can be a positive effect since it works towards the anticipation of the injected fluids breakthrough. Thus, for this case, our workflow indicated that the use of pseudo-relative permeability curves to mimic the fine-scale dynamic behavior is recommended, and the final coarse model presented close results with the reference (Figure 9).

For Model B, the stable water flooding evaluation emphasized that the permeability simplification on the coarse model presented a high impact on the results (Figure 10 – left). In this reservoir model, the flow behavior is non-homogeneous and mainly concentrated on the high permeability area. At this point, the DP/DP upscaling procedure was suggested and provided a consistent improvement on the coarse model permeability representation, which can be observed by the results presented in Figure 10 – right. As previously mentioned, if the objective of this problem was to evaluate stable immiscible displacement, the coarse model would not require the use of pseudo functions, only the DP/DP permeability representation. However, due to the near-miscible WAG strategy, further changes in the relative permeability curves were suggested. The final result was an accurate coarse model (Figure 13), despite the large difference in the results initially observed (Figures 3 and 6 – right).

Finally, based on our results and investigations, it is worth highlighting that our work presents a robust global upscaling procedure that can be applied to any kind of reservoir model with any type of recovery method.

Conclusions

In this work, we proposed and tested a new general workflow to guide the upscaling procedure and enable a proper choice of the upscaling techniques to be considered in each

problem. The workflow is simple and, by following the steps, it is possible to better deal with the real limitations of an upscaling process.

The main advantages of applying the new workflow are: (1) the possibility to improve any coarse-scale simulation results with a consistent stepwise procedure and (2) a better understanding of the upscaling problem and the nature of the limitations to be overcome.

The specific conclusions of this work are:

- With the proposed procedure, we can verify when an especial permeability upscaling procedure (DP/DP approach) is recommended and in which situations the use of pseudo-relative permeability curves are necessary.
- The upscaling problem can be divided into G1 (static modeling limitations) and G2 (flow-dynamics specifics) types, and techniques were suggested for each of these scenarios.
- The proposed case studies were important to illustrate each step of the workflow and to highlight the different nature of upscaling problems. Model A was typically G2 type, and pseudo-relative permeability curves were generated to improve the results. Model B, on the other hand, required G1 and G2 techniques, and DP/DP permeability upscaling associated with the use of pseudo-curves provided improved results for the coarse-model.
- The proposed workflow can be useful for the industry demands since it allows the reservoir simulation engineers to dedicate their effort on the most important features to improve the coarse-scale simulation results.
- The upscaling investigation on Expanded Model B provided important results. The final coarse model obtained for Model B satisfactorily reproduced the fine-scale results without any further treatment. Although more investigations must be conducted in this direction, this result is important because it indicates that our approach can be applied to sector-models of giant reservoirs and, then, expanded for the full-field applications.

Acknowledgments

The authors would like to thank Petrobras (Petróleo Brasileiro S.A.), UNISIM, DE-FEM/UNICAMP, CEPETRO, ANP, and CMG for all the support for this work. Energi Simulation, Canada, is thanked for funding the chair in EOR at the University of Bergen held by prof. Arne Skauge and the chair in Integration of Reservoir Simulation and Facilities at UNICAMP, Brazil, held by prof. Denis José Schiozer.

7 ARTICLE 6: DIFFERENCES IN THE UPSCALING PROCEDURE FOR COMPOSITIONAL RESERVOIR SIMULATIONS OF IMMISCIBLE AND MISCIBLE GAS FLOODING

Victor de Souza Rios, Arne Skauge, Ken Sorbie, Gang Wang, Denis José Schiozer, Luiz O. S. dos Santos

To be presented at SPE Reservoir Simulation Conference held in Galveston, Texas, USA, 4-6 Oct 2021

Abstract

Compositional reservoir simulation is essential to represent the complex interactions associated with gas flooding processes. Generally, an improved description of such small-scale phenomena requires the use of very detailed reservoir models, which impact the computational cost. We provide a practical and general upscaling procedure to guide a robust selection of the upscaling approaches considering the nature and limitations of each reservoir model, exploring the differences between the upscaling of immiscible and miscible gas injection problems.

We highlight the different challenges to achieve improved upscaled models for immiscible and miscible gas displacement conditions with a stepwise workflow. We first identify the need for a special permeability upscaling technique to improve the representation of the main reservoir heterogeneities and sub-grid features, smoothed during the upscaling process. Then, we verify if the use of pseudo-functions is necessary to correct the multiphase flow dynamic behavior. At this stage, different pseudoization approaches are recommended according to the miscibility conditions of the problem.

This study evaluates highly heterogeneous reservoir models submitted to immiscible and miscible gas flooding. The fine models represent a small part of a reservoir with a highly refined set of grid-block cells, with 5 x 5 cm^2 area. The upscaled coarse models present grid-block cells of 8 x 10 m^2 area, which is compatible with a refined geological model in reservoir engineering studies. This process results in a challenging upscaling ratio of 32 000. We show a consistent procedure to achieve reliable results with the coarse-scale model under the different miscibility conditions. For immiscible displacement situations, accurate results can be obtained with the coarse models after a proper permeability upscaling procedure and the use of pseudo-relative permeability curves to improve the dynamic responses. Miscible displacements, however, requires a specific treatment of the fluid modeling process to overcome the limitations arising from the thermodynamic equilibrium assumption. For all the situations, the workflow can lead to a robust choice of techniques to satisfactorily improve the coarse-scale simulation results.

Our approach works on two fronts. (1) We apply a dual-porosity/dual-permeability upscaling process, developed by Rios et al. (2020a), to enable the representation of sub-grid heterogeneities in the coarse-scale model, providing consistent improvements on the upscaling results. (2) We generate specific pseudo-functions according to the miscibility conditions of the gas flooding process. We developed a stepwise procedure to deal with the upscaling problems consistently and to enable a better understanding of the coarsening process.

Introduction

In numerical reservoir simulation studies, upscaling fine-scale detailed models to coarser systems is a common need to improve the numerical performance of the simulation models. However, this process can degenerate results due to some critical consequences of the coarsening, such as: loss of resolution of the small-scale phenomena, averaging sub-grid heterogeneity and preferential pathways, and numerical dispersion, especially in oil fields with miscible gas flooding as an enhanced oil recovery method, continuously or alternatively with water (WAG). For this reason, various upscaling techniques have been proposed throughout the years with an increasing level of complexity, depending on the static and dynamic challenges represented by each reservoir and production strategy. Detailed and comprehensive reviews on several techniques are provided by Wen and Gomez-Hernández (1996), Renard and de Marsily (1997), Farmer (2002), and Durlofsky (2003).

In practical studies, single-phase upscaling techniques are valuable tools and the most commonly applied methods. They can provide satisfactory results for some two- and three-phase flow problems when the reservoir system is not highly heterogeneous or the mobility-ratio is not high. However, even when single-phase upscaling fails to capture the main features of the system, it is a prerequisite for more evolved solutions (Salehi, 2019). The most frequently used method to upscale porosity from a fine-scale model is the volumetric weighted arithmetic mean, because the pore volume is preserved (Durlofsky, 2003). For permeability upscaling, there are three important methods: averaging, which considers horizontal arithmetic average and vertical harmonic average; Cardwell-Parsons directional averaging (Cardwell and Parsons, 1945); and flow-based upscaling with closed boundary conditions (Christie, 1996; Kumar et al., 1997). In general, flow-based upscaling methods are more widely considered as reference approaches because of their generality and flexibility (Chen and Durlofsky, 2006).

For multiphase flow applications, additional effort is usually required to obtain a useful upscaled model. Generally, for water or immiscible gas flooding simulation processes, a two-phase upscaling procedure is recommended. In this case, the use of pseudo-relative permeability curve is a popular method when fine-scale simulation results are available. Barker and Thibeau (1997) reviewed several existing relative permeability upscaling approaches. They noted some limitations when considering pseudo-relative permeability curves while upscaling fine-grid geological models to coarse-scale simulation models. It is worth highlighting that the various pseudoization approaches require that one must either be able to run the fine grid, or select a representative section of the fine grid, and assert that the pseudo functions are appropriate for use elsewhere in the model (Fayazi et al., 2016). This limitation is well-known

when applying pseudo-relative permeability curves to reproduce fine-scale results using coarse models.

Specific approaches have been proposed for upscaling compositional flow simulations, and they can be roughly divided into four categories. The first type is the method of transport coefficients (also known as α-factors), proposed by Backer and Fayers (1994). The α-factors consist of modifiers introduced in the flow terms to relate compositions of the fluids flowing out of a large grid block to the average compositions of those fluids within the grid block. Together with pseudo-relative permeability curves, the coefficients are then considered to improve coarse-scale compositional simulations. Christie and Clifford (1998) also used the α-factor approach, but they used streamline techniques to generate a fine-scale solution. However, no pseudo-relative curves were used because they only considered single-phase flow problems.

A second type is the S_{orm} method (Hiraiwa and Suzuki, 2007), which models a bypassed oil fraction in the porous media by excluding this immobile saturation from the flash calculations. In this method, there is no mass transfer between the bypassed oil saturation and the flowing fluids. This is the main disadvantage of this method, which makes the bypassed oil totally unrecoverable.

A third type is to introduce a dual-porosity/dual-permeability (DP/DP) representation of the reservoir in which the porous space is divided into two systems, one with the most important flowing areas and another with the regions more likely to be bypassed. The mass transfer between the flowing and bypassed systems can represent the non-equilibrium behavior at the sub-grid scale. This type of approach was recently considered by Evazi and Jessen (2014), Zhang and Okuno (2015), and Rios et al. (2020a). However, only the methodology proposed by Zhang and Okuno (2015) focused on representing the bypassed oil fraction in a compositional simulation of gas flooding. The other two studies proposed a more generical methodology to represent the fine-scale heterogeneous features on a coarse-scale model.

The fourth type of method is to work on the components' thermodynamic properties to match fine-scale fluxes in a coarse-scale. This approach is valid to overcome one important and fundamental limitation of compositional simulation: the local equilibrium assumption, which allows the fluids to become perfectly mixed and in equilibrium within each grid block. This condition may be valid at fine-scale systems, but it is not reasonable for typical simulation grid block sizes. Iranshahr et al. (2014) developed a new compositional upscaling formulation, considering a non-thermodynamic equilibrium condition on the coarse-scale models. They

introduced the use of upscaled functions to reproduce this effect. This approach was extended by Salehi (2013, 2016), introducing a physical non-equilibrium term for the local thermodynamic constraints, which was also converted to a transport coefficient similar to the α-factors. These approaches allowed the coarse-scale simulation results to better represent the small-scale curves and component rates, but with an impact on the simulation time. Rios et al. (2017, 2019) proposed a methodology applied in two steps: first, an alternative fluid model is generated to deal with the compositional local equilibrium limitation. Then, pseudo relative permeability curves are used to better fit the simulated fine-scale model production curves. The authors showed that the proposed technique improved the coarse-scale results – production curves, sweep efficiency, and gas saturation map profile – in different scenarios of heterogeneity, with lower simulation time impact, compared to previously mentioned work.

The upscaling problems tend to be more challenging in highly heterogeneous systems since coarse-scale models usually fail to represent the main reservoir heterogeneities and sub-grid non-uniform flow behavior with traditional single-phase upscaling techniques. Besides, when fluid is injected into the reservoir promoting a high mobility-ratio displacement, viscous fingering instabilities are often ignored at the reservoir scale because it is impossible to capture such small-scale phenomena with large grid-blocks in simulation models. In addition, upscaling errors become more severe for large upscaling ratios where the numerical dispersion can significantly affect transport.

Despite the numerous published upscaling techniques, there is no universal method to provide reliable coarse-scale simulation models. In that sense, Rios et al. (2020b) proposed and tested a general upscaling workflow that provides a practical stepwise procedure. The authors, considering the nature of the effects, generically divide the upscaling problem into two groups that require different approaches: static modeling limitations (Group 1) and flow-dynamics specificities (Group 2). Their work presented two important features that represented an improvement in terms of how to deal with upscaling problems. It (1) guides the upscaling process by enabling the selection of the proper approach according to the problem's limitations - Group 1 or Group 2. Also, it (2) allows a better understanding of the upscaling problem as a whole, resulting in improved and robust coarse-scale simulation models.

In practical upscaling situations, the generation of a coarse model can be dominated by one of the above-mentioned groups or a combination of both. Working on Group 1 alone may be enough when immiscible fluid is injected in a highly heterogeneous reservoir, where the preferential pathways concentrate the overall flow dynamics. Group 2 tends to be the focus when a near-miscible or miscible gas injection is performed (continuously or WAG) in a low

heterogeneous reservoir. Lastly, both groups are important when a combination of the earlier scenarios occurs (Rios et al. 2020b).

In this work, we focus on the upscaling problems associated with gas flooding processes. We first discuss the differences between immiscible and miscible conditions and how it can affect the way an upscaled model must be generated. Then, we apply the general upscaling workflow proposed by Rios et al. (2020b) to guide the upscaling of two highly heterogeneous fine-scale models submitted to immiscible and miscible gas flooding strategies. The models represent a small sector of a reservoir with an area of 50 x 10 m^2 and present a highly refined set of grid-block cells, with a 5 x 5 cm^2 area. We upscaled the models to coarser systems with grid-block cells of 8 x 10 m^2, which is compatible with a refined geological model in reservoir engineering studies. This results in a challenging upscaling ratio (UR) of 32 000 in a 1D coarse-scale model.

We work on Group 1 (G1) limitations with the DP/DP upscaling proposed by Rios et al. (2020a). For Group 2 (G2), pseudo-relative permeability curves can be considered for immiscible processes, and the two-step methodology proposed by Rios et al. (2017,2019) is recommended for miscible gas flooding.

Objectives

The objectives of this work are:

- Explore the different upscaling procedures proposed for immiscible and miscible gas flooding processes; and
- Provide consistent and robust coarse-scale results with the proposed upscaling workflow for two highly heterogeneous fine-scale reservoirs under immiscible and miscible conditions.

Methodology

In this work, we summarize methodologies presented in some previous publications to better explain and describe the upscaling of numerical reservoir models under immiscible and miscible gas flooding process. First, the general upscaling workflow proposed by Rios et al. (2020b) is the global strategy to guide the generation of coarse models with a better treatment of the specifics of each problem. This workflow is summarized in Figure 1, and it is a useful tool to assist the upscaling process by highlighting the most critical limitations to the problem. With this procedure, it is possible to create consistent coarse-scale simulation models with a coherent stepwise approach and obtain a better understanding of the upscaling problem and the nature of the limitations to be overcome. Details of each step are provided by Rios et al. (2020b).

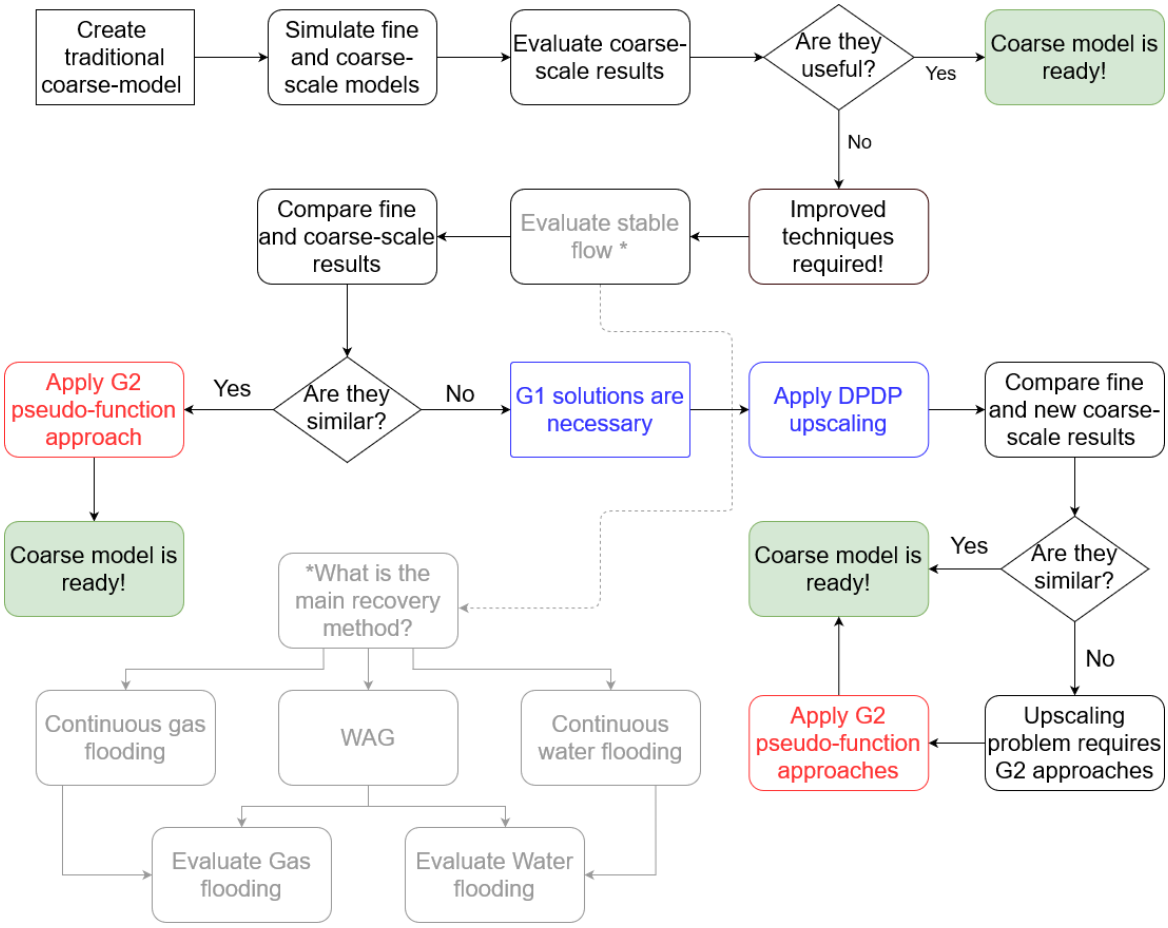

Figure 1. Flowchart to guide a general upscaling procedure. Adapted from Rios et al. 2020b

This general upscaling workflow is divided into three main parts, as follows: (i) verify if the traditional single-phase upscaling is useful and sufficient for the problem; (ii) evaluate whether the problem is G1 or G2 type; and (iii) investigate the need for G2 solutions after working on G1.

In the first part, we generate the coarse model with a traditional flow-based upscaling methodology and simulate coarse and fine-scale models with the desired recovery method. Then, the results are compared to verify if the coarse model is acceptable to be used. If not, the next step is required. It is worth noting that, when the fine model is highly time-consuming to simulate the full model, the use of representative sector-models is a recommended alternative for this evaluation.

If the upscaled model requires improvement after the first verification part, it is critical to understand the main reason for the observed deviations. This check is the second part of the workflow, whose objective is to investigate whether it is the averaging of the permeability field and the smoothing of sub-grid heterogeneities that are compromising the coarse-scale results (G1 type of problem). If this is true, a more robust permeability upscaling technique

should be considered, and the DP/DP upscaling proposed by Rios et al. (2020a) is recommended, given its capability for improving upscaling results for highly heterogeneous reservoirs has been demonstrated (Rios et al. 2020a, 2020b, 2021). On the other hand, if the permeability upscaling is shown not to be an important limitation, then the problem is of G2 type; therefore, pseudo-functions are indicated to improve the coarse-scale results.

The third part is a final inspection after the G1 solution, in case that it is applied. At this point, G2 solutions may be used to conclude the upscaling process, if required.

Next, we will show some information about the recommended approaches to overcome G1 and G2 type of problems.

A solution for G1: DP/DP Upscaling to Improve Permeability Representation

As previously discussed, for highly heterogeneous reservoirs, the traditional techniques have limited conditions to represent the main reservoir features and sub-grid heterogeneities in coarse-scale models. Therefore, to deal with this deficiency, the DP/DP upscaling approach proposed by Rios et al. (2020a, 2021), summarized in Figure 2, is a consistent option to improve G1 limitations on the upscaling problem.

This upscaling technique uses flow and storage capacity analysis, and the Lorenz Coefficient applied to the static information of a fine-scale model to split the porous media into two levels: one representing the main flow regions and the other, the secondary flow regions. With the splitting of fine-scale cells, the coarse-scale properties are calculated. The volumetric weighted arithmetic mean is considered for porosity, while directional Cardwell-Parsons upscaling is performed for permeability.

Once the porous media is ranked and divided into two systems, flow and transport need to be modeled in a way that allows two different continua to coexist, with interaction between them. Thus, the flow in the upscaled model can be approximated with a DP/DP approach formulation (Rios et al., 2020a, 2021). The resulting DP/DP coarse-scale models can adequately reproduce the reference fine-scale results and properly represent the non-homogeneous flow behavior within a coarse-scale grid-block in highly heterogeneous reservoir models.

For these reasons, we consider this solution recommended when G1 limitations are important in the upscaling procedure.

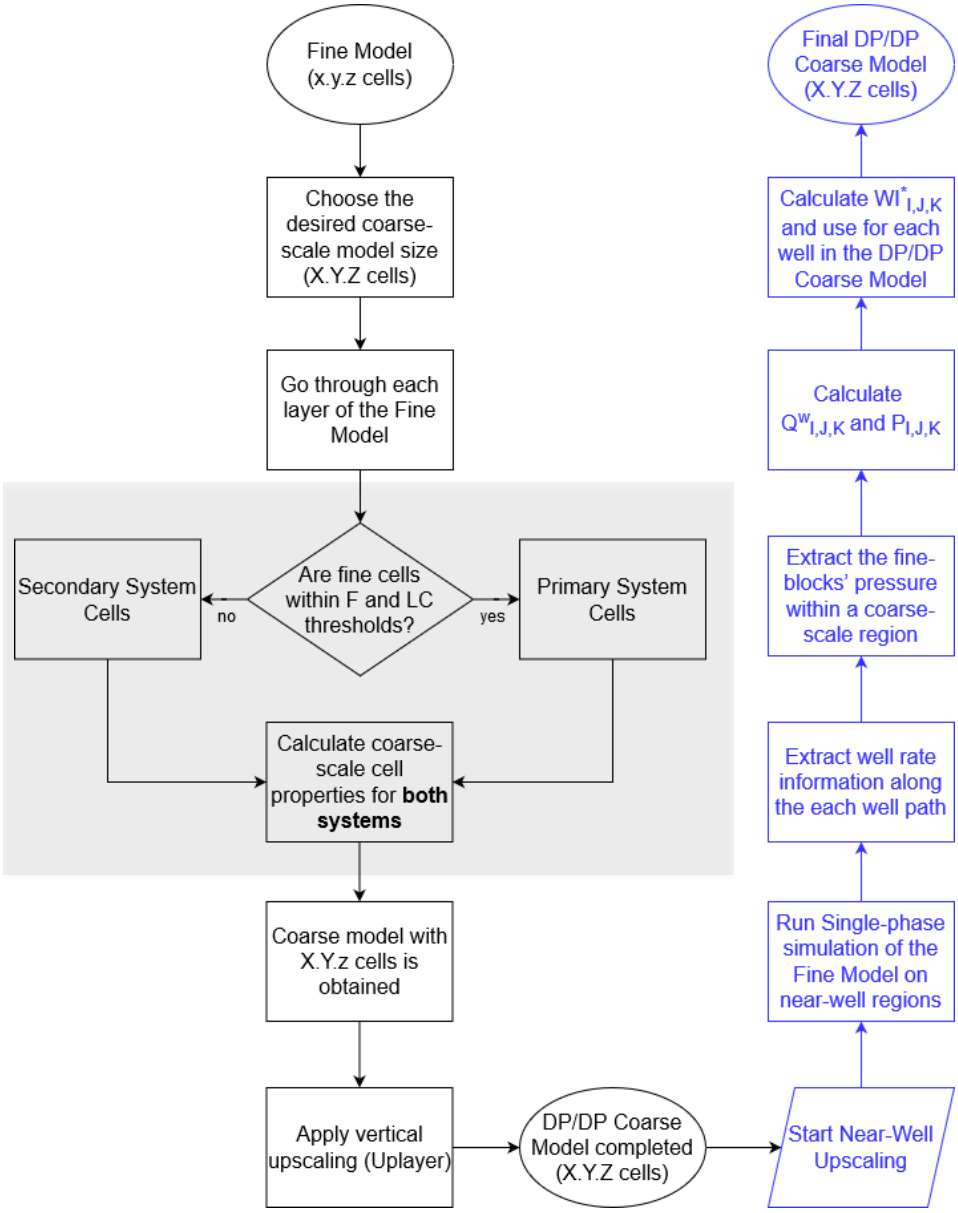

Figure 2. Flowchart summarizing the steps of the DP/DP upscaling procedure (Rios et al. 2021). The highlighted steps are detailed in Rios et al. (2020a)

Solutions for G2: Pseudo-functions to Improve Dynamic Behavior

When the dynamic features of the problem become an important limitation to obtain acceptable upscaled models, the use of pseudo-functions can be an effective tool to improve the coarse models' results. This group of techniques aims at mimicking the dynamic responses of a fine-scale reference model by changing some functions on the coarse model. The pseudo-relative permeability curve is the most well-known strategy for this task and can provide good results for immiscible displacements with a high mobility-ratio.

In this work, adjusting pseudo-relative permeability curves is equivalent to a history matching task. We consider a 3-parameter analytical correlation for relative permeability, proposed by Lomeland et al., 2005. This correlation, known as LET correlation, promotes more

flexibility in fitting pseudo-relative permeability curves. It allows varying three parameters during the history matching procedure to reproduce the fine-scale reference results. To assist this pseudo-relative permeability curves tuning task, we used a commercial software capable of running the compositional simulator and optimizing the LET parameters to fit reference curves. Alternatively, the usual Corey relative permeability correlation can be used for this step, and the same procedure can be performed (Rios et al., 2019).

For a miscible gas flooding process, pseudo-relative permeability curves cannot be directly applied since there is no gradual variation in the grid-blocks' gas saturation. In fact, only 0 or 1 values are obtained on first contact miscibility conditions. In coarse-scale models, this thermodynamic consequence, combined with the local equilibrium during the simulations, tend to overestimate the oil recovery. To overcome this problem, we consider the two-step methodology proposed by Rios et al. (2019).

This approach is based on employing an alternative fluid model, also known as pseudo-fluid, with a pseudo minimum miscibility pressure (PMMP) above experimental values to provide an immiscible-like displacement. This solution does not violate the phase behavior and ensures the formation of two hydrocarbon phases in the reservoir. Therefore, the gas relative permeability plays a role in the simulation results and can be used to improve the coarse model production curves. The technique is applied in two steps: first, the pseudo-fluid model is generated, and then pseudo relative permeability curves are used to better fit the production curves. Details of this methodology are provided in the original publication.

Therefore, in this work, we suggest the use of pseudo-relative permeability curves for immiscible displacement and the two-step compositional upscaling approach for miscible conditions. These techniques can provide improvements to G2 limitations.

Case Studies Description

In this work, we consider the 2D highly detailed reservoir models created by Wang et al. (2019). They introduced two heterogeneous reservoirs, named Model A and Model B, which were considered to investigate full-physics simulations of near-miscible CO_2 WAG injection. Both models present the same Dykstra-Parsons (Dykstra and Parsons, 1950) coefficient ($V_{DP} = 0.7$) but different dimensionless correlation ranges (RL). Model A presents a short correlation length ($R_L = 0.1$) with the idea of triggering possible fingering flow. Model B is characterized by a long correlation length ($R_L = 1$) to enable a channelized flow pattern. Figure 3 shows the permeability field for both models.

In the fine-scale, Model A and Model B are 2D areal models described on a regular Cartesian grid with dimensions of 50 x 10 x 0.1 m^3. The size of all the grid-blocks is 0.05 x 0.05 x 0.1 m3, except in the first and last columns, with 1 x 0.05 x 0.1 m^3. A horizontal injector is completed along the entire length of the first column, and a horizontal producer is completed along the entire length of the last column. Therefore, there are 192 400 cells in total (962 x 200 x 1).

Although models A and B are considered, only static properties (permeability and porosity) and relative permeability curves are kept as considered by Wang et al. (2019). We adapted the fluid properties, initial conditions, and well constraints to enable a better discussion regarding the differences between the upscaling solutions for immiscible and miscible gas flooding process.

The reservoir fluid is a light oil represented by seven pseudo-components, as presented by Rios et al. (2017, 2019). The initial GOR is 215 m^3/m^3 and the saturation pressure is 400 bar, while the initial reservoir temperature and pressure are set at 93.9 °C and 500 bar, respectively. There is no free gas, and the initial water saturation is 0.1. More information about the numerical models is summarized in Table 1 and Table 2.

Table 1 - Summary of Model A and Model B properties.

	Porosity	**Average K (mD)**	**V_{dp}**	**R_L**
Model A	0.1	1000	0.7	0.1
Model B	0.1	1800	0.7	1

Table 2 – Additional information about the numerical models (BHP is bottom hole pressure and EoS is equation of state)

Number of cells	Fine-Scale = 192400 Coarse-Scale = 20
Simulator type	Compositional
Fluid Model	EoS with 7 components (see Rios et al. (2017, 2019))
Producer BHP	500 bar
Injection Rate	0.4 PV/day
Relative Permeability curves	Corey type (see Wang et al. 2019)

As previously mentioned, Model A and Model B represent different heterogeneity and flow behavior and are critical challenges to stress-test the methodology. As described in the “Introduction” section, both models are upscaled to coarse models with a UR of 32 000 (Figure 4). The high level of coarsening (the fine model is a highly refined 2D system, while the coarse model is 1D) combined with the specifics of the miscibility conditions during the

gas flooding process make these upscaling problems more complex. These factors enable a complete discussion about the global upscaling workflow and the differences in the upscaling procedure when immiscible and miscible displacement are considered.

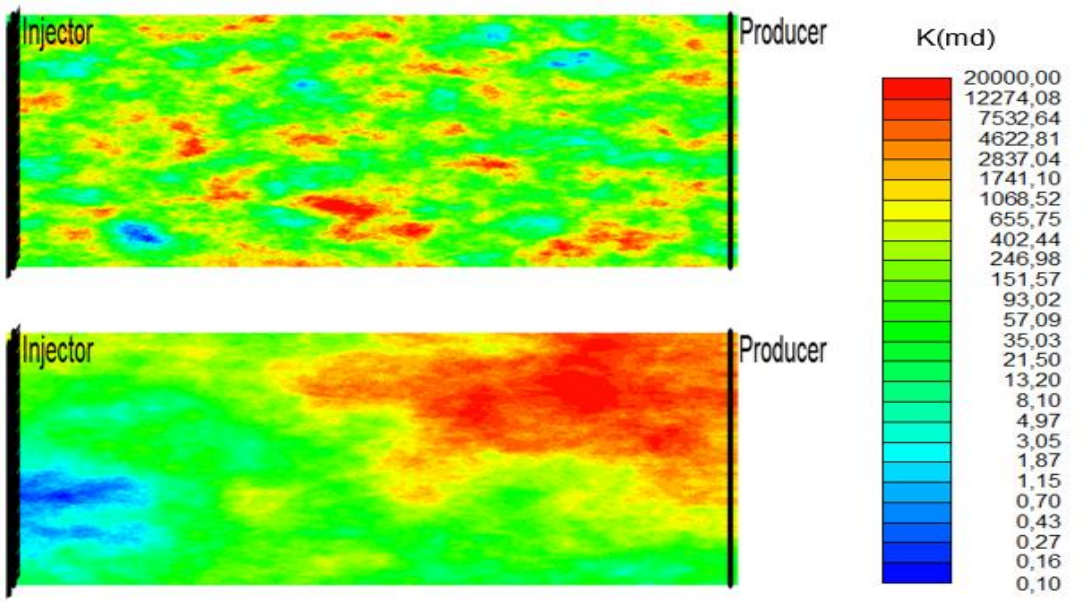

Figure 3. Permeability Field for Models A (upper image) and B (lower image)

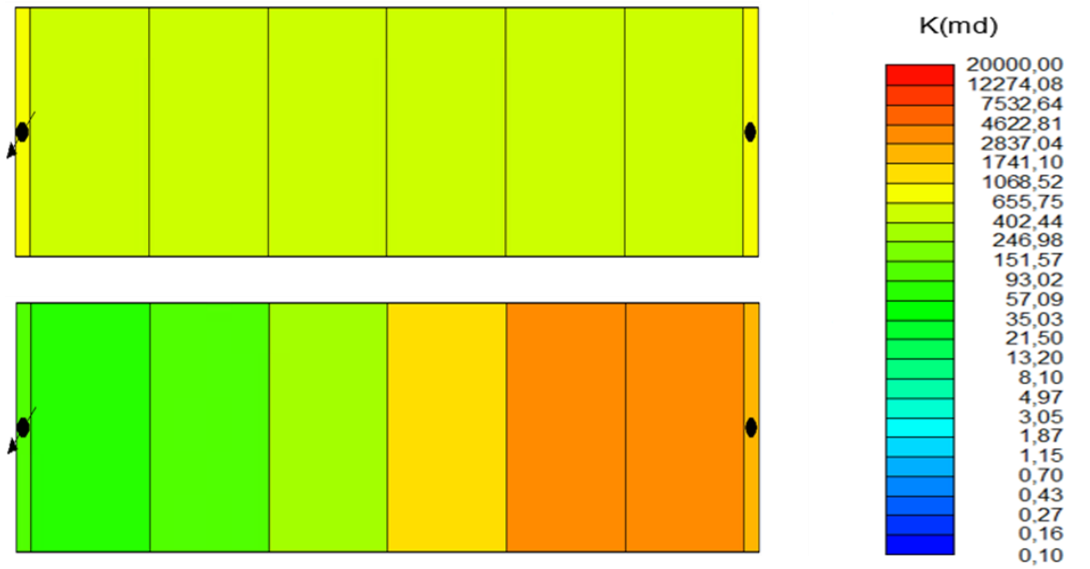

Figure 4. Permeability Field for coarse models with UR 32 000: Models A (upper image) and B (lower image)

Numerical Evaluations

In our numerical investigations, we first focus on discussing the main differences between immiscible and miscible gas flooding conditions on the selection of the appropriate upscaling strategies. Then, we apply the global upscaling workflow combined with the

methodologies described in the “Methodology” section to obtain accurate and useful coarse-scale models for Model A and Model B under different miscibility conditions.

Key Differences Between Immiscible and Miscible Conditions

When gas is injected into an oil reservoir, the mass exchange between the fluids may vary considerably depending on their composition and the reservoir pressure and temperature. In immiscible displacements, the compositional exchange and mass transfer between the injected gas and the reservoir fluid is usually limited to light and some medium components, while heavy components are left behind, leading to a low oil recovery. In such a condition, free gas and oil are distinct phases, and the flow is related to the fluids' saturations. However, if the gas flooding process is conducted under miscible conditions, strong compositional interactions occur, and there is no interfacial tension between gas and oil. This situation leads the system to achieve thermodynamic equilibrium as a single-phase with residual oil saturation approaching zero, and the saturation variations have limited meaning.

The above-mentioned differences have an important impact on the selection of proper upscaling approaches. To illustrate these aspects, we perform comparisons between fine- and coarse-scale simulation models under miscible and immiscible conditions for Model A and Model B. For this evaluation, we consider matched viscosity between injected gas and the reservoir oil to isolate the miscibility behavior effects and mitigate the viscous instabilities in the gas front. Besides, the coarse-scale models were numerically refined in the flow direction to present the same level of numerical dispersion as the fine models. This means that each grid cell in the coarse models showed in Figure 4 was divided into 160 refined blocks. Thus, the numerical dispersion effect does not introduce any bias to the overall comparisons.

For immiscible cases, we consider a black-oil version of the fluid model described in Table 2, so we can capture the extreme of no compositional effect. On the other hand, for miscible displacement cases, CO_2-rich gas is considered in the same configuration presented by Rios et al. (2017, 2019).

The gas saturation profiles for fine- and coarse-scale models when an immiscible gas displacement is performed are shown in Figure 5. Note that, as a reference, the coarse models were generated using the flow-based upscaling technique. The images represent the gas breakthrough time for the fine models A and B. The upper figures show the fine-scale responses, where we can observe the main difference between Model A and Model B. While the first present a nearly homogeneous sweep behavior, the second is highly dependent on the main permeability area, located at the top of the reservoir. The lower images show the coarse-scale responses for each model at the equivalent time. We note that, despite the high coarsening

level, the resultant gas saturation profile is in close agreement with the fine response for Model A, while coarse Model B presents a completely different profile once it fails to model the main (and sub-grid) heterogeneities in a 1D representation.

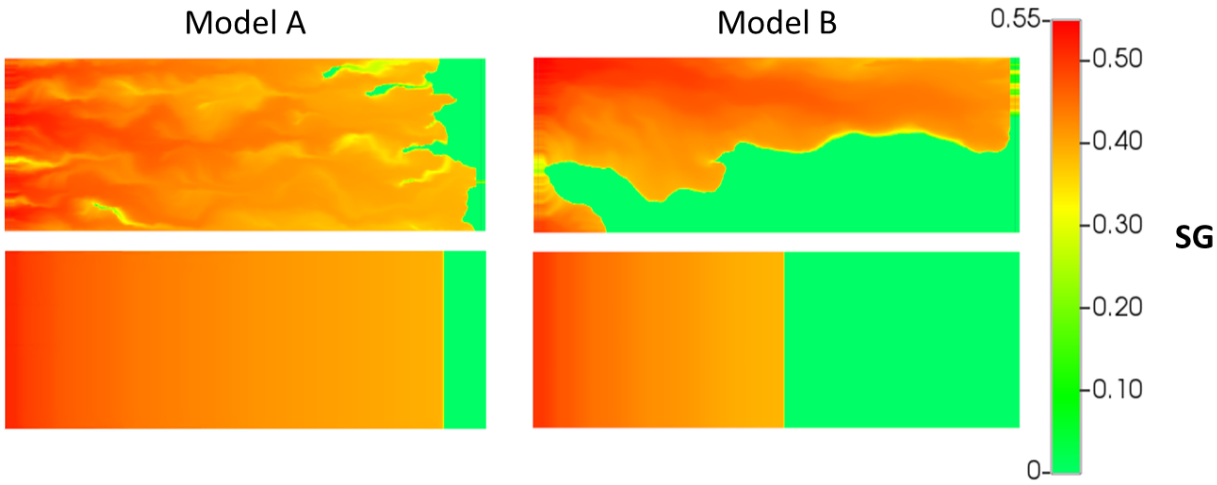

Figure 5. Gas Saturation profile at the gas breakthrough time of the fine model for immiscible gas flooding process. Model A on the left and Model B on the right. The upper images refer to the fine-scale reference models while the lower represent the respective coarse models

For the miscible gas flooding process, the small-scale phenomena are more complex to be well represented in coarse models due to the compositional effects and the high local displacement efficiency. The global CO_2 mole fraction for fine- and coarse-scale models A and B are shown in Figure 6, while Figure 7 shows the gas saturation profiles. Again, the images capture the gas breakthrough time for the fine models A and B.

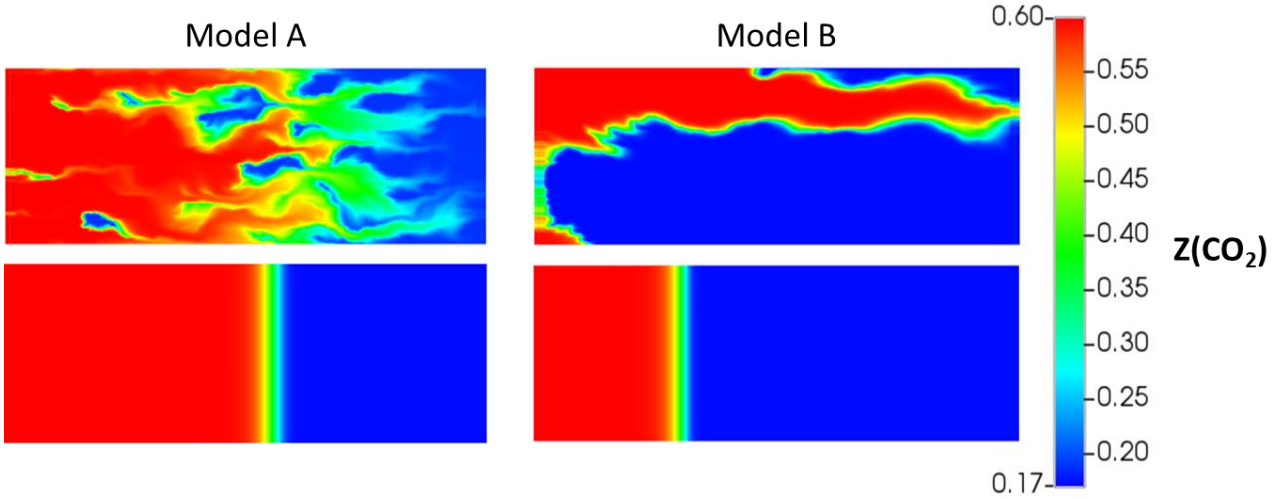

Figure 6. Global CO_2 mole fraction at the gas breakthrough time of the fine model for miscible gas flooding process. Model A on the left and Model B on the right. The upper images refer to the fine-scale reference models while the lower represent the respective coarse models

From the upper images in Figure 6, we observe that the compositional effects are more present on Model A, where it is possible to note a wider variation on the CO_2 mole

fraction. For Model B, heterogeneity is a dominant factor, and compositional effects become relatively less important, as pointed out by Wang et al. (2019). Both cases, however, are not well represented by the equivalent coarse-scale models. The lower images in Figure 6 show that the loss of resolution in the upscaled models smooths the CO_2 diffusion representation (which is emphasized in the high-resolution permeability heterogeneity in the fine-scale - upper images in Figure 6). For Model A, this effect is clearer if we compare it with the immiscible case. The absence of compositional effects was a key factor in enabling a proper representation of the fine-scale results with the coarse model. The same behavior is not observed with the miscible displacement, and the upscaled model fails to reproduce the CO_2 propagation front and delays the gas breakthrough (CO_2-rich gas dissolved in oil). For Model B, the coarse model also presents a limited prediction of the small-scale compositional effects; however, the heterogeneity representation seems to be the critical modeling limitation.

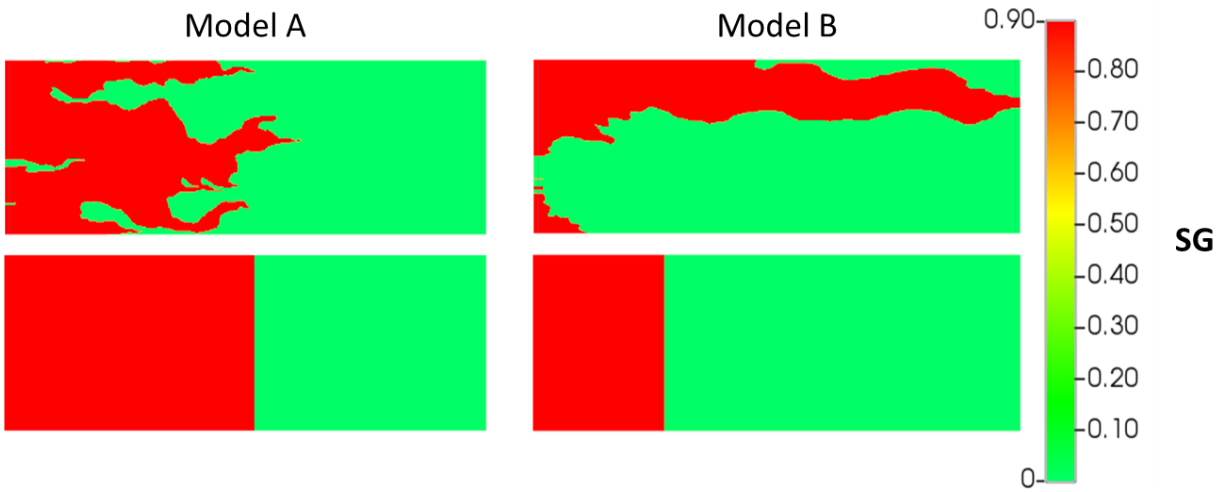

Figure 7. Gas Saturation profile at the gas breakthrough time of the fine model for miscible gas flooding process. Model A on the left and Model B on the right. The upper images refer to the fine-scale reference models while the lower represent the respective coarse models.

The comparison between immiscible and miscible fine-scale gas saturation profiles (Figure 5 and Figure 7) shows that the higher local displacement efficiency during the miscible processes (residual oil saturation goes to zero) makes the overall sweep efficiency lower when compared with the immiscible scenario. The same behavior happens for Model A and Model B, although it has more emphasis on Model A, once Model B is more dominated by a channeling flow regime. This observation has a critical consequence for the upscaling process. For Model A, the better sweep promoted by the injected gas (despite the lower local efficiency) allows the simplified coarse model to represent the average gas saturation profile. However, the small-scale unswept zones under miscible conditions are not well represented by the coarse model. For Model B, the same situation happens, but it is restricted to the upper high permeability area.

In other words, for immiscible displacement, the main limitation for Model B is the permeability representation, while both permeability upscaling and compositional effects are challenges when a miscible gas process is considered.

Therefore, the most critical difference between immiscible and miscible conditions for the upscaling problem is the challenge in incorporating the small-scale compositional effects on the coarse model. This is a well-known limitation of traditional upscaling techniques and a useful solution was proposed by Rios et al. (2019).

Global Upscaling Workflow Applied to Model A and Model B

Once the key differences between the upscaling problem for immiscible and miscible gas flooding were discussed, we apply the general upscaling workflow and the suitable group of techniques to build consistent coarse-scale simulation models with a challenging UR of 32 000 for models A and B. For both models, we investigate immiscible and miscible problems in two dynamic evaluations with a highly unfavorable viscosity.

Next, we first present the results and discussions for Model A, then for Model B. The upscaling process follows the steps provided in Figure 1, which enables a better understanding of the nature of the upscaling limitations (G1, G2, or both) and guides the appropriate techniques to be considered.

Model A

a) Immiscible gas flooding with a viscosity ratio of 75:

As mentioned earlier, once the scale of the desired coarse model is selected, we consider the flow-based upscaling as the reference technique for permeability to generate the initial upscaled model. Then, to begin with the upscaling procedure, the first part of the general workflow shown in Figure 1 is to evaluate fine- and coarse-scale simulation results and verify if the traditional solution is satisfactory or not.

Figure 8 shows the Oil Recovery Factor (ORF) and Gas Oil Ratio (GOR) curves for fine and coarse models. Besides the fine-scale results, this figure shows the coarse-scale (UR 32 000) and the refined coarse-scale (which is the same coarse model numerically refined in the flow direction to represent the same level of numerical dispersion as the fine model) responses, with the objective to discuss the numerical dispersion effect on the results. From the observed results, we note that the coarse-scale responses are fairly close to the reference fine-scale, despite the unfavorable viscosity ratio in which the displacement is performed. It is worth mentioning, however, that when we diminish the numerical dispersion by refining the coarse model, the coarse-scale curves present a more optimistic behavior. This response happens because the numerical dispersion can partially cancel the upscaling errors associated with the

loss of small-scale phenomena representation (Haajizadeh et al., 2000), as illustrated in Figure 9.

In practical studies, we could consider this coarse model as useful for the decision-making process for this dynamic condition. However, to evaluate the general upscaling approach, we proceed with the workflow to verify if it is possible to achieve an even more accurate result and how it should be done.

Following the workflow, once we consider that the coarse model can be improved, the next step is to check if G1 solution is necessary. For this purpose, stable flow investigation is required. In this step, highlighted in gray in Figure 1, we evaluate matched viscosity gas flooding and compare fine- and coarse-scale results. The idea is to better isolate the impact of permeability upscaling and verify if the DP/DP technique is recommended to improve sub-grid heterogeneity representation (Rios et al. 2020b). The results are shown in Figure 10, and we note that fine and coarse models are in close agreement. Again, to diminish the numerical dispersion effect, we also simulated the refined coarse model. It is possible to verify that, once it is a stable flow, the dynamic small-scale phenomena (such as viscous fingering) are controlled (Figure 5 upper left image), and the refined coarse model presents a slightly better performance. Nevertheless, this investigation shows a good agreement between fine and coarse models, which means that flow-based upscaling is adequate for the permeability upscaling and G1 solution is not necessary.

Therefore, to improve the final coarse model for this application, we must work on G2 solutions. Since it is an immiscible displacement, the well-known pseudo-relative permeability curves is an effective technique.

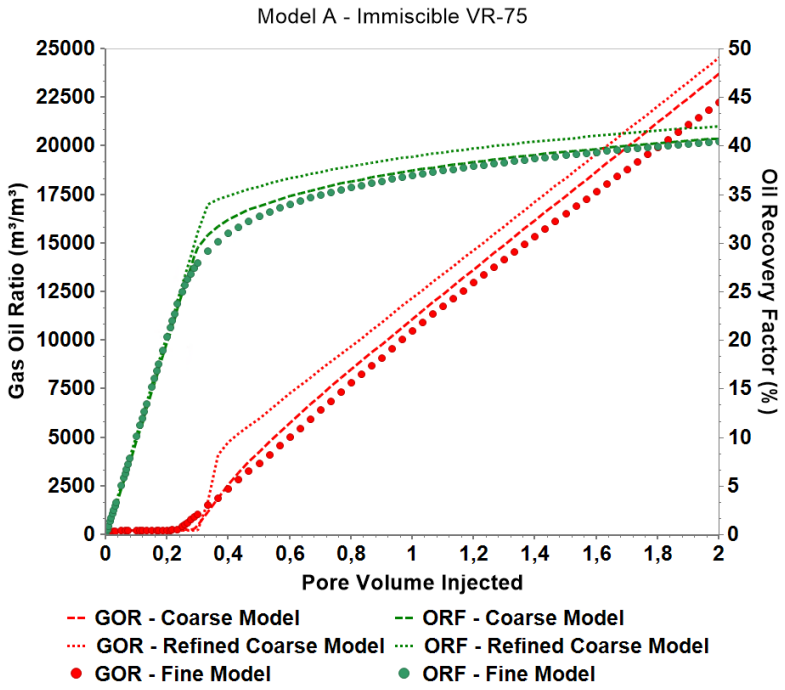

Figure 8. Oil Recovery Factor and Gas Oil Ratio for fine, refined coarse, and coarse models

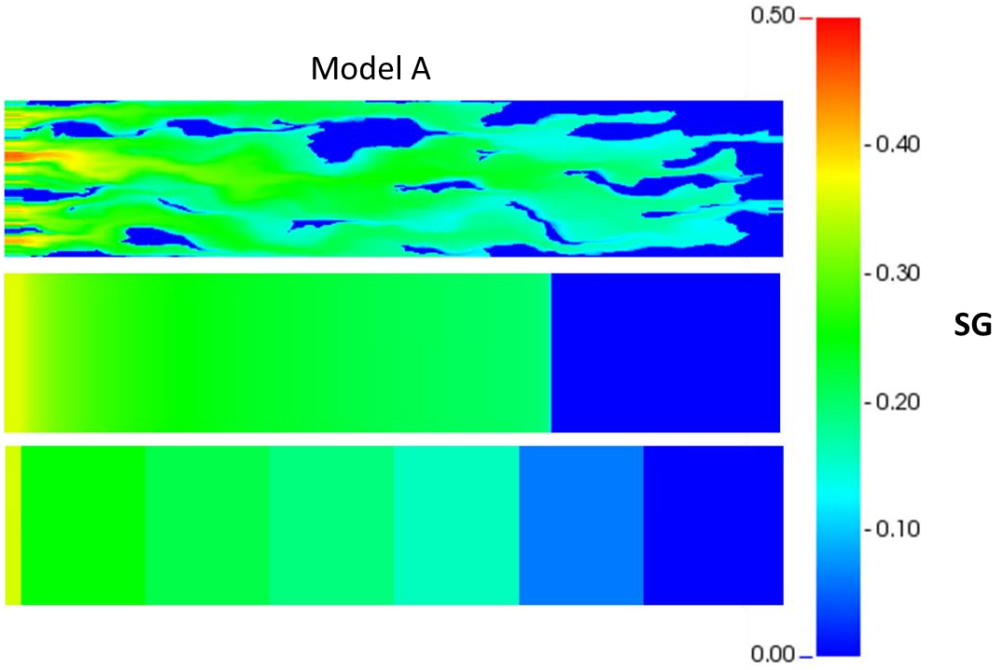

Figure 9. Gas Saturation profile at the gas breakthrough time of the fine Model A for immiscible gas flooding process. Upper image is the fine model, middle is the refined coarse model and lower is the coarse model (UR 32 000).

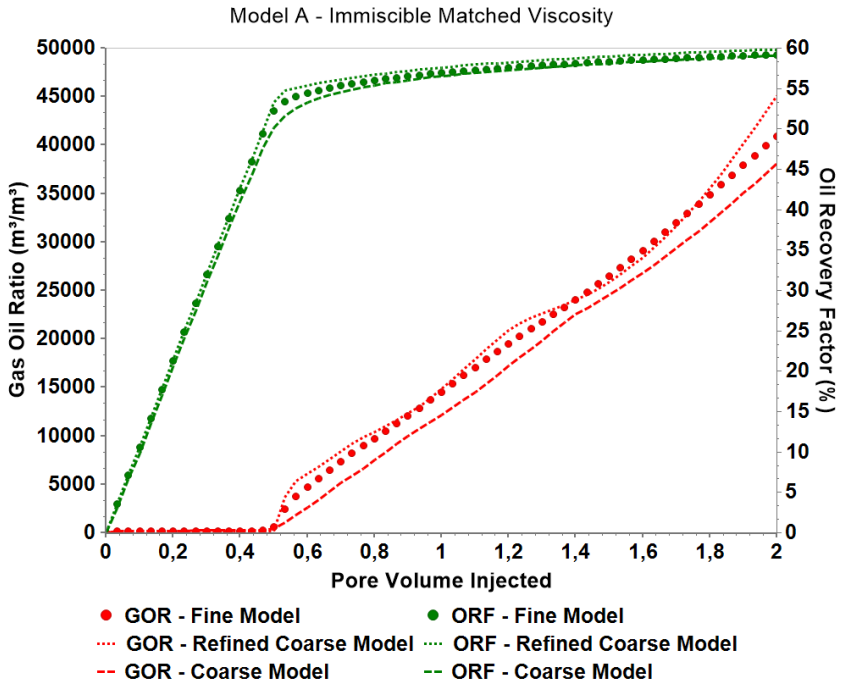

Figure 10. Oil Recovery Factor and Gas Oil Ratio for fine, refined coarse, and coarse models. Stable-flow evaluation.

After the history matching process, pseudo-relative permeability curves were generated to improve the coarse model results. The comparison between the final coarse model and the reference fine model is shown in the left image of Figure 11. It is possible to note that the results are nearly identical without a great change in the relative permeability curves since the results were already close. The original and pseudo fractional flow curves for gas are presented on the right image of Figure 11.

Finally, it is worth highlighting that, despite the clear improvement on the final coarse-scale results, this immiscible gas flooding application was already well represented by the initial coarse model. However, we showed that the general upscaling workflow is useful to guide the proper choice of upscaling technique suitable for the problem. In this case, small dynamic corrections were necessary; thus, pseudo-relative permeability curves were employed.

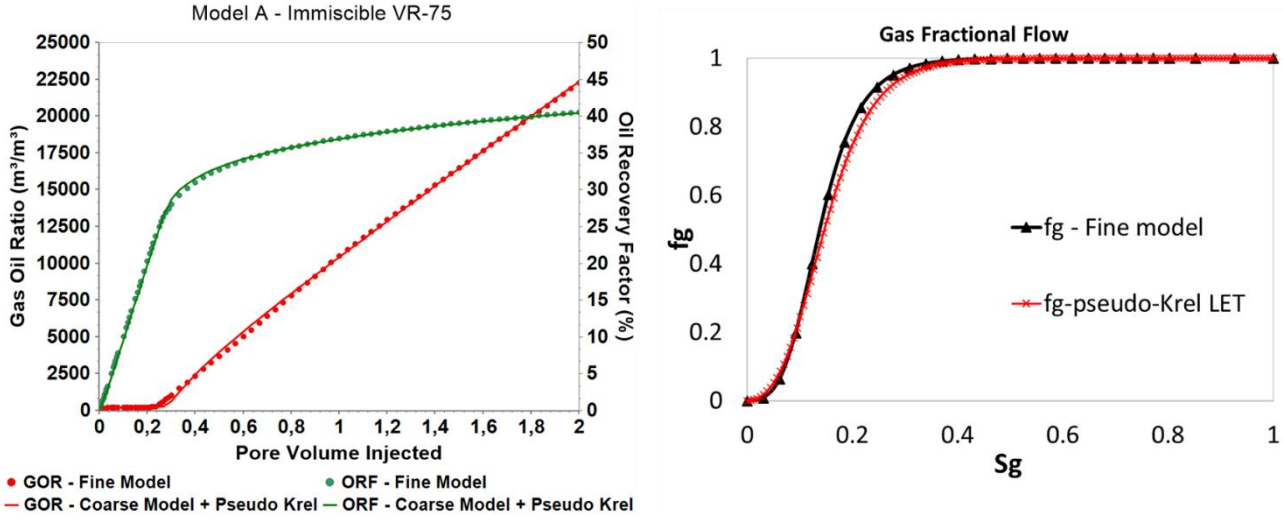

Figure 11. Left: Oil Recovery Factor and Gas Oil Ratio for fine and final coarse models. Right: Fractional flow curves for original relative permeability curves and pseudo-relative

b) Miscible gas flooding with viscosity ratio of 75:

The second application with Model A is to improve, if necessary, the coarse-scale results when miscible gas is injected into the reservoir under an unfavorable viscosity ratio of 75. This dynamic evaluation combines two critical challenges for the upscaling procedure: intense compositional effects and small-scale viscous fingering. Besides, as previously discussed, the numerical dispersion acts as a "positive" effect.

Again, the first step is to compare the traditional coarse model responses with the reference. The left image in Figure 12 shows the ORF and GOR comparison between the fine model and the initial coarse model. The difference in the results is expressive, and the coarse model presents a highly optimistic behavior, as expected. The highly unfavorable viscosity ratio miscible gas flooding process is one of the most challenging scenarios for the upscaling problem. The unstable gas front establishes viscous fingers, which has a great impact on the sweep efficiency. Besides, the miscible displacement presents a high local displacement efficiency, 100% in this case, which means that all the oil contacted by the injected gas tends to be displaced. On the coarse scale, however, the small-scale viscous fingers are impossible to be reproduced, which artificially increases the sweep efficiency at this scale. This fact, combined with the miscible nature of the gas injection, makes the coarse models highly optimistic, displacing 100% of the contacted oil in a highly coarse grid cell. This problem can be exemplified by the gas saturation profiles shown in the right image of Figure 12. At the same simulation time, the fine-scale gas saturation presents a high amount of bypassed oil (A), while the coarse model behaves homogeneously. Therefore, improvements are required to generate a useful coarse model on this scale.

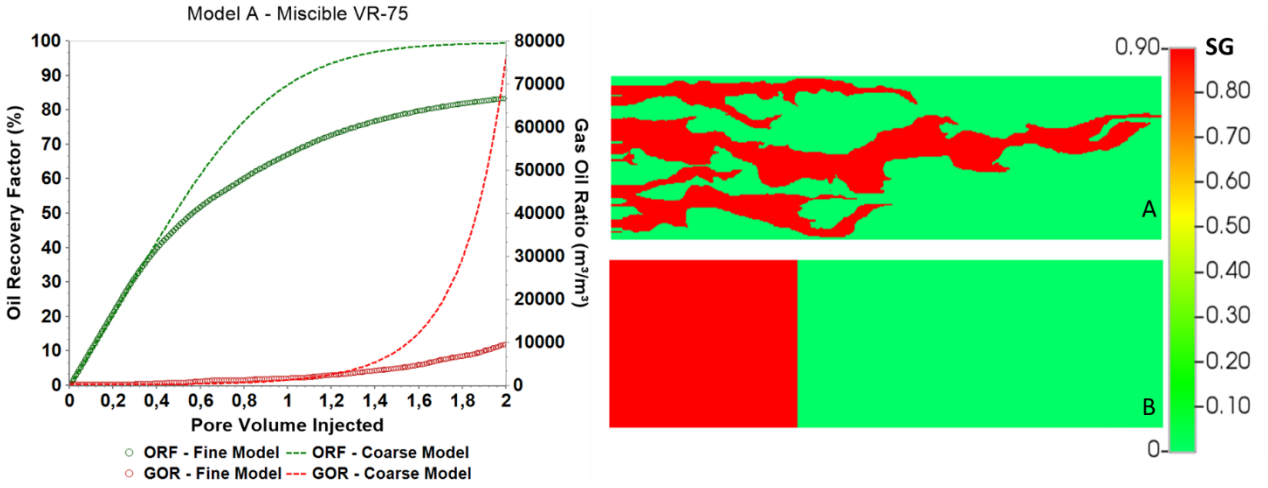

Figure 12. ***Left:*** **Oil Recovery Factor and Gas Oil Ratio for fine and initial coarse models.** ***Right:*** **Gas Saturation profile at the same time for fine and coarse models under miscible gas flooding process.**

The next step is to verify if G1 solution is necessary. For this purpose, we evaluate matched viscosity gas flooding and compare fine- and coarse-scale results. This procedure is the same performed for the immiscible case, thus it is not necessary to be repeated since we already acknowledged that this problem is not G1 type and flow-based upscaling is a proper representation for the coarse-scale permeability.

Accordingly, this upscaling problem is a G2 type, and pseudo functions can be applied to improve the coarse-scale results. Nevertheless, for miscible conditions, the use of pseudo-relative permeability curves directly has no impact due to the absence of continuous variation on the saturations (each block is 100% gas or 100% oil, there is not a continuous variation in between). Therefore, the two-step methodology proposed by Rios et al. (2019) is suggested to overcome the upscaling limitations in this case.

The first part of this compositional upscaling technique is the generation of a pseudo-fluid model with an “immiscible” behavior at the reservoir pressure and temperature. This is important to properly represent, in the coarse model, the average gas saturation behavior that a coarse block area presents in the fine-scale model (which is not 0 or 1 but varies between these values). Since the fluid model we consider in this application is the same one used by Rios et al. (2019), we use the same pseudo-fluid model presented by the authors to mimic the desired “immiscible-like” behavior in the coarse-scale. Figure 13 shows the main difference between the original fluid model and the pseudo-fluid. It can be noted that, at the reservoir pressure, only the original presents a miscible behavior, while the pseudo-fluid has a minimum miscibility pressure above the reservoir pressure. Other comparisons between the fluid models are available in Rios et al. (2019).

Once the pseudo-fluid is generated, it becomes the new fluid model for the coarse model. With this change, the displacement efficiency of the gas injection in the coarse model is reduced and becomes more representative of the small-scale inefficiencies that occur in the fine-scale (Figure 12, right, A). Thus, after this first step, the results already present an important improvement, as can be seen in the left image of Figure 14. At this point, we have conditions to further improve the coarse-scale results by working on the second step, which is the generation of pseudo-relative permeability curves. Finally, the fractional flow curve related to the new set of relative permeability curves is presented in the right image of Figure 14. The highly unfavorable mobility ratio combined with the compositional effects (weaker in this pseudo-fluid, but still present) made the fractional flow become extremally favorable to the gas flow, which resulted in improved results. Accordingly, the resultant upscaled model can accurately represent the fine-scale results, as shown in the continuous curves on the left image of Figure 14, and the coarse model is now satisfactory to represent the reference responses.

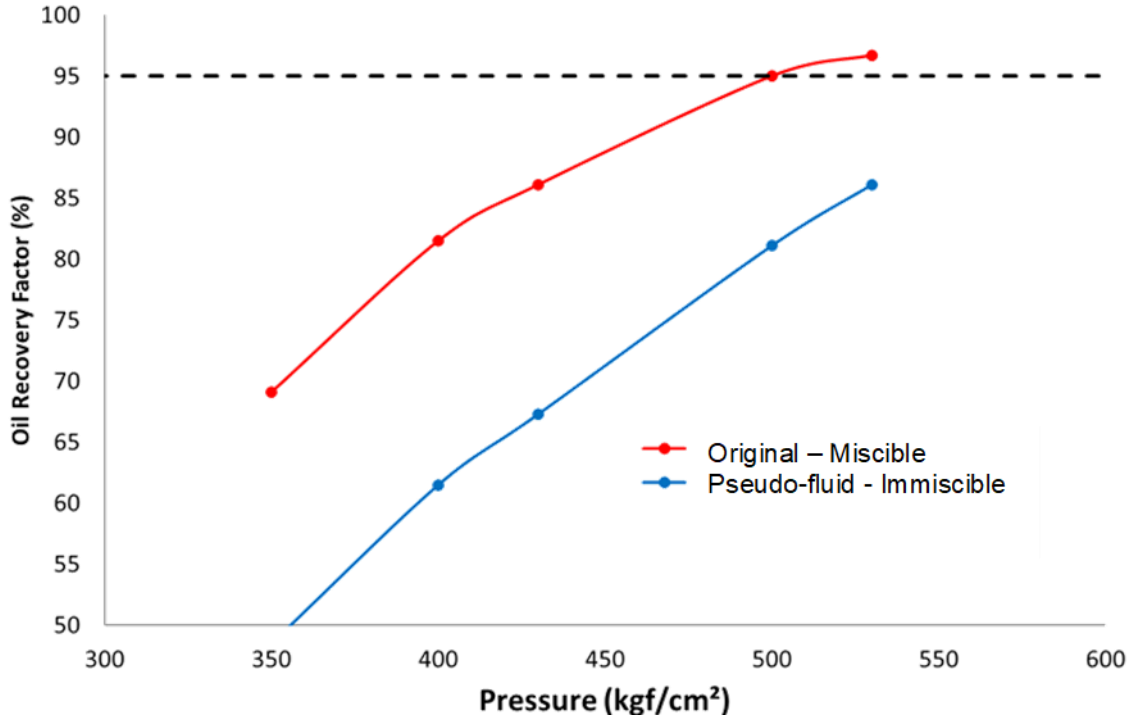

Figure 13. Oil recovery factor versus pressure after 1.2 PV injected of gas for miscible gas and pseudo-fluid adjustment. Adapted from Rios et al. (2019).

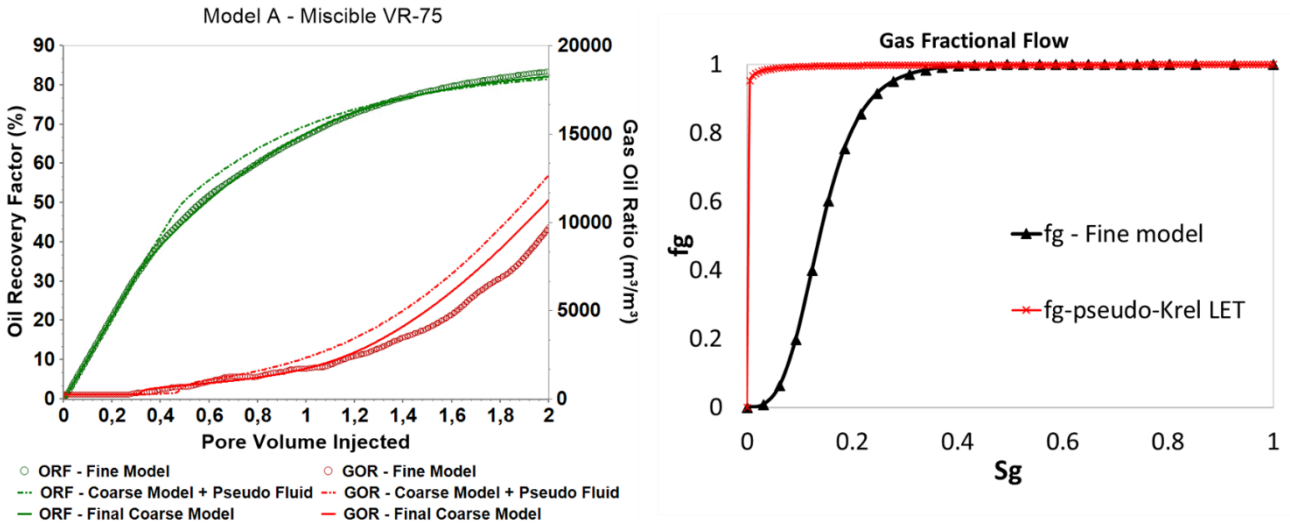

Figure 14. ***Left:*** **Oil Recovery Factor and Gas Oil Ratio for fine model, coarse model with pseudo-fluid, and final coarse model with pseudo fluid and pseudo K_r.** ***Right:*** **Fractional flow curves for original relative permeability curves and pseudo-relative**

Model B

a) Immiscible gas flooding with a viscosity ratio of 75:

As previously discussed, Model B presents a high permeability region in the top part of the reservoir. This characteristic triggers a channeling flow pattern, which is challenging to be captured by the coarse model. For this reason, the use of a structured upscaling workflow to guide the improvement of the generated coarse model is critical. As we employed for Model A applications, the first step is to verify the quality of the initial coarse-scale model compared to the reference solution. The left image in Figure 15 shows the ORF and GOR comparison between the fine model and the initial coarse model, while the right image shows the gas saturation profiles for both models. We note that the coarse model fails to represent the desired results. The curves and the gas saturation profiles are highly different, and the coarse model presents an optimistic behavior for two main reasons: poor representation of the main reservoir heterogeneities and difficulties in reproducing the small-scale unstable gas front.

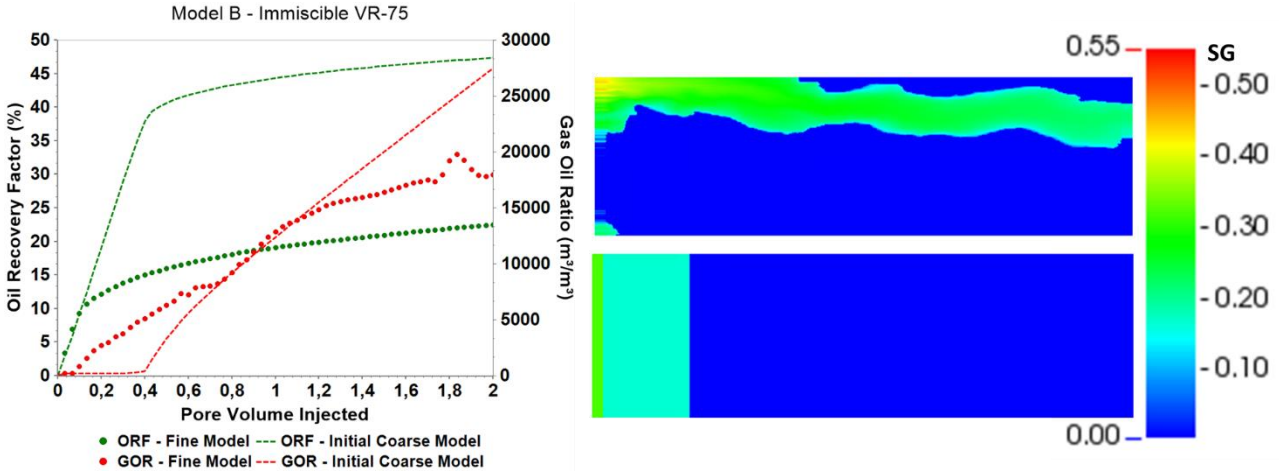

Figure 15. Left: Oil Recovery Factor and Gas Oil Ratio for fine and initial coarse models. Right: Gas Saturation profile at the same time for fine and coarse models under miscible gas flooding process.

Therefore, in order to generate an effective coarse model for this problem, additional improvements are required. We then follow the workflow to evaluate which approaches are useful for this task.

To investigate if this problem is G1 type, we conduct the stable flow analysis. For that, immiscible gas is injected with matched viscosity related to the reservoir fluid. The coarse model was numerically refined to mitigate the impacts of numerical dispersion and better isolate the heterogeneity effects on the results. Figure 16 shows the ORF and GOR results of this comparison. From this evaluation, different from what was observed on Model A, it is clear the impacts of the loss on the heterogeneity representation on coarse Model B. The coarse-scale results are highly optimistic even for stable flow without compositional effects. Thus, this upscaling problem requires G1 improvements and the DP/DP upscaling technique is indicated.

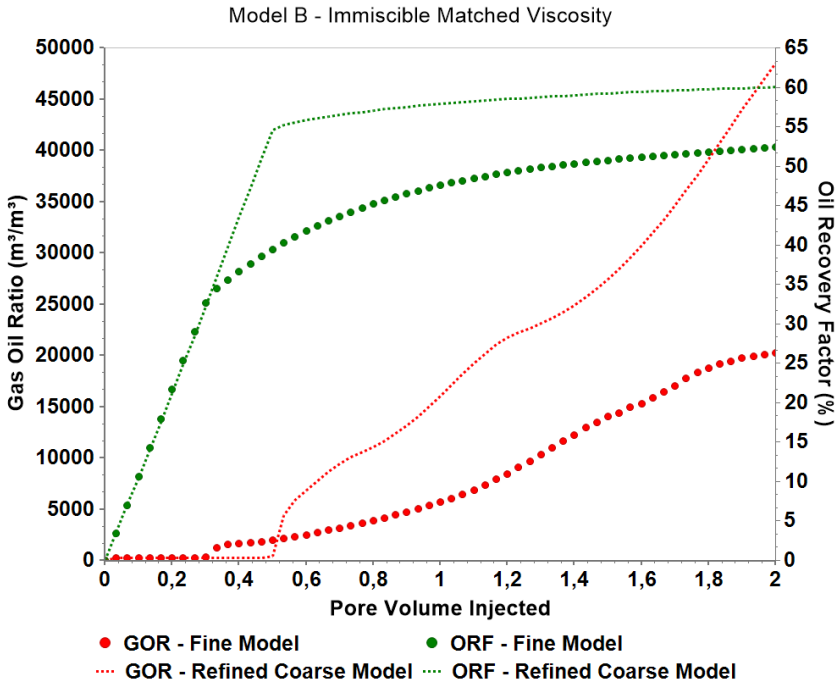

Figure 16. Oil Recovery Factor and Gas Oil Ratio for fine model and refined coarse model. Stable-flow evaluation.

According to Rios et al. (2020a), the first step of the DP/DP upscaling technique is to divide the fine-scale porous medium into two systems – primary and secondary -, and the second is to calculate the final properties for each coarse-scale grid block cell.

In the first step, classical flow and storage capacity theory is used as a global guide, based on static data of the fine-scale reference model, to select the fine cells with a higher theoretical contribution for the flow. The Lorenz coefficient is calculated for each group of fine cells that compose a coarse-scale cell. This second criterion is considered a local guide.

In the second step, the coarse-scale properties are calculated. Porosity and permeability are obtained for both primary and secondary systems. The volumetric weighted arithmetic mean is considered for porosity, while directional Cardwell-Parsons upscaling is performed for permeability.

Since the porous media is ranked and divided into two systems, flow and transport need to be modeled in a way that allows two different continua to coexist with interaction between them. To achieve this, the flow in the new upscaled model can be approximated with a DP/DP approach formulation. The dynamic of the fluid flow will have a preferential system (primary system) modeled as “fracture” and a passive system (secondary system), modeled as “matrix”. Following the procedure proposed by Rios et al. (2020a), we generate the DP/DP coarse model with a UR 32 000 for Model B. Figure 17 summarizes the final permeability upscaling and Figure 18 shows the ORF and GOR comparison between the DP/DP coarse

model and the fine-scale reference model. Again, to minimize numerical dispersion effects, the coarse model was refined in the flow direction in this comparison, so the main contribution becomes related to the heterogeneity representation. We note that the upscaled model with an improved representation of the sub-grid heterogeneities can satisfactorily represent the fine-scale responses. Hence, the G1 limitation was consistently overcome, and we can move to the next step of the global workflow upscaling shown in Figure 1.

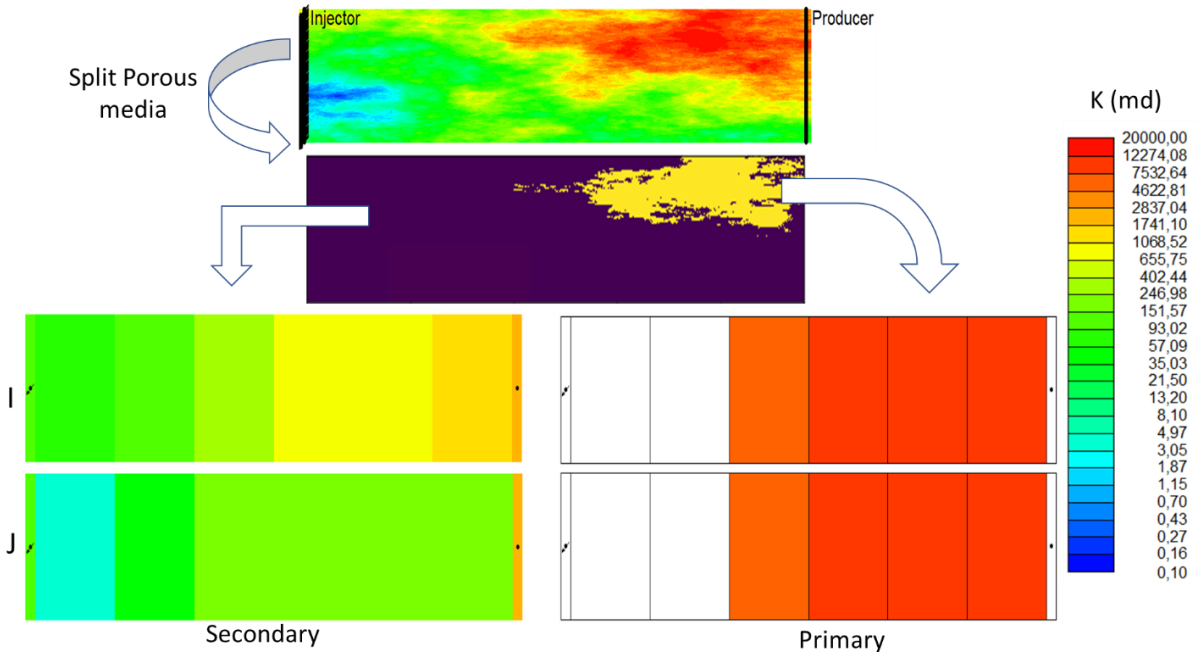

Figure 17. Summary of DP/DP upscaling for Model B. The Coarse-scale model with UR 32 000 now can represent sub-grid heterogeneities (Rios et al. 2020b).

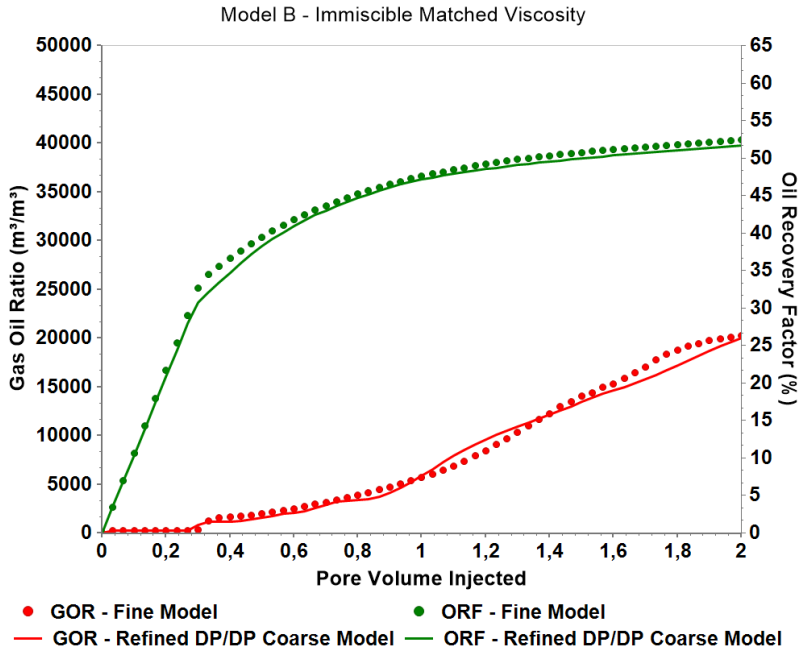

Figure 18. Oil Recovery Factor and Gas Oil Ratio for fine model and refined DP/DP coarse model. Stable-flow evaluation.

We proceed with the evaluation by simulating the DP/DP coarse model considering the actual goal of this application, which is the immiscible gas flooding with an unfavorable viscosity ratio of 75. From this point on, we do not consider the refined coarse model because the final coarse model needs to be improved considering all the effects and the coarse-scale with the desired UR 32 000.

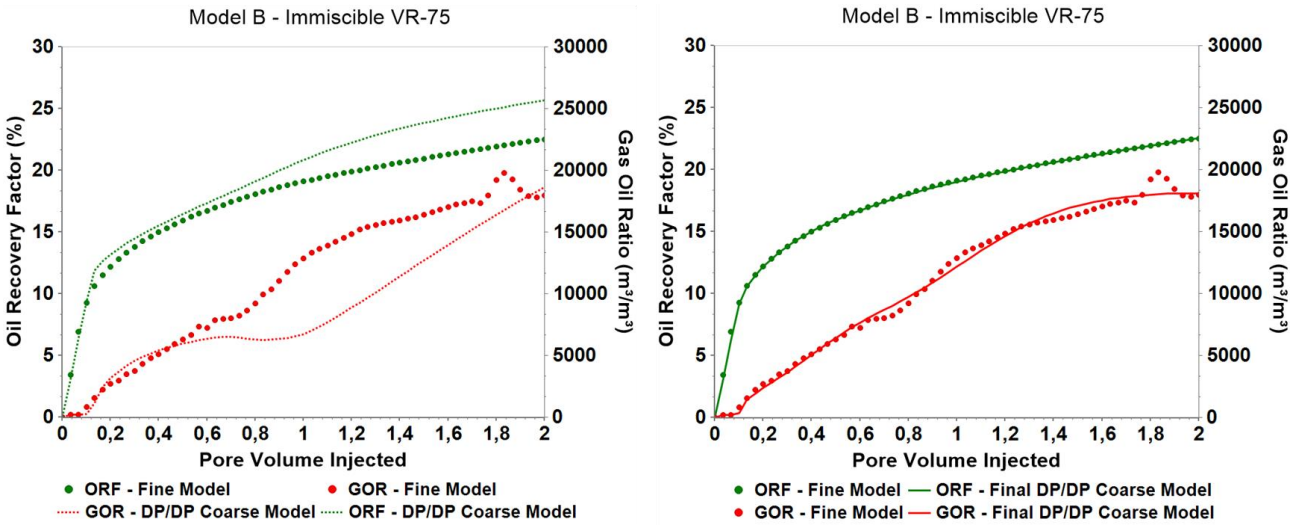

Figure 19. ***Left:*** **Oil Recovery Factor and Gas Oil Ratio for fine model and DP/DP coarse model.** ***Right:*** **Oil Recovery Factor and Gas Oil Ratio for fine model and DP/DP coarse model + Pseudo K_r**

The left graph in Figure 19 shows the performance of the DP/DP coarse model compared with the fine model. The responses are close to each other, and the improvement in the results is remarkable when we compare with the initial coarse model results shown on the left graph in Figure 15. This difference in the coarse-scale results is due to the better representation of the main reservoir heterogeneities, which, for this problem, showed to be the main limitation.

Nevertheless, we observe that the DP/DP coarse model can still be improved. Following the global upscaling workflow, we can work on G2 techniques to obtain the final improvements on the results. Since this is an immiscible gas flooding process, we can generate pseudo-relative permeability curves, as before, and achieve the final DP/DP coarse model with a new set of relative permeability curves. The only difference for this application is that, once we have a DP/DP representation, we can create pseudo-curves for primary and secondary systems separately, which gives more flexibility and representativity for this step.

The right graph in Figure 19 shows the final comparison after the generation of pseudo-relative permeability curves, whose resultant gas fractional flow curves are presented in Figure 20. We note that the final coarse model is now presenting accurate results when

compared to the fine-scale results and the global upscaling workflow provided a useful guide for selecting the appropriate techniques.

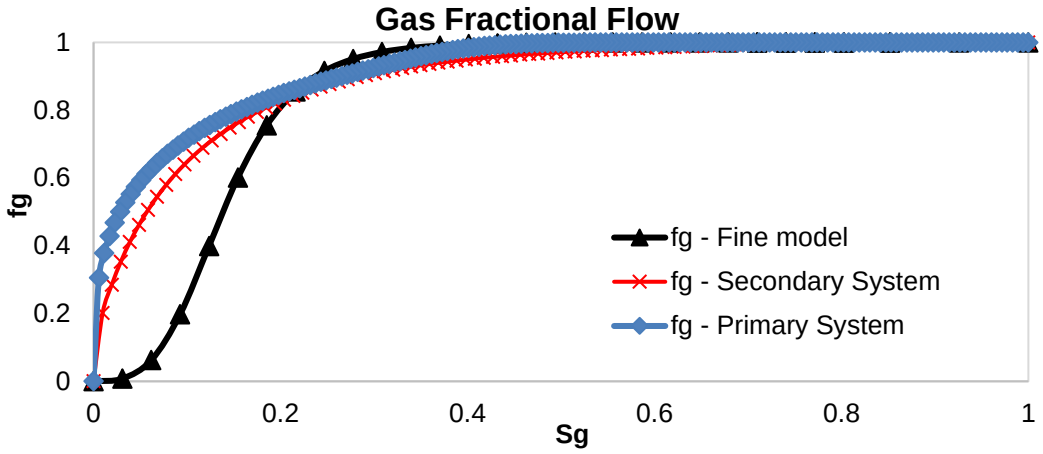

Figure 20. Fractional flow curves for original relative permeability curves and pseudo-relative permeability curves for Primary and Secondary systems on the final DP/DP coarse model.

b) Miscible gas flooding with a viscosity ratio of 23:

The challenges for this application are a combination of the previous application and the compositional effects discussed on application b) for Model A. At this point, we know that Model B requires G1 solutions, and the DP/DP coarse model obtained for the first application is also recommended for this case. Thus, we begin this evaluation by showing a comparison between the fine-scale results and two coarse models, the initial one (flow-based upscaling) and the DP/DP coarse model. The results for ORF and GOR are presented in Figure 21.

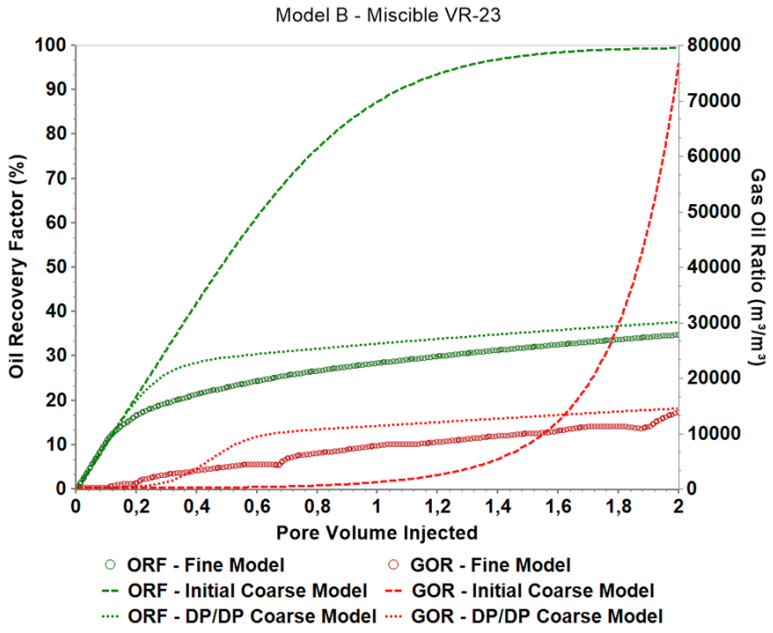

Figure 21. Oil Recovery Factor and Gas Oil Ratio for fine model, initial coarse Model and DP/DP coarse model.

The interpretation of Figure 21 provides important information about this upscaling problem. First, we observe that the initial coarse model is not useful and fails to represent the reference curves since it presents highly optimistic results. Then, it is possible to verify the importance of an improved representation of the reservoir heterogeneities, which can be demonstrated by the notable improvement in the results with the DP/DP coarse model. Nevertheless, a deviation between the results is still observed. Then, following the general upscaling procedure, we must apply G2 solutions to achieve a better coarse model.

Since it is a miscible displacement, we again consider the compositional upscaling technique proposed by Rios et al. (2019), following the same procedure already performed for application b) on Model A. After the first step, the change of the original fluid for the pseudo-fluid, the results became closer to the fine-scale solutions, as presented in Figure 22. Moreover, an accurate coarse model is obtained after the generation of pseudo-relative permeability curves (second step of Rios et al., 2019), as shown in the continuous curves of Figure 22. To accomplish this final improvement, the pseudo-curves for primary and secondary systems promote a different gas fractional flow, as highlighted in Figure 23.

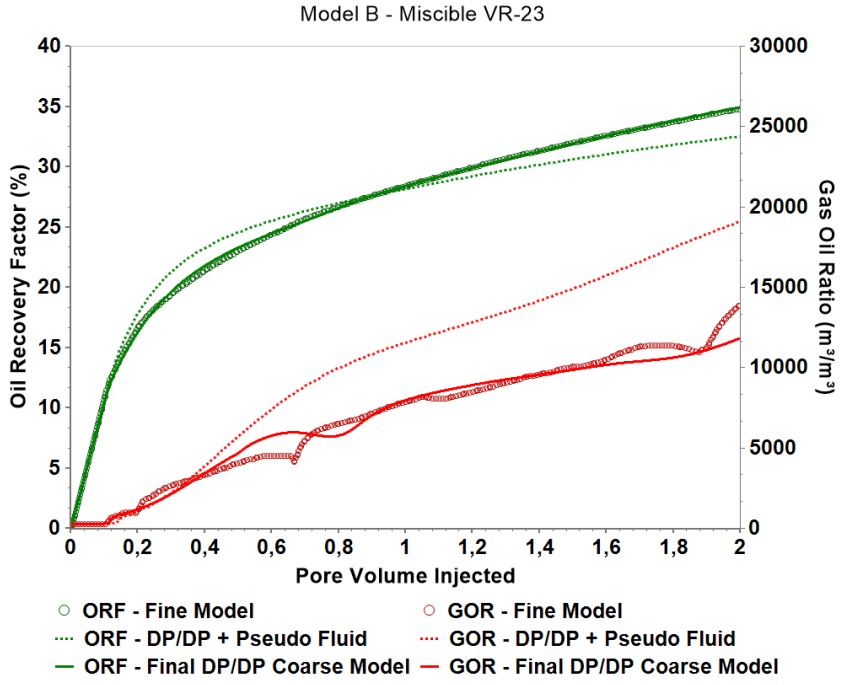

Figure 22. Oil Recovery Factor and Gas Oil Ratio for fine model, DP/DP coarse model + Pseudo Fluid and Final DP/DP coarse model (DP/DP + Pseudo Fluid + Pseudo K_r).

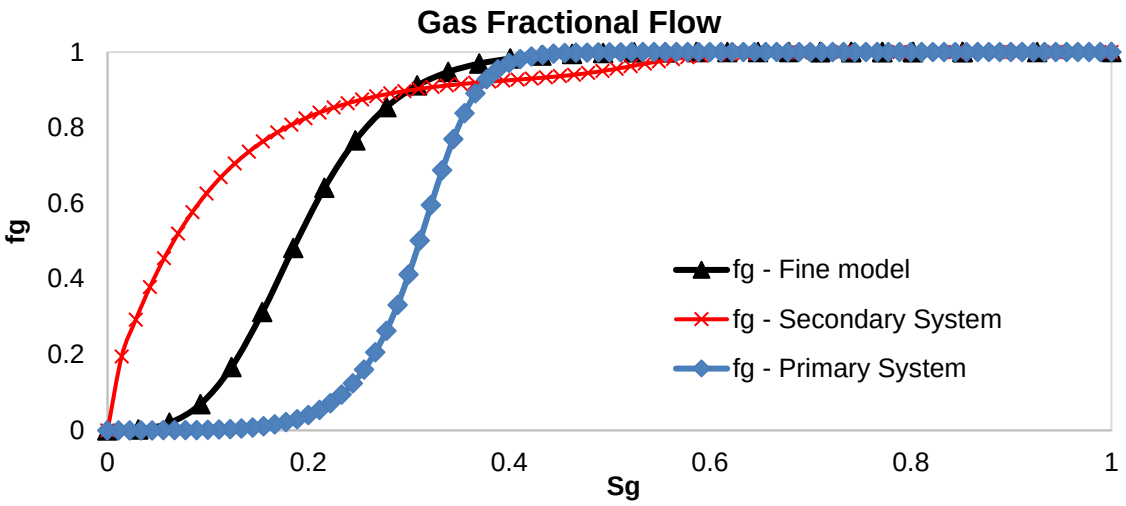

Figure 23. Fractional flow curves for original relative permeability curves and pseudo-relative permeability curves for Primary and Secondary systems on the final DP/DP coarse model.

It is worth mentioning the results and discussions presented for the above applications focused on the general upscaling workflow and on the differences between miscible and immiscible upscaling problems. Moreover, another important consideration is regarding the simulation time using coarse-scale models. When compared with the fine-scale, coarse models require only a fraction of the run-time. For all cases, the final coarse models require less than 0.005 % of the total time used for a single fine-scale simulation run. It is important to mention that no numerical optimization was performed on the models; therefore, the results are a relative comparison. Nevertheless, all models can be numerically improved, as shown by Avansi et al. (2019) and Rios et al. (2020c).

Finally, we showed in two different applications for each fine model that there are important differences in the upscaling problem when immiscible and miscible gas flooding process is considered. Additionally, the general upscaling workflow showed to be a robust procedure to guide the upscaling problem, and the approaches we suggested to overcome the limitations of each group are effective in providing useful coarse-scale models no matter the complexity level of the problem.

Final comments and conclusions

In this work, we discussed the differences in the upscaling problem when immiscible or miscible gas flooding process is considered. Additionally, we tested the general workflow, proposed by Rios et al. (2020b), to guide the upscaling procedure and enable a proper choice of the upscaling techniques to be considered in each problem. We suggested specific techniques to be considered depending on the limitations of the upscaling problem.

The main advantages of applying the workflow and the suggested upscaling techniques are: (1) the possibility to improve any coarse-scale simulation results with a consistent stepwise procedure and (2) a better understanding of the upscaling problem and the nature of the limitations to be overcome.

The specific conclusions of this work are:

- Upscaling immiscible and miscible gas injection problems is different and requires attention. Usually, due to the limited compositional effects, pseudo-relative permeability curves can play an effective role in immiscible displacements. However, for miscible conditions, a compositional upscaling approach is recommended in order to better represent small-scale inefficiencies on the coarse-scale cells.
- With the general upscaling procedure, we can verify when an especial permeability upscaling approach (DP/DP approach) is recommended and in which situations the use of pseudo-functions, such as pseudo-fluid and pseudo-relative permeability curves, are necessary.
- The upscaling problem can be divided into G1 (static modeling limitations), and G2 (flow-dynamics specifics) types and the techniques suggested for each of these scenarios were successfully tested.
- The applications we evaluated for Model A and Model B provided important discussions about the upscaling problem. While Model A was satisfactorily represented by the flow-based permeability upscaling, Model B required a more robust approach to represent the channelized flow behavior. Besides, the use of pseudo-functions was the main solution for Model A, while only a “final improvement” for Model B.
- The proposed workflow can be useful for the industry demands since it allows the reservoir simulation engineers to dedicate their effort to the most important features to improve the coarse-scale simulation results.

Acknowledgments

The authors would like to thank Petrobras (Petróleo Brasileiro S.A.), UNISIM, DE-FEM/UNICAMP, CEPETRO, ANP, and CMG for all the support for this work. Energi Simulation, Canada, is thanked for funding the chair in EOR at the University of Bergen held by prof. Arne Skauge and the chair in Integration of Reservoir Simulation and Facilities at UNICAMP, Brazil, held by prof. Denis José Schiozer.

8 CONCLUSIONS

In this research, we aimed at working on techniques and procedures to overcome key limitations of the upscaling problem in numerical reservoir simulation. We conducted studies to provide structured solutions for important gaps in the upscaling literature. The main contributions of our work were: (1) proposition of a robust upscaling technique for highly heterogeneous systems; and (2) development of an effective compositional upscaling procedure for miscible gas flooding processes. Additionally, we worked on secondary objectives that led to two additional contributions for making the upscaling process more consistent: (1) creation of a general upscaling workflow to guide the coarsening procedure according to the most important limitations of each problem; and (2) proposition of upscaling techniques suitable to be applied at an ensemble-level, not only for deterministic studies. We worked on each of the contributions mentioned above and presented six scientific articles to support the specific conclusions highlighted in the next paragraphs.

To overcome the difficulties of representing highly heterogeneous systems in a coarse-scale model, we developed a new dual porosity/dual permeability (DP/DP) upscaling procedure. With this technique, we ranked and split the porous medium into primary and secondary systems based on the fine-scale model's static properties. This step allowed an improved representation of the sub-grid heterogeneities and preferential pathways without using any simulation results of fine-scale models as inputs. Moreover, since dynamic responses from the fine-scale full-field simulation are not used, this methodology improves the coarse-scale results even when different well-strategies and flow patterns are considered.

Furthermore, our results showed that the new DP/DP coarse models are consistently less sensitive to the level of upscaling and robust to provide reliable results for different viscosity ratios. These characteristics offer more flexibility and enable a more aggressive upscaling procedure without jeopardizing the decision-making process guided by simulation results.

We also tested our DP/DP methodology at the ensemble-level, with 500 realizations. The results showed remarkable improvement in the behavior of uncertainty curves for different upscaling ratios, injected fluid and well pattern. Therefore, based on the presented results and discussions, we conclude that the new DP/DP upscaling technique is an effective and robust tool for creating coarse-scale models and can be used in deterministic and probabilistic reservoir engineering studies.

For miscible gas flooding processes, we proposed a technique with two important contributions for a robust upscaling procedure in a compositional simulation. It improved the representation of the coarse-scale gas saturation behavior with the pseudo-fluid model. Besides, it enabled the generation of pseudo-relative permeability curves to better reproduce production curves. Consequently, the final coarse models could capture the small-scale inefficiencies with the pseudo-fluid model and the production curves presented a close agreement with the reference fine-scale models after the generation of the pseudo-relative permeability curves. We also validated the results by simulating different operational conditions and drainage plans, showing the robustness and flexibility of the proposed methodology.

Following, inspired by the lack of practical probabilistic upscaling procedures in the literature, we extended the compositional upscaling technique to be applied to multiple realizations in probabilistic studies. The proposed workflow improved coarse-scale simulation results when multiple realizations were considered. The final simulation results removed the biases and maintained global fine-scale variability, essential to probabilistic studies and decision-making process. With this approach, we showed that the correlation between the Koval factor and oil recovery is a useful guide to extrapolate the pseudo-curves obtained for each selected representative model. We successfully applied the methodology to different upscaling ratios, flow conditions and recovery method, which showed its robustness in better representing coarse-scale simulation results in multiple realization scenarios. Furthermore, the proposed workflow is very cost-effective, since it only requires a few fine models to be simulated (roughly 1%) to improve the entire ensemble of coarse-scale models simulation results.

Additionally, once we developed consistent methodologies for the upscaling of highly heterogeneous reservoirs and miscible gas flooding processes, we proposed a new general workflow to guide the upscaling procedure and enable a proper choice of the upscaling techniques for each problem. The workflow is simple and, by following the steps, it is possible to better deal with the real limitations of an upscaling process. The issues were divided into G1 (static modeling limitations) and G2 (flow-dynamics specifics) types, with techniques suggested for each of these scenarios.

The proposed procedure allowed verifying when a special permeability upscaling procedure (DP/DP approach) is recommended and in which situations the use of pseudo-functions was necessary. We showed that the upscaling of immiscible and miscible gas injection problems was different and required attention. Usually, due to the limited compositional effects, pseudo-relative permeability curves could play an effective role in immiscible displacements. However, for miscible conditions, a compositional upscaling approach was recommended to

better represent small-scale inefficiencies on the coarse-scale cells. Nevertheless, the proposed workflow can be useful for the industry demands since it allows the reservoir simulation engineers to dedicate their effort to the most important features to improve the coarse-scale simulation results.

Finally, the results of the thesis, compiled in the presented scientific articles, aggregates key contributions for some important previously mentioned gaps presented in the upscaling literature. The methodologies were stress-tested with challenging case-studies and showed robustness, flexibility, and consistency in generating useful and fast coarse-scale simulation models.

8.1 RECOMMENDATIONS FOR FUTURE WORK

In this work, we presented techniques and procedures that improved the current upscaling literature. Still, some important investigations can be the focus of future research studies:

- The use of pseudo-relative permeability curves is an important ally to improve the dynamic results of coarse-scale models. Classically, the relative permeability is a function of the fluid phases' saturations and this condition can fairly represent immiscible displacements. However, this approach is highly limited for near-miscible and miscible conditions. The main reasons for this limitation are the compositional effects and mass exchange between the reservoir fluid and the injected gas. In such conditions, at some point, the fluid in a grid block can be considered either gas or oil; however, its composition varies in a much more intense way, which is not captured by the relative permeability curves. Therefore, the development of a procedure to determine the relative permeability curves as a function of compositions, rather than saturations only, is a remarkable improvement for better modeling the fluid flow in porous media. Additionally, it makes the upscaling problem more straightforward since the use of pseudo-functions, if necessary, will not be limited to the phases' saturations.
- The use of submodels to improve full-field coarse-scale models can be an effective strategy; however, the selection of a proper representative submodel can rely on the user's experience. Depending on the reservoir heterogeneity and facies distribution, more than one submodel can be required and a manual selection becomes less effective. In that sense, the development of an automated manner to perform this task can be helpful.

- The proposed DP/DP upscaling technique is currently prepared to deal with uniform upscaling. However, a non-uniform coarsening can provide interesting results, especially considering a more aggressive upscaling on the secondary system.
- For naturally fractured and heterogeneous reservoirs, the DP/DP upscaling technique can be applied in combination with the EDFM (de Sousa Junior et al, 2016) method. The first focusing on better representing the sub-grid heterogeneities, and the second improving the representation of the fractures. Although the DP/DP technique could capture the overall heterogeneities, this combined approach tends to result in lower computational cost and provide a better description of the fractures.
- The near-well upscaling procedure for 3D problems with the DP/DP technique can be improved to better represent the alternation of water and gas in the same injector well. Also, it can be evaluated, for fractured systems, the possibility of not considering all the well blocks as the secondary system only.
- In the probabilistic workflow presented in Article 3, instead of considering only oil recovery factor, the use of multiple dynamic functions and the identification of their correlation with static functions (such as Koval) could be achieved in a more automated manner, using machine learning and clustering techniques.

REFERENCES

- Araktingi, U. G., & Orr Jr, F. M., 1993. Viscous Fingering in Heterogeneous Porous Media. *Society of Petroleum Engineers*. https://doi:10.2118/18095-PA.
- Avansi, G., Rios, V., & Schiozer, D. 2019. Numerical tuning in reservoir simulation: it is worth the effort in practical petroleum applications. *Journal of the Brazilian Society of Mechanical Sciences and Engineering*, 41(1), 59.
- Barker, J.W. & Fayers, F. J. 1994. Transport Coefficients for Compositional Simulation with Coarse Grids in Heterogeneous Media. *SPE Journal*, *2*(2), 103–112. https://doi.org/10.2118/22591-PA.
- Barker, J. W. & Thibeau, S. 1997. A critical review of the use of pseudorelative permeabilities for upscaling. SPE Reservoir Engineering, 12(02):138–143.
- Cardwell, W. T. Jr., & Parsons, R. L. 1945. Average Permeabilities of Heterogeneous Oil Sands. Transactions of the AIME, 160(01), 34-42.
- Chaves, J. M. P., 2018. Multiscale Approach to Construct a Carbonate Reservoir Model with Karstic Features and Brazilian Pre-Salt Trends UsingNumerical Simulation. *Master's thesis, University of Campinas, Campinas, Brazil* (November 2018).
- Chen, Y., Durlofsky, L. J., Gerritsen, M., & Wen, X. H. 2003. A coupled local–global upscaling approach for simulating flow in highly heterogeneous formations. *Advances in Water Resources*, 26(10), 1041-1060.
- Chen, Y., & Durlofsky, L. J. 2006. Adaptive local–global upscaling for general flow scenarios in heterogeneous formations. *Transport in porous Media*, 62(2), 157-185.
- Chen, Y., & Durlofsky, L. J. 2008. Ensemble-level upscaling for efficient estimation of fine-scale production statistics. *SPE Journal*, 13(04), 400-411.
- Christie, M. A. 1996. Upscaling for reservoir simulation. Journal of Petroleum Technology, 48(11), 1-004.
- Christie, M. A., and Blunt, M. J. 2001. Tenth SPE Comparative Solution Project: A Comparison of Upscaling Techniques. SPE-66599-MS, *SPE Reservoir Evaluation & Engineering*, 4(04):308–317, August 2001.
- Christie, M. A., Clifford, P. J., & Exploration, B. P. 1998. Fast Procedure for Upscaling Compositional Simulation, (February), 8–11. http://doi.org/10.2118/50992-PA.

- Coats, K. H., Thomas, L.K. and Pierson. R. G. 2004.Simulation of Miscible Flow Including Bypassed Oil and Dispersion Control. In SPE-90898-MS, *Annual Technical Conference and Exhibition. Society of Petroleum Engineers*.
- Completamos dez anos de produção no pré-sal. **Petrobras Blog Fatos e Dados**, 2018. Available in: https://petrobras.com.br/fatos-e-dados/completamos-dez-anos-de-producao-no-pre-sal.htm. Access in: 01 Dez. 2020.
- Computer Modelling Group Ltd., 2018. CMOST User Guide. Computer Assisted History Matching, Optimization and Uncertainty Assessment Tool.
- Correia, M. G., von Hohendorff Filho, J. C., & Schiozer, D. J., 2019. Multiscale Integration for Karst-Reservoir Flow-Simulation Models. *SPE Reservoir Evaluation & Engineering*. doi:10.2118/195545-PA.
- de Sousa Junior, Luis Carlos, et al., 2016. Methodology for geomechanically controlled transmissibility through active natural fractures in reservoir simulation. *Journal of Petroleum Science and Engineering*, 147: 7-14
- Ding, Y., 1995. Scaling-up in the vicinity of wells in heterogeneous field. In *SPE Reservoir Simulation Symposium*. Society of Petroleum Engineers.
- Doorwar, S., & Mohanty, K. K., 2015. Fingering Function for Unstable Immiscible Flows. *Society of Petroleum Engineers*. https://doi:10.2118/173290-MS.
- Durlofsky, L. J. 2003. Upscaling of geocellular models for reservoir flow simulation: a review of recent progress. *In 7th International Forum on Reservoir Simulation Bühl/Baden-Baden*, Germany (pp. 23-27). Citeseer
- Dykstra, H., & Parsons, R. L., 1950. The prediction of oil recovery by water flood. *Secondary recovery of oil in the United States*, 2, 160-174.
- Evazi, M., & Jessen, K. 2014. Dual-porosity Coarse-scale Modeling and Simulation of Highly Heterogeneous Geomodels. *Transport in porous media,* 105(1), 211-233.
- Farmer, C. L. 2002. Upscaling: a review. *International journal for numerical methods in fluids*, 40(1-2), 63-78.
- Fayazi, A., Bagherzadeh, H., & Shahrabadi, A. 2016. Estimation of pseudo relative permeability curves for a heterogeneous reservoir with a new automatic history matching algorithm. *Journal of Petroleum Science and Engineering, 140, 154-163*.
- Fernandes, B. R. B., Marcondes, F., & Sepehrnoori, K. 2013. Investigation of Several Interpolation Functions for Unstructured Meshes in Conjunction with Compositional Reservoir Simulation. *Numerical Heat Transfer, Part A: Applications*, 64(12), 974-993.

- Fernandes, B. R. B., Gonçalves, A. D. R., Filho, E. P. D., da Costa Menezes Lima, I., Marcondes, F., & Sepehrnoori, K. 2015. A 3D Total Variation Diminishing Scheme for Compositional Reservoir Simulation Using the Element-based Finite-volume Method. *Numerical Heat Transfer, Part A: Applications*,67(8), 839-856.
- Gilman, J. R., & Kazemi, H. 1983. Improvements in simulation of naturally fractured reservoirs. *Society of petroleum engineers Journal*, 23(04), 695-707.
- Haajizadeh, M., Fayers, F. J., & Cockin, A. P., 2000. Effects of Phase Behavior, Dispersion and Gridding on Sweep Patterns for Nearly Miscible Gas Displacement. *In SPE Annual Technical Conference and Exhibition. Society of Petroleum Engineers*. SPE-62995-MS.
- Hiraiwa, T., & Suzuki, K. (2007). New Method of Incorporating Immobile and Non-vaporizing Residual Oil Saturation Into Compositional Reservoir Simulation of Gasflooding. *SPE Reservoir Evaluation & Engineering*, *10*(01), 60-65.
- Iranshahr, A., Chen, Y., & Voskov, D. V. 2014. A Coarse-scale Compositional Model. *Computational Geosciences*, 18(5), 797–815.
- Jensen, J., Lake, L. W., Corbett, P. W., & Goggin, D. 2000. *Statistics for petroleum engineers and geoscientists* (Vol. 2). Gulf Professional Publishing.
- Jessen, K., & Evazi Yadecuri, M. 2013. Simulation of waterflooding with coarse-scale dual-porosity representation of highly heterogeneous reservoirs. *In SPE Western Regional & AAPG Pacific Section Meeting 2013 Joint Technical Conference*. Society of Petroleum Engineers.
- Koval, E.J. 1963, A method for predicting the performance of unstable miscible displacements in heterogeneous media, SPE Journal 3 (2): 145-154.
- Kumar, A., Farmer, C. L., Jerauld, G. R., & Li, D. 1997. Efficient upscaling from cores to simulation models. In SPE Annual Technical Conference and Exhibition. Society of Petroleum Engineers. https://doi.org/10.2118/38744-MS. January.
- Lake, L. W., & Jensen, J. L. 1989. A review of heterogeneity measures used in reservoir characterization.
- Lake, L. W. 1989. *Enhanced oil recovery*, Prentice Hall.
- Lomeland, F., Ebeltoft, E., & Thomas, W. H. (2005, August). A New Versatile Relative Permeability Correlation. *In International Symposium of the Society of Core Analysts*, Toronto, Canada (Vol. 112).

- Lorenz, M. O. 1905. Methods of measuring the concentration of wealth. *Publications of the American statistical association*, 9(70), 209-219.
- Li, H. Compositional Upscaling for Individual Models and Ensembles of Realizations. PhD thesis, Stanford University, 2014.
- Li, H., Durlofsky, L.J, 2016. Ensemble level upscaling for compositional flow simulation. Computational Geosciences, 20 (3), pp. 525-540.
- Li, L. and Lee, S. H. 2008. Efficient Field-Scale Simulation of Black Oil in Naturally Fractured Reservoir Through Discrete Fracture Networks and Homogenized Media.*SPE Res Eval & Eng* 11(4): 750–758. SPE-103901-PA. https://doi.org/10.2118/103901-PA.
- Luo, H., Mohanty, K. K., Delshad, M., & Pope, G. A., 2016. Modeling and Upscaling Unstable Water and Polymer Floods: Dynamic Characterization of the Effective Finger Zone. *Society of Petroleum Engineers*. https://doi:10.2118/179648-MS.
- Maschio, C., & Schiozer, D. J. 2003. A new upscaling technique based on Dykstra–Parsons coefficient: evaluation with streamline reservoir simulation. *Journal of Petroleum Science and Engineering*, 40(1-2), 27-36.
- Moczydlower, B., Figueiredo Junior, F. P., & Pizarro, J. O. S. A., 2019. Libra Extended Well Test-An Innovative Approach to De-Risk a Complex Field Development. In *Offshore Technology Conference*. Offshore Technology Conference.
- Moinfar, A., Varavei, A., Sepehrnoori, K. et al. 2014. Development of an Efficient Embedded Discrete Fracture Model for 3D Compositional Reservoir Simulation in Fractured Reservoirs.*SPE J.*19(2): 289–303. SPE-154246-PA. https://doi.org/10.2118/154246-PA.
- Pizarro, J. O. D. S., Poli, R. E. B., Rosa, M. B., Silva, V. C. D., Branco, C. C. M., Cunha, B. M., ... & Pinto, A. C., 2017. Optimizing Production of Santos Basin Pre-Salt Fields through Sound Reservoir Management Practices. In *OTC Brasil*. Offshore Technology Conference.
- Renard, P., & De Marsily, G. 1997. Calculating equivalent permeability: a review. *Advances in water resources*, 20(5-6), 253-278.
- Renard, P., Le Loc'h, G., et al. 2000. A fast algorithm for the estimation of the equivalent hydraulic conductivity of heterogeneous media. *Water Resources Research* 36 (12), 3567– 3580.

- Rios, V.S.; Santos, L.O.S. & Espósito, R.O., 2016. Methodology to Incorporate the Miscibility on the Adjust of the Equations of State. *Rio Oil & Gas Expo and Conference 2016*. IBP2213_16.
- Rios, V. S., Santos, L. O.S., Quadros, F. B., Lykawka, R., & Schiozer, D. J. 2017. Methodology to Improve Miscible Gas Injection Forecast Based on a Field Scale Simulation Model. In *OTC Brazil*. Offshore Technology Conference.
- Rios, V. S., Santos, L. O. S., Quadros, F. B., & Schiozer, D. J. 2019. New upscaling technique for compositional reservoir simulations of miscible gas injection. *Journal of Petroleum Science and Engineering*, 175, 389-406.
- Rios, V. S., Santos, L. O., Schiozer, D. J., 2020a. Upscaling Technique for Highly Heterogeneous Reservoirs Based on Flow and Storage Capacity and the Lorenz Coefficient. *SPE Journal, 25(4).*
- Rios, V. S.; Skauge, A., Sorbie, K. S., Wang, G., Santos, L. O., Schiozer, D. J., 2020b. A General Upscaling Workflow Applied to Highly Detailed Heterogeneous Reservoirs Under Near-Miscible WAG flood. *To be submitted*.
- Rios, V. S., Avansi, G. D., & Schiozer, D. J., 2020c. Practical workflow to improve numerical performance in time-consuming reservoir simulation models using submodels and shorter period of time. *Journal of Petroleum Science and Engineering, 195*, 107547.
- Rios, V. S., Santos, L. O., Schiozer, D. J., Skauge, A., 2021. Improving Coarse-Scale Simulation Models with a Dual-Porosity Dual-Permeability Upscaling Technique and a Near-Well Approach. *Journal of Petroleum Science and Engineering*, 198, 108-132.
- Sajjadi, M., & Azaiez, J., 2012. Thermo-Viscous Fingering in Heterogeneous Media. *Society of Petroleum Engineers*. https://doi:10.2118/157722-MS.
- Salehi, A., 2016. Upscaling of Compositional Flow Simulation Based on a Non-equilibrium Formulation. PhD Thesis. Stanford University.
- Salehi, A., Voskov, D.V., Tchelepi, H.A., 2013. Thermodynamically consistent transport coefficients for upscaling of compositional processes. In: Society of Petroleum Engineers - SPE Reservoir Simulation Symposium 2013 1. pp. 1–16.
- Wang, G., Pickup, G. E., Sorbie, K. S., & Mackay, E. J., 2019a. Analysis of compositional effects on global flow regimes in CO_2 near-miscible displacements in heterogeneous systems. Transport in Porous Media, 129(3), 743-759.

- Wang, G., Pickup, G., Sorbie, K., Mackay, E., & Skauge, A., 2019b. Analysis of Near-Miscible CO_2-WAG Displacements: The Distinction between Compositional and Interfacial Tension Effects. In SPE Reservoir Simulation Conference. Society of Petroleum Engineers.
- Wang, G., Pickup, G., Sorbie, K., Mackay, E., & Skauge, A., 2020a. Numerical study of CO_2 injection and the role of viscous crossflow in near-miscible CO_2-WAG. Journal of Natural Gas Science and Engineering, 74, 103112.
- Wang, G., Pickup, G. E., Sorbie, K. S., & Mackay, E. J., 2020b. Detailed assessment of compositional and interfacial tension effects on the fluid behavior during immiscible and near-miscible CO_2 continuous and WAG displacements. Transport in Porous Media, 131(3), 805-830.
- Wen, X. H., & Gómez-Hernández, J. J., 1996. Upscaling hydraulic conductivities in heterogeneous media: An overview. *Journal of Hydrology*, 183(1-2), ix-xxxii.
- Zhang, B., & Okuno, R., 2015. Modeling of capacitance flow behavior in EOS compositional simulation. *Journal of Petroleum Science and Engineering*, *131*, 96-113.

APPENDIX A – Complementary Article #1 (Article 7)

METHODOLOGY TO IMPROVE MISCIBLE GAS INJECTION FORECAST BASED ON A FIELD SCALE SIMULATION MODEL

V.S. Rios, L.O.S Santos, F.B. Quadros, R. Lykawka, D.J. Schiozer

Presented at the Offshore Technology Conference Brasil held in Rio de Janeiro, Brazil, 24–26 October 2017

Abstract

The use of coarse scales in reservoir simulation is necessary to reduce computational time; however it can degenerate results due to loss of resolution of the small-scale phenomena, especially in oil fields in which a miscible gas is injected in an enhanced oil recovery method. Errors of the upscaling process are usually mitigated with the use of pseudo relative permeability curves. In cases of miscible gas injection, these techniques cannot be used directly, since there is no saturation variation. Therefore, the proposed methodology is based on employing a fluid model with a minimum miscibility pressure (MMP) above experimental values in order to ensure an immiscible displacement. This solution does not violate the phase behavior and ensures formation of two hydrocarbon phases in the reservoir. Therefore, the gas relative permeability plays a role in the simulation results and can be used to better fit the refined model production curves. In this study, problems that occur when upscaling is applied in various levels of refinement, from fine-scale grid (necessary to preserve geological characteristics) to simulation grid (necessary to preserve flow characteristics) in large fields with miscible gas injection were investigated. As expected, (1) simulations in coarser scales were not able to represent small-scale phenomena and (2) an increased numerical dispersion effect was observed and evaluated with higher order numerical schemes. An alternative solution to better reproduce small-scale production curves using a coarser scale model and a modified fluid model is proposed.

Introduction

Miscible gas injection is an effective enhanced oil recovery method and has gained special attention recently, especially after the Pre-Salt's oil fields discoveries. This method can improve oil production due to the formation of a miscible front, but field scale representation is challenging since several small-scale phenomena are smoothed in simulation grid.

In this context, the highlight is the formation of an unstable front, known as viscous fingers, and the channeling effect, which happens due to permeability contrasts in heterogeneous environments. Several authors have studied the mechanisms and solutions for the representation of these phenomena.

Wagoner et al. (1991) evaluated, for different degrees of heterogeneity measured by the Dykstra-Parson index, whether a given flow condition would be dominated by viscous fingers, dispersion, or channeling. Araktingi & Orr (1993) studied the dominance conditions between viscous fingers and channeling, in addition, these authors proposed an index of heterogeneity capable of evaluating the dominant process.

Haajizadeh et al. (2000) showed that an optimal configuration for grid block size of simulation model which allows to partially cancel errors associated to the loss of smaller scale heterogeneities can exist. The authors also emphasize that the simulations in coarse meshes present a large numerical dispersion, which softens the forward front, masking the viscous fingers. On the other hand, refining the grid without refining the geological discretization potentiates the grid orientation effects.

Many authors studied problems related to grid discretization in cases of unstable flow. Sajjadi & Azaiez (2006) evaluated the unstable flow in thermal processes in which the miscible front propagates faster than the thermal front due to the formation of viscous fingers. Doorwar and Mohanty (2015) proposed a methodology for grouping the fingers observed in small scale in a single finger that would represent the total set and thus would correct the final recovery estimates. Lou et al. (2016) studied the representation of viscous fingers in cases of water injection in viscous oil. In this work the authors proposed a correlation to estimate parameters to be incorporated in the simulation with the objective of better represent the recovery obtained for different speeds of exploitation.

Methodology and Results

In the management of an oil field, it is common to create a refined model in order to properly represent the main reservoir heterogeneities. However, to evaluate the dynamic behavior, it is usual to perform upscaling for a geocellular model with a reduced number of cells, thus enabling the reservoir flow simulation in a time compatible with the needs of the industry. In order to evaluate the effect of this upscaling in the simulation flow, a refined model was initially constructed with cells of 5 x 5 m² and average thickness of approximately 0.5 m. The first upscaling was performed only vertically, resulting in average thicknesses of approximately 1.7 m and preserving the remaining dimensions in 5 x 5 m². Further transfers were then made to grids with 10 x 10 m², 50 x 50 m² and 100 x 100 m² cells, maintaining the mean vertical thickness of 1.7 m. In this work, the horizontal influence of the upscale performed was evaluated. It was considered a single layer representative of a stratigraphic subzone with different levels of refinement, forming a 2D evaluation. Figure 1 shows the permeability maps for the four different levels of refinement used.

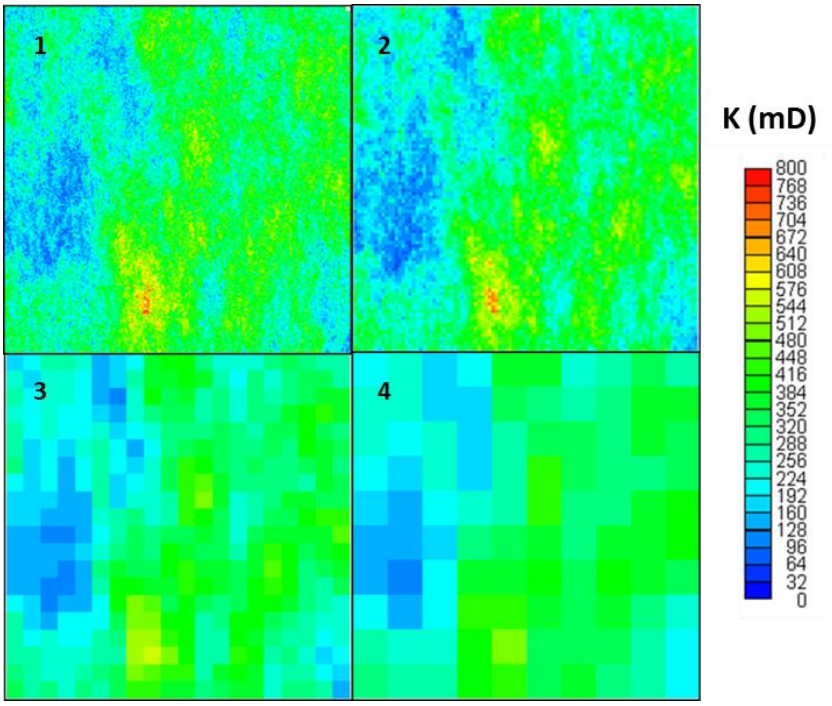

Figure 1. Absolute permeability map with emphasis on the different scales of the reservoir model and associated loss of heterogeneity. In the figure, we have: 1) 5 x 5 m², 2) 10 x 10 m², 3) 50 x 50 m² and 4) 100 x 100 m²

The main objective of the present study is to evaluate the impacts of upscaling from geological to simulation scale on miscible injection problems. For this purpose, a seven-pseudo-component fluid model was used. Table 1 highlights the parameters used on the Peng-Robinson (PR) equation of state (EoS), while Table 2 shows the binary interaction coefficients.

Table 1. Parameters of the equation of state for a miscible fit - Peng-Robinson

	P_c(MPa)	T_c(K)	□	MW	Vshift
PC1	7.38	304.2	0.23	44.0	-0.0718
PC2	4.59	190.2	0.01	16.1	0.0468
PC3	3.42	369.0	0.20	36.8	0.0282
PC4	2.40	614.9	0.51	168.2	0.0075
PC5	1.82	778.5	0.72	241.1	-0.0053
PC6	1.09	796.7	1.18	363.5	0.1956
PC7	0.71	1078.1	1.33	785.3	0.1741

Table 2. Binary interaction coefficients for a miscible fit

PC1	0						
PC2	0.15	0					
PC3	0.16	0.03	0				
PC4	0.15	0.07	0	0			
PC5	0.13	0.09	0	0	0		
PC6	0.09	0.12	0	0	0	0	
PC7	0.02	0.16	0	0	0	0	0

Upscale effects in the dynamic results

First, the quality of the models with different levels of refinement was evaluated by simulation of conventional recovery methods, e.g., depletion and water injection. Figures 2 shows that the dynamic answer for the depletion, with a production period followed by a static period, is the same in all cases, which indicates the equivalence among the geological models, despite de different refinements. The same behavior is observed considering water injection, Figure 3. These analyses indicate a good agreement between the thin model (5 x 5 m^2 mesh) and the coarser model (100 x 100 m^2 mesh).

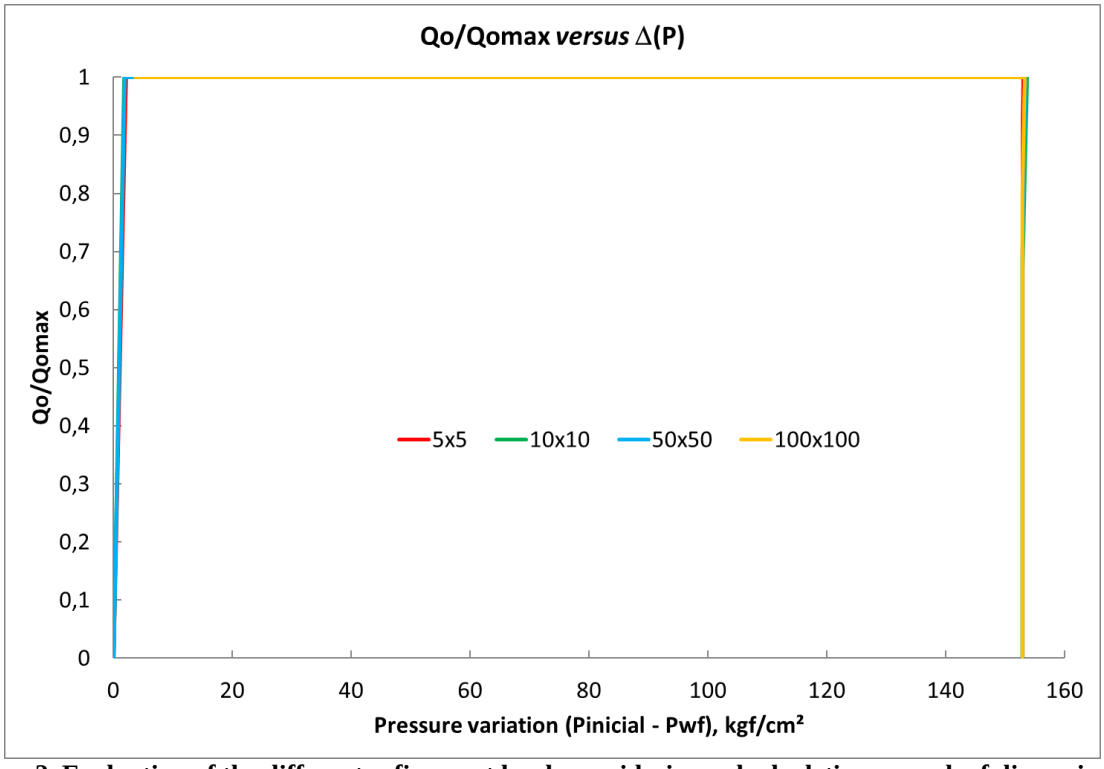

Figure 2. Evaluation of the different refinement levels considering only depletion - graph of dimensionless flow rate versus pressure variation (in kgf / cm^2) during process.

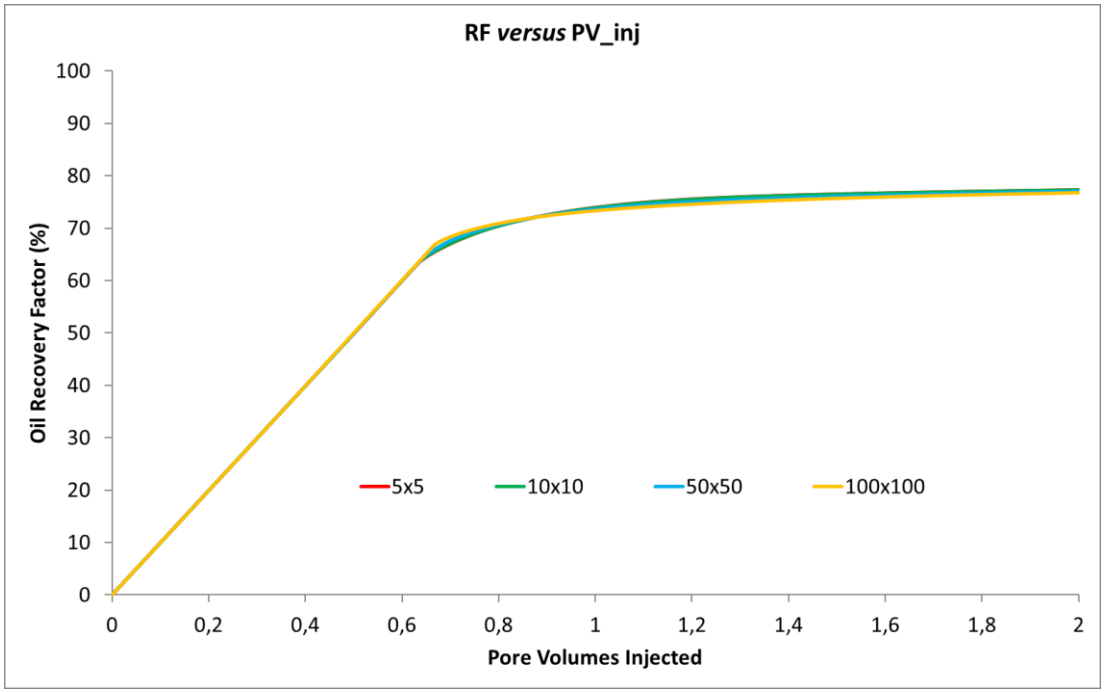

Figure 3. Recovery factor versus injected pore volumes for the case of water injection.

The second step was to evaluate the injection of CO_2-rich gas. Figure 4 shows the four simulated cases of miscible gas injection for the different levels of refinement. It is observed that there is great difference in the results; furthermore, the coarser meshes tend to overestimate the final recovery (more optimistic results). Figure 5 shows saturation maps for the four simulated cases. This figure indicates viscous finger effect acting strongly on the miscible injection.

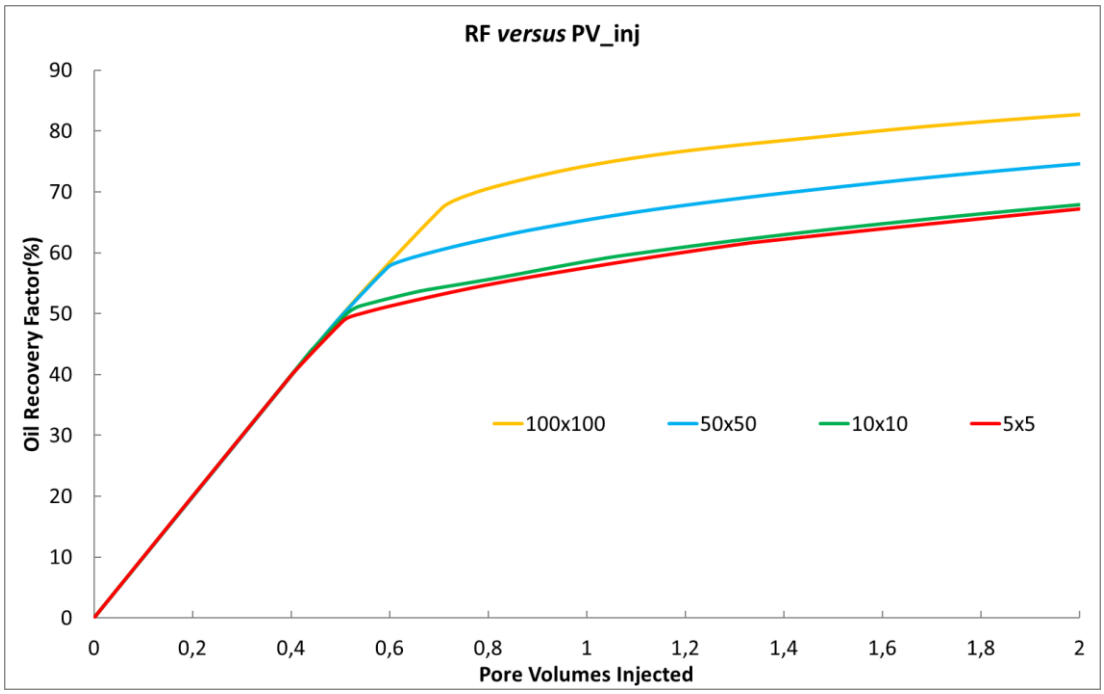

Figure 4. Recovery factor versus pore volumes injected for the case of CO_2-rich gas injection

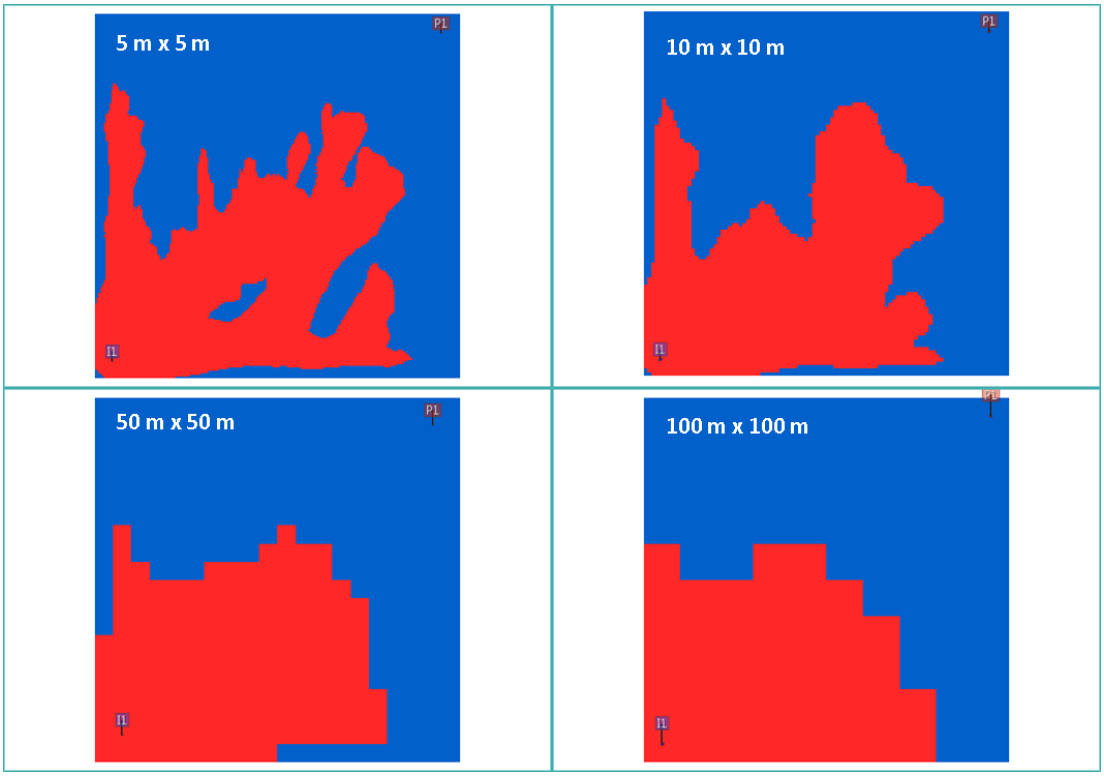

Figure 5. Behavior of the miscible gas front in different levels of refinement, at the same simulation time

In order to evaluate the grid orientation effects and to minimize numerical dispersion, additional analyses were performed in the most refined case (5 x 5 m²). This model was also simulated using 9-point scheme and TVD. These solutions were used together and separately and compared with the conventional solution (5-point and *upwind*).

Figure 6 shows the behavior of the refined case recovery factor in four configurations: conventional solution, 9-point, TVD and the last two combined. To illustrate the difference among the analyzed cases in relation to the front of miscible gas, Figures 7 and 8 show, for two distinct instants, the behavior of the gas front for each of the solutions investigated for the most refined case. Figure 7 represents an initial injection moment, while Figure 8 highlights the time of gas breakthrough in the most premature case.

The analysis of Figures 6 to 8 indicates some important aspects of the investigated model. Firstly, it is observed that there is a considerable variation in the behavior of the recovery factor as a function of the solution used, in addition, it is noticed that the characteristic of the gas miscible front is quite different in each solution.

By analyzing the TVD solution, which reduces the truncation error and decreases numerical dispersion, it can be seen from Figures 7 and 8 that there is a greater emphasis on viscous fingers. On the other hand, the problem of grid orientation becomes even more intense, which justifies the recovery factor slightly higher than that observed in the conventional solution. These results suggest that, while reducing the undesirable effects of numerical

dispersion, simulations using high order methods in problems with unstable fronts do not necessarily result in more reliable results. Fernandes et al. (2013) and Fernandes et al. (2015) compared different interpolation functions for TVD in unstructured grids and identified that the results in terms of grid orientation effect vary.

The 9-point solution, in turn, shows a noticeable reduction of the grid orientation effect, which is easily verified with Figures 7 and 8. This reduction leads to smaller recovery factors, as it drives the injected gas more directly to the producing well.

Finally, the combination of the two solutions incorporates the aforementioned effects. The result of this is a miscible gas front with lower numerical dispersion, better defined fingers, and lower mesh orientation effect. Factors that lead to a lower recovery factor compared to the other configurations.

It is worth noting that the above observations are consistent with those reported in the literature. The grid orientation effect tends to be important in cases where there are predominant viscous fingers, not channeling due to heterogeneity. In the analyzed cases, there was a great reduction of the grid orientation effect with the 9-point solution and, in addition, a better definition of the fingers with the application of TVD. These factors are in agreement with what is observed in the literature and complement each other in the analysis.

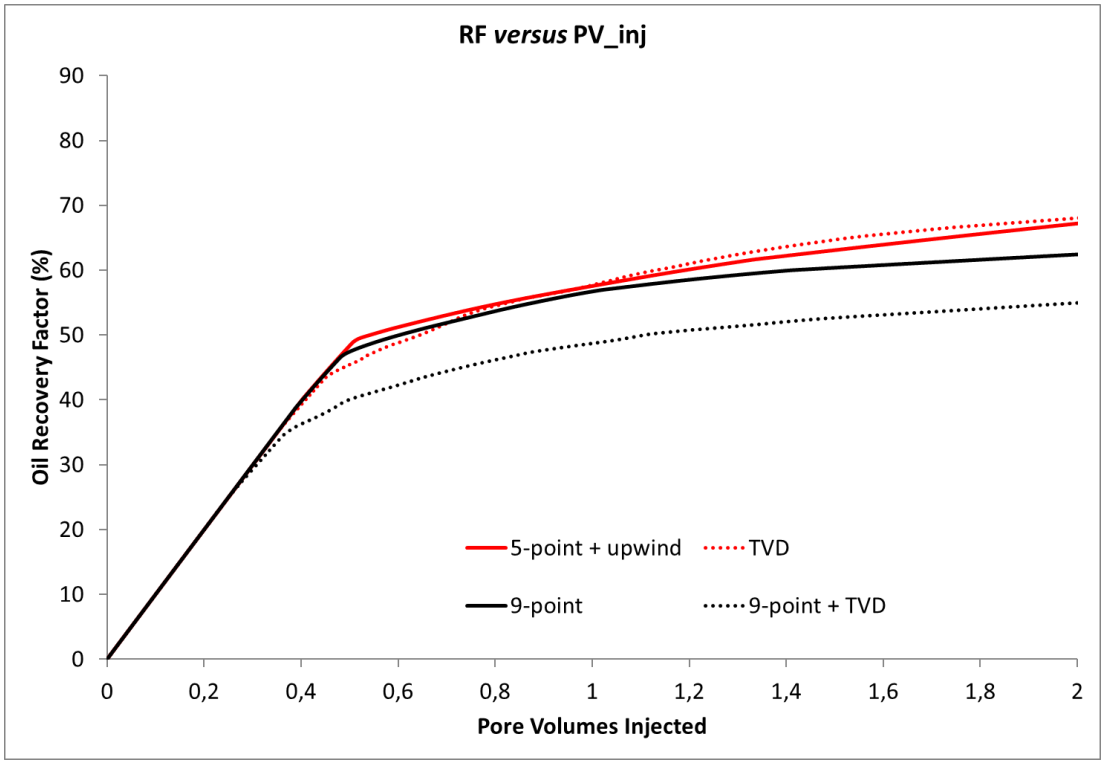

Figure 6. Recovery factor versus pore volumes injected for the most refined case (5 x 5 m²). Continuous curve, conventional case (upwind + 5-point). Dotted red curve, TVD. Continuous black curve, 9 points. Dotted black curve, 9 points + TVD

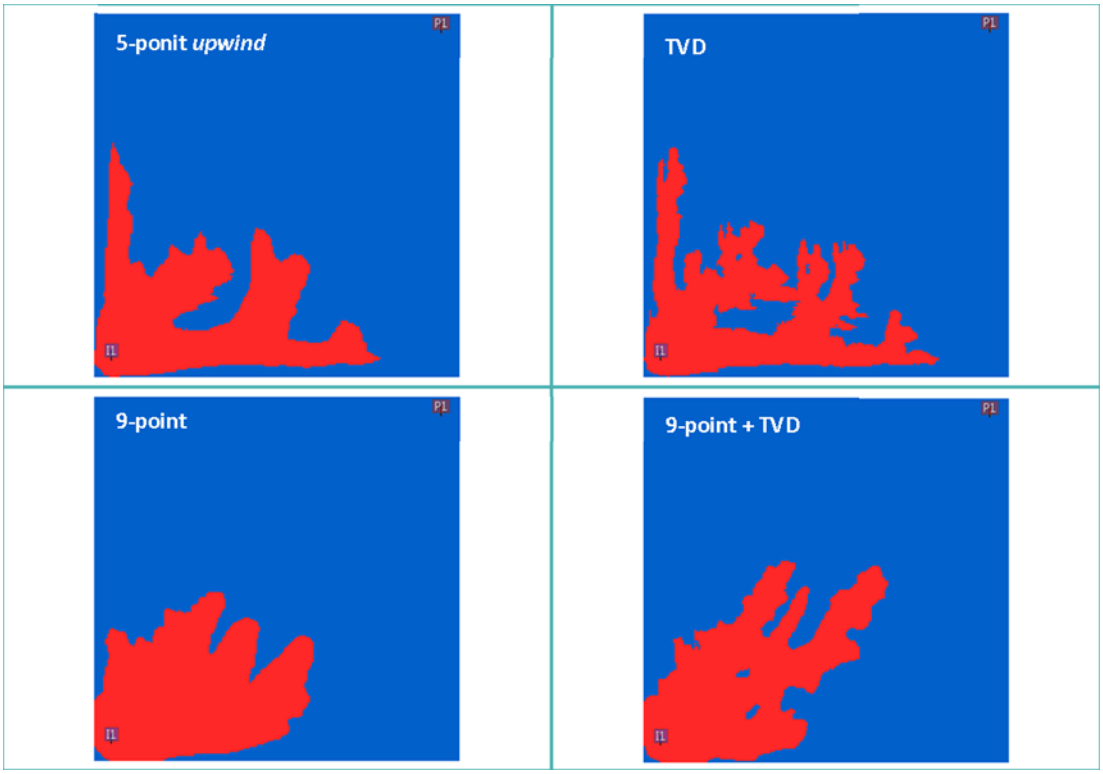

Figure 7. Behavior of the miscible gas front for four different configurations of the most refined case, 5 x 5 m², at an initial time of the gas injection.

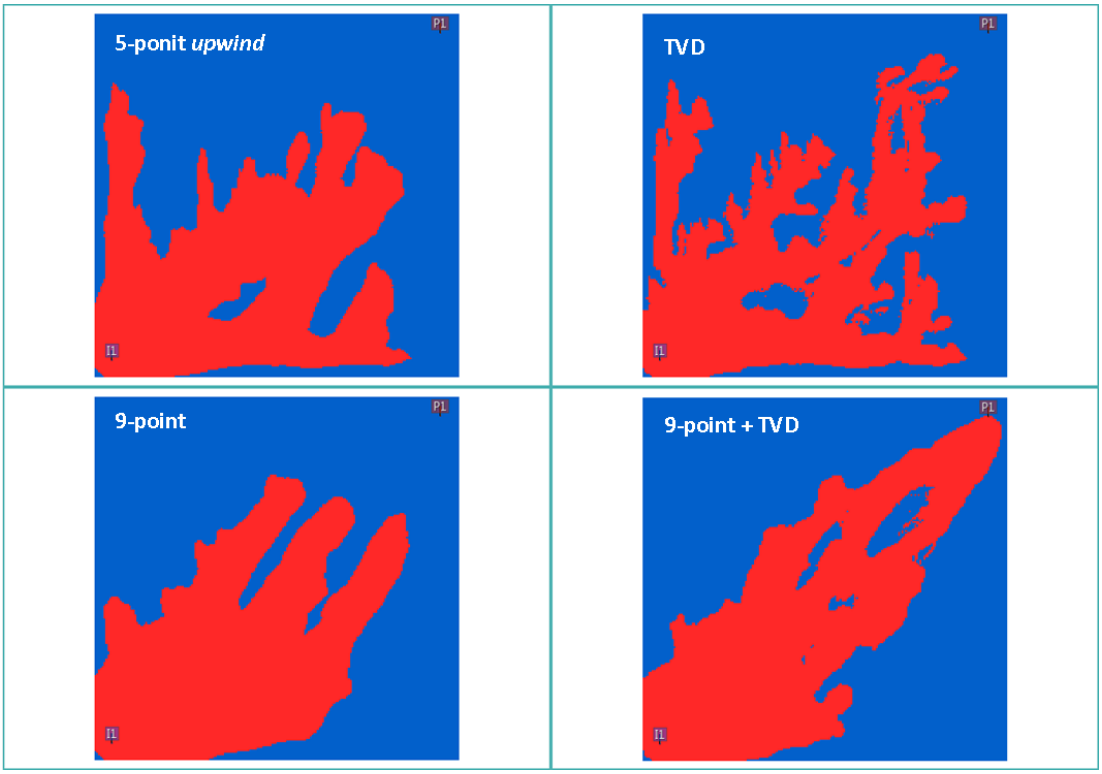

Figure 8. Behavior of the miscible gas front for the four different solutions of the most refined case, 5 x 5 m², all solutions on the same date corresponding to the breakthought of the solution 9-point + TVD

Proposed Solution

In water injection cases, the problems associated with upscaling can be corrected by techniques to generate pseudo curves of relative permeability. Inspired by this solution, it is proposed the use of a fluid model with a minimum miscibility pressure (MMP) above the experimental values and the pressure conditions evaluated in the simulations, which is, in average, 550 kgf / cm², in order to guarantee an immiscible displacement.

Under these conditions, the formation of two hydrocarbon phases is guaranteed. Therefore, there is variation of saturations in the porous medium. Table 3 shows the parameters of the adjusted EoS to represent immiscible displacement, while Table 4 shows the binary interaction coefficients.

Table 3. Parameters of the state equation for immiscible fit - Peng-Robinson

	P_c(MPa)	**T_c(K)**	□	**MW**	**Vshift**
PC1	7.38	304.2	0.23	44.0	-0.0718
PC2	4.59	190.2	0.01	16.1	-0.0553
PC3	4.89	383.8	0.17	33.0	-0.03827
PC4	3.08	621.0	0.36	115.0	-0.01237
PC5	1.99	750.0	0.58	216.4	0.00133
PC6	1.23	780.0	1.21	386.8	0.02593
PC7	0.72	1149.7	1.35	991.5	0.04019

Table 4. Binary interaction coefficients for the immiscible fit

PC1	0						
PC2	0.20	0					
PC3	0.19	0.01	0				
PC4	0.19	0.03	0	0			
PC5	0.19	0.04	0	0	0		
PC6	0.18	0.06	0	0	0	0	
PC7	0.18	0.09	0	0	0	0	0

The immiscible fluid model must be equivalent to the reference model in relation to the adjustment of the laboratory data, differing only in the behavior of the miscibility to the injected gas. In this context, Figure 9 shows the phase envelopes for the two adjustments of fluid models considered, in two distinct compositions of the fluid in the reservoir. It can be seen that the shape and the critical point are very similar in both cases, which shows equivalence between the fitted models.

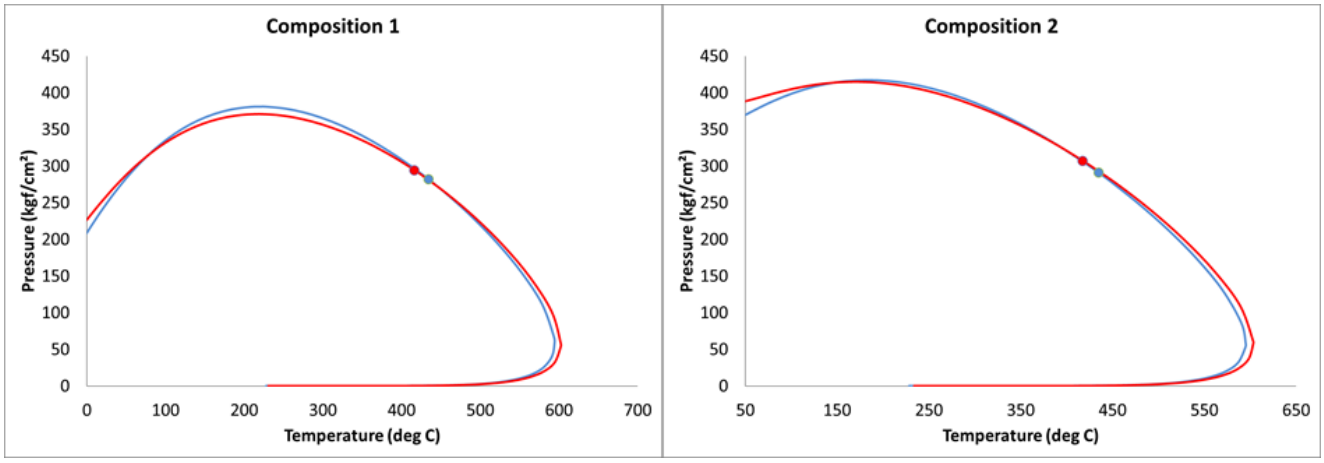

Figure 9. Behavior of the phase envelope for the two fluid models analyzed in two different global compositions. Data in red refer to the miscible realization, while in blue, the immiscible

As previously mentioned, the fluid model with immiscible characteristic is a realization with the MMP higher than the experimental data and the pressure conditions of the reservoir during production period. To show this observation, numerical evaluations were carried out reproducing the slimtube experiment, Rios et al. (2016).

There is no universally accepted method for defining the MMP from slimtube experiments. A widely adopted criterion for determining the MMP is the construction of a graph of the oil recovery factor after the injection of 1.2 pore volumes (Vp) of gas against the injection pressure. The MMP is considered with the injection pressure value at which the oil recovery reaches 90 to 95%.

Figures 10 and 11 show the oil recovery factor curves after the injection of 1.2 Vp of gas at different pressures for miscible and immiscible fluid models, respectively.

It is observed that only the first adjustment, Figure 10, presents PMM for the investigated pressure range, obtaining a characteristic recovery factor of slimtube miscibility between 430 and 500 kgf / cm². The immiscible case, Figure 11, shows no miscible behavior in the evaluated range.

Thus, once obtained a fluid model that allows the existence of immiscible displacement conditions in the reservoir, it is possible to act on relative pseudo-permeability curves also to correct the gas behavior.

The stage of adjusting pseudo relative permeability curves (gas-oil in this case, because it is the injection of only gas in oil reservoir) is equivalent to a task of history matching. In this case, starting from the coarser model, 100 x 100 m², miscible fluid model was replaced by the immiscible one and, later, the relative permeability curve was modified so as to better adjust the recovery observed in the refined reference model, 5 x 5 m². Figure 12 shows the oil

recovery factor curves for (i) the coarse models with miscible fluid model (yellow curve), (ii) the coarse model with immiscible fluid model (dashed black curve), and (iii) the refined model with miscible fluid model (red curve). It is worth mentioning that for this step, the reference model with conventional solution was considered, i.e. 5-point and upwind.

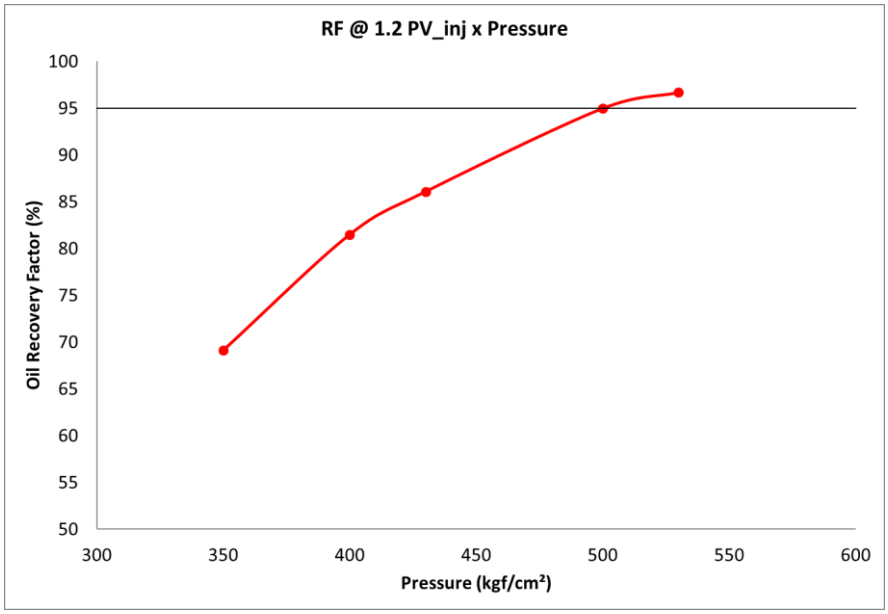

Figure 10. Graph of oil recovery factor against pressure after 1.2 PV injected gas for miscible adjustment

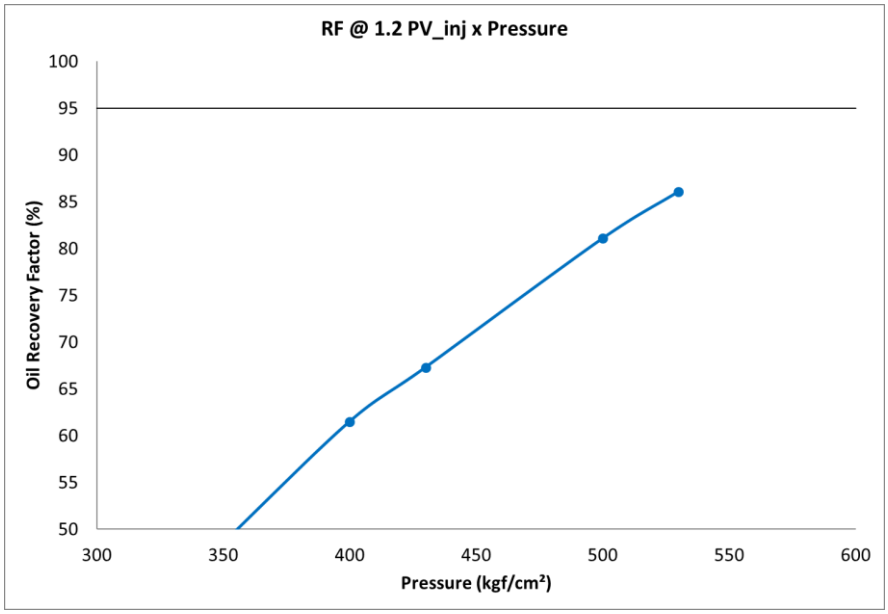

Figure 11. Graph of oil recovery factor against pressure after 1.2 PV injected gas for immiscible adjustment

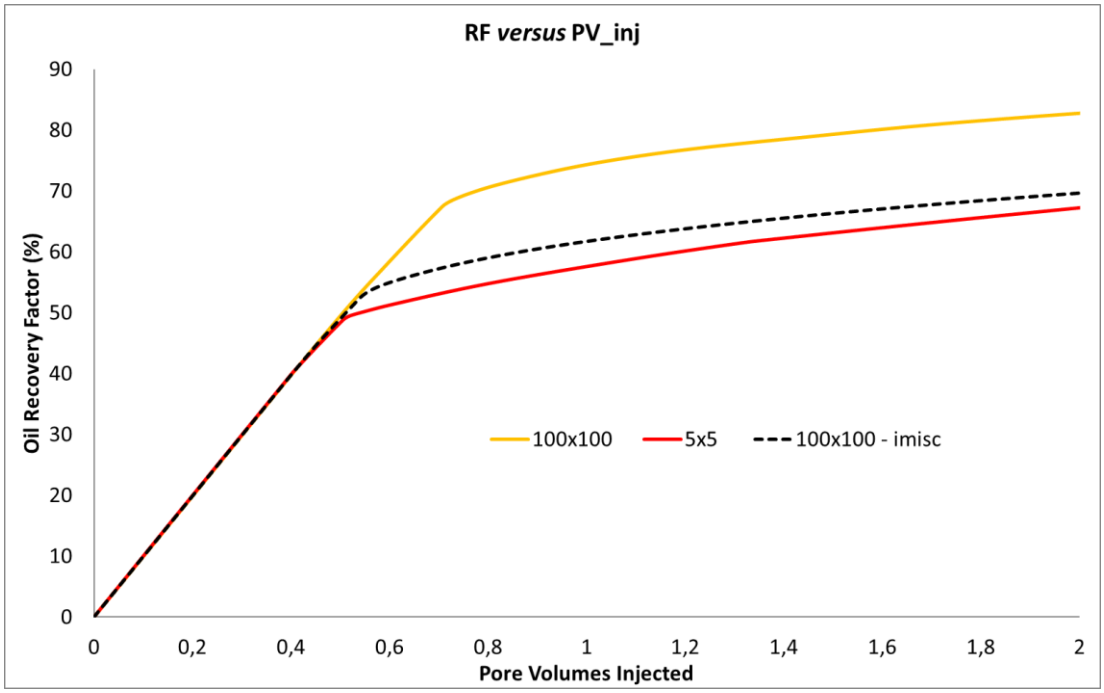

Figure 12. Graph of oil recovery factor against injected pore volume of gas for cases with coarse model (miscible and immiscible) and refined model.

It is possible to observe in Figure 12 that the alteration of the fluid model has already allowed a greater approximation between the recoveries of the coarse and refined models. It is observed, however, that there is still a slightly optimistic behavior of the 100 x 100 m² model. However, as the coarse case now presents two-phase flow in the reservoir, acting on the gas-oil relative permeability curve, it is possible to reproduce satisfactorily the recovery behavior observed in the refined reference model.

Figure 13 presents the same curves of Figure 12, but after adjusting a pseudo relative permeability curve for the coarse model with immiscible fluid model, it is possible to verify the optimal reproduction of the response obtained in the refined reference model.

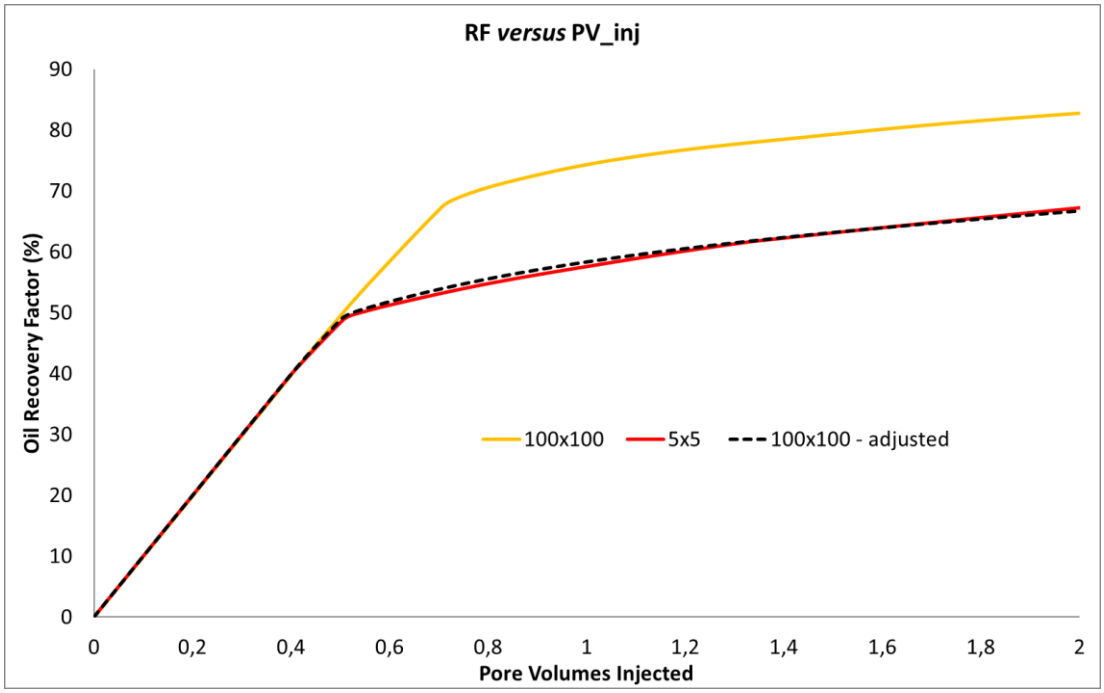

Figure 13. Graph of oil recovery factor against injected pore volume of gas for cases with coarse model (miscible and immiscible adjusted) and refined model.

Finally, Figure 14 shows the gas-oil relative permeability curves for both cases, i.e. the original curve and the adjusted curve in order to reproduce in the coarse model the recovery observed in the refined reference model.

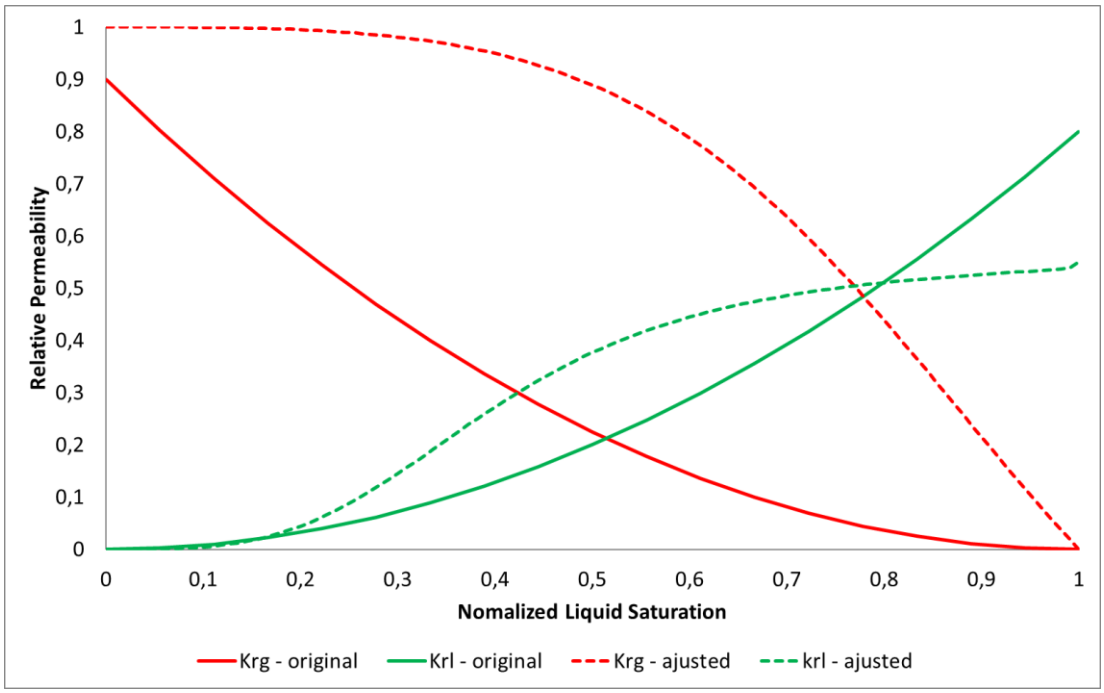

Figure 14. Original and adjusted gas-oil (gas-liquid) relative permeability curves.

Conclusions

In this work, the problem arising from the grid upscaling process (geological model to flow simulation model) was evaluated. It was verified that the coarser scale simulations tend to present optimistic production results in relation to the simulations in a more refined scale.

The main reason observed is the difficulty to represent the unstable flow and channeling on a reduced (coarse) scale. These phenomena tend to disappear with the smoothing of the forward fronts, represented by the so-called numerical dispersion derived from the truncation error.

It was evaluated the use of a 9-point scheme and TVD to mitigate the grid orientation and numerical dispersion effects, but the results were not conclusive. The TVD solution, for example, may present different results for different interpolation functions. In this way, more specific tests are necessary to have a conclusive evaluation about this technique.

Finally, it was possible to obtain good results in coarser models with the use of a fluid model that guaranteed the immiscible displacement and consequent formation of two hydrocarbon phases, with subsequent adjustment of pseudo relative permeability curves. Therefore, this technique is recommended to be applied in cases similar to the case tested here.

References

- Waggoner, J. R., Zapata, V. J., & Lake, L. W., 1991. Viscous Mixing In Unstable Miscible Displacements. *Society of Petroleum Engineers*. SPE-22235-MS
- Araktingi, U. G., & Orr Jr, F. M., 1993. Viscous Fingering in Heterogeneous Porous Media. *Society of Petroleum Engineers*. doi:10.2118/18095-PA
- Haajizadeh, M., Fayers, F. J., & Cockin, A. P., 2000. Effects of phase behavior, dispersion and gridding on sweep patterns for nearly miscible gas displacement. *In SPE Annual Technical Conference and Exhibition. Society of Petroleum Engineers*. SPE-62995-MS
- Sajjadi, M., & Azaiez, J., 2012. Thermo-Viscous Fingering in Heterogeneous Media. *Society of Petroleum Engineers*. doi:10.2118/157722-MS
- Doorwar, S., & Mohanty, K. K., 2015. Fingering Function for Unstable Immiscible Flows. *Society of Petroleum Engineers*. doi:10.2118/173290-MS
- Luo, H., Mohanty, K. K., Delshad, M., & Pope, G. A., 2016. Modeling and Upscaling Unstable Water and Polymer Floods: Dynamic Characterization of the Effective Finger Zone. *Society of Petroleum Engineers*. doi:10.2118/179648-MS

- Fernandes, B. R. B., Marcondes, F., & Sepehrnoori, K. 2013. Investigation of several interpolation functions for unstructured meshes in conjunction with compositional reservoir simulation. *Numerical Heat Transfer, Part A: Applications*, 64(12), 974-993.
- Fernandes, B. R. B., Gonçalves, A. D. R., Filho, E. P. D., da Costa Menezes Lima, I., Marcondes, F., & Sepehrnoori, K. 2015. A 3D total variation diminishing scheme for compositional reservoir simulation using the element-based finite-volume method. *Numerical Heat Transfer, Part A: Applications*,67(8), 839-856.
- Rios, V.S.; Santos, L.O.S. & Espósito, R.O., 2016. Methodology to incorporate the miscibility on the adjust of the equations of state. *Rio Oil & Gas Expo and Conference 2016*. IBP2213_16

APPENDIX B - Complementary Article #2 (Article 8)

PRACTICAL WORKFLOW TO IMPROVE NUMERICAL PERFORMANCE IN TIME-CONSUMING RESERVOIR SIMULATION MODELS USING SUBMODELS AND SHORTER PERIOD OF TIME

V.S. Rios, Avansi, G. D., D.J. Schiozer

Journal of Petroleum Science and Engineering, v. 195, December 2020, 107547

Abstract

Numerical reservoir simulation is a valuable tool to support the decision-making process in oil field projects. For this purpose, current reservoir engineering studies request numerous simulations runs for complex workflows, such as numerical reservoir characterization, data assimilation process, strategy optimization, well placement studies, production management and supplementary project support. Thus, providing efficient and effective simulation numerical models is a critical task in reservoir simulation studies before starting the daily run demands.

In this work, we propose, test and evaluate a practical workflow to improve the numerical performance of time-consuming reservoir simulation models. We provide a procedure to select representative numerical submodels and representative snapshots interval from simulation time (RSIST) to reduce the total time spent in numerical optimization. The first approach allows the optimization of the numerical parameters without the drawback of simulating long execution runtime. The second enables to select a range of simulation time where typical convergence problems of timestep cuts occur. The numerical parameters are then optimized using submodels and RSIST, where we highlight a workflow to reduce runtime of the optimization of slow reservoir models. Following, the resultant set of parameters is applied to the entire (original) reservoir numerical model, improving its performance and allowing more effective execution of several simulation-runs in reservoir engineering studies.

To conclude, we provide a workflow to be applied to any reservoir simulation model, especially those with complex structural grid and high-time consuming to run. Our results demonstrated remarkable improvements in the numerical performance of simulation models, with a high potential of saving days of work during probabilistic evaluations. Furthermore, we recommend this workflow as a first step before starting studies using reservoir simulation to avoid unphysical and time-demanding simulation runs that may affect future decisions.

Introduction

In practical reservoir simulation, it is common to build a numerical model for dynamic study purposes which requires many stages before starting to solve the actual reservoir engineering problems (Galas, 1997). Firstly, structural information is required, which includes: overall geometry, grid size specification, elevation (top and base) for each grid block, faults and limits of the reservoir (Caumon et al., 2009). The second step is to render geological interpretation and conceptual geological model into a suitable input format for reservoir

simulation software, i.e., provide an image (porosity, permeability, net-to-gross and facies distributions) that represents the same variability and phenomena into the structural model as we understand the real petroleum field (Dubrule, 1998; Mallet, 2002). Relative permeability and capillary pressure curves are also important inputs to build the reservoir model. In addition, fluid PVT (Pressure, Volume and Temperature) properties, including: formation volume factors, solution gas, viscosities, which are also obtained by laboratory tests, are included to our numerical model (Dalen, 1986; Dodson et al., 1953; Whitson and Brule, 1993). Finally, well locations, perforated intervals (Morris and Ayoub, 1989), productivity and injectivity indices (PI and II's) (Aziz, 2000; Van Wingen, 1949), initial and well operational conditions are the last information to include in our reservoir simulation model (Stags and Herbeck, 1971). The general idea is to build a reservoir numerical model to represent the pore-scale flow behavior of a real field (Odeh, 1969).

Building a numerical reservoir simulation model is not an easy task, especially when the focus is to build consistent and efficient models. Consistent models mean (1) respecting geological descriptions and spatial correlations of reservoir properties (Johnson and Jones, 1988) and (2) obtaining a solution of nonlinear partial differential equations (PDEs) which converges to true solution respecting the set of geological information (Coats, 1982). Efficient models mean ones which run with a minimum amount of effort based on the level of importance of the study (objective), available time and resources. This stage is one of the most important steps of reservoir integrated studies as proposed by Schiozer et al., (2019). They proposed a model-based decision methodology using reservoir numerical models based on 12 steps to be applied in decision analysis process in petroleum fields where the second step is to represent a real petroleum field in thousands of PDEs that cannot be analytically solved.

Despite having a large number of complicated problems (coupled oil, water and gas equations, PDEs in time and space (1, 2 and 3D) and variable properties, such as porosity and permeability) to be solved, we need to guarantee that all created reservoir models must be consistent, both geologically (preserving spatial correlation of reservoir properties), and numerically (convergence to true solution). These must also be efficient (computational effort). To create numerical models from complex and time-consuming numerical models representing real fields, such as those from the pre-salt area in Brazil, we must work on numerical parameters of reservoir simulator in order to obtain reliable production output and also save computational effort on probabilistic reservoir development and management workflows.

From our experience, reservoir simulation engineers do not always select the most suitable numerical parameters to provide an efficient solution to most simulation problems. A

practical approach to increase efficiency without losing geological and numerical consistency of simulation models in a full workflow of petroleum reservoir simulations is then presented, and it is the focus of this proposed article. It is also important to highlight that overriding the numerical parameters is not a simple task and requires good understanding of the problem and solution of the methods involved. A bad combination of numerical parameters can greatly increase the running execution time for a specific simulation activity. Above all, it seems reasonable to include an appropriate numerical screening step after building the numerical model to enhance the decision analysis procedure with a consistent and efficient numerical model, apart from just improving petroleum work process speed and productivity, especially with high complex and heterogeneous reservoirs.

Avansi et al. (2019) evaluated the impacts of performing an optimization of the numerical parameters in reservoir simulation models. They showed expressive time-saving results not only regarding single simulation runs, but considering some workflows usually performed in reservoir engineering activities. Enhance the numerical tuning of complex models that demands higher runtime demands additional research and, as a result; this is the main motivation of this work proposal.

We identified that tuning numerical parameters is effective, however for slow reservoir models, which usually take a long time to run a single realization, the solution gets more complex as the problem does. While these models are the most potential beneficiaries of an improvement in numerical performance, it is harder to conduct optimization using the entire model because of the required time to run the models. To overcome this limitation, we propose a new and practical workflow in which representative numerical submodels are extracted from the original one. Then, numerical optimization, as proposed by Avansi et al. (2019), is performed for this model. Moreover, as another attempt to improve the performance, it is usually not necessary to simulate the entire production period, thus, we propose the selection of a RSIST, which is the total production period to be considered for each simulation run. Therefore, the optimization process applied to the submodels becomes more effective to obtain the desired results.

The Problem

Reservoir engineering studies usually require many simulations in several activities within a practical workflow, such as reservoir characterization, data assimilation, production/injection and well control optimization, among others. However, no special attention is usually given to define a proper set of numerical parameters for the simulation runs. Thus, in general, the simulations are performed using default numerical control internally set

in the numerical simulator. These numerical parameters, despite the effort of the developers, tend to be ineffective, increasing the total simulation time and also the risk of getting high material balance errors (Avansi et al., 2019).

The idea of a practical procedure to increase numerical performance of black oil reservoir simulations without losing geological and numerical consistency of reservoir models was discussed by Avansi et al., (2019). The proposed methodology achieved remarkable improvements in the numerical performance of the simulation models, with straightforward procedure to optimize numerical parameters. Despite the need to perform several simulation runs to achieve an optimized numerical control, the benefits in a complete reservoir engineering workflow were shown to be consistent. Moreover, the application of the whole methodology is challenging in high-time-consuming and large-scale reservoir dimension.

The present work proposes a practical workflow to enhance numerical tuning with complex and time-consuming reservoir numerical models. We propose a process to select representative submodels to reduce runtime of the numerical tuning. In addition, we can choose representative simulation run period of time for this task which is important to improve the performance of the proposed workflow, reducing not only the runtime of the process but also the simulation time that we need to run the numerical tuning. Thus, the numerical optimization of a large-scale reservoir model is obtained using a submodel and simulating part of the total development and management plan time for that oil field. Both strategies combined make the present work an effective and practical workflow to improve numerical performance of large-scale models.

Objectives

This work proposes a workflow to improve numerical performance in time-consuming reservoir simulation models. The key objectives are, then:

- Establish a procedure to proper select representative submodels - from the numerical point of view - using the information of a previous simulation run of a large-scale model to be optimized;
- Define, from the available simulation run, the necessary period of time to be considered in the submodels simulation runs in order to obtain a more effective result in terms of runtime-saving; and
- Perform a numerical optimization in the selected representative submodel and use the resultant numerical parameters to improve the performance of the original model.

Assumptions

In this work, the following assumptions were considered:

- Black-oil fluid models;
- Base case reservoir numerical model with default numerical parameter settings;
- Parallel computing is one technique that can be used to accelerate the solution of computationally expensive optimization problems. Nonetheless, we are not considering it into our optimization procedure because we focused our analysis on comparing numerical submodel runs on the same basis in terms of hardware and we know that the effects of the parallelism are not linear; and
- Different stochastic optimization methods were not tested. We are assuming a pre-defined commercial algorithm named as CMG Designed Exploration and Controlled Evolution - CMG-DECE (Computer Modelling Group Ltd., 2012) based on the proposal of Yang et al., (2007) to tune the numerical parameters of the reservoir simulation model.

Methodology

The proposed methodology of numerical tuning using submodels is highlighted in Figure 1.

Base-Case Simulation

The initial analysis starts with the first simulation results, which are obtained considering the default numerical parameter choice.

Numerical Model Diagnosis

At this stage, we are performing a numerical diagnosis of the model based on four indicators suggested by Avansi et al. (2019) for a complex corner-point grid that is extremely helpful in order to check if there are problems related with long execution times. In most of the times, these problems are related to convergence failures. When all primary variables or all the primary equation residuals have converged to their tolerance values (Computer Modelling Group Ltd., 2015) this means that we obtain a better physical behavior of our real problem, i.e., the representation of the flow in a porous media (Avansi et al., 2019). The benefits of performing a numerical tuning will be then not expressive in cases that we do not have any problem with the numerical model. As a result, we can move forward directly to the application (Step 10); otherwise, we must check where the convergence problems occurs (Step 3) to check in Step 4 if is necessary or not to build a submodel to reduce the total execution time of the numerical tuning.

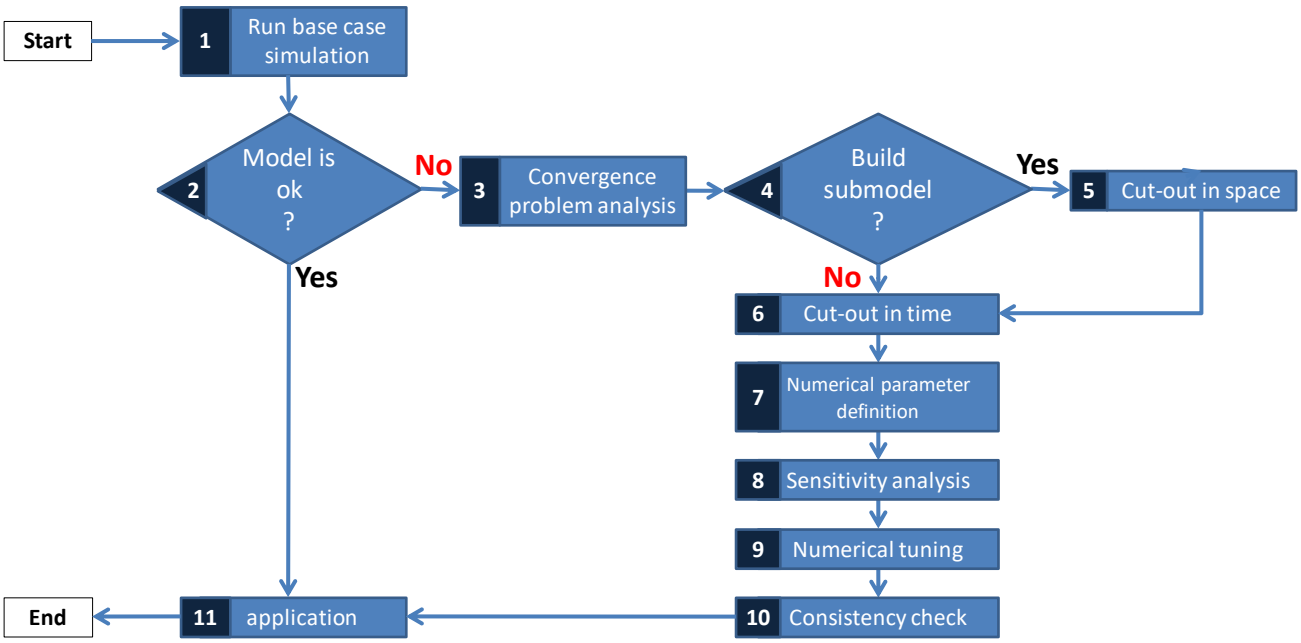

Figure 1. Flowchart highlighting the proposed methodology.

Convergence Problem Analysis

At this stage, we must perform a quality analysis to check regions of the reservoir numerical model where the convergence problems occur that affect the total elapsed time to run the numerical model. This step is important for the next stage in order to check if is possible or not to cluster the problematic regions highlighted.

Submodel Construction Decision

We must check if it is possible to build a submodel with the highlighted problematic regions. If yes, we must move on to the next stage that is to create the submodel based on the convergence problematic regions. Otherwise, we move on to Step 6 to evaluate if we can reduce the total time simulated during the tuning procedure.

Cut out in Space: Submodel

To build our submodel, it is necessary to cut out the submodel from the full field in space. The idea is to use the submodel in the whole workflow of tuning the numerical parameters inputs (Avansi et al., 2019), focusing on problematic regions that increase the total execution time of the full field numerical model.

In order to build our submodel we suggest analyzing the convergence problems that affects the execution time in space. Figure 2 gives us an idea of the step-by-step that will be used cut out our submodel from the model in space.

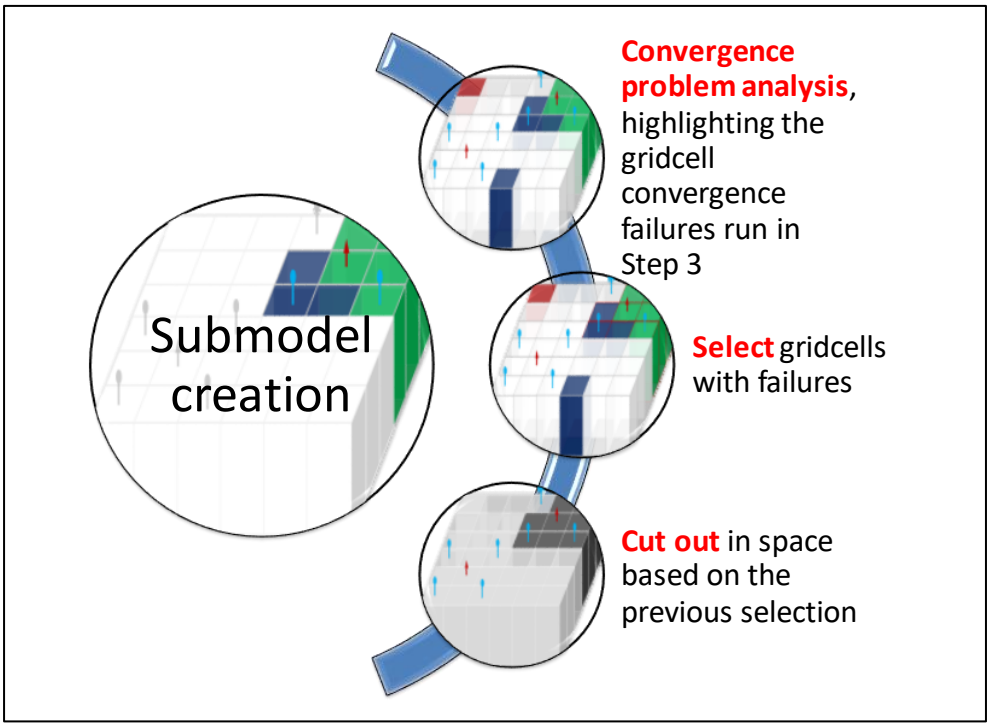

Figure 2. Diagram highlighting the cutout in space to build the submodel.

Quality Analysis of Convergence Failures

First, we need to remember that we are now checking how we can build our submodel. After running the numerical model with the default numerical parameters and performing the convergence problem analysis (Step 3), we can post-process the results of the solution obtained by the simulator. We then plot a 2D graph that provides information on grid cell location of Newtonian iteration convergence failures caused by changes in fluid saturation and pressure that exceeds the maximum previous defined by default.

Selection and Cutout

After highlighting the problematic grid cells that fail, we select a region and then cut out in space to build our submodel which is treated as no flux at the boundary. This is an important step of the procedure because it is possible to have more than one region to be selected. This selection will then be based on the experience of the user and the idea is to select a region that has at least one producer and one injector.

Cutting-time simulation: representative snapshots interval from simulation time (RSIST)

After cutting out in space, we also analyse the frequency of timestep cuts in the total simulation runtime as shown as an example in Figure 3. This is an addition step that helps us to decreasing the total simulation runtime for the numerical tuning, allowing us to select the most frequent and critical time interval that the convergence failures occur.

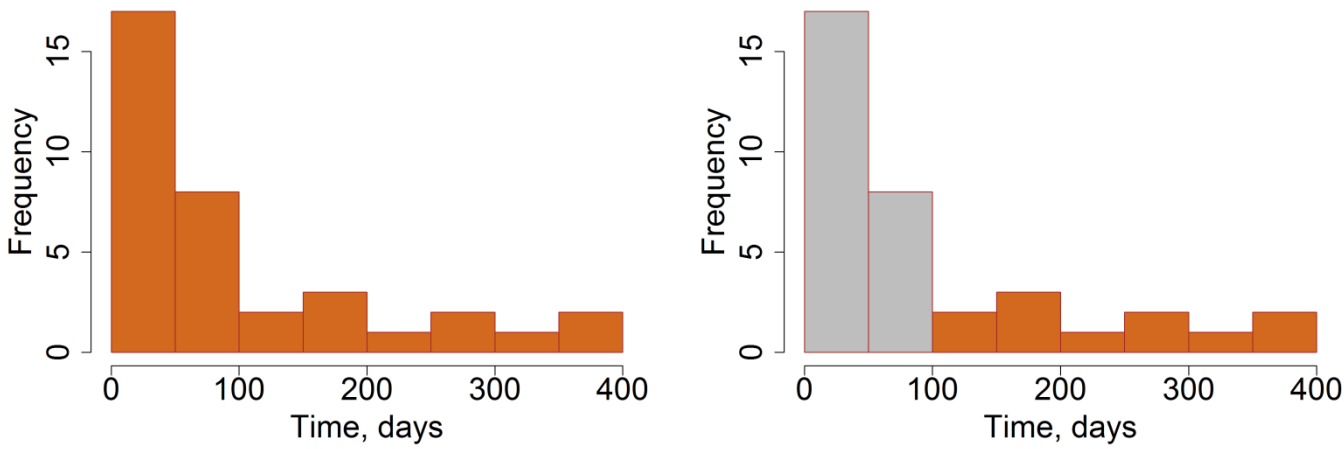

(a) (b)

Figure 3. Example of convergence failures frequency occurring in 400 days of simulation runtime

From Figure 3, it is possible to observe that there is a significant decrease in the frequency when the simulation runtime reaches 100 days, and then keep almost constant until the end of the simulation. As a result, the main problematic time interval is between 0 and 100 days, i.e., we can stop the simulation runtime on 100 days for our numerical tuning procedure.

Building submodels through cutout in space (selecting the most critical regions that fail to converge) and in time (selecting a period of simulation time that the simulation model fail to converge – avoiding unnecessary runtime during the optimization) are worthy to increase the potential of using numerical tuning techniques.

Numerical Parameter Definition

The most critical numerical parameters of the model are surveyed after the numerical diagnosis. The interval of the optimization for each parameter is generated. After this survey, we must perform a sensitivity analysis.

Sensitivity Analysis

At this stage, we must provide a measure of sensitivity of all input's parameters. Through this analysis, it is possible to have an overview of the most sensitive inputs of the numerical model that affects the simulation runtime. The idea is to avoid unnecessary inputs during the numerical tuning.

Numerical Tuning

Some numerical parameters were previously selected, as discussed in the previous section, and the optimization is conducted to tune computational time. For a consistent numerical tuning, it is important to guarantee that all machines used for tuning are identical in

performance and set up (Avansi et al., 2019). Therefore, a consistency check of the machines, i.e., a test to verify inconsistencies in the computer infrastructure (e.g., same reservoir model with different execution times), must be run to guarantee these criteria. In addition, filter and numerical model selection is carried out to select the most suitable combination of inputs and acceptable outputs as presented by Avansi et al., (2019).

Consistency Check of Numerical Model

After performing the numerical tuning, a consistency check is performed in order to verify the quality of the results in the full reservoir numerical model. If the results are acceptable, we can then use for the future applications.

Application

The idea of this topic is to compare the performance of the numerical tuning against the default parameters. For this purpose, several applications can be used such as: history matching with uncertainty reduction, production strategy optimization, risk analysis and so on.

Case Studies: UNISIM-I-D

The study case, UNISIM-I-D (Avansi and Schiozer, 2015; Gaspar et al., 2015), is a synthetic model that was built based on a real dataset from the Namorado Field, Campos Basin, Brazil. UNISIM-I-D (UNISIM, 2013) is a benchmark case create for oil field development and production strategy selection. We proposed two different levels of fidelity in terms of running time of the UNISIM-I-D to create fast (UNISIM-I-D-h7v7) and slow (UNISIM-I-D-hfm) models to test and validate the proposed methodology.

The numerical model named as UNISIM-I-D-h7v7 (U-I-D-h7v7) has a corner-point grid with 81 x 58 x 23 grid cells (41,096 active total cells) and a grid cell resolution of 100 x 100 x 6 m. On the other hand, the validation case UNISIM-I-D-hfm (U-I-D-hfm) has the same corner-point grid, although with 326 x 234 x 157 grid cells (365,820 active total cells) and a grid cell resolution of 25 x 25 x 1 m. Figure 4 highlights the porosity and permeability distribution with well positions for both models.

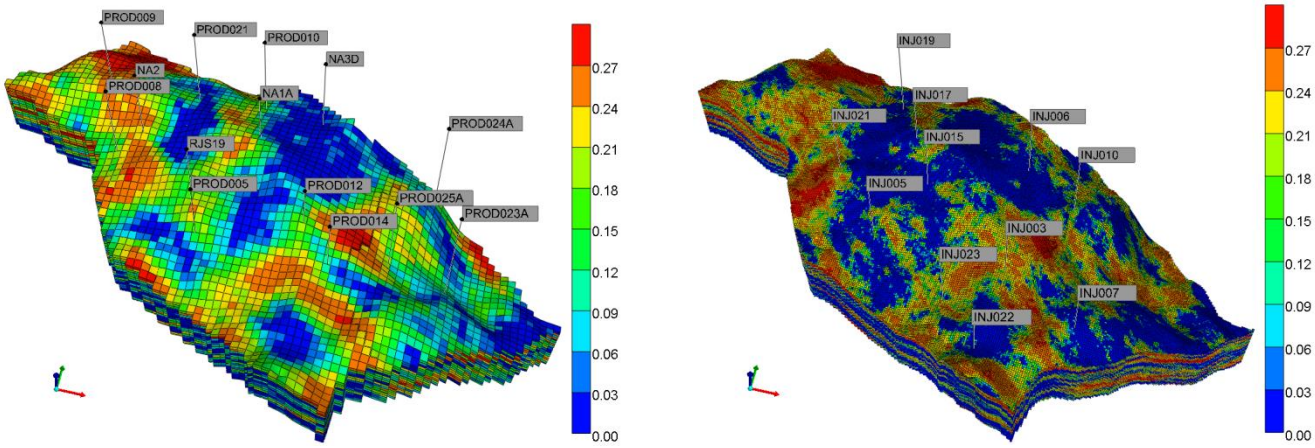

(a) U-I-D-h7v7: porosity highlighting all producers, including the four original wells (NA1A, NA2, NA3D and RJS19)

(b) U-I-D-hfm: permeability showing all injectors

Figure 4: Reservoir properties distribution of both case studies.

Rock-fluid properties, fluid model, operating and monitoring well and platform conditions from both reservoir numerical models are the identical and they are from the original case studies (Avansi and Schiozer, 2015; Gaspar et al., 2015). The rock compressibility is $5.3\,E\times10^{-5}\ (kgf/cm^2)^{-1}$ ($5.2\,E\times10^{-3}\ kPa^{-1}$) and bubble point pressure is $210\ kgf/cm^2$ ($20{,}597\ kPa$). There is a historical production of 1,461 days (4 years). The total forecast production time for the model is 9,496 days (26 years) under the following operating and monitoring well conditions:

- Liquid rates are produced with the maximum possible rate for the field: 2,000 m³/day;
- Minimum production pressure is 190 kgf/cm² (18,633 kPa);
- Water cut is 90%, maximum gas-oil ratio is 200 m³/m³ and minimum oil rate is 20 m³/day for monitoring and closing conditions for producers, if the condition is reached;
- Water is injected at the maximum possible rate for the field: 5,000 m³/day;
- Maximum injection pressure is 350 kgf/cm² (34,323 kPa).

We used a black oil commercial reservoir numerical simulator from CMG (Computer Modelling Group Ltd., 2018) to run the simulation models for 10,957 days and the average simulation running time of U-I-D-h7v7 and U-I-D-hfm for a single scenario are 788 and 458,094 seconds using 1 single and 2 parallel processors respectively.

Results and Discussions

The results presented in the following topics are for U-I-D-h7v7 and U-I-D-hfm models. The complete procedure, using the flowchart in Figure 1 is presented as follows.

Steps 1 and 2: base case simulation run and numerical diagnosis

After running the base case simulation with all default numerical parameters, we performed the numerical model diagnosis as shown in Table 1.

Table 1. U-I -D-h7v7 and U-I-D-hfm: numerical diagnosis highlighting a summary of the numerical outputs.

Reservoir Numerical Model	Total$_{(o+w+g)}$ MBE Error, %	Time-step (TS)	Newtonian Cycles (NC)	Time-step Cuts (TSC)	Solver Iterations (SI)
UNISIM-I-D-h7v7	0.00	977	2,099	42	39,012
UNISIM-I-D-hfm	0.03	13,658	23,274	598	421,974

Next, it is necessary to calculate the numerical parameters defined by Avansi et al., (2019) to check if the model is acceptable or not as illustrated in Table 2 to skip the numerical tuning stage.

Table 2. U-I-D-h7v7 and U-I-D-hfm: numerical diagnosis highlighting the eligible numerical parameters in red that justify the importance of tuning the numerical model based on our experience for a Black-Oil numerical model.

Computational Statistics	Total$_{(o+w+g)}$ MBE Error, %	Number of Time-step Cuts (TSC) per Time-step (TS), %	Number of Newtonian Cycles (NC) per Time-step (TS)	Number of Solver Iterations (SI) per Newtonian Cycle (NC)
Acceptance Criteria	-0.5% ≤ MBE Error ≤ 0.5%	TSC/TS ≤ 1 %	NC/TS ≤ 1.5	SI/NC ≤ 20
UNISIM-I-D-h7v7	0.00	**4.3**	**2.1**	18.6
UNISIM-I-D-hfm	0.03	**4.4**	**1.7**	18.1

From the analysis in Table 2, we identified that the model is not acceptable mainly because of the high number of time-step cuts per time-step (more than 1%), showing that is possible to enhance the numerical section of the model. Based on our experience, 788 seconds and 458,094 seconds are considered high to run one single realization for U-I-D-h7v7 and U-I-

D-hfm respectively. So, there is another alternative to increase the power of the numerical tuning procedure that is cutting them out in space and time.

Steps 3, 4 and 5: cut out submodel from the entire model and cutting-time simulation

As we know, the number of possible solutions using the numerical simulator increased exponentially when the number of dimension increases (active cells). After checking if the model is suitable for the numerical tuning or not, we must evaluate if the effects in reducing runtime through this is worthy or not.

So, the next step is to check where the convergence problems occur in order to cut out the submodel and save computational time for the numerical tuning. Figure 5 illustrates a 2D-gridcell map where we highlighted when maximum allowed changes per time-step exceed the limit (this is an input of the numerical section that the user can change it).

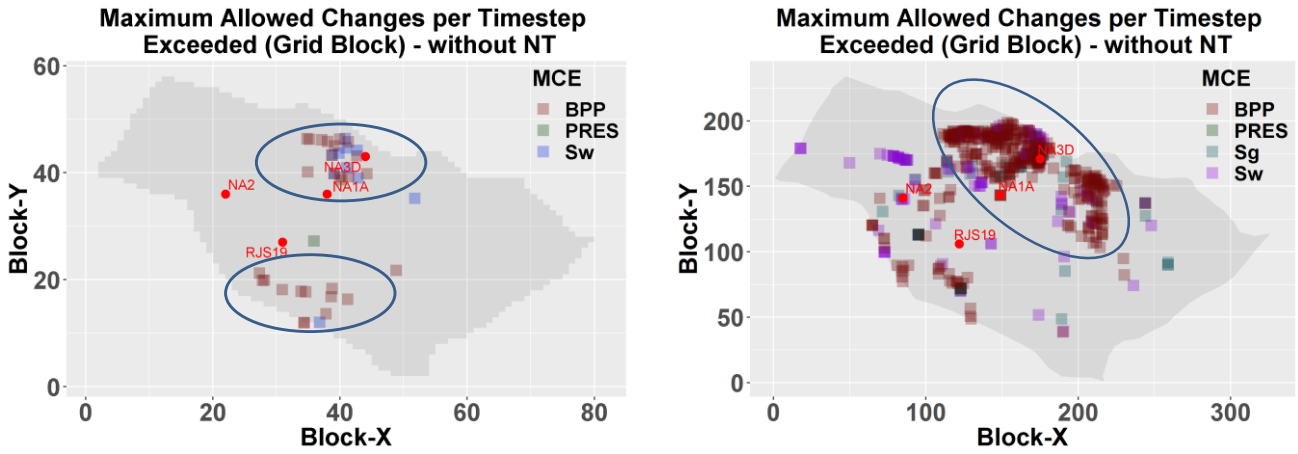

(a) U-I-D-h7v7 (b) U-I-D-hfm

Figure 5. Maximum allowed changes per timestep exceed by grid block without the numerical tuning (NT) for bubble-point pressure (BPP) in light brown; pressure (PRES) in light green, water saturation (Sw) in light blue and gas saturation (Sg) in light purple. Dark blue circle highlights the potential region to be cut out.

As we can see in Figure 5, the number of convergence problems in U-I-D-hfm is higher than U-I-D-h7v7 because increases the number of finite elements (resolution) used to compute an approximate solution of the physical problem (flow in porous media). In general, higher resolution increases accuracy of the solution but also requires longer computational times due to higher convergence problems. In addition, most of the numerical problems are concentrated in regions highlighted in the blue area. So, it is feasible to cut out in space the numerical model since it spends 788 (1-processor) and 458,094 (2-parallel-processors) seconds to run.

Based on our experience, the numerical tuning usually spends about 500 runs. In order to avoid computer performance effects using different machines and architecture, we ran this procedure for the entire field in a local machine with 4 processors. In this context, we spent about 98,460 seconds (27 hours) and 114,523,500 seconds (80 days) to perform the numerical tuning for each case respectively.

In this context, using submodels for this procedure is an important step to save time during the reservoir simulation workflow. As a result, we move to the following step that is building the submodel. Figure 6 shows the numerical model before and after the cutout. It is important to note that the limit of the reservoir, after cutting out the submodels inside the blue circles, are treated as no-flux.

After highlighting the 2D quality map (Figure 6) of time-step cuts per maximum change in pressure and saturation within a time-step during 10,957 days of total runtime, we build our submodel based on the problematic regions of the reservoir. As a result, we reduced the runtime of the model to 179 and 2,381 seconds for U-I-D-h7v7 and U-I-D-hfm correspondingly, likewise saving 77% and 99% for each one in comparison to the entire model (without no cutout).

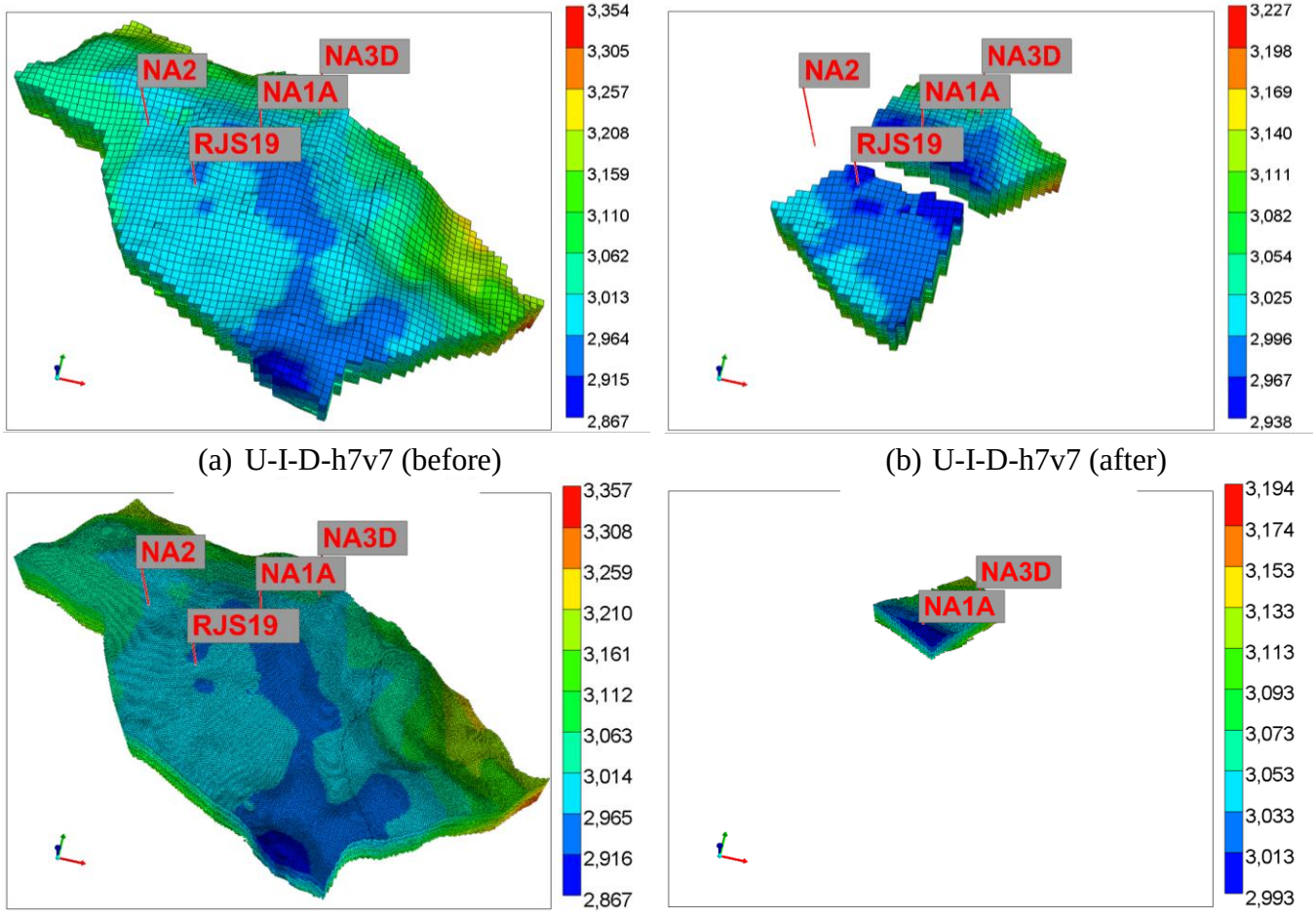

(a) U-I-D-h7v7 (before) (b) U-I-D-h7v7 (after)

(c) U-I-D-hfm (before) (d) U-I-D-hfm (after)

Figure 6. Reservoir numerical model before (entire field) and after performing the cut-out in space to create the submodel.

We are then ready to check if we can also cut them out in time as the next step. For this, we plot the histogram of timestep cuts during the simulation run for each reservoir numerical model as we can see in Figure 7.

As we can see in Figure 7, it is unnecessary to run the numerical model for the entire period of production (10,957 days) because the most frequent occurrence of timestep cuts occurs at the beginning of the simulation run time because of the massive number of operational changes that occurs with wells and platforms (known as boundary conditions for numerical simulation of petroleum reservoir model). As a result, we cut time simulation of total simulation time for both models and simulate the U-I-D-h7v7 and U-I-D-hfm until 16.5 and 11.0 years respectively.

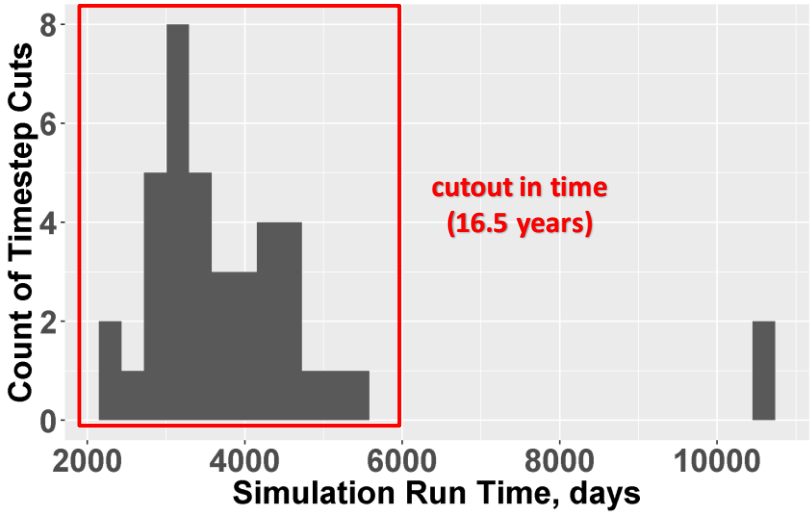

(a) UNISIM-I-D-h7v7

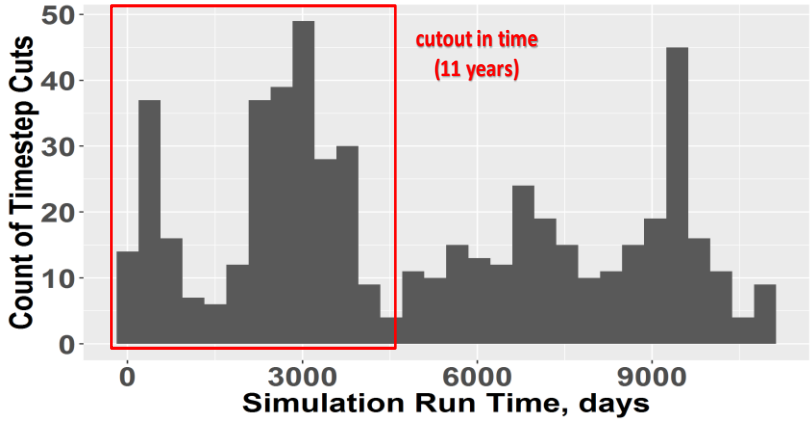

(b) UNISIM-I-D--hfm

Figure 7. Histogram of the number of timestep cuts within a certain range (commonly known as bins) of 250 and 333 days for U-I-D-h7v7 and U-I-D-hfm respectively until the end of the simulation run time (10,957 days). Red square highlights the region to be cut- time histogram for the simulation time.

Steps 6, 7 and 8: numerical parameter definition, sensitivity analysis and numerical tuning

After cutting out both models in space and time, we now have a practical reservoir numerical model to be used in the numerical tuning process.

Before starting the numerical tuning, we must define the numerical parameter inputs that we will be used in the optimization procedure. Table 3 highlights the inputs that we characterize during our studies. As we are working with a Black-Oil model, the same one used by Avansi et al., (2019), we are assuming the same inputs as following.

Table 3. Numerical inputs used in the optimization procedure, including the default values and the optimum value to reach the minimum running time for U-I-D-h7v7 and U-I-D-hfm.

Parameter	Probability Distribution	Default Value	Probability Density Function (pdf)	Optimum Value (with filter)	
				UNISIM-I-D-h7v7	UNISIM-I-D-hfm
Maximum Time-step Size, *days*	continuous (uniform)	365	0, x < 1 1/(31-1), 1 ≤ x ≤ 31 0, x > 31	31	14
Normal Variation in Pressure per Time-step, *kgf/cm²*[1]	continuous (uniform)	3,000	0, x < 1,000 1/(5,000-1,000), 1,000 ≤ x ≤ 5,000 0, x > 5,000	49 *kgf/cm²*	46 *kgf/cm²*
Normal Variation in Saturation per Time-step, *dimensionless*	continuous (uniform)	0.10	0, x < 0.05 1/(0.50-0.05), 0.05 ≤ x ≤ 0.50 0, x > 0.50	0.35	0.20
Maximum Change in Pressure per Time-step, *kgf/cm²*[1]	continuous (uniform)	6,000	2*(Normal Variation in Pressure)	98 *kgf/cm²*	92 *kgf/cm²*
Maximum Change in Saturation per Time-step, *dimensionless*	continuous (uniform)	0.2	2*(Normal Variation in Saturation)[2]	0.70	0.40
Convergence of Newton's Method[3], *dimensionless*	continuous (uniform)	0.1	0, x < 0.01 1/(0.01-1.00), 0.01 ≤ x ≤ 1.00 0, x > 1.00	1	1
Convergence Tolerance for Linear Solver - Globally[4], *dimensionless*	continuous (uniform)	0.0001	0, x < 0.00001 1/(0.00001-0.01000), 0.00001 ≤ x ≤ 0.01000 0, x > 0.01000	0.00334	0.00889
Hybrid Stability-Threshold Adaptative Implicity Switching for Bubble Point Pressure (p_b) and Fluid Saturations (S_f), *dimensionless*	constant	p_b = 0.25 S_f = 0.25	p_b= 0.25 S_f = 0.25	p_b= 0.25 S_f = 0.25	p_b= 0.25 S_f = 0.25
Maximum Number of Linear Iterations, *dimensionless*	constant	40	200	200	200
Maximum Number of Orthogonalisations, *dimensionless*	constant	30	100	100	100
Maximum Number of Newtonian Cycles, *dimensionless*	constant	10	10	10	10
Maximum Number of Time-step Size Cuts, *dimensionless*	constant	4	20	20	20

Before this, it is important to perform a sensitivity analysis in order to target the input parameters that most affect the reservoir numerical output. Figure shows a tornado plot of linear effects estimates using a Plackett-Burman design (Plackett and Burman, 1946) with 20 trials for U-I-D-h7v7.

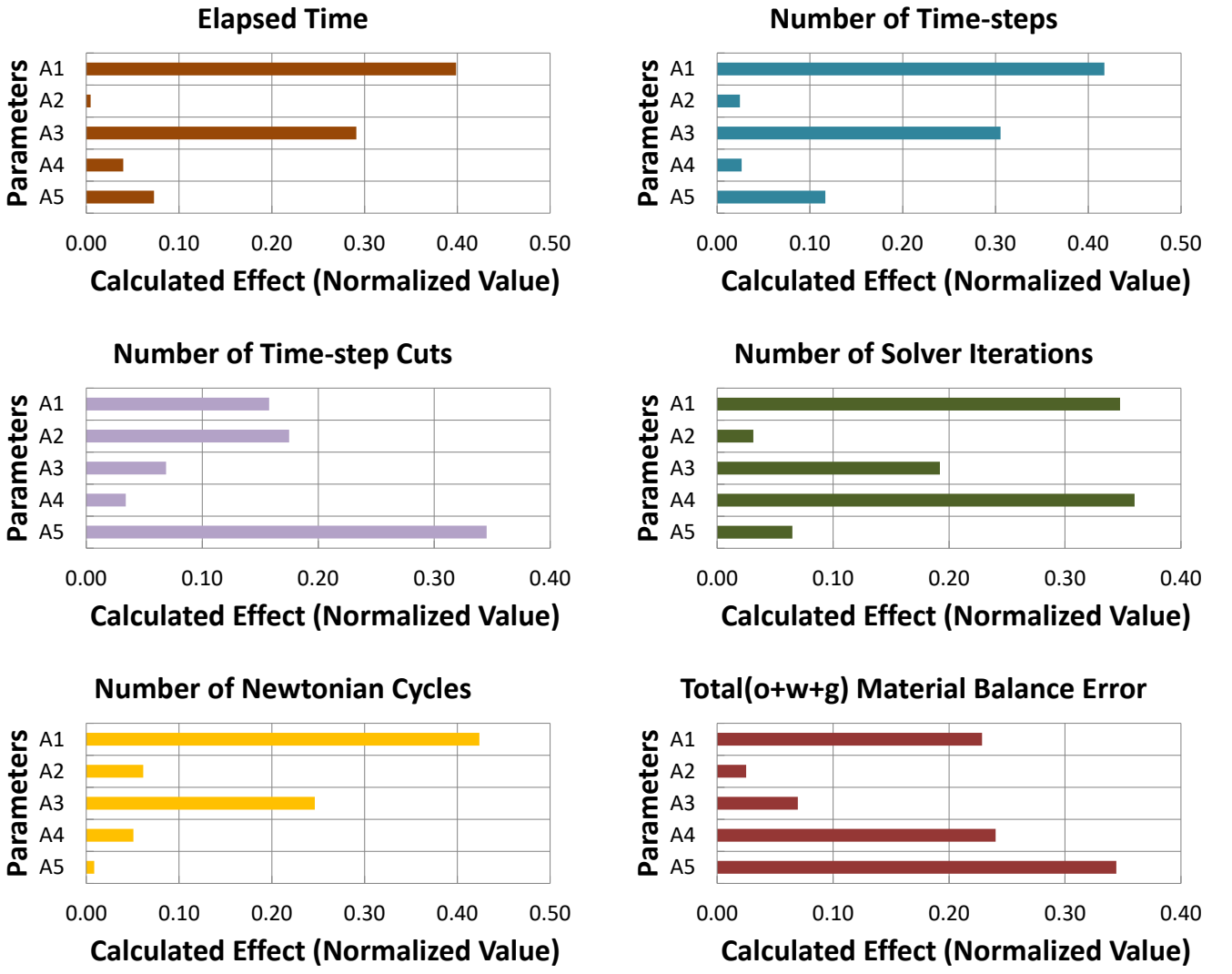

Figure 8. U-I-D-h7v7: Sensitivity Analysis of the submodels – cut out in space and cutting-time simulation.

As we can see in Figure 8, the linear effect estimates from the tornado plots show us that we must consider all the inputs to perform the numerical tuning. This happens mainly

[1] Pressure unit conversion between kilopascal and kilogram-force/square centimeter: 1 *kgf/cm²* = 98.0665 *kPa*.
[2] Maximum value is 0.90.
[3] Global Maximum Convergence Criteria for Newton's Method.
[4] All equations: oil, water, gas (when appropriate).

because we do not have a common input parameter insignificant for all outputs that impact the numerical tuning and are considered in the proposed methodology. For practical purposes, we are not showing the results of the sensitivity analysis for U-I-D-hfm; we also concluded we cannot eliminate any input parameter for our next stage, the numerical tuning. As we observe, it is difficult to generalize and choose the most influential parameters that affect the objective functions related to runtime. Filtering the parameters is one alternative instead of ranking the input influence and we are also performing this by the end of the numerical tuning.

After the sensitivity analysis, we noticed that all selected inputs are important to the process. So, we run the numerical tuning procedure which demands a high number of runs. The procedure is highlight in Figure 9 for both case studies.

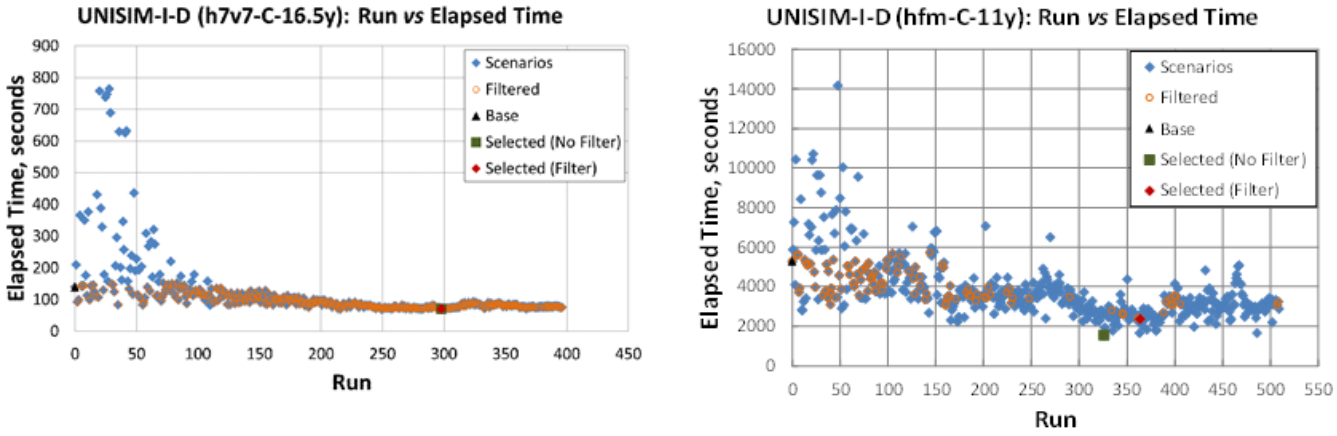

(a) UNISIM-I-D-h7v7. (b) UNISIM-I-D-hfm.

Figure 9. Numerical tuning using the submodel – cut out in space and cutting-time simulation. Elapsed time over execution run of the tuning procedure. Base simulation run (black triangle) used as a reference; all scenarios used during the procedure (blue diamonds); all scenarios using a total material balance equation error cut-off (orange circle) to highlight acceptable runs; the minimum running time with (dark red square) and without (dark green circle) the cut-off.

From Figure 9 it is possible to observe that the elapsed time dropped gradually until the simulation run 100 for both case applications. Then, the trend fluctuated steadily until the end of the tuning for UNISIM-I-D-h7v7 (Figure 9a), with almost all runs inside the quality criteria that we are calling “filter” (orange circles). For the other case in Figure 9b, the trend fluctuated between 2,000 and 6,000 runs until the end of the tuning, but with less filtered scenarios than the other case. To conclude this stage, we can analyse the results with and without using the proposed technique in Table 4.

Table 4. Numerical tuning of U-I-D-h7v7 and U-I-D-hfm models comparing the total elapsed time with and without the proposed methodology.

Model	Total elapsed time (seconds) spent to tune the numerical model considering		Saving time (%)
	entire model	proposed methodology	
UNISIM-I-D-h7v7	39,240	6,420	84
UNISIM-I-D-hfm	5,702,160	121,380	98

From Table 4, we concluded that we saved 84 and 98% for the U-I-D-h7v7 and U-I-D-hfm model cut out in space and cutting-time simulation, respectively.

Step 9: Consistency check

After performing the numerical tuning with the submodel, the optimized parameters were used into the entire field to check the consistency of the results as highlighted in Table 5. As we can see and as expected, it is clear the runtime saved (44 and 39%, respectively for U-I-D-h7v7 and U-I-D-hfm) after performing the numerical tuning using the proposed methodology, keeping the same order of magnitude.

Table 5. U-I-D-h7v7 and U-I-D-hfm: consistency check of both models after performing the numerical tuning using cut out in space and cutting-time simulation.

Model	Total elapsed time (seconds)		Saving time (%)
	Before	After	
UNISIM-I-D-h7v7	788	443	44
UNISIM-I-D-hfm	458,094	278,309	39

After checking the results of one model, it is important to check the behavior for a practical application in reservoir studies.

Step 10: Application

The idea of this section is to check how the tuning procedure performs after tuning the numerical model using the cut out in space and cutting-time simulation. The uncertainties and their levels considered in the processes are the same described by Gaspar et al., (2015).

Test case: UNISIM-I-D-h7v7

In order to achieve the results of the tuning procedure in a practical application of risk analysis, we run 500 scenarios, combining reservoir, technical and economic uncertainties for U-I-D-h7v7. Figure 6 shows the results after running the numerical simulator for each scenario.

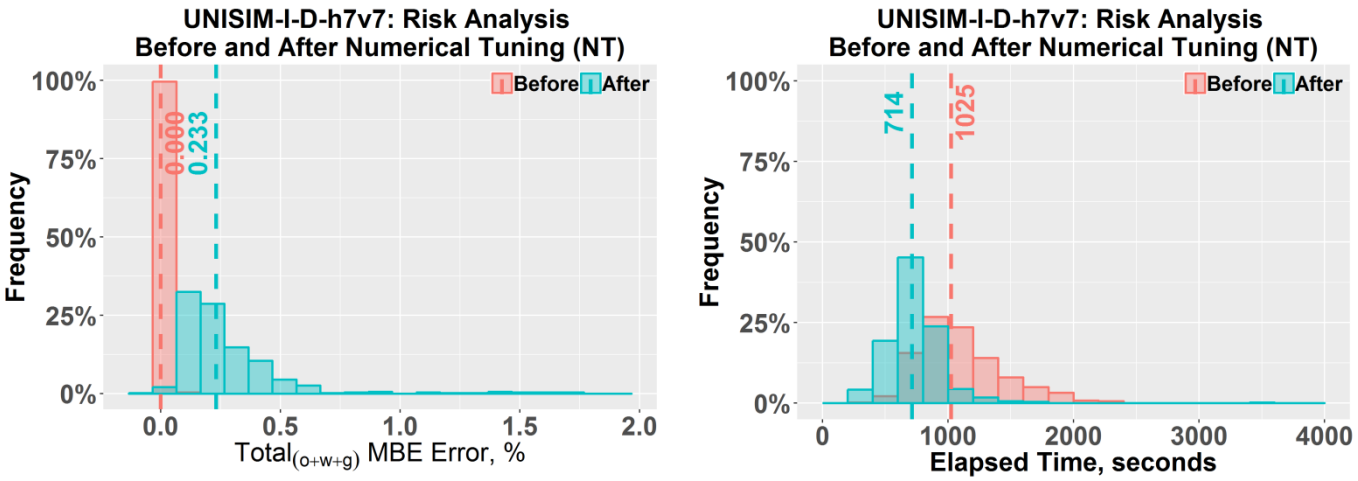

Figure 10. UNISIM-I-D-h7v7: statistical analysis after the risk analysis application before and after the numerical tuning.

It can be clearly seen in Figure 10 that the elapsed time were reduced considerably after performing the numerical tuning and, consequently, diminished the execution time of each simulation run. It is important to note that the total MBE Error increased, although is still in the proposed discrepancy criterion of 0.5% (Avansi et al., 2019).

Validation case: UNISIM-I-D-hfm

Due to this model is highly-time consuming (278,309 seconds - 77 hours - after the numerical tuning), we decide to evaluate three representative models based on cumulative oil production (Np) of UNISIM-I-D-h7v7 instead of 500 trials. We selected the optimistic, probable and pessimist based on Np and we run the numerical simulator for these models with default and optimized numerical conditions. Following, we check if is feasible or not to optimize the numerical section using submodels and cutting-time simulation. Figure 11 highlights the results before and after the numerical tuning.

When we compared before and after performing the numerical tuning in Figure 11, it is thoroughly explicit that the elapsed time has intelligible decreased about 23% (330,000 to 255,000) and the total MBE Error increased (0.1 to 0.2%). It is important to note that the benefits of increasing the total computational time saved is greater than increasing the total MBE errors that is still in our discrepancy tolerance defined (0.5%).

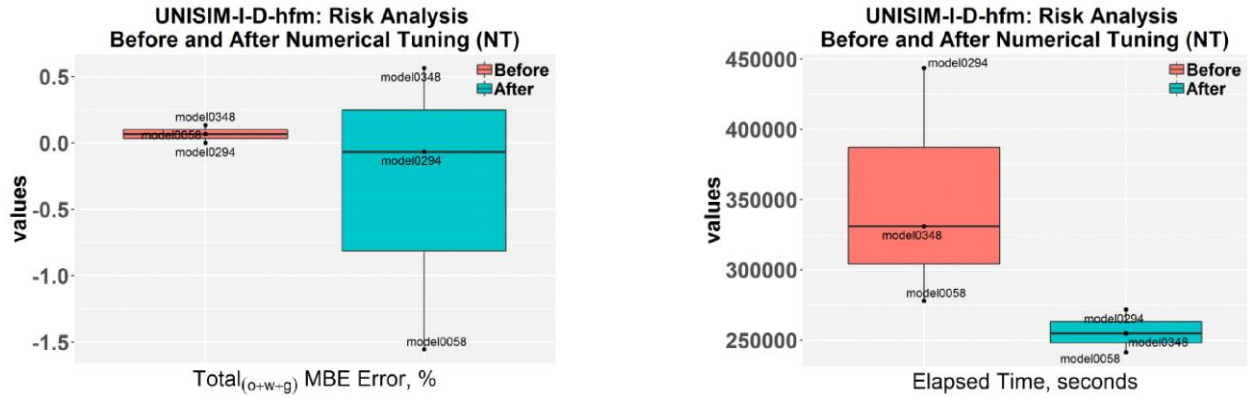

(a) (b)

Figure 11. UNISIM-I-D-hfm: statistical analysis after the risk analysis application before and after the numerical tuning.

Furthermore, it is important to consider the total time spend to tune the numerical parameters in the total runtime after performing the numerical tuning. Figure 12 shows the case studies with and without tuning over the elapsed time used to run the optimization.

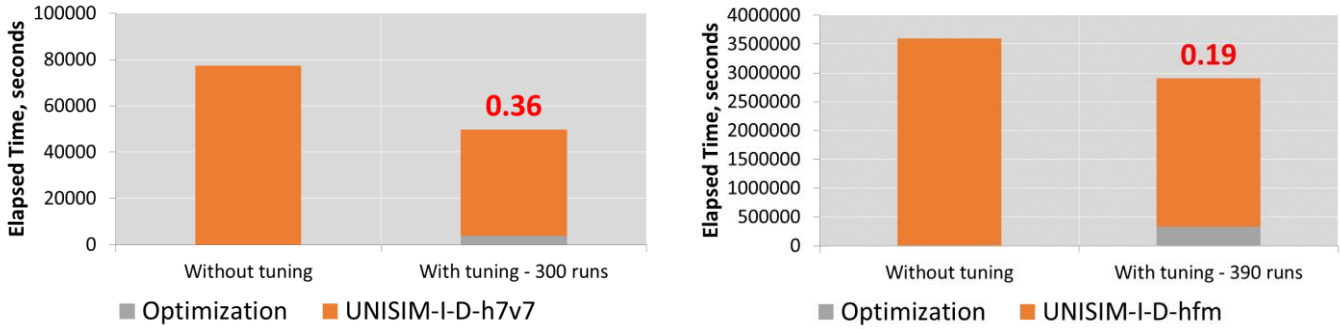

Figure 12. UNISIM-I-D-h7v7 and UNISIM-I-D-hfm: results of the application considering a traditional approach (all numerical parameters at default conditions) and a tuned approach, including the time spent to optimize the numerical parameters. We also highlighted a fraction of the reduction (in red) for both cases in comparison to the original case.

From Figure 12, considering just one activity of reservoir simulation studies (build risk curves), we can notice that it is worthy to execute the proposed methodology to save precious time in daily activities, especially because we considered the time spent during the numerical tuning. As we can see, this time has fallen by 36% for U-I-D-h7v7 and 19% for U-I-D-hfm in comparison to the original application (default numerical parameters). Notwithstanding being a small gain compared what we can expected from using the proposed methodology, it is justified because the technique is simple and easy to apply and we are also running only a few simulations and just one application of several that can be daily perform, tending to increase in probabilistic approaches.

As a result, we can conclude that the proposed procedure is helpful and significantly reduce tuning efforts and time spent in practical numerical reservoir studies, saving days of works.

Conclusions

In the proposed work, we highlight a straightforward methodology to reduce runtime of the tuning procedure and improve numerical performance of their simulation models with accurate results.

We considered two case studies: U-I-D-h7v7 (least time-consuming) and U-I-D-hfm (most time-consuming) to test and validate the proposed methodology. We also evaluate this proposed methodology in a practical and common-daily situation in a petroleum reservoir simulation of building uncertainty curves to show how impressive is the proposed technique if an additional treatment to the numerical model is previous given before starting the numerical tuning.

The results show that using cut out in space and cutting-time simulation is effective to optimize the time spend to run a simulation of a petroleum reservoir model that demands a huge computational time and detecting convergence problems during the simulation run.

In addition, instead of optimising the entire simulation period, we detected the period where convergence problems occurred, that is, cuts in time-steps due to a change beyond the maximum allowed that is defined by the user.

To conclude, the methodology proved to be efficient and simple to reproduce, being indispensable to improve simulation study workflows. It also shows the potential to save even more when several applications, using the same model, are carried out.

Acknowledgments

This work was conducted with the support of Energi Simulation and in association with the ongoing Project registered as "BG-32 – Análise de Risco para o Desenvolvimento e Gerenciamento de Campos de Petróleo e Potencial uso de Emuladores" (UNICAMP/Shell Brazil/ANP) funded by Shell Brazil, under the ANP R&D levy as "Compromisso de Investimentos com Pesquisa e Desenvolvimento". The authors also thank UNISIM, DE-FEM-UNICAMP, CEPETRO and PETROBRAS for supporting this work and CMG, Emerson and Schlumberger for software licenses.

Nomenclature

S	Saturation	-
C	Cut out in space	-
y	Number of years	-
BBP	Bubble Point Pressure	kPa
PRES	Pressure	kPa
CMG	(Computer Modelling Group Ltd	-
DECE	Designed Exploration and Controlled Evolution	-
Np	Cumulative oil production	m^3
MBE	Material Balance Equation	-
UNISIM-I-D-h7v7 / U-I-D-h7v7	Numerical model created with 41,096 active total cells	-
UNISIM-I-D-hfm / U-I-D-hfm	Numerical model created with 365,820 active total cells	-
PDEs	partial differential equations	-
SI	Solver Iterations	-
PI	productivity index	$m^3/day/kgf/cm^2$
II	injectivity index	$m^3/day/kgf/cm^2$
NC	Newtonian Cycles	-
TSC	Time-step Cuts	-
TS	Time-step	-
CPU	Central Processing Unit	sec
NT	Numerical tuning	-
RSIST	representative snapshots interval from simulation time	-
Subscripts		
F	Fluid phase (oil, water or gas)	-
O	Oil	-
W	Water	-
G	Gas	-

References

- Avansi, G., Rios, V., Schiozer, D., 2019. Numerical tuning in reservoir simulation: it is worth the effort in practical petroleum applications. J. Brazilian Soc. Mech. Sci. Eng. 41, 59. doi:10.1007/s40430-018-1559-9.
- Avansi, G.D., Schiozer, D.J., 2015. UNISIM-I: Synthetic Model for Reservoir Development and Management Applications. Int. J. Model. Simul. Pet. Ind. 9, 21–30.
- Aziz, K., 2000. Productivity and injectivity of horizontal wells. Tulsa, OK. doi:10.2172/751965.
- Caumon, G., Collon-Drouaillet, P., Le Carlier de Veslud, C., Viseur, S., Sausse, J., 2009. Surface-Based 3D Modeling of Geological Structures. Math. Geosci. 41, 927–945. doi:10.1007/s11004-009-9244-2.

- Coats, K., 1982. Reservoir Simulation: State of the Art (includes associated papers 11927 and 12290). J. Pet. Technol. 34, 1633–1642. doi:10.2118/10020-PA.
- Computer Modelling Group Ltd., 2012. CMOST User Guide. Computer Assisted History Matching, Optimization and Uncertainty Assessment Tool.
- Computer Modelling Group Ltd., 2015. IMEX User Guide. Three-Phase, Black-Oil Reservoir Simulator.
- Dalen, V., 1986. Fluid properties in reservoir simulation. Fluid Phase Equilib. 29, 93–108. doi:10.1016/0378-3812(86)85014-2.
- Dodson, C.R., Goodwill, D., Mayer, E.H., 1953. Application of Laboratory PVT Data to Reservoir Engineering Problems. J. Pet. Technol. 5, 287–298. doi:10.2118/953287-G.
- Dubrule, O., 1998. Geostatistics In Petroleum Geology. AAPG Special Volumes, Tulsa, Oklahoma, U.S.A.
- Galas, C., 1997. The Future of Reservoir Simulation. J. Can. Pet. Technol. 36. doi:10.2118/97-01-GE.
- Gaspar, A.T.F.., Avansi, G.D., Santos, A.A., Hohendorff Filho, J.C.V., Schiozer, D.J., 2015. UNISIM-I-D: Benchmark Studies for Oil Field Development and Production Strategy Selection. Int. J. Model. Simul. Pet. Ind. 9, 47–55.
- Johnson, C.R., Jones, T.A., 1988. Putting Geology Into Reservoir Simulations: A Three-Dimensional Modeling Approach, in: Society of Petroleum Engineers (U.S.) (Ed.), SPE Annual Technical Conference and Exhibition. Society of Petroleum Engineers, Houston, Texas, USA. doi:10.2118/18321-MS.
- Mallet, J.-L., 2002. Geomodeling. Oxford University Press.
- Morris, C.W., Ayoub, J.A., 1989. Engineered Perforation Design and Evaluation, in: SPE Production Operations Symposium. Society of Petroleum Engineers. doi:10.2118/18840-MS.
- Odeh, A.S., 1969. Reservoir Simulation ...What Is It. J. Pet. Technol. 21, 1383–1388. doi:10.2118/2790-PA.
- Plackett, R.L., Burman, J.P., 1946. The Design of Optimum Multifactorial Experiments. Biometrika 33, 305–325. doi:10.1093/biomet/33.4.305.
- Schiozer, D.J., de Souza dos Santos, A.A., de Graça Santos, S.M., von Hohendorff Filho, J.C., 2019. Model-based decision analysis applied to petroleum field

development and management. Oil Gas Sci. Technol. – Rev. d'IFP Energies Nouv. 74, 46. doi:10.2516/ogst/2019019.

- Stags, H.M., Herbeck, E.F., 1971. Reservoir Simulation Models An Engineering Overview. J. Pet. Technol. 23, 1428–1436. doi:10.2118/3304-PA.
- UNISIM, 2013. UNISIM-I-D: Case Study for Selection of Production Strategy [WWW Document]. URL https://www.unisim.cepetro.unicamp.br/benchmarks/br/unisim-i/unisim-i-d.
- Van Wingen, N., 1949. Injectivity Indices-Their Prediction and Determination. Drill. Prod. Pract.
- Whitson, C.H., Brule, M.R., 1993. Phase Behavior, in: SPE Monograph Volume 20. Henry L. Doherty Memorial Fund of AIME, Society of Petroleum Engineers., Richardson, TX.
- Yang, C., Nghiem, L.X., Card, C., Bremeier, M., 2007. Reservoir Model Uncertainty Quantification Through Computer-Assisted History Matching, in: SPE Annual Technical Conference and Exhibition. Society of Petroleum Engineers. doi:10.2118/109825-MS.

APPENDIX C – Examples of alternative fluid models for the same set of experimental PVT data

When we proposed the compositional upscaling for miscible gas flooding process, one key step was the generation of the "pseudo-fluid" model. We showed in the publications the differences between the original and the "immiscible-like" EoS. In this appendix, we present two additional EoS, fitted reproducing the same experimental data. The objective is to show that, since the EoS fitting process is an inverse problem, the step 1 of our compositional upscaling methodology is a practical procedure and easy to obtain.

In total, we created four EoS. EOS1 and EOS2 are, respectively, the "Original-Miscible" and the "Immiscible", as named in Article 1, while EOS3 and EOS4 are new realizations. Table 1 to Table 8 summarizes the parameters for the four EoS, and Figure 1.A to Figure 1.C show some examples of PVT experiments and the equivalence among all the realizations. Again, the difference is only regarding the interaction between the injected gas and the reservoir oil, as we highlight in Figure 1.D with the numerical slimtube simulation results.

Additionally, to emphasize the equivalence between the fluid models, we repeated the consistency test performed considering the coarse-scale Case A in Article 1. The test consisted of simulating water injection and comparing the results with the four fluid models. Figure 2 shows the total equivalence between the curves, as expected.

Therefore, it is possible to verify the miscibility behavior (see Rios et al. 2016) predicted by a specific EoS and work on alternative fluid models according to the need. Note that the binary coefficients are key parameters to change for obtaining different miscibility predictions.

Table 1 - Parameters of the equation of state for EOS1 - Peng-Robinson

	P_c(MPa)	T_c(K)	ω	MW	Vshift
PC1	7.38	304.2	0.23	44.0	-0.0718
PC2	4.59	190.2	0.01	16.1	0.0468
PC3	3.42	369.0	0.20	36.8	0.0282
PC4	2.40	614.9	0.51	168.2	0.0075
PC5	1.82	778.5	0.72	241.1	-0.0053
PC6	1.09	796.7	1.18	363.5	0.1956
PC7	0.71	1078.1	1.33	785.3	0.1741

Table 2 - Binary interaction coefficients for the EOS1

PC1	0						
PC2	0.15	0					
PC3	0.16	0.03	0				
PC4	0.15	0.07	0	0			
PC5	0.13	0.09	0	0	0		
PC6	0.09	0.12	0	0	0	0	
PC7	0.02	0.16	0	0	0	0	0

Table 3 - Parameters of the state equation for EOS2 - Peng-Robinson.

	P_c(MPa)	T_c(K)	ω	MW	Vshift
PC1	7.38	304.2	0.23	44.0	-0.0718
PC2	4.59	190.2	0.01	16.1	-0.0553
PC3	4.89	383.8	0.17	33.0	-0.03827
PC4	3.08	621.0	0.36	115.0	-0.01237
PC5	1.99	750.0	0.58	216.4	0.00133
PC6	1.23	780.0	1.21	386.8	0.02593
PC7	0.72	1149.7	1.35	991.5	0.04019

Table 4. Binary interaction coefficients for the EOS2

PC1	0						
PC2	0.20	0					
PC3	0.19	0.01	0				
PC4	0.19	0.03	0	0			
PC5	0.19	0.04	0	0	0		
PC6	0.18	0.06	0	0	0	0	
PC7	0.18	0.09	0	0	0	0	0

Table 5 - Parameters of the state equation for EOS3 - Peng-Robinson.

	P_c(MPa)	T_c(K)	ω	MW	Vshift
PC1	7.38	304.20	0.23	44.01	-0.0718
PC2	4.59	190.23	0.01	16.11	0.044627
PC3	4.89	383.78	0.17	33.02	0.018142
PC4	2.28	601.64	0.52	115.10	-0.26422
PC5	1.46	702.81	0.67	218.93	-0.08374
PC6	0.89	731.87	1.57	389.43	0.287817
PC7	0.64	1125.37	1.78	994.43	0.574626

Table 6. Binary interaction coefficients for the EOS3

PC1	0.00						
PC2	0.17	0.00					
PC3	0.17	0.00	0.00				
PC4	0.16	0.00	1.22E-03	0.00			
PC5	0.16	0.09	3.21E-03	4.92E-04	0.00		
PC6	0.16	0.10	6.00E-03	1.92E-03	4.79E-04	0.00	
PC7	0.16	0.12	9.40E-03	4.16E-03	1.85E-03	4.56E-04	0.00

Table 7 - Parameters of the state equation for EOS4 - Peng-Robinson.

	P_c(MPa)	T_c(K)	ω	MW	Vshift
PC1	7.38	304.20	0.23	44.01	-0.0718
PC2	4.59	190.23	0.01	16.11	-0.05537
PC3	4.89	383.78	0.17	33.02	-0.03827
PC4	2.28	601.64	0.52	115.10	-0.16422
PC5	1.48	726.67	0.84	216.52	0.017734
PC6	0.91	755.74	1.74	387.01	0.335916
PC7	0.53	1113.97	1.94	992.02	0.533767

Table 8. Binary interaction coefficients for the EOS4

PC1	0						
PC2	0.15	0					
PC3	0.15	0.00	0				
PC4	0.14	0.00	0	0			
PC5	0.14	0.09	0	0	0		
PC6	0.14	0.10	0	0	0	0	
PC7	0.13	0.12	0	0	0	0	0

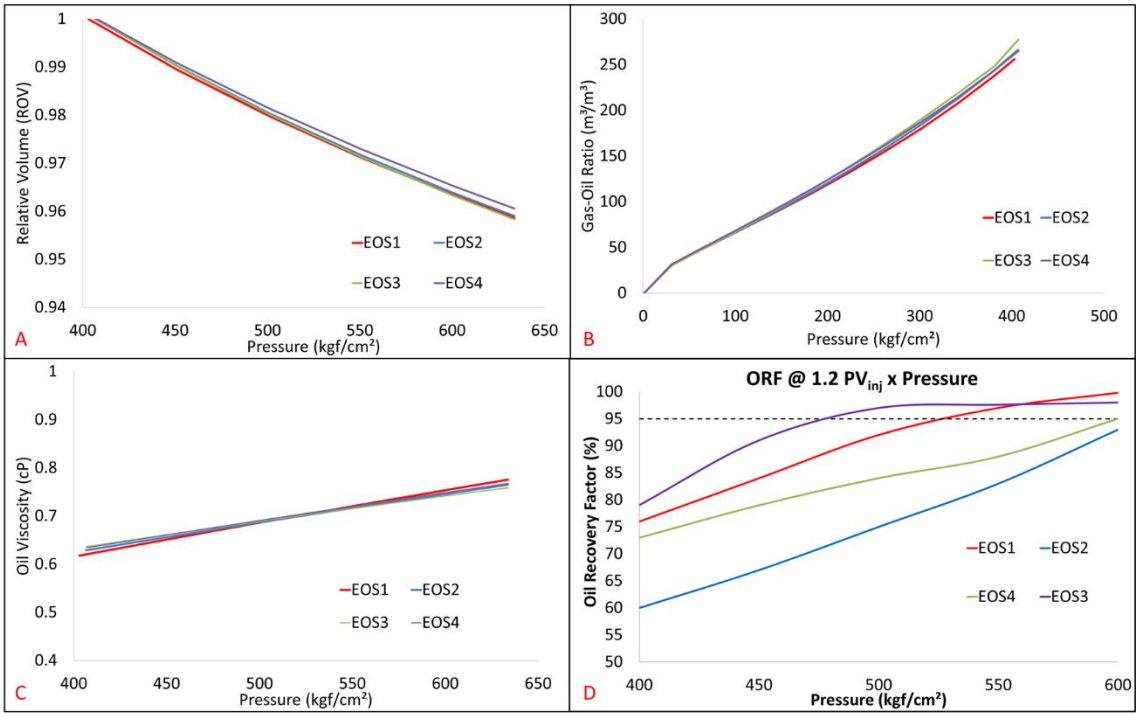

Figure 1 – Comparison of EOS1, EOS2, EOS3, and EOS4. A, B, and C are some PVT experiment simulations; D refers to the slimtube numerical results.

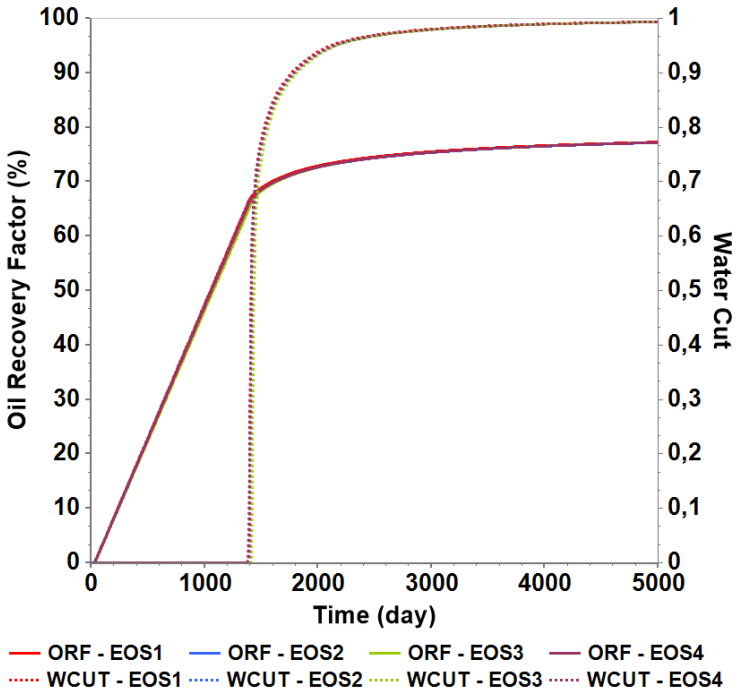

Figure 2 – Consistency test with water flooding to verify the total equivalence among the four EoS when no gas is injected in the system.

APPENDIX D – LICENSE AGREEMENTS FROM PUBLISHERS GRANTING PERMISSION TO REPRODUCE PUBLISHED ARTICLES IN THIS THESIS

Copyright Clearance Center | RightsLink®

Home | Help | Email Support | Sign in | Create Account

New upscaling technique for compositional reservoir simulations of miscible gas injection

Author: V.S. Rios,L.O.S. Santos,F.B. Quadros,D.J. Schiozer

Publication: Journal of Petroleum Science and Engineering

Publisher: Elsevier

Date: April 2019

© 2018 Elsevier B.V. All rights reserved.

Please note that, as the author of this Elsevier article, you retain the right to include it in a thesis or dissertation, provided it is not published commercially. Permission is not required, but please ensure that you reference the journal as the original source. For more information on this and on your other retained rights, please visit: https://www.elsevier.com/about/our-business/policies/copyright#Author-rights

BACK | CLOSE WINDOW

Copyright Clearance Center Marketplace™

Society of Petroleum Engineers (SPE) - License Terms and Conditions

This is a License Agreement between Victor de Souza Rios / Unicamp ("You") and Society of Petroleum Engineers (SPE) ("Publisher") provided by Copyright Clearance Center ("CCC"). The license consists of your order details, the terms and conditions provided by Society of Petroleum Engineers (SPE), and the CCC terms and conditions.

All payments must be made in full to CCC.

Order Date	01-Feb-2021	Type of Use	Republish in a thesis/dissertation
Order license ID	1094658-1		
ISSN	1086-055X	Publisher	THE SOCIETY,
		Portion	Chapter/article

LICENSED CONTENT

Publication Title	SPE JOURNAL -RICHARDSON-	Country	United States of America
		Rightsholder	Society of Petroleum Engineers (SPE)
Author/Editor	SOCIETY OF PETROLEUM ENGINEERS (U.S.)	Publication Type	Journal
Date	01/01/1996		
Language	English		

REQUEST DETAILS

Portion Type	Chapter/article	Rights Requested	Main product
Page range(s)	19	Distribution	Worldwide
Total number of pages	19	Translation	Original language of publication
Format (select all that apply)	Print, Electronic	Copies for the disabled?	No
Who will republish the content?	Academic institution	Minor editing privileges?	No
		Incidental promotional use?	No
Duration of Use	Life of current and all future editions	Currency	USD
Lifetime Unit Quantity	Up to 9,999		

NEW WORK DETAILS

Title	NEW METHODOLOGIES FOR UPSCALING OF HIGHLY HETEROGENEOUS RESERVOIRS AND MISCIBLE GAS FLOODING PROCESSES IN NUMERICAL RESERVOIR SIMULATION	Institution name	Unicamp
		Expected presentation date	2021-02-26
Instructor name	Denis José Schiozer		

ADDITIONAL DETAILS

Order reference number	SPE-200484-PA	The requesting person / organization to appear on the license	Victor de Souza Rios / Unicamp

REUSE CONTENT DETAILS

Title, description or numeric reference of the portion(s)	Full article	Title of the article/chapter the portion is from	N/A
Editor of portion(s)	N/A	Author of portion(s)	SOCIETY OF PETROLEUM ENGINEERS (U.S.)
Volume of serial or monograph	N/A	Issue, if republishing an article from a serial	N/A
Page or page range of portion	Full article	Publication date of portion	2020-03-05

PUBLISHER SPECIAL TERMS AND CONDITIONS

The person requesting republication permission is an author of SPE-200484-PA.

Copyright Clearance Center Marketplace™

Society of Petroleum Engineers (SPE) - License Terms and Conditions

This is a License Agreement between Victor de Souza Rios / Unicamp ("You") and Society of Petroleum Engineers (SPE) ("Publisher") provided by Copyright Clearance Center ("CCC"). The license consists of your order details, the terms and conditions provided by Society of Petroleum Engineers (SPE), and the CCC terms and conditions.

All payments must be made in full to CCC.

Order Date	01-Feb-2021	Type of Use	Republish in a thesis/dissertation
Order license ID	1094661-1	Publisher	Society of Petroleum Engineers
ISBN-13	9781613997123	Portion	Chapter/article

LICENSED CONTENT

Publication Title	SPE Europec featured at 82nd EAGE Conference and Exhibition (20EURO)	Country	United States of America
		Rightsholder	Society of Petroleum Engineers (SPE)
Date	01/01/2020	Publication Type	e-Book
Language	English		

REQUEST DETAILS

Portion Type	Chapter/article	Rights Requested	Main product
Page range(s)	20	Distribution	Worldwide
Total number of pages	20	Translation	Original language of publication
Format (select all that apply)	Print, Electronic	Copies for the disabled?	No
Who will republish the content?	Academic institution	Minor editing privileges?	No
		Incidental promotional use?	No
Duration of Use	Life of current and all future editions	Currency	USD
Lifetime Unit Quantity	Up to 9,999		

NEW WORK DETAILS

Title	NEW METHODOLOGIES FOR UPSCALING OF HIGHLY HETEROGENEOUS RESERVOIRS AND MISCIBLE GAS FLOODING PROCESSES IN NUMERICAL RESERVOIR SIMULATION	Institution name	Unicamp
		Expected presentation date	2021-02-26
Instructor name	Denis José Schiozer		

ADDITIONAL DETAILS

Order reference number	SPE-200616-MS	The requesting person / organization to appear on the license	Victor de Souza Rios / Unicamp

REUSE CONTENT DETAILS

Title, description or numeric reference of the portion(s)	Full article	Title of the article/chapter the portion is from	N/A
Editor of portion(s)	N/A	Author of portion(s)	N/A
Volume of serial or monograph	N/A	Issue, if republishing an article from a serial	N/A
Page or page range of portion	Full article	Publication date of portion	2020-12-03

PUBLISHER SPECIAL TERMS AND CONDITIONS

The person requesting republication permission is an author of SPE-200616-MS.

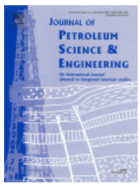

Improving coarse-scale simulation models with a dual-porosity dual-permeability upscaling technique and a near-well approach

Author: Victor de Souza Rios,Denis José Schiozer,Luiz O.S. dos Santos,Arne Skauge

Publication: Journal of Petroleum Science and Engineering

Publisher: Elsevier

Date: March 2021

Offshore Technology Conference - License Terms and Conditions

This is a License Agreement between Victor de Souza Rios / Unicamp ("You") and Offshore Technology Conference ("Publisher") provided by Copyright Clearance Center ("CCC"). The license consists of your order details, the terms and conditions provided by Offshore Technology Conference, and the CCC terms and conditions.

All payments must be made in full to CCC.

Order Date	01-Feb-2021	Type of Use	Republish in a thesis/dissertation
Order license ID	1094660-1		
ISBN-13	978-1-61399-541-9	Publisher	Offshore Technology Conference
		Portion	Chapter/article

LICENSED CONTENT

Publication Title	OTC Brasil	Country	United States of America
Author/Editor	Offshore Technology Conference	Rightsholder	Offshore Technology Conference
Date	01/01/2017	Publication Type	e-Book
Language	English		

REQUEST DETAILS

Portion Type	Chapter/article	Rights Requested	Main product
Page range(s)	13	Distribution	Worldwide
Total number of pages	13	Translation	Original language of publication
Format (select all that apply)	Print, Electronic	Copies for the disabled?	No
Who will republish the content?	Academic institution	Minor editing privileges?	No
Duration of Use	Life of current and all future editions	Incidental promotional use?	No
Lifetime Unit Quantity	Up to 9,999	Currency	USD

NEW WORK DETAILS

Title	NEW METHODOLOGIES FOR UPSCALING OF HIGHLY HETEROGENEOUS RESERVOIRS AND MISCIBLE GAS FLOODING PROCESSES IN NUMERICAL RESERVOIR SIMULATION	Institution name	Unicamp
		Expected presentation date	2021-02-26
Instructor name	Denis José Schiozer		

ADDITIONAL DETAILS

Order reference number	OTC-28008-MS	The requesting person / organization to appear on the license	Victor de Souza Rios / Unicamp

REUSE CONTENT DETAILS

Title, description or numeric reference of the portion(s)	Full Article	Title of the article/chapter the portion is from	N/A
Editor of portion(s)	N/A	Author of portion(s)	Offshore Technology Conference
Volume of serial or monograph	N/A	Issue, if republishing an article from a serial	N/A
Page or page range of portion	Full article	Publication date of portion	2017-10-26

PUBLISHER SPECIAL TERMS AND CONDITIONS

The person requesting republication permission is an author of OTC-28008-MS.

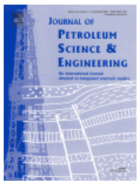

Practical workflow to improve numerical performance in time-consuming reservoir simulation models using submodels and shorter period of time

Author: V.S. Rios,G.D. Avansi,D.J. Schiozer

Publication: Journal of Petroleum Science and Engineering

Publisher: Elsevier

Date: December 2020